

<https://doi.org/10.15388/vu.thesis.284>

<https://orcid.org/0000-0002-2707-7724>

VILNIAUS UNIVERSITETAS

Aistė

ZENTELYTĖ

Vaisiaus vandenų kamieninių ląstelių  
diferenciacijos molekuliniai tyrimai  
sveikų nėštumų ir nėštumų su vaisiaus  
patologija atvejais

**DAKTARO DISERTACIJA**

Gamtos mokslai,  
Biochemija (N 004)

---

VILNIUS 2022

Disertacija rengta 2017– 2021 metais Vilniaus universitete Gyvybės mokslų centre Biochemijos institute.

Mokslinius tyrimus rėmė Lietuvos mokslo taryba (projektas „Epigenetinių veiksmų ir mikro RNR vaidmuo vaisiaus vandenų kamieninių ląstelių funkcionavime“, MIP-57/2015; gauta Lietuvos mokslo tarybos stipendija už akademinis pasiekimus), Vilniaus universitetas (Mokslo skatinimo fondo finansuotas projektas „Žmogaus vaisiaus vandenų kamieninių ląstelių nervinės diferencijos tyrimas“, MSF-JM-4; Mokslo skatinimo fondo finansuota išvyka į konferenciją; gauta vienkartinė tikslinė stipendija) ir Gyvybės mokslų centras (gauta GMC vardinė stipendija už akademinis pasiekimus)

**Mokslinė vadovė:**

**Dr. Veronika V. Borutinskaitė** (Vilniaus universitetas, gamtos mokslai, biochemija – N 004)

**Mokslinė konsultantė:**

**Prof. Dr. Rūta Navakauskienė** (Vilniaus universitetas, gamtos mokslai, biochemija – N 004).

Gynimo taryba:

Pirmininkė – **Dr. Daiva Baltriukienė** (Vilniaus universitetas, gamtos mokslai, biochemija N004).

Nariai:

**Dr. Daiva Bironaitė** (Valstybinis mokslinių tyrimų institutas Inovatyvios medicinos centras, gamtos mokslai, biochemija – N 004);

**Prof. Dr. Dainius Characiejus** (Vilniaus universitetas, medicinos ir sveikatos mokslai, medicina – M 001);

**Prof. Dr. Gediminas Čepinskas** (Lawson Sveikatos mokslų institutas, Kanada, gamtos mokslai, biochemija – N 004);

**Prof. Dr. Vytenis Arvydas Skeberdis** (Lietuvos sveikatos mokslų universitetas, gamtos mokslai, biologija – N 010).

Disertacija ginama viešame Gynimo tarybos posėdyje 2022 m. vasario mėn. 25 d. 14 val. Vilniaus universiteto Gyvybės mokslų centro R-401 auditorijoje.

Adresas: Saulėtekio al. 7, LT-10527, Vilnius, Lietuva

Tel. +37052234416; el. paštas [info@gmc.vu.lt](mailto:info@gmc.vu.lt) .

Disertaciją galima peržiūrėti Vilniaus universiteto bibliotekoje ir VU interneto svetainėje adresu: <https://www.vu.lt/naujienos/ivykiu-kalendorius>

<https://doi.org/10.15388/vu.thesis.284>

<https://orcid.org/0000-0002-2707-7724>

VILNIUS UNIVERSITY

Aistė

ZENTELYTĖ

# Molecular studies of differentiation in amniotic fluid stem cells of healthy and fetus affected gestations

**DOCTORAL DISSERTATION**

Natural Sciences,  
Biochemistry (N 004)

---

VILNIUS 2022

This dissertation was written between 2017 and 2021 at Vilnius University Life Sciences Center Institute of Biochemistry.

The research was supported by Research Council of Lithuania (project „Regulation of amniotic fluid-derived stem cell functioning by microRNA and epigenetic factors”, MIP-57/2015; granted a scholarship for academic accomplishments), Vilnius University (project „Neurogenic differentiation of human amniotic fluid mesenchymal stem cells“, MSF-JM-4; granted a scholarship to attend a conference; granted a one-time targeted scholarship) and Life Sciences Center (granted LSC nominal scholarship).

**Academic supervisor:**

**Dr. Veronika V. Borutinskaitė** (Vilnius University, Natural Sciences, Biochemistry – N 004).

**Academic consultant:**

**Prof. Dr. Rūta Navakauskienė** (Vilnius University, Natural Sciences, Biochemistry – N 004).

Dissertation Defence Panel:

Chairman – **Dr. Daiva Baltriukienė** (Vilnius University, Natural Sciences, Biochemistry – N 004).

Members:

**Dr. Daiva Bironaitė** (State Research Institute Centre for Innovative Medicine, Natural Sciences, Biochemistry – N 004);

**Prof. Dr. Dainius Characiejus** (Vilnius University, Medicine and Health Sciences, Medicine – M 001);

**Prof. Dr. Gediminas Čepinskas** (Lawson Health Research Institute, Canada, Natural Sciences, Biochemistry – N 004);

**Prof. Dr. Vytenis Arvydas Skeberdis** (Lithuanian University of Health Sciences, Natural Sciences, Biology – N 010).

The dissertation shall be defended at a public meeting of the Dissertation Defence Panel at 14 h on 25th February 2022 in Room R-401 of Vilnius University Life Sciences Center.

Address: Sauletekio av. 7, LT-10257, Vilnius, Lithuania

Tel. +37052234416; e-mail: info@gmc.vu.lt

The text of this dissertation can be accessed at the library of Vilnius University, as well as on the website of Vilnius University:

[www.vu.lt/lt/naujienos/ivykiu-kalendorius](http://www.vu.lt/lt/naujienos/ivykiu-kalendorius)



## TURINYS

PUBLIKACIJŲ SĄRAŠAS .....	7
SANTRUMPOS .....	8
ĮVADAS.....	11
1. METODAI.....	17
1.1. VVKL išskyrimas, kultivavimas, kariotipavimas ir poveikiai .	17
1.2. VVKL diferenciacijos indukcija.....	17
1.3. RNR skyrimas ir TL-kPGR.....	18
1.4. Paviršinių ir viduląstelių baltymų analizė tėkmės citometru.	19
1.5. Baltymų išskyrimas ir Western Blot analizė .....	19
1.6. Imunofluorescencinė analizė .....	19
1.7. Imunofermentinė sekretuojamų baltymų analizė .....	20
1.8. VVKL energetinio profilio ir ROS analizė .....	20
1.9. Statistinė analizė.....	20
2. REZULTATAI IR JŲ APTARIMAS .....	21
2.1. Sveikų nėštumų ir nėštumų su vaisiaus patologija VVKL charakterizavimas.....	21
2.2. Sveikų nėštumų ir nėštumų su vaisiaus patologija VVKL diferenciacijos potencialas riebaline, kauline, raumenine ir nervine kryptimis .....	24
2.2.1. Diferencijuotų VVKL morfologiniai ir genų raiškos pokyčiai .....	24
2.2.2. Epigenetiniai pokyčiai VVKL diferenciacijos metu .....	27
2.3. Sveikų ir polihidramniono nėštumų VVKL nervinė diferenciacija.	31
2.3.1. Ląstelių morfologiniai pokyčiai diferenciacijos metu.....	31
2.3.2. Genų raiškos pokyčiai diferenciacijos metu.....	33
2.3.3. Baltymų raiškos pokyčiai diferenciacijos metu.....	35
2.4. Mažųjų molekulių poveikių įtaka VVKL savybėms ir nervinės diferenciacijos potencialui.....	36

2.4.1. Mažųjų molekulių poveikių įtaka VVKL genų ir baltymų raiškai .....	37
2.4.2. VVKL metabolizmo pokyčiai poveikių mažosiomis molekulėmis metu .....	38
2.4.3. Mažųjų molekulių poveikių įtaka VVKL nervinės diferenciacijos potencialui .....	39
IŠVADOS.....	41
SUMMARY .....	42
LITERATŪROS SĄRAŠAS/REFERENCES.....	50
REZULTATŲ VIEŠINIMAS .....	63
PADĖKA.....	64
CURRICULUM VITAE .....	65
PRIEDAI .....	66
PUBLIKACIJŲ KOPIJOS .....	69

## PUBLIKACIJŲ SĄRAŠAS

Disertacija rengta remiantis žemiau išvardintomis publikacijomis:

1 publikacija. M. Gasiūnienė, **A. Zentelytė**, G. Treigytė, S. Baronaitė, J. Savickienė, A. Utkus, R. Navakauskienė. Epigenetic alterations in amniotic fluid mesenchymal stem cells derived from normal and fetus-affected gestations: a focus on myogenic and neural differentiations. *Cell Biology International*, 2019, 43:299-312. doi: 10.1002/cbin.11099

Autorės indėlis: prisidėjo prie publikacijos rašymo ir parengimo spausdinimui, atliko ląstelių charakterizavimo, genų raiškos eksperimentus.

2 publikacija. **A. Zentelytė**, M. Gasiūnienė, G. Treigytė, S. Baronaitė, J. Savickienė, V. Borutinskaitė, R. Navakauskienė. Epigenetic Regulation of Amniotic Fluid Mesenchymal Stem Cell Differentiation to the Mesodermal Lineages at Normal and Fetus-Diseased Gestation. *Journal of Cellular Biochemistry*, 2020, 121:1811-1822. doi: 10.1002/jcb.29416

Autorės indėlis: prisidėjo prie publikacijos rašymo ir parengimo spausdinimui, atliko ląstelių charakterizavimo, genų ir miR raiškos eksperimentus.

3 publikacija. **A. Zentelytė**, D. Žukauskaitė, I. Jacerytė, V.V. Borutinskaitė, R. Navakauskienė. Small Molecule Treatments Improve Differentiation Potential of Human Amniotic Fluid Stem Cells. *Frontiers in Bioengineering and Biotechnology*, 2021, 9:623886. doi: 10.3389/fbioe.2021.623886

Autorės indėlis: parašė ir parengė publikaciją spausdinimui, atliko ląstelių charakterizavimo, energetikos, genų ir baltymų raiškos eksperimentus.

4 publikacija. G. Valiulienė, **A. Zentelytė**, E. Beržanskytė, R. Navakauskienė. Metabolic Profile and Neurogenic Potential of Human Amniotic Fluid Stem Cells from Normal vs. Fetus-Affected Gestations. *Frontiers in Cell and Developmental Biology*, 2021, 9:700634. doi: 10.3389/fcell.2021.700634

Autorės indėlis: prisidėjo prie publikacijos rašymo ir parengimo spausdinimui, atliko ląstelių charakterizavimo, energetikos, baltymų raiškos eksperimentus.

## SANTRUMPOS

8-Br-cAMP	8-Bromadenozino 3',5'-ciklinis adenzino monofosfatas (angl. <i>8-Bromoadenosine 3',5'-cyclic monophosphate</i> )
APC	alofikocianinas (angl. <i>allophycocyanin</i> )
ATP	adenozin 5' trifosfatas (angl. <i>adenosine triphosphate</i> )
BDNF	smegenų neurotrofinis veiksnys (angl. <i>brain-derived neurotrophic factor</i> )
BMI1	pirmojo Polikombo slopinančio komplekso subvienetas (angl. <i>B Lymphoma Mo-MLV Insertion Region 1 Homolog</i> )
dbcAMP	dibutiril ciklinis adenzino monofosfatas (angl. <i>dibutyryl cyclic adenosine monophosphate</i> )
DMEM	Dulbecco's modifikuota Eagle terpė (angl. <i>Dulbecco's Modified Eagle Medium</i> )
DNMT	DNR metiltransferazė
ECAR	užląstelinio rūgštėjimo greitis (angl. <i>extracellular acidification rate</i> )
EGF	endotelio augimo veiksnys (angl. <i>endothelial growth factor</i> )
ELISA	fermentinė imuninė reakcija (angl. <i>enzyme-linked immunosorbent assay</i> )
EZH2	antrojo Polikombo slopinančio komplekso subvienetas (angl. <i>enhancer of zeste 2 polycomb repressive complex 2 subunit</i> )
FBS	fetalinis veršiuko serumas (angl. <i>fetal bovine serum</i> )
FGF	fibroblastų augimo veiksnys (angl. <i>fibroblast growth factor</i> )
FITC	fluoresceino izotiocianatas (angl. <i>fluorescein isothiocyanate</i> )
H3K4me3	histono H3 4-ojo lizino trimetilinimas
H3K9me3	histono H3 9-ojo lizino trimetilinimas
H3K27me3	histono H3 27-ojo lizino trimetilinimas
H3K9ac	histono H3 9-ojo lizino acetilinimas

H4hyperAc	histono H4 hiperacetilinimas
HDAC	histonų deacetilazė (angl. <i>histone deacetylase</i> )
IBMX	3-izobutil-metilksantinas (angl. <i>3-isobutyl-1-methylxanthine</i> )
IKK	NFκB signalinį kelią aktyvuojanti kinazė (angl. <i>IκB kinase</i> )
IL	interleukinas
KCl	kalio chloridas
kDNR	komplementari DNR
KL	kamieninė ląstelė
MHC	didysis audinių suderinamumo kompleksas (angl. <i>major histocompatibility complex</i> )
miR	mikro RNR
NaBut	natrio butiratas
NCAM	nervinių ląstelių adhezinė molekulė (angl. <i>neural cell adhesion molecule</i> )
NFκB	branduolio veiksnys kapa B (angl. <i>nuclear factor kappa-light-chain-enhancer of activated B cells</i> )
NGF	nervų augimo veiksnys (angl. <i>nerve growth factor</i> )
OCR	deguonies suvartojimo greitis (angl. <i>oxygen consumption rate</i> )
OxPhos	oksidacinis fosforilinimas (angl. <i>oxidative phosphorylation</i> )
PE	fikoeritinas (angl. <i>phycoerythrin</i> )
PKL	pluripotentinės kamieninės ląstelės
PRC	Polikombo slopinantis kompleksas (angl. <i>Polycomb repressive complex</i> )
RA	retinoinė rūgštis (angl. <i>all-trans retinoic acid</i> )
ROS	reaktyvios deguonies rūšys (angl. <i>reactive oxygen species</i> )
SUZ12	antrojo Polikombo slopinančio komplekso subvienetas (angl. <i>suppressor of zeste 12 protein</i> )

TET	fermentas, katalizuojantis 5-metilcitozino virsmą į 5-hidroksimetilcitoziną (angl. <i>ten-eleven translocation</i> )
TNF $\alpha$	naviko nekrozės veiksnys alfa (angl. <i>tumor necrosis factor alpha</i> )
TSA	trichostatinas A
TUBB3	III klasės $\beta$ -tubulinas (angl. <i>class III <math>\beta</math>-tubulin</i> )
VEGF	kraujagyslių endotelio augimo veiksnys (angl. <i>vascular endothelial growth factor</i> )
ViC	vitaminas C
VV	vaisiaus vandenys
VVKL	vaisiaus vandenų kamieninė ląstelė

## ĮVADAS

Pastaruoju metu pasaulyje pastebima tendencija, kad didėja nėščiujų ir gimdyvių amžius, nes vis daugiau moterų planuoja vėlesnį nėštumą. Vyresnis besilaukiančiųjų moterų amžius siejamas su padidėjusia chromosominių anomalijų ir persileidimo rizika (Frederiksen ir kt., 2018). Pasaulinės sveikatos organizacijos (PSO) duomenimis, apie 6 % naujagimių diagnozuojamos įgimtos ligos, tačiau šis skaičius gali būti ir didesnis, kadangi dažnai į statistinius duomenis yra neįtraukiami nėštumo nutraukimo dėl vaisiaus apsigimimų atvejai ar negyvagimių atvejai (<https://www.who.int/health-topics/congenital-anomalies>). Taip pat pastebima, jog įgimtų ligų paplitimas skiriasi tarp skirtingų regionų/valstybių, toks pasiskirstymas siejamas su besiskiriančiomis socialinėmis, rasinėmis, ekonominėmis ir ekologinėmis ypatybėmis. Nustatyta, kad 40-60 % įgimtų sutrikimų etiologija yra neaiški, 30-40 % sutrikimų lemia genetinės priežastys, o 5-10 % siejami su aplinkos veiksniais (Rizk ir kt., 2014). Įgimtos širdies ligos, nervinio vamzdelio raidos defektai, Dauno sindromas – tai dažniausiai pasitaikantys įgimti sutrikimai (Morris ir kt., 2018). Prenatalinėje diagnostikoje taikomi metodai padeda anksti (choriono gaurelių biopsija atliekama nuo 11-os nėštumo savaitės, amniocentezė - nuo 15 savaitės) išaiškinti galimą vaisiaus ligą, tačiau yra sutrikimų, kurie išsivysto vėlyvesniame nėštumo laikotarpyje. Vienas jų – polihidramnionas – tai nėštumo sutrikimas, siejamas su padidėjusiu vaisiaus vandenų (VV) kiekiu. Įvairių šaltinių duomenimis, polihidramniono nėštumai nustatomi 0,2-3,9 % visų nėštumų (Allaf ir kt., 2015). Motinos ligos (diabetas, vaistų vartojimas) ar placentos sutrikimai (monochorioninis dvynių nėštumas) siejami su polihidramniono išsivystymu, tačiau įgimti vaisiaus sutrikimai, tokie kaip virškinamojo trakto ligos, centrinės nervų sistemos sutrikimai, raumenų sistemos ar kvėpavimo takų anomalijos bei įgimta diafragmos išvarža, labiausiai siejami su polihidramniono diagnoze, nors dauguma atvejų ligos etiologija taip pat neaiški (Kornacki ir kt., 2017). Nustatyta, jog polihidramniono atvejais dažniausiai pasitaikantis vaisiaus sutrikimai yra centrinės nervų sistemos ir nervinio vamzdelio raidos defektai, pavyzdžiui *Spina bifida occulta*, meningocele, mielomeningocelė, anencefalija, hidrocefalija (Kouamé ir kt., 2013). Todėl, VV esančios ląstelės, tarp jų ir kamieninės ląstelės (KL), galėtų būti panaudojamos ne tik terapiniais tikslais, bet ir ligų atsiradimo priežasčių bei ankstyvų biožymenų paieškos tyrimams.

Kamieninės ląstelės išsiskiria iš kitų ląstelių tipų dėl kelių savo savybių. Šios ląstelės pasižymi gebėjimu pasidalyti daug kartų išlaikant nepakitusias

ląstelių savybes, taip pat KL geba diferencijuoti į specializuotas tam tikrų tipų ar audinių ląsteles. Šios ypatybės leidžia KL tyrinėti ir bandyti pritaikyti jas regeneracinėje medicinoje gydant įvairias ligas, audinių ir organų pažeidimus, pagerinti sutrikusias natyvių ląstelių funkcijas. Klinikiniams tikslams KL gali būti naudojamos dviem būdais – pakeičiant pažeistas ląsteles arba pagerinant augimo aplinką natyvioms ląstelėms per parakrininių veiksmų sekreciją. Terapiniams tikslams gali būti panaudojamos donorų kamieninės ląstelės arba autologinės paciento ląstelės, kurios buvo saugotos audinių ar ląstelių banke (pvz., kaulų čiulpu, virkštelės kraujo KL) ar šviežiai išskirtos iš kažkurio audinio ar organo. Sąlyginai naujas ir daug žadantis KL šaltinis yra vaisiaus vandenys, iš kurių galima išskirti gausią KL kultūrą (Loukogeorgakis ir De Coppi, 2017). Skelbiama, kad vaisiaus vandenų kamieninės ląstelės (VVKL) galėtų būti panaudojamos autoimuninių ligų (Yang ir kt., 2021), širdies ligų (Fang ir kt., 2021), Alzheimerio ligos (Gatti ir kt., 2020) ir kitų sutrikimų gydymui. Taip pat kaip vienas svarbiausių šių ląstelių panaudojimo būdų – įgimtų ligų, tokių kaip *Spina Bifida*, diafragmos išvarža ar įgimtos širdies ligos, gydymas (Di Bernardo ir kt., 2014; Abe ir kt., 2019).

Žinoma, kad vaisiaus vandenyse aptinkama ląstelių populiacija yra heterogeniška (Bossolasco ir kt., 2006) ir ją sudaro įvairios kilmės ir skirtingo diferenciacijos lygio ląstelės, pasižyminčios skirtingomis savybėmis. Vaisiaus vandenyse esančių ląstelių kiekis priklauso nuo nėštumo laikotarpio, tačiau jis gali kisti esant įvairioms vaisiaus ir nėštumo patologijoms (Prusa ir Hengstschlāger, 2002). Pirmieji darbai, kuriuose skelbiama apie identifikuotą kamieninių ląstelių populiaciją vaisiaus vandenyse, paskelbti beveik prieš 20 metų (Prusa ir kt., 2003; In `t Anker ir kt., 2003; Kaviani ir kt., 2003). Per šį laikotarpį VVKL susilaukė daug dėmesio ir buvo plačiai tyrinėjamos. Dabar jau žinoma, kad šios ląstelės pasižymi plačiu diferenciacijos potencialu, geba diferencijuoti į ląstelių linijas iš visų trijų gemalinių lapelių (De Coppi ir kt., 2007; Perin ir kt., 2008), VVKL greitai proliferuoja ir sąlyginai lėtai sensta *in vitro* kultūroje (Alessio ir kt., 2018; Gasiunienė ir kt., 2020), transplantavus nesukelia imuninio atsako ir neformuoja teratomų *in vivo*, taip pat pasižymi priešūždegiminėmis savybėmis (Trohatou ir kt., 2013), o šių ląstelių gavimas nesukelia beveik jokių etinių problemų.

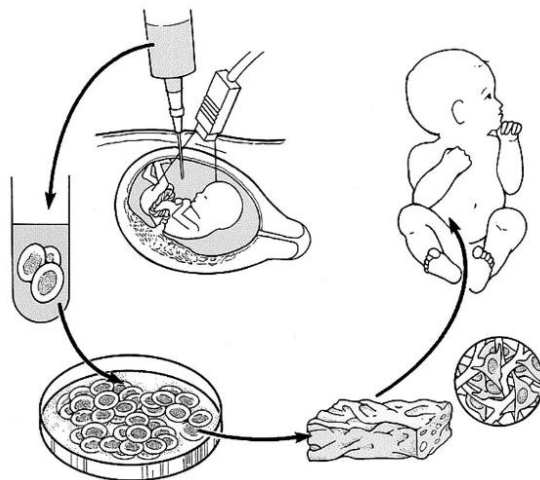
VVKL galėtų būti plačiai pritaikomos regeneracinėje medicinoje (Joo ir kt., 2012; Kim ir kt., 2014), kadangi jos yra autogeninės vaisiui ir gali būti panaudojamos prenataliniu ir neonataliniu laikotarpiu gydymo tikslais (Kunisaki ir kt., 2007; Ekblad ir kt., 2015; Ramasamy ir kt., 2018; Shaw ir kt., 2021) (1 pav.), taip pat šios ląstelės yra pusiau alogeninės kiekvienam iš tėvų, tad jos potencialiai galėtų būti panaudojamos ir kitų šeimos narių gydymui



(Siegel ir kt., 2007; Cananzi ir kt., 2009). VVKL savo savybėmis yra pranašesnės už kamienines ląsteles išskirtas iš kitų šaltinių, įskaitant kaulų čiulus, virkštelės kraują, endometriumą, placentą (Roubelakis ir kt., 2007; Yan ir kt., 2013; Bonaventura ir kt., 2015; Alessio ir kt., 2018; Jain ir kt., 2019). VVKL panaudojimas klinikinėje praktikoje yra logiškas ir praktiškas pasirinkimas, kadangi KL gali būti išskiriamos iš VV, kurie surenkami amniocentezės būdu, dar prieš gimdymą. Amniocentezė yra rutiniškai klinikinėje diagnostikoje taikomas metodas, kuomet nedidelis VV kiekis paimamas genetinių ligų ir aneuploidijų nustatymui (Daum ir kt., 2019). Tuo tarpu KL gavimas iš kitų prenatalinių audinių, pavyzdžiui choriono gaureliai, virkštelės kraujas, vaisiaus oda, kepenys ar raumuo, yra ir techniškai sudėtingesnis, ir pavojingesnis vaisiui metodas (Cadrin ir Golbus, 1993; Cheng, 2018). VV įprastai diagnostiniams tyrimams surenkami antrojo nėštumo trimestro metu (16-22 savaitę), tačiau esant tam tikriems nėštumo ir vaisiaus vystymosi sutrikimams, tokiems kaip polihidramnionui, kuriam būdingas padidėjęs VV kiekis, amniocentezė taikoma kaip vienas iš gydymo būdų trečiojo nėštumo trimestro laikotarpiu (28-34 savaitę), kuomet pašalinamas perteklinis VV kiekis. Palyginus VVKL, išskirtas iš panašaus laikotarpio nėštumo vaisiaus vandenų, šių ląstelių savybės buvo panašios, nors ir pastebimi tam tikri skirtumai tarp skirtingų donorų bei tarp ląstelių, išskirtų iš ankstyvo ir vėlyvo nėštumų VV (Maguire ir kt., 2013; Casciaro ir kt., 2018).

Viena iš svarbiausių kamieninių ląstelių funkcijų yra jų gebėjimas diferencijuotis ir specializuotis. Ši KL savybė leidžia jas tyrinėti stengiantis tokias ląsteles pritaikyti terapiniais tikslais. Moksliniuose darbuose skelbiama, kad VVKL galėtų būti naudojamos daugelio ligų ir sutrikimų gydymui, pavyzdžiui miokardo infarktas, širdies nepakankamumas, centrinės nervų bei virškinimo sistemų pažeidimai, plaučių ir inkstų ligos (Loukogeorgakis ir De Coppi, 2017; Azargoon ir Negahdari, 2018; George ir kt., 2019; Yu ir kt., 2019). Taip pat įvairios įgimtos ligos ir net naujagimių sepsis (Kunisaki ir kt., 2018; Sato ir kt., 2020). Tačiau didžiosios dalies moksliniuose tyrimuose, orientuotuose į VVKL pritaikymą klinikinėje praktikoje, tiriamos kamieninės ląstelės, išskirtos iš sveikų nėštumų vaisiaus vandenų. Šių tyrimų rezultatai ir surinkti duomenys galėtų apriboti VVKL panaudojimą terapiniams tikslams tuo atveju, jei būtų nustatyti esminiai kamieninių ląstelių savybių skirtumai tarp ląstelių, išskirtų iš sveikų nėštumų ir nėštumų su vaisiaus sutrikimais. Ankstesniuose laboratorijos kolegų darbuose buvo nustatyta, kad iš sveiko nėštumo vaisiaus vandenų išskirtos VVKL geba diferencijuoti mezoderminę ir neuroektoderminę kryptimis (Savickienė ir kt., 2015; Glemžaitė ir Navakauskienė, 2016; Gasiūnienė ir kt., 2019a; 2019b; 2019c), tačiau apie

žmogaus VVKL, išskirtas iš nėštumo su vaisiaus patologija, žinoma dar sąlyginai nedaug.



**1 pav.** VVKL pritaikymo klinikinėje praktikoje koncepcija. Vaisiaus vandenys surenkami amniocentezės būdu, išskirtos ląstelės auginamos ir padauginamos *in vitro* kultūroje, gali būti auginamos ir ant įvairių karkasų imituojančių organų erdvinę struktūrą. Ląstelės ar ląstelių ir karkasų dariniai transplantuojami vaisiui prenataliniu ar neonataliniu laikotarpiu (Kaviani ir kt., 2003).

Ląstelių vystymosi ir diferenciacijos metu be galo svarbų vaidmenį atlieka epigenetinė šių procesų reguliacija, kuri apima tokius veiksnius kaip mikro RNR, DNR metilinimas, histonų modifikacijos, chromatino persitvarkymo baltymai (Wu ir Sun, 2006). Kartu su transkripcijos veiksniais Oct4, Nanog ir Sox2 epigenetiniai reguliatoriai kontroliuoja pluripotentinių kamieninių ląstelių (PKL) savęs atsinaujinimą, proliferaciją ir diferenciaciją (Kashyap ir kt., 2009). Somatinių kamieninių ląstelių, taip pat ir mezenchiminių kamieninių ląstelių, funkcionavime ir diferenciacijos valdyme epigenetinė reguliacija yra be galo svarbi (Avgustinova ir Benitah, 2016; Ozkul ir Galderisi, 2016). VVKL kamieninių ląstelių hierarchijoje užima tarsi tarpinę padėtį tarp embrioninių ir somatinių kamieninių ląstelių, jų diferenciacijos reguliacijos mechanizmai dar nėra iki galo išaiškinti ir nėra žinoma ar jie nesiskiria tarp sveiko ir nėštumo su vaisiaus patologija KL. Tad šių procesų tyrimai reikšmingai prisidėtų prie abiejų šaltinių VVKL savybių išaiškinimo ir galimo pritaikymo klinikinėje praktikoje.

Epigenetinėje reguliacijoje dalyvaujančius veiksnius veikiančios (juos aktyvinančios ar slopinančios) medžiagos ir jų poveikiai gali būti naudojami įvairių ląstelėje vykstančių procesų inicijavimui ir reguliavimui. Šių medžiagų, dar vadinamų mažosiomis molekulėmis, panaudojimas ląstelių

pluripotentiškumo ar (trans)diferenciacijos indukcijai yra pakankamai naujas jų pritaikymo būdas (Kim ir kt., 2020). Naudojant mažąsias molekules nesunkiai galima reguliuoti jų koncentracijas, kombinacijas, poveikio laiką, taip pat jos lengvai patenka į ląsteles, nėra imunogeniškos ir gali būti skiriamos pacientams kaip vaistiniai preparatai, skatinantys ląstelių atsinaujinimą ir regeneraciją (Baranek ir kt., 2017; Ma ir kt., 2017). Mažosios molekulės plačiai taikomos kamieninių ląstelių diferenciacijos (Maioli ir kt., 2013; Deng ir kt., 2016) ar transdiferenciacijos indukcijai (Cipriano ir kt., 2017), taip pat gali būti pritaikytos PKL diferenciacijai į mezenchimines kamienines ląsteles (Chen ir kt., 2012). Didelė mažųjų molekulių įvairovė ir dar didesnė jų kombinacijų apimtis rodo, kad šios medžiagos turėdamos daug taikinių gali padėti reguliuoti įvairius ląstelinius procesus. Mokslinių tyrimų duomenys rodo didžiulį mažųjų molekulių pritaikymo potencialą kamieninių ląstelių tyrimuose, pasitelkiant šias medžiagas galima pagerinti ląstelių savybes, diferenciacijos efektyvumą, skatinti proliferaciją ir slopinti senėjimą bei uždegiminiuosius procesus.

**Darbo tikslas:** įvertinti sveikų nėštumų ir nėštumų su vaisiaus patologija vaisiaus vandenų kamieninių ląstelių molekulinis (genetinius, epigenetinius, baltyminius, energetinius) pokyčius diferenciacijos riebaline, kauline, raumenine ir nervine kryptimis metu.

**Darbo uždaviniai:**

1. Charakterizuoti sveikų nėštumų ir nėštumų su vaisiaus patologija VVKL pagal paviršiaus ir kamieniškumo genetinius žymenis, mikro RNR raišką ir metabolinius profilius.
2. Nustatyti abiejų šaltinių VVKL diferenciacijos potencialą riebaline, kauline, raumenine ir nervine kryptimis bei įvertinti morfologinius ir molekulinis pokyčius.
3. Ištirti sveikų ir polihidramniono nėštumų VVKL nervinės diferenciacijos potencialą indukuojant skirtingomis medžiagomis ir jų kombinacijomis bei nustatyti morfologinius, genetinius ir baltyminius pokyčius.
4. Įvertinti mažųjų molekulių poveikių įtaką VVKL savybėms ir nervinės diferenciacijos potencialui nustatant molekulinis pokyčius, įvykstančius diferenciacijos metu.

**Mokslinis naujumas ir praktinė reikšmė**

Šiame darbe tyrėme vaisiaus vandenų kamienines ląsteles (VVKL), išskirtas iš sveikų nėštumų ir nėštumų su vaisiaus patologija. Lyginome šių

ląstelių charakteristikas bei diferenciacijos potencialą riebaline, kauline, raumenine ir nervine kryptimis, gilinomės į galimus kamieninių ląstelių savybių skirtumus. Parodėme, jog visgi esti tam tikri fenotipiniai skirtumai tarp abiejų šaltinių VVKL, kurie ypač išryškėja trečiojo nėštumo trimestro metu esant vaisiaus patologijai (polihidramionui). Taip pat parodėme, jog polihidramniono nėštumo VVKL yra energetiškai aktyvesnės, kadangi pasižymi aktyvesniu oksidaciniu fosforiliniu ir didesniu ATP lygiu, ir joms būdingi didesni ROS kiekiai. Nustatėme, kad antrojo nėštumo trimestro sveikų nėštumų ir nėštumų su vaisiaus patologija VVKL diferenciacijos potencialas riebaline, kauline, raumenine ir nervine kryptimis yra panašus, taip pat ir epigenetiniai abiejų šaltinių VVKL yra panašūs. Mes pirmieji ištyrėme ir palyginome sveikų bei polihidramniono nėštumų VVKL diferenciaciją nervine kryptimi indukuojant ją neurotrofinėmis ir signalinius kelius aktyvuojančiomis molekulėmis bei parodėme, kad polihidramniono atveju nervinė diferenciacija sumažina uždegiminę ląstelių būseną, kadangi reikšmingai sumažėja TNF $\alpha$  sekrecija. Taip pat parodėme, kad epigenetiškai aktyvios molekulės turi įtakos sveiko nėštumo VVKL kamieniškumo savybėms bei pagerina šių ląstelių nervinės diferenciacijos potencialą.

Šiame darbe gauti rezultatai papildo esamas žinias apie VVKL, išskirtas iš sveiko nėštumo ir nėštumo su vaisiaus patologija, jų charakteristikas ir diferenciacijos potencialą įvairiomis kryptimis. Gauti duomenys pagilina žinias apie galimą šių ląstelių pritaikymą regeneracinėje medicinoje įvairių ligų, įskaitant ir įgimtų sutrikimų, gydymui.

#### **Ginamieji teiginiai:**

- VVKL skiriasi savo morfologija, genų ir paviršinių žymenų raiška bei metaboliniu profiliu antrojo trimestro sveikų nėštumų ir trečiojo trimestro nėštumų su vaisiaus patologija atvejais.
- Nepriklausomai nuo antrojo nėštumo trimestro nėštumo būsenos (sveikas nėštumas ar nėštumas su vaisiaus patologija), VVKL geba diferencijuotis riebaline, kauline, raumenine ir nervine kryptimi ir šių procesų epigenetinė reguliacija yra panaši.
- Geresniu nervinės diferenciacijos potencialu pasižymi antrojo nėštumo trimestro sveikų nėštumų VVKL nei trečiojo nėštumo trimestro polihidramniono VVKL.
- Mažųjų molekulių kombinacijų poveikiai pagerina VVKL nervinės diferenciacijos efektyvumą.

## 1. METODAI

Tyrimuose naudotų prietaisų, reagentų ir komercinių rinkinių gamintojų sąrašas pateiktas priede nr. 1.

### 1.1. VVKL išskyrimas, kultivavimas, kariotipavimas ir poveikiai

Vaisiaus vandenų mėginiai (3-5 ml) surinkti amniocentezės būdu antro (16-24 savaitė) ar trečio (28-32 savaitė) nėštumo trimestrų metu. Mėginių surinkimui ir tyrimams gautas Vilniaus regioninio biomedicininio tyrimų etikos komiteto leidimas (Nr. 158200-18/7-1049-550), visos tyrimuose dalyvavusios pacientės pasirašė informuoto asmens sutikimo formą.

VVKL skirtos naudojant dviejų etapų skyrimo protokolą (Savickiene ir kt., 2015; 1-4 publikacijos) ir augintos *AmnioMAX™ C-100* bazinėje terpėje su *AmnioMAX™ C-100* priedu (1 ir 2 publikacijos) arba DMEM (4,5 g/l gliukozės) su 10 % FBS (3 ir 4 publikacijos), abi terpės papildytos 100 U/ml penicilino ir 100 µg/ml streptomicino. Išskirtos ląstelės auginamos 37 °C termostate su 5 % CO<sub>2</sub>.

VVKL vaisiaus kilmės patvirtinimui atliktas ląstelių kariotipavimas (tyrimams naudoti mėginiai, kuomet vaisius vyriškos lyties). VVKL preparatai paruošti, dažyti 5 % Giemsa dažų tirpale ir analizuoti *Nikon ECLIPSE E200* mikroskopu su ×1000 padidiniu (3 publikacija). Taip pat tirti epigenetiškai aktyvių medžiagų, tokių kaip trihostatinas A (TSA), natrio butiratas (NaBut), retinoinė rūgštis (RA) ir vitaminas C (VitC), įtaka VVKL. Ląstelių gyvybingumas po poveikių šiomis medžiagomis ir jų kombinacijomis įvertintas naudojant 0,2 mg/ml MTT reagento tirpalą ir apskaičiuotas kaip santykis nuo neveiktos kontrolės (3 publikacija).

### 1.2. VVKL diferenciacijos indukcija

Tyrimuose VVKL diferenciacija indukuota keturiomis kryptimis naudojant skirtingus diferenciacijos protokolus ir induktorius.

a) Riebalinė diferenciacija indukuota naudojant komercinę terpę *StemPro™ Adipogenesis Differentiation Kit* ir diferenciacija vykdyta 9 dienas. Diferenciacijos įvertinimas aprašytas 2 publikacijoje.

b) Kaulinė diferenciacija indukuota naudojant komercinę terpę *StemPro™ Osteogenesis Differentiation Kit*. Diferenciacija vykdyta 9 dienas ir įvertinta kaip aprašyta 2 publikacijoje.

c) Raumeninė diferenciacija indukuota naudojant terpę, susidedančią iš DMEM (1 g/l gliukozės), 10 % FBS ir 2 % inaktyvuoto arklio serumo, diferenciacija vykdyta 12 dienų ir įvertinta kaip aprašyta 1 publikacijoje.

d) Nervinė diferenciacija indukuota skirtingomis sąlygomis naudojant kelis protokolus:

- DMEM/F12 su *GlutaMax*<sup>TM</sup> terpę papildant 1 % N2 priedu ir 1,5 μM RA, diferenciacija vykdyta 12 dienų ir įvertinta kaip aprašyta 1 publikacijoje.

- DMEM/F12 su *GlutaMax*<sup>TM</sup> terpę papildant 3 μM RA ir 1 % N2 priedu, 2 % B27 priedu ar jų kombinacija. Taip pat diferenciacijai indukuoti naudotas pirminės indukcijos žingsnis su epigenetiškai aktyviomis medžiagomis (VitC, TSA, RA). Diferenciacija vykdyta 12 dienų. Detalesni diferenciacijos protokolų ir diferenciacijos įvertinimo aprašai pateikti 3 publikacijoje.

- DMEM/F12 su *GlutaMax*<sup>TM</sup> terpę papildant 1 % N2 priedu ir 2 μM RA, *BrainPhys*<sup>TM</sup> su 1 % *NeuroCult*<sup>TM</sup> terpę papildant įvairiomis induktorių (8-Br-cAMP, IBMX, KCl, RA, BDNF, NGF) kombinacijomis, taip pat naudotas ir pirminės indukcijos etapas su augimo veiksniais (FGF ir EGF). Diferenciacija vykdyta 3 dienas ir įvertinta kaip aprašyta 4 publikacijoje.

### 1.3.RNR skyrimas ir TL-kPGR

Visuminė RNR išskirta naudojant komercinį TRIzol® reagentą pagal gamintojo rekomendacijas. Komplementarios DNR (kDNR) sintezė atlikta naudojant *Maxima First Strand cDNA Synthesis Kit* (1 ir 2 publikacijos) arba *SensiFAST<sup>TM</sup> cDNA Synthesis Kit* (3 ir 4 publikacijos). Tikro laiko kiekybinė polimerazės grandininė reakcija (TL-kPGR) vykdyta naudojant *Maxima SYBR Green qPCR Master Mix* (1 ir 2 publikacijos) arba *SensiFAST<sup>TM</sup> SYBR® No-ROX Kit* (3 ir 4 publikacijos) ir *Rotor-Gene<sup>TM</sup> 6000* termociklerį su programine įranga. Santykinė genų raiška (lyginant su neveikta ar nediferencijuota kontrole) apskaičiuota  $\Delta\Delta C_t$  metodu, normalizavus pagal GAPDH ir RPL13A raišką. Naudotos pradmenų sekos pateiktos 1, 2, 3 ir 4 publikacijose.

Mikro RNR (miR) raiškos analizei naudoti *TaqMan<sup>TM</sup> MicroRNA Assays*. kDNR sintezė atlikta panaudojant komercinį rinkinį *TaqMan<sup>TM</sup> MicroRNA Reverse Transcription Kit*, o miR raiškos lygis nustatytas panaudojant termociklerį *Rotor-Gene<sup>TM</sup> 6000* su programine įranga bei komercinius rinkinius *TaqMan<sup>TM</sup> MicroRNA Assay* ir *TaqMan<sup>TM</sup> Universal PCR Master Mix II, no UNG* pagal gamintojo rekomendacijas. miR raiška normalizuota pagal RNU48 ir santykinė raiška (lyginant su nediferencijuota kontrole) apskaičiuota naudojant  $\Delta\Delta C_t$  metodą (1 ir 2 publikacijos).

#### 1.4. Paviršinių ir viduląstelinių baltymų analizė tėkmės citometru

VVKL charakterizuotos pagal paviršinių (1-4 publikacijos) žymenų raišką. Ląstelės inkubuotos su antikūnais konjuguotais su vienu iš fluoroforu (PE, FITC, *Alexa Fluor*® 488, *Alexa Fluor*® 647, APC). Darbuose tirti paviršiniai žymenys siejami su hematopoetinėmis ir endotelio ląstelėmis (CD9, CD15, CD31, CD34, CD133, CD309), taip pat įvairūs pluripotentinių ir multipotentinių kamieninių ląstelių žymenys (CD13, CD44, CD56, CD73, CD90, CD105, CD146, CD166, CD117, CD338, SSEA4, TRA-1-60, TRA-1-81, Notch1) ir keli imuniniai žymenys (HLA-ABC, HLA-DR). Tirta ir VVKL viduląstelinių žymenų raiška (3 ir 4 publikacijos). Darbuose naudoti antikūnai prieš Sox2, Nanog, Oct4, Lin28a, c-Myc, Nestin, Musashi1, TUBB3. Baltyminių žymenų raiškos analizė atlikta naudojant *Guava*® *easyCyte 8HT* tėkmės citometrą su *InCyte 2.2.2* programa arba *BD FACSCanto*™ II tėkmės citometrą su *BD FACSDIVA*™ programa.

#### 1.5. Baltymų išskyrimas ir Western Blot analizė

Baltymai iš VVKL išskirti ir paruošti analizei kaip aprašyta 1 ir 2 publikacijose. Tiriamiems baltymams detektuoti naudoti antikūnai prieš DNMT1, HDAC1, EZH2, SUZ12, H4hyperAc, H3K9ac, H3K4me3, H3K9me3, H3K27me3, BMI1, GAPDH, H4. Po inkubacijos membranos ryškintos chemiliuminescenciniu būdu naudojant komercinį rinkinį pagal gamintojo rekomendacijas. Išryškintų baltymų juostelių densitometrinė analizė atlikta ImageJ (NIH) programa, santykinis kiekvienos juostelės tankis normalizuotas pagal GAPDH (DNMT1, HDAC1, EZH2, SUZ12 ir BMI1) arba bendrą H4 baltymo kiekį (taikoma histonų modifikacijoms), o pokytis (kartais) diferencijuotose ląstelėse apskaičiuotas lyginant su kontrole.

#### 1.6. Imunofluorescencinė analizė

Baltymų imunofluorescencinei analizei VVKL augintos ir diferencijuotos ant stikliukų. Ląstelių baltymai vizualizuoti naudojant antikūnus prieš NCAM, TUBB3 ir Vimentin. F-aktinas žymėtas naudojant *Alexa Fluor*® 594 Phalloidin. Ląstelių branduoliai dažyti 300 nM DAPI tirpalu. Paruošti ląstelių mėginiai analizuoti *Zeiss Axio Observer* fluorescenciniu mikroskopu, naudojant ×63 imersinį objektyvą. Detalesnė preparatų paruošimo procedūra aprašyta 3 ir 4 publikacijose.

### 1.7. Imunofermentinė sekretuojamų baltymų analizė

Imunofermentinis ELISA metodas naudotas nustatyti sekretuojamus BDNF, VEGF, TNF $\alpha$ , IL-1 $\beta$ , IL-6 ir IL-10 kiekius kontrolinėse ir nervine kryptimi diferencijuotose VVKL. Sekretomui surinkti naudota *NutriStem*<sup>®</sup> *hPSC XF* terpė, o baltymų kiekių analizė atlikta naudojant komercinius rinkinius, visos procedūros atliktos pagal gamintojo rekomendacijas. Sugertis plokštelėse išmatuota naudojant spektrofotometrą *Infinite M200 Pro*. Sekretuotų baltymų kiekiai normalizuoti pagal bendrą ląstelių baltymų kiekį. Detalesnis protokolo aprašymas pateiktas 3 ir 4 publikacijose.

### 1.8. VVKL energetinio profilio ir ROS analizė

VVKL metabolinis profilis charakterizuotas naudojant *Seahorse XFp Extracellular Flux Analyzer* kartu su *Cell Energy Phenotype Test Kit* kaip aprašyta 3 publikacijoje. Šiuo rinkiniu nustatytas deguonies suvartojimo greitis (angl. *oxygen consumption rate (OCR)*) bei užląstelinio rūgštėjimo greitis (angl. *extracellular acidification rate (ECAR)*), visos procedūros atliktos pagal gamintojo rekomendacijas. OCR ir ECAR vertės normalizuotos pagal bendrą ląstelių baltymą ir metabolinio fenotipo parametrai apskaičiuoti naudojant *Seahorse Wave Desktop Software* programą.

VVKL metabolinis aktyvumas nustatytas naudojant komercinius rinkinius *Glycolysis Assay*, *Extracellular O<sub>2</sub> Consumption Assay*, *TMRE Mitochondrial Membrane Potential Assay* ir *Luminescent ATP Detection Assay*. Procedūros atliktos pagal gamintojo reikalavimus kaip aprašyta 4 publikacijoje. Matavimams naudotas plokštelių skaitytuvas *Varioskan Flash Multimode Reader* ir tėkmės citometras *Guava*<sup>®</sup> *easyCyte 8HT* su *InCyte 2.2.2* programa.

ROS kiekiai VVKL nustatyti naudojant komercinį rinkinį *DCFDA Cellular ROS Detection Assay Kit*, visos procedūros atliktos pagal gamintojo reikalavimus kaip aprašyta 4 publikacijoje. Kiekybiškai ROS lygis įvertintas tėkmės citometru *Guava*<sup>®</sup> *easyCyte 8HT* su *InCyte 2.2.2* programa, kokybinė ROS analizė atlikta naudojant fluorescencinį mikroskopą *EVOS FL*.

### 1.9. Statistinė analizė

Visi eksperimentai kartoti mažiausiai tris kartus, duomenys pateikti kaip aritmetiniai vidurkiai su standartiniu nuokrypiu. Statistinis patikimumas įvertintas naudojant Stjudento t-testą, vienakryptę ANOVA su Tukey testu ar dvikryptę ANOVA su Bonferroni testu naudojant *GraphPad Prism* programą.



## 2. REZULTATAI IR JŲ APTARIMAS

Šioje dalyje aptariami svarbiausi doktorantūros metu atlikti tyrimai ir gauti rezultatai, kurie yra publikuoti su disertacijos tema susijusiose publikacijose. Pirmoje dalyje aptariamas KL, išskirtų iš sveikų nėštumų ir nėštumų su vaisiaus patologija vaisiaus vandenų, charakteristikos ir savybės (1-4 publikacijos). Antroje dalyje pateikiami sveikų nėštumų ir ankstyvų nėštumų su vaisiaus patologija VVKL diferenciacijų riebaline, kauline, raumenine ir nervine kryptimis charakterizavimas bei epigenetinės šių diferenciacijų reguliacijos tyrimų rezultatai (1 ir 2 publikacijos). Trečioje dalyje plačiau gilinamasi į sveikų ir polihidramniono nėštumų VVKL diferenciaciją nervine kryptimi panaudojant skirtingus induktorius (4 publikacija). Ketvirtojoje dalyje nagrinėjama mažųjų molekulių poveikių įtaka sveikų nėštumų VVKL savybėms ir nervinės diferenciacijos potencialui (3 publikacija).

### 2.1. Sveikų nėštumų ir nėštumų su vaisiaus patologija VVKL charakterizavimas

Šiame darbe tirtos žmogaus vaisiaus vandenų kamieninės ląstelės išskirtos iš sveikų nėštumų vaisiaus vandenų (16-20 savaitė) ir nėštumų su vaisiaus patologija vaisiaus vandenų (18-32 savaitė) (1-4 publikacijos). Išskirtų ląstelių vaisiaus kilmė buvo patvirtinta kariotipavus ląsteles ir identifikavus Y chromosomą, patvirtinančią vaisiaus vyrišką lytį (3 publikacija). Šiame darbe tirtos įvairios vaisiaus patologijos – trisomija 21 (Dauno sindromas), daugybiniai vaisiaus apsigimimai ir universali vaisiaus vandenė, *Russell-Silver* sindromas ir kraujotakos sutrikimai, centrinės nervų sistemos patologija ir išsiplėtę smegenų skilveliai, neimuninė vaisiaus vandenė ir anemija, dvynių transfuzijos sindromas (1 ir 2 publikacijos) bei polihidramnionas, išsivystęs dėl vaisiaus stemplės atrezijos, *Treacher-Collins* sindromo ar vaisiaus skrandžio atonijos (4 publikacija).

Kamieninės ląstelės iš vaisiaus vandenų išskirtos naudojant dviejų etapų skyrimo protokolą. Gauta sveiko nėštumo VVKL kultūra pasižymėjo būdinga verpstės formos morfologija, panašiai atrodė ir 2-ojo trimestro nėštumo su vaisiaus patologija VVKL (1 ir 2 publikacijos), tuo tarpu pastebėta, jog polihidramniono mėginių, kurie gauti 3-ąjį nėštumo trimestrą, VVKL pasižymi apvalesne ląstelių forma (4 publikacija) (2 pav.). Išmatavus visų šaltinių VVKL ilgį ir plotį, nustatėme, jog sveiko nėštumo ir 2-ojo trimestro nėštumo su vaisiaus patologija VVKL ilgio ir pločio santykis buvo panašus (atitinkamai  $9,3 \pm 2,3$  ir  $9,16 \pm 3,2$ ), tuo tarpu polihidramniono VVKL ilgio ir

pločio santykis buvo kur kas mažesnis ( $1,6 \pm 0,4$ ) (duomenys nepublikuoti). Iš abiejų šaltinių (sveikų nėštumų ir nėštumų su vaisiaus patologija) išskirtas ląsteles charakterizavome pagal paviršinių žymenų raišką. Nustatėme, jog VVKL nebūdinga įvairių hematopoetinių ir endotelio žymenų raiška (CD9, CD15, CD31, CD34, CD133, CD309), tačiau pasižymi kamieninėms ląstelėms būdingų žymenų raiška (CD13, CD44, CD56, CD73, CD90, CD105, CD146, CD166), taip pat šios ląstelės pasižymi HLA-ABC raiška (MHC I), bet nepasižymi HLA-DR (MHC II) raiška (1-4 publikacijos). Tokia imuninių žymenų raiškos dinamika parodo, jog VVKL yra neimunogeniškos, nes transplantavus tokias ląsteles, jos nesukeltų imuninio atsako (Kot ir kt., 2019). Vertinant skirtumus ląstelėse, išskirtose iš sveikų mėginių ir ankstyvų (2-ojo trimestro) nėštumų su vaisiaus patologija mėginių, mes nustatėme, kad reikšmingai skyrėsi tik CD90 raiška (1 ir 2 publikacijos), o lyginant sveikų ir polihidramniono nėštumų VVKL pastebėta reikšmingai mažesnė CD13, CD73, CD90 ir CD105 žymenų raiška patologiniuose mėginiuose (4 publikacija). Taip pat VVKL charakterizavome pagal pluripotentiskumo ir kitų su kamieniškumu susijusių genų raišką ir parodėme, kad tirtos ląstelės pasižymi *SOX2*, *OCT4*, *NANOG*, *REX1*, *LIN28A*, *NOTCH1* ir *c-MYC* raiška (1-4 publikacijos). Lyginant sveikų nėštumų ir ankstyvų nėštumų su vaisiaus patologija mėginius reikšmingų genų raiškos skirtumų nenustatėme (1 ir 2 publikacijos), tačiau vertinant polihidramniono nėštumų VVKL parodėme reikšmingai didesnę *OCT4*, *NOTCH1* ir *MYC* genų raišką lyginant su sveikų nėštumų VVKL (4 publikacija). Tokie morfologijos bei paviršinių ir genetinių žymenų raiškos skirtumai galimi dėl ganėtinai vėlyvo polihidramniono nėštumų laikotarpio (32 savaitė, kai tuo tarpu sveikų nėštumų mėginiai gauti 16-17 savaitę). Kaip teigiama kitų mokslininkų darbuose, nagrinėjančiuose VVKL, išskirtas iš gimdymo metu (37-40 savaitė) surinktų vaisiaus vandens, multipotentinėms kamieninėms ląstelėms būdingų paviršinių žymenų CD73, CD90, CD105 raiška vėlyvojo nėštumo laikotarpio kamieninėse ląstelėse yra mažesnė nei antrojo trimestro metu surinktų ir išskirtų VVKL, taip pat, kad trečiojo nėštumo trimestro VVKL paviršinių žymenų raiška labai skiriasi tarp mėginių iš skirtingų pacienčių (Gao ir kt., 2016; Moraghebi ir kt., 2017; Iampietro ir kt., 2020).



**2 pav.** Sveikų nėštumų ir nėštumų su vaisiaus patologija VVKL morfologija ląstelių kultivavimo metu, mastelis – 400  $\mu\text{m}$  (pagal 1 ir 4 publikacijas).

Šiame darbe VVKL charakterizavome ir pagal mikro RNR (miR), dalyvaujančių ląstelių proliferacijos ir diferenciacijos procesuose (miR-17, miR-21, miR-34a, miR-148b), raišką. Nustatėme, kad tirtų miR raiškos lygis sveikų nėštumų ir nėštumų su vaisiaus patologija ląstelėse beveik nesiskiria, tačiau reikšmingus skirtumus pastebėjome ląstelių kultivavimo metu lyginant ankstyvą, tarpinį ir vėlyvą pasaužus. Tyrimų rezultatai parodė, jog miR-17 ir miR-21 raiška kultivavimo metu reikšmingai mažėja, o miR-34a ir miR-148b raiška – reikšmingai didėja (2 publikacija). Ankstesniuose mūsų darbuose nustatėme, jog miR-17 ir miR-21 raiškos sumažėjimas gali būti siejamas su sumažėjusiu VVKL proliferacijos potencialu (Savickienė ir kt., 2016), tai patvirtina ir kitų mokslininkų darbai (Hackl ir kt., 2010; Kongcharoensombat ir kt., 2010). Mes nustatėme, jog miR-34a ir miR-148b raiška VVKL kultivavimo metu padidėja ir taip yra stabdoma ląstelių proliferacija. Toks augimo slopinimas galėtų vykti aktyvuojant SIRT1 (Zhang ir kt., 2015) ir WNT1/ $\beta$ -catenin (Zhang ir kt., 2017) signalinius kelius.

Šiame darbe taip pat apibūdinome sveikų ir polihidramniono nėštumų VVKL metabolinį potencialą. Nustatėme, jog polihidramniono grupės VVKL reikšmingai sparčiau vartoja deguonį (aktyvesnis oksidacinis fosforilimas) ir joms būdingas didesnis viduląstelinio ATP kiekis bei reikšmingai didesnė *NRF1* geno raiška. Nustatyta, jog transkripcijos veiksnys *NRF1* yra vienas pagrindinių mitochondrinio kvėpavimo reguliatorių (Yuan ir kt., 2018). Taip pat šiame darbe nustatėme, jog sveiko nėštumo VVKL pasižymi aukštesniu mitochondrijų membranos potencialu (4 publikacija). Kitų autorių gauti duomenys rodo, kad aukštas mitochondrijų membranos potencialas mažėja esant aktyviam mitochondriniam kvėpavimui (Nicholls, 2004). Žinoma, kad PKL nepasižymi labai aktyviu oksidaciniu fosforilimu ir palaiko aukštą mitochondrijų membranos potencialą (Tsogtbaatar ir kt., 2020), taip pat teigiama, jog aukštu potencialu pasižyminčios KL geba diferencijuoti visų

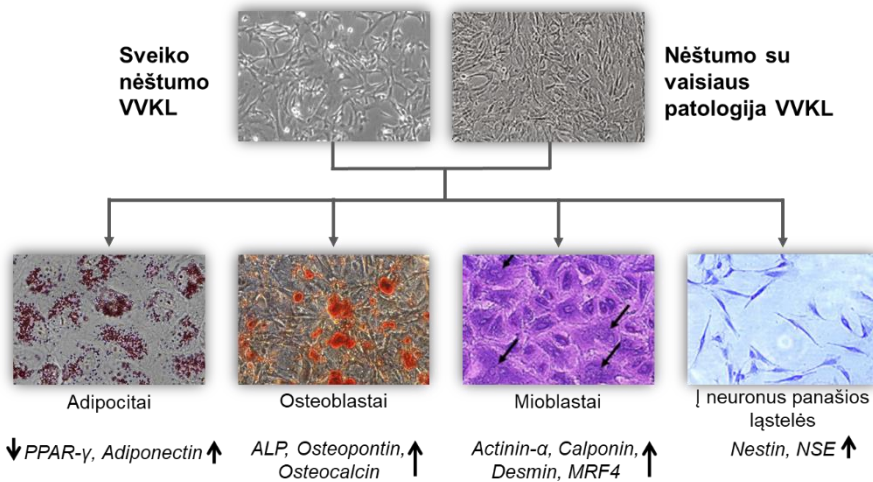
trijų gemalinių lapelių kryptimis, o tuo tarpu žemesniu mitochondrijų membranos potencialu pasižyminčios ląstelės geba diferencijuoti tik mezodermine kryptimi (Schieke ir kt., 2008). Mes nustatėme, kad užląstelinio rūgštėjimo (glikolizės) greitis buvo panašus abejose tirtose VVKL grupėse, nors tokių glikolizės reguliatorių, kurie siejami ir su ląstelių kamieniškumu, kaip LIN28A (Tsogtbaatar ir kt., 2020), OCT4 (Kim ir kt., 2015; Yu ir kt., 2019) ar c-MYC (Cao ir kt., 2015), didesnė genų raiška nustatyta polihidramniono VVKL.

Skelbiama, kad nėštumo laikotarpis neturi didelės įtakos VVKL diferenciacijai tam tikromis kryptimis (Vadasz ir kt., 2014; Moraghebi ir kt., 2017; Spitzhorn ir kt., 2017), tačiau yra tyrimų, kuriuose priešingai nurodoma, jog ankstyvesnių nėštumų VVKL pasižymi kur kas geresniu diferenciacijos potencialu (Shaw ir kt., 2017; Huang ir kt., 2020). Tad būtina išaiškinti ar nėštumo laikotarpis ir galimos vaisiaus patologijos keičia ląstelių savybes bei jų gebėjimą diferencijuoti įvairiomis kryptimis.

## 2.2. Sveikų nėštumų ir nėštumų su vaisiaus patologija VVKL diferenciacijos potencialas riebaline, kauline, raumenine ir nervine kryptimis

### 2.2.1. Diferencijuotų VVKL morfologiniai ir genų raiškos pokyčiai

Vaisiaus vandenų kamieninės ląstelės sulaukia daug susidomėjimo dėl savo plataus diferenciacijos potencialo. Skirtingai nei dauguma somatinių kamieninių ląstelių, VVKL geba diferencijuoti ne tik mezodermos, bet ir ektodermos ir endodermos kryptimis (Perin ir kt., 2008; Loukogeorgakis ir De Coppi, 2017). Doktorantūros metu atliktuose tyrimuose vertinome sveiko nėštumo ir ankstyvo nėštumo su vaisiaus patologija VVKL diferenciacijos riebaline, kauline, raumenine ir nervine kryptimis potencialą. Riebaline ir kauline kryptimis ląstelės buvo indukuotos diferencijuoti 9 dienas (2 publikacija), o raumenine ir nervine – 12 dienų (1 publikacija). Vertinant sveikų nėštumų ir nėštumų su vaisiaus patologija VVKL diferenciacijos metu vykstančius morfologinius pokyčius skirtumai tarp šių grupių nepastebėti, visose diferencijuotose ląstelių kultūrose vyko būdingi morfologiniai pokyčiai bei diferenciacijų metu susidarantys specifiniai dariniai dažėsi atitinkamais dažais (3 pav.).



**3 pav.** Riebalinei, kaulinei, raumeninei ir nervinei diferenciacijoms būdingi morfologiniai pokyčiai ir tirti specifiniai genai. Riebalinė diferenciacija vertinta riebalines vakuoles dažant *Oil Red O* dažu ir tiriant *PPAR-γ* ir *Adiponectin* genų raišką. Kaulinė diferenciacija vertinta pagal *Alizarin Red S* dažu nusidariusius kalcifikatus ir tiriant *ALP*, *Osteopontin* bei *Osteocalcin* genų raišką. Raumeninei ir nervinei diferenciacijai vaizdinti ląstelės dažytos kristalo violeto dažu, raumeninės diferenciacijos metu susidariusios daugianbranduolės ląstelės pažymėtos juodomis rodyklėmis. Tirta raumeninės diferenciacijos genų *Actinin-α*, *Calponin*, *Desmin* ir *MRF4* raiška, nervinė diferenciacija vertinta pagal *Nestin* ir *NSE* genų raišką (pagal 1 ir 2 publikacijas).

Šiame darbe riebaline kryptimi diferencijavusios ląstelės dažėsi specifiniais *Oil Red O* dažais. Parodyta, kad šie dažai yra specifiški viduląsteliniam lipidams (Ramírez-Zacarias ir kt., 1992). Diferenciacijos metu vertinant genų raišką nustatėme sumažėjusią ankstyvosios adipogenezės žymens *PPAR-γ* raišką ir labai išaugusią vėlyvojo adipocitų žymens *Adiponectin* raišką, kuri buvo šiek tiek mažesnė VVKL iš nėštumų su vaisiaus patologija. Tirti genai siejami su adipogenezės iniciacija ir adipocitų brendimu (Tontonoz ir Spiegelman, 1994; Fu ir kt., 2005). Mūsų gauti rezultatai rodo, kad abiejų šaltinių VVKL labiau diferencijavo į brandžius adipocitus (2 publikacija).

Kaulinės diferenciacijos metu vertinome ląstelių mineralizaciją monosluoksnį dažant *Alizarin Red S* dažais. Šis dažymas pasirinktas, kadangi šie dažai specifiskai jungiasi prie kalcio druskų (Puchtler ir kt., 1969). Vertinant genų raišką diferenciacijos metu nustatėme stipriai išaugusią

šarminės fosfatazės *ALP* geno raišką, kiek mažiau išaugusią *Osteocalcin* raišką, kuri sveikų nėštumų VVKL buvo didesnė bei labai nežymiai padidėjusią *Osteopontin* geno raišką. Kadangi diferenciacijos metu stipriau išaugo *ALP* nei *Osteocalcin* raiška, kurie literatūroje žinomi kaip atitinkamai ankstyvųjų bei subrendusių osteoblastų žymenys (Miron ir Zhang, 2012), galime teigti, kad mūsų tyrime diferenciacijos metu VVKL specializavosi iki ankstyvųjų osteoblastų, tačiau pailginus diferenciacijos trukmę, šios ląstelės galimai diferencijuotų ir iki brandesnių osteoblastų (2 publikacija).

Raumeninės diferenciacijos indukcijai naudota terpė, kurios sudėtis pasižymi nedidele arklio serumo koncentracija, terpėje nedaug ląstelių proliferaciją stimuliuojančių veiksnių, tad stabdomas ląstelės ciklas ir skatinama diferenciacija bei ląstelių susilieėjimas (Yaffe ir Saxel, 1977; Franke ir kt., 2014; Saini ir kt., 2018). Diferenciacijos metu stebėjome daugiabranduolių ląstelių formavimąsi kultūroje, o vertinant genų raišką nustatėme, jog stipriausiai išaugo *Actinin- $\alpha$*  raiška, kuri buvo reikšmingai didesnė nėštumų su vaisiaus patologija VVKL, *Calponin* ir *Desmin* raiška reikšmingai nesiskyrė tarp abiejų šaltinių VVKL, o *MRF4* geno didesnę raišką nustatėme sveiko nėštumo VVKL. *Actinin- $\alpha$*  yra siejamas su griaučių raumenų ląstelėmis (Sjöblom ir kt., 2008), *MRF4* genas koduoja veiksnį, dalyvaujantį griaučių raumenų diferenciacijoje kartu su kitais reguliaciniais baltymais (Lazure ir kt., 2020; Zammit, 2017), o *Calponin* ir *Desmin* laikomi lygiųjų raumenų žymenimis (Frid ir kt., 1994). Taigi, naudojant šį diferenciacijos protokolą abiejų šaltinių VVKL labiau specializuojasi griaučių raumenų kryptimi (1 publikacija).

Nervinė diferenciacija indukuota pasitelkiant retinoinę rūgštį, kuri, kaip žinoma, dalyvauja ankstyvoje neurogenezėje bei ląstelių nervinėje diferenciacijoje (Yu ir kt., 2012; Janesick ir kt., 2015). Diferenciacijos metu keitėsi ląstelių morfologija, ląstelės įgavo pailgesnę formą, formavosi į neuritus panašios ląstelių atšakos. Ištyrus nervinei diferenciacijai būdingų genų raišką, kuri vertinta 5-ąją ir 12-ąją diferenciacijos dieną, nustatėme, kad *Nestin* raiška 5-ąją diferenciacijos dieną reikšmingai išaugo nėštumų su vaisiaus patologija VVKL ir susilygino su sveikų nėštumų VVKL 12-ąją diferenciacijos dieną. *NSE* geno raiška diferenciacijos metu išaugo palaipsniui, 5-ąją diferenciacijos dieną šio geno raiška buvo panaši abiejų šaltinių VVKL, o 12-ąją diferenciacijos dieną *NSE* raiška buvo stipriau išreikšta nėštumų su vaisiaus patologija VVKL. *Nestin* yra žinomas kaip nervinių kamieninių ląstelių žymuo (Bernal ir Arranz, 2018), o *NSE* laikomas neuronų ir neuroendokrinių ląstelių žymeniu (Haque ir kt., 2018). Šiame darbe stipriau išaugusi *Nestin* raiška parodė, jog diferenciacijos metu abiejų

šaltinių VVKL kultūroje labiau dominavo nervinės progenitorinės ląstelės (1 publikacija).

Indukavus VVKL diferenciaciją, ląstelės specializavosi atitinkamų linijų kryptimis, diferenciacijos metu keitėsi ląstelių morfologija, išryškėjo linijoms būdingi bruožai, taip pat suaktyvinta specifinių riebalinių, kaulinių, raumeninių ir nervinių genų raiška.

### 2.2.2. Epigenetiniai pokyčiai VVKL diferenciacijos metu

Diferenciacijos metu vykstančius fenotipinius ir funkcinius kamieninių ląstelių virsmus lemia pasikeitusi genų raiška. Šiuos genų raiškos profilio pokyčius reguliuoja epigenetiniai veiksniai, apimantys trumpas nekoduojančias RNR sekas (mikro RNR), chromatiną modifikuojančius baltymus (PRC1 ir PRC2 kompleksai), histonų modifikacijas bei DNR metilinimą. Šiame darbe tyrėme VVKL riebalinės, kaulinės, raumeninės ir nervinės diferenciacijos epigenetinę reguliaciją, taip pat siekėme palyginti šios reguliacijos profilius sveikų nėštumų ir nėštumų su vaisiaus patologija VVKL (1 lentelė).

Šiame darbe tyrinėjome mikro RNR (miR) raiškos pokyčius VVKL diferenciacijų metu. miR – tai trumpos 20-25 nukleotidų ilgio nekoduojančios RNR sekos, kurios reguliuoja genų raišką potranskripciniame lygyje, taip miR reguliuoja ląstelių proliferacijos, diferenciacijos, senėjimo ir kitus procesus. Taip pat miR reguliuoja ir epigenetinėje reguliacijoje dalyvaujančių baltymų, tokių kaip DNR (de)metilazės, histonų (de)acetilazės ir (de)metilazės, Polikombo komplekso baltymai, raišką (Sato ir kt., 2011). Viena iš mūsų pasirinktų miR sekų miR-17 skatina ląstelių proliferaciją ir palaiko jų kamieniškumą bei blokuoja diferenciaciją, taip pat parodyta, jog ši miR tiesiogiai slopina ALP aktyvumą ir mineralizaciją (Li ir kt., 2011; Kang ir Hata, 2015). Mūsų tyrimuose visų indukuotų diferenciacijų metu miR-17 raiška reikšmingai sumažėjo (1 ir 2 publikacijos), taip pat nustatėme, jog kaulinės bei nervinės diferenciacijos metu miR-17 raiška labiau sumažėjo sveikų nėštumų nei nėštumų su vaisiaus patologija VVKL. Žinoma, kad miR-21 funkcionuoja kaip kaulinės diferenciacijos jungtukas (Kang ir Hata, 2015; Sun ir kt, 2015), tą parodė ir mūsų tyrimuose nustatyta reikšmingai padidėjusi miR-21 raiška kaulinės diferenciacijos metu ir stipresnis raiškos padidėjimas pastebėtas sveikų nėštumų VVKL (2 publikacija), raumeninės ir nervinės diferenciacijos metu miR-21 raiška išliko beveik nepakitusi, o riebalinės diferenciacijos metu reikšmingai sumažėjo. Taip pat nustatėme, kad miR-34a ir miR-146a raiškos profiliai tirtų diferenciacijų metu buvo panašūs, kuomet

jų raiška riebalinės ir kaulinės diferenciacijos metu reikšmingai sumažėjo (2 publikacija), o raumeninės ir nervinės diferenciacijos metu šių miR raiška reikšmingai padidėjo (1 publikacija), taip pat nustatėme, jog šių miR raiška stipriau padidėja nėštumų su vaisiaus patologija VVKL mėginiuose, tik ne toks ryškus skirtumas pastebėtas tiriant miR-146 raišką nervinės diferenciacijos metu. Kitų mokslininkų darbuose nustatyta, kad miR-34a ir miR-146a funkcionuoja kaip kaulinės diferenciacijos slopikliai (Chen ir kt., 2014; Huszar ir Payne, 2014), tačiau šios miR nervinėje diferenciacijoje ir neuritų formavimesi vaidina labai svarbų vaidmenį (Aranha ir kt., 2011; Nguyen ir kt., 2018).

**1 lentelė.** Epigenetinė reguliacijoje dalyvaujančių veiksnių pokyčiai VVKL diferenciacijos įvairiomis kryptimis metu (pagal 1 ir 2 publikacijas).

Epigenetinis veiksnys		Diferenciacija			
		Riebalinė	Kaulinė	Raumeninė	Nervinė
Mikro RNR	miR-17	↓	↓	↓	↓
	miR-21	↓	↑	~	~
	miR-34a	↓	↓	↑	↑
	miR146a	↓	↓	↑	↑
Atviro chromatino modifikacijos ir baltymai	H4hiperAc	↓	↓	↓	↓
	H3K9ac	↓	↓	↓	↓
	H3K4me3	↓	↓	↓	↓
	HDAC1	↓	↓	↓	↓
Uždaro chromatino modifikacijos	H3K9me3	↓	~	↓	↓
	H3K27me3	↑	↑	↑	↑
PRC1	BMI1	↓	↓	↓	↓
PRC2	SUZ12	↓	↓	↓	↓
	EZH2	↓	↓	↓	↓
DNR metilinimas	DNMT1	↓	↓	↓	↓
	<i>DNMT3a</i>	netirta	netirta	↑	↑
	<i>DNMT3b</i>	netirta	netirta	↑	↑

Diferencijuojant kamieninėms ląstelėms aktyvuojama specifinių linijai genų raiška ir slopinama kamieniškumą palaikančių genų raiška, tokį genų raiškos persitvarkymą reguliuoja chromatina modifikuojantys baltymai, histonų modifikacijos, DNR metilinimas. Riebalinės ir kaulinės diferenciacijos metu vykstantys epigenetinių veiksnių raiškos pokyčiai vertinti 9-ąją diferenciacijos dieną (2 publikacija), o raumeninės ir nervinės diferenciacijos metu – 5-ąją ir 12-ąją diferenciacijos dieną (1 publikacija), ištyrus visų tirtų baltymų lygius ir jų modifikacijas reikšmingų skirtumų tarp



sveikų nėštumų ir nėštumų su vaisiaus patologija VVKL nenustatėme, tačiau pastebėjome, jog šių veiksmų raiška nežymiai keitėsi diferenciacijų metu.

Genų transkripcinį aktyvumą lemia chromatino konformacija, kuri gali būti atvira (euchromatinas) arba uždara (heterochromatinas), o tai lemia histonų modifikacijos, kurios taip pat skirstomos į aktyvinančias ir slopinančias. Tyrimų metu nustatėme, jog visų tirtų diferenciacijų metu aktyvių histonų modifikacijų H4hiperAc, H3K9ac ir H3K4me3 lygis buvo reikšmingai sumažėjęs, sumažėjo ir heterochromatino modifikacijos H3K9me3 raiška (tik kaulinės diferenciacijos metu šis sumažėjimas nežymus), tačiau padidėjo slopinančios H3K27me3 modifikacijos kiekis (1 ir 2 publikacijos). Taip pat nustatėme, jog raumeninės ir nervinės diferenciacijų metu histonų modifikacijų raiškos mažėjimas vyksta palaipsniui, tik H3K27me3 raiška ankstyvosios diferenciacijos metu sumažėja, o vėlyvuojau diferenciacijos laikotarpiu padidėja. Literatūroje skelbiama, kad pilnai diferencijavusiuose adipocituose H3K4me3 kiekis adipocitinių genų promotoriuose labai žemas (Musri ir kt. 2006), tačiau taip pat yra duomenų, jog riebalinės diferenciacijos metu specifinių genų raiškos aktyvacija siejama su H3K27 demetilinimu bei padidėjusiu H3K9 acetiliniu (Noer ir kt., 2009). Kaulinės diferenciacijos metu vyksta visuminis H3K9ac kiekio sumažėjimas bei H3K9me2 padidėjimas ir nepakitęs bivalentinių modifikacijų H3K4me3/H3K27me3 kiekis, o specifinių „osteo“ genų raiškos aktyvinimas siejamas su H3K9 acetiliniu, bet nepakitusiu H3K9me2 kiekiu (Tan ir kt., 2009; Håkeliën ir kt., 2014). Tačiau mūsų tyrimų metu gauti rezultatai parodė kitokią tendenciją, kuomet visuminis H3K4me3 kiekis sumažėja, o H3K27me3 padidėja (2 publikacija). Raumenų ląstelių specializacijos metu genų raiškos aktyvacija siejama su H3K9 demetilinimu bei H3K27 hipometilinimu (Sincennes ir kt., 2016). Mūsų gauti duomenys rodo, jog VVKL raumeninės diferenciacijos metu vyksta H3K9me3 kiekio sumažėjimas, tačiau H3K27me3 lygis sumažėja 5-ąją diferenciacijos dieną, o 12-ąją dieną stebimas padidėjimas (1 publikacija). Nervinėse kamieninėse ląstelėse tolimesnei diferenciacijai reikalingų genų promotoriai pasižymi bivalentinėmis modifikacijomis (H3K4me3 ir H3K27me3), ląstelėms pradėjus diferencijuoti nespecifinių genų promotoriai slopinami H3K27me3, o specifinių genų promotoriai pasižymi aktyvinančia H3K4me3 modifikacija arba išlieka bivalentiniai (Burney ir kt., 2013).

Nustatėme, kad VVKL diferenciacijų metu Polikombo slopinančio komplekso 1 (angl. *Polycomb repressive complex 1*, *PRC1*) baltymo BMI1 bei Polikombo slopinančio komplekso 2 (angl. *Polycomb repressive complex 2*, *PRC2*) baltymų SUZ12 ir EZH2 (1 ir 2 publikacijos) kiekis reikšmingai

sumažėjo. Žinoma, kad PRC2, kurį sudaro EZH2 (histonų metiltransferazė) ir SUZ12 (palaiko EZH2 veikimą), diferenciacijos metu inicijuoja su kamieniškumu ir proliferacija susijusių baltymų raiškos slopinimą kartu su PRC1 ir BMI1, kurie palaiko uždara chromatiną būseną (Richly ir kt., 2011). Mūsų gauti rezultatai atitinka ir kitų mokslininkų paskelbtus duomenis, rodančius, jog kaulinės diferenciacija gali būti siejama su sumažėjusiu PRC1/2 baltymų kiekiu (Wei ir kt., 2011), o riebalinės diferenciacijos metu BMI1 komplekso sumažėjimas nustatytas kaulų čiulpų kamieninių ląstelių diferenciacijos metu (Hu ir kt., 2019). Taip pat skelbiama, kad Polikombo kompleksų baltymai dalyvauja ir raumeninėje bei nervinėje diferenciacijose, EZH2 ir BMI1 reguluoja raumeninių genų raišką (Caretti ir kt., 2004; Asp ir kt., 2011) ir valdo neurogenezės procesus (Corley ir Kroll, 2015; Shan ir kt., 2017) įvairiuose organizmo vystymosi etapuose.

Epigenetinėje genų raiškos reguliacijoje taip pat dalyvauja tokie fermentai kaip histonų deacetilazės (HDAC) ir DNMT metiltransferazės (DNMT). Mes ištyrėme HDAC1 ir DNMT1 baltymų kiekio bei DNMT3a ir DNMT3b genų raiškos pokyčius. Šiame darbe nustatėme, kad visų diferenciacijų metu HDAC1 bei DNMT1 kiekiai reikšmingai mažėja (1 ir 2 publikacijos). Kaip ir mūsų gauti rezultatai, literatūroje yra duomenų, jog riebalinės ir kaulinės diferenciacijos metu HDAC1 kiekis sumažėja (Yoo ir kt., 2006; Lee ir kt., 2006). Tokia pati tendencija pastebima ir raumeninės bei nervinės diferenciacijos metu, kuomet specifinių genų raiškos aktyvacija yra siejama su DNMT1 ir HDAC1 sumažėjimu (Laker and Ryall, 2016; Jang ir kt., 2018). Tirdami *de novo* metiltransferazių DNMT3a ir DNMT3b genų raišką raumeninės ir nervinės diferenciacijos metu nustatėme tam tikrus raiškos skirtumus sveikų nėštumų ir nėštumų su vaisiaus patologija VVKL. Raumeninės diferenciacijos metu abiejų tirtų metiltransferazių genų raiška palaipsniui didėjo ir stipresnis raiškos didėjimas nustatytas nėštumų su vaisiaus patologija VVKL. Nervinės diferenciacijos metu taip pat nustatyta reikšmingai didėjanti DNMT3b raiška, tik intensyvesnis padidėjimas nustatytas sveikų nėštumų VVKL, o DNMT3a raiška diferenciacijos pradžioje buvo labiau išaugusi nei diferenciacijos pabaigoje ir stipresnis raiškos didėjimas nustatytas nėštumų su vaisiaus patologija VVKL (1 publikacija). Literatūroje žinoma, kad tiek DNMT3a, tiek DNMT3b atlieka labai svarbų vaidmenį raumeninės ir nervinės ląstelių diferenciacijos metu reguliuojant ir įtvirtinant genų raiškos profilius (Watanabe ir kt., 2006; Hatazawa ir kt., 2018).

Ištyrus epigenetinius pokyčius riebalinės, kaulinės, raumeninės ir nervinės diferenciacijos metu sveiko nėštumo ir nėštumo su vaisiaus patologija VVKL,

galime teigti, jog epigenetinė diferenciacijų reguliacija vyksta vienodai abiejų šaltinių VVKL. Visuotinis chromatinio persitvarkymas, histonų modifikacijų pokyčiai vyksta universaliai visų diferenciacijų metu, o mikro RNR raiška pasižymi tam tikru specifiškumu diferenciacijoms.

### 2.3. Sveikų ir polihidramniono nėštumų VVKL nervinė diferenciacija

Tolimesniuose doktorantūros metu atliktuose tyrimuose pasirinkome plačiau panagrinėti trečiojo nėštumo trimestro (32 savaitė) nėštumų su vaisiaus patologija VVKL, tokios ląstelės tyrimams išskirtos iš polihidramniono nėštumų VV. Kaip jau minėta 2.1 skyriuje, polihidramniono nėštumų VVKL pasižymėjo aktyviu oksidaciniu fosforiliniu bei žemu mitochondrijų membranos potencialu, o tokios ląstelių charakteristikos gali būti siejamos su prastesniu diferenciacijos potencialu trimis gemalinių lapelių kryptimis (Schieke ir kt., 2008; Tsogtbaatar ir kt., 2020). Todėl tolesni tyrimai buvo atliekami lyginant sveikų ir polihidramniono nėštumų VVKL diferenciacijos potencialą nervine (ektodermos) kryptimi.

#### 2.3.1. Ląstelių morfologiniai pokyčiai diferenciacijos metu

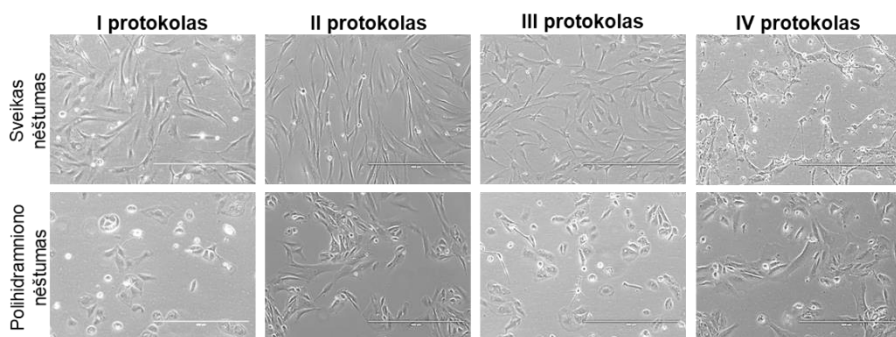
Abiejų šaltinių VVKL buvo indukuotos diferencijuoti nervine kryptimi keturiais skirtingais protokolais, į kurių sudėtį įeina įvairios su neurogeneze siejamos signalinės molekulės – 8-Bromadenozino 3',5'-ciklinis adenozino monofosfatas (8-Br-cAMP), 3-izobutil-metilksantinas (IBMX), kalio chloridas (KCl) ir retinoinė rūgštis (RA) bei trofiniai veiksniai – smegenų neurotrofinis veiksnys (BDNF) ir nervų augimo veiksnys (NGF) (2 lentelė). VVKL diferenciacija vykdyta 3 dienas.

**2 lentelė.** Nervinės diferenciacijos indukcijai naudotos medžiagos ir jų funkcijos (pagal 4 publikaciją).

Protokolas	Induktorius	Funkcija
I ir III	cAMP	Signalinė molekulė, kuri per baltymų kinazę A aktyvuoja nervinių genų raišką, stimuliuoja neuritų susidarymą (Zhang ir kt., 2011).
I ir III	IBMX	Fosfodiesterazių slopiklis, apsaugantis cAMP nuo degradavimo (Shahbazi ir kt., 2016).
II ir III	BDNF	Neurotrofinas, dalyvaujantis nervinėje diferenciacijoje per MAPK, PLC ir PI3K signalinius kelius (Lim ir kt., 2008).
II ir III	NGF	Neurotrofinas, dalyvaujantis nervinėje diferenciacijoje per MAPK, PLC ir PI3K signalinius kelius (Martorana ir kt., 2018).

2 lentelės tęsinys		
Protokolas	Induktorius	Funkcija
I, II ir III	KCl	Skatina membranos depoliarizaciją (Rienecker ir kt., 2020).
I, II, III ir IV	RA	Dalyvauja ankstyvoje neurogenezėje ir nervinėje diferenciacijoje, stabdo proliferaciją, aktyvuoja specifinių genų raišką (Janesick ir kt., 2015).
IV	N2 priedas	Komercinis priedas, skirtas nervinės diferenciacijos indukcijai.

Indukavus diferenciaciją įvertinome ląstelių morfologinius pokyčius ir pastebėjome, kad sveikų nėštumų VVKL nervinėms ląstelėms būdingi požymiai buvo ryškesni nei polihidramniono nėštumo VVKL (4 pav). Šiuos ląstelių virsmus įvertinome ir kiekybiškai matuodami susidariusių neuritų ilgi ir neuritus formuojančių ląstelių dažnį diferencijuotoje kultūroje. Nustatėme, jog ilgiausius neuritus formavo sveiko nėštumo VVKL indukuotos I-ojo protokolo (8-Br-cAMP, IBMX, KCl, RA) diferenciacijos terpe (mediana 78,695  $\mu\text{m}$ ), o didžiausias diferenciacijai būdinga morfologija pasižyminčių ląstelių dažnis nustatytas III-ojo protokolo (8-Br-cAMP, IBMX, BDNF, NGF, KCl, RA) terpe indukuotų sveikų nėštumų VVKL diferencijuotoje kultūroje (0,95/1) (4 publikacija).



**4 pav.** Sveikų ir polihidramniono nėštumų VVKL morfologija nervinės diferenciacijos metu. VVKL indukuotos diferencijuoti naudojant skirtingų medžiagų kombinacijas – I protokolas: cAMP, IBMX, RA, KCl; II protokolas: BDNF, NGF, RA, KCl; III protokolas: cAMP, IBMX, BDNF, NGF, RA, KCl; IV protokolas: N2 priedas, RA. Mastelis – 400  $\mu\text{m}$  (pagal 4 publikaciją).

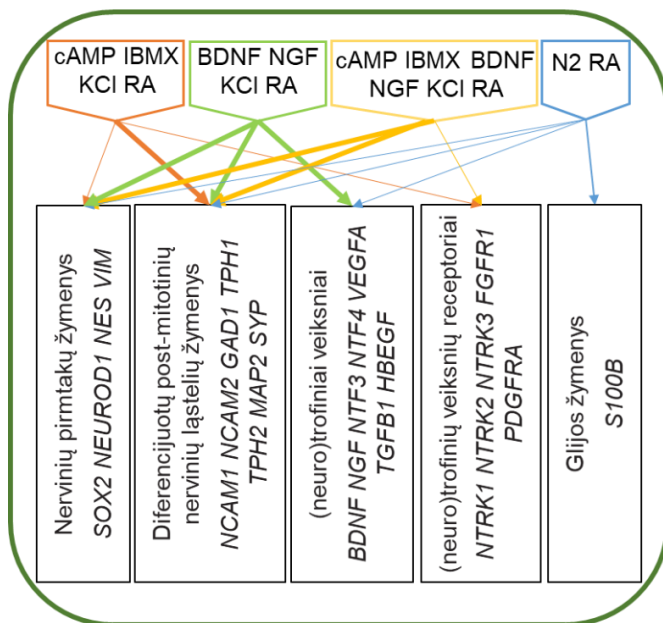
Ląstelių indukuotos diferenciacijos metu pastebėjome, kad indukavus abiejų šaltinių VVKL III-ojo protokolo induktorių kombinacija, morfologiniai pokyčiai įvyksta labai greitai. Po indukcijos pradžios praėjus tik 3-ims valandoms ląstelių kultūroje buvo galima matyti nervinių ląstelių morfologija pasižyminčias VVKL. Šiuos pokyčius vizualizavome pasitelkiant

imunofluorescencinę mikroskopiją ir nustatėme ryškų citoskeleto baltymų, tokių kaip  $\beta$ -tubulinas III, vimentinas, F-aktinas, persitvarkymą ir nervinio žymens NCAM1 persiskirstymą ląstelėse (4 publikacija).

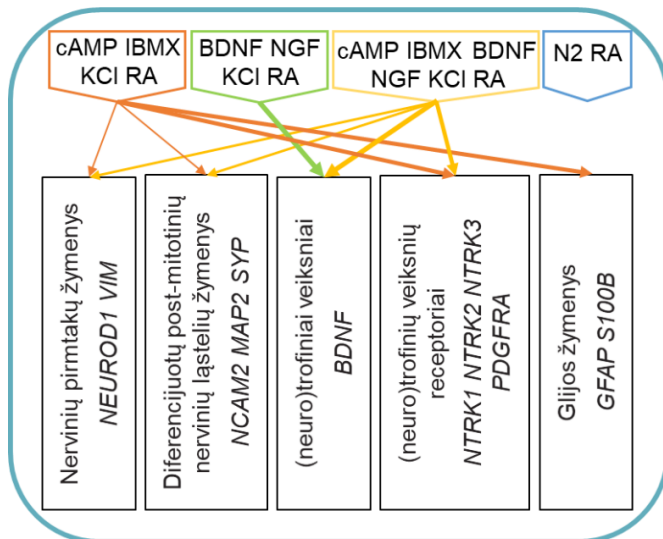
### 2.3.2. Genų raiškos pokyčiai diferenciacijos metu

Nors polihidramniono nėštumo VVKL morfologiniai pokyčiai nervinės diferenciacijos metu nebuvo ryškūs, atlikome specifinių genų raiškos tyrimus indukuojant diferenciaciją visų keturių protokolų terpėmis. Ištyrus nervinių pirmtakų žymenų (*SOX2*, *NES*, *NEUROD1* ir *VIM*), diferencijuotų postmitotinių nervinių ląstelių žymenų (*NSE*, *NCAM1*, *NCAM2*, *GAD1*, *TPH1*, *TPH2*, *MAP2* ir *SYP*), glijos žymenų (*GFAP* ir *S100B*), (neuro)trofinių veiksnių (*BDNF*, *NGF*, *NTF3*, *NTF4*, *VEGFA*, *TGFB1*, *HBEGF*) ir jų receptorių (*NTRK1*, *NTRK2*, *NTRK3*, *FGFR1* ir *PDGFRA*) genų raišką, nustatėme, jog sveiko nėštumo VVKL specifinių nervinei diferenciacijai genų raiška aktyvuota intensyviau, išskyrus glijos žymenis (*GFAP* ir *S100B*), kurių didesnė raiška nustatyta polihidramniono VVKL (4 publikacija) (5 pav.). Visomis diferenciacijos indukcijos sąlygomis ypatingai stipriai aktyvuota *NEUROD1* geno, koduojančio transkripcijos veiksnių aktyvuojantį neurogenezės programą ląstelėse (Pataskar ir kt., 2016), raiška. Taip pat stipriai aktyvuota ir diferenciaciją stimuliuojančio veiksnio *NCAM1* (Shin ir kt., 2002) geno raiška, kurią galimai aktyvavo *NEUROD1*, kadangi *NCAM1* yra tiesioginis šio transkripcijos veiksnio taikinytis (Osborne ir kt., 2013). Susumavus duomenis įvertinome, jog II-ojo protokolo induktorių kombinacija, į kurios sudėtį įeina *BDNF*, *NGF*, *KCl* ir *RA*, geriausiai inicijavo VVKL specializacijos nervine kryptimi programą. Papildomai ištyrėme šio protokolo terpe indukuotų ląstelių jonų kanalų *HCN2* ir *KCNJ2* genų raišką, kuri sveikų nėštumų VVKL išaugo smarkiau (4 publikacija).

## Sveiko nėštumo VVKL



## Polihidramniono nėštumo VVKL



**5 pav.** Sveikų ir polihidramniono nėštumų VVKL genų raiškos aktyvacija ląsteles indukuojant diferencijuoti nervine kryptimi bei naudojant skirtingas induktorių kombinacijas. Tirta nervinių pirmtakų žymenų, diferencijuotų post-mitotinių nervinių ląstelių žymenų, glijos žymenų, (neuro)trofinių veiksmių ir jų receptorių genų raiška. Paryškintos rodyklės nurodo stipriau aktyvuotą genų raišką atitinkamoje tirtų genų grupėje (pagal 4 publikaciją).

Nors charakteringus morfologinius pokyčius intensyviau inicijavo cAMP, IBMX, BDNF, NGF, KCl ir RA induktorių kombinacija (III-as protokolai), geresni genų raiškos rezultatai nustatyti naudojant tik BDNF, NGF, KCl ir RA (II-as protokolai). Pasitelkiant panašios sudėties diferenciacijos terpę (dbcAMP, IBMX, EGF, bFGF, NGF, BDNF) Bonaventura ir kolegos pademonstravo, jog iš visų tirtų kamieninių ląstelių šaltinių (kaulų čiulpai, virkštelės kraujas, endometriumas, vaisiaus vandenys), VVKL pasižymėjo geriausiu diferenciacijos nervine kryptimi potencialu, kuris buvo patvirtintas ir funkciškai (Bonaventura ir kt., 2015). Kadangi II-ojo protokolo kombinacija geriausiai inicijavo nervinių genų, ypač neurotrofinių veiksnių, raišką, pasirinkome šį protokolą tolimesniems tyrimams viduląstelių ir sekretuojamų baltymų lygyje.

### 2.3.3. Baltymų raiškos pokyčiai diferenciacijos metu

Baltyminiame lygyje tyrėme viduląstelių baltymų (tarpinis filamentas Nestin, kamieninių ląstelių ir nervinių progenitorių transkripcijos veiksnys Musashi1 ir transkripcijos veiksnys LIN28a) bei sekretuojamų baltymų (neurotrofinis veiksnys BDNF bei trofinis veiksnys VEGF) kiekių pokyčius sveikų ir polihidramniono mėginių VVKL diferenciacijos metu naudojant II-ojo protokolo induktorių kombinaciją (BDNF, NGF, KCl, RA). Nustatėme, jog diferenciacijos metu šių baltymų kiekis reikšmingai didėja ir vertinant nuo nediferencijuotos kontrolės baltymų kiekio padidėjimas didesnis sveikų nėštumų VVKL, tačiau verta paminėti, jog neveiktose polihidramniono nėštumų VVKL nustatytas tirtų baltymų kiekis buvo didesnis nei nediferencijuotose sveikų nėštumų VVKL (4 publikacija). Nors mūsų eksperimentuose po diferenciacijos tirtų trofinių molekulių sekrecija padidėja, Castelli ir kolegos parodė, jog net ir nediferencijuotų VVKL sekretomas per BDNF signalinius kelius aktyvuoja ląstelių išgyvenamumo ir slopina apoptozę skatinančio signalo perdavimą išemijos/reperfuzijos SH-SY5Y ląstelių modelyje (Castelli ir kt. 2020).

Taip pat vertinome sekretuojamų citokinų IL-1 $\beta$ , IL-6 ir IL-10 kiekių pokyčius ir nustatėme, jog abiejų šaltinių VVKL nepasižymi uždegimą skatinančio citokino IL-1 $\beta$  ir priešuždegiminio citokino IL-10 sekrecija, tačiau pasižymi uždegimą skatinančio citokino IL-6 sekrecija, kuri diferenciacijos metu sveikų nėštumų VVKL sumažėjo, o polihidramniono VVKL suintensyvėjo, nors šie skirtumai nereikšmingi (4 publikacija). IL-6 žinomas kaip vienas iš pagrindinių imuninio ir uždegiminio atsako dalyvių, tačiau

duomenys rodo, jog šis citokinas skatina nervinių kamieninių ląstelių diferenciaciją glijos ląstelių kryptimi (Islam ir kt., 2009).

Tyrimų metu nustatėme, kad tik polihidramniono VVKL pasižymi uždegimą skatinančio citokino TNF $\alpha$  sekrecija, kuri diferenciacijos metu reikšmingai sumažėja. Taip pat nustatėme, jog citokiną koduojančio *TNFA* geno raiška neveiktose VVKL reikšmingai didesnė nei polihidramniono mėginiuose, o receptorinio geno *TNFR1* raiška diferenciacijos metu stipriau išaugo sveikų nėštumų VVKL (4 publikacija). TNF $\alpha$  sekrecija polihidramniono mėginiuose galėtų būti siejama su reikšmingai didesne *c-MYC* geno raiška, kadangi žinoma, jog *c-MYC* skatina TNF $\alpha$  raišką (Liu ir kt., 2015). Taip pat žinoma, jog TNF $\alpha$  skatina ROS gamybą (Kastl ir kt., 2014), o CD13 (aminopeptidazė N) slopina ROS produkciją vėžinėse ląstelėse (Kim ir kt., 2012). Tai patvirtina ir mūsų tyrimuose gautus duomenis, parodančius reikšmingai intensyvesnę ROS generaciją bei mažesnę CD13 raišką polihidramniono VVKL lyginant su sveikų nėštumų VVKL. Tokios polihidramniono VVKL ypatybės galėtų būti paaiškintos visumine uždegimine nėštumo būseną, kadangi viena iš polihidramniono gydymo ar bent komplikacijų išvengimo strategijų yra nesteroidinių priešuždegiminių vaistų vartojimas nėštumo metu (Hamza ir kt., 2013).

Tyrimais parodėme, kad nervine kryptimi indukuotos diferencijuoti sveikų ir polihidramniono nėštumų VVKL skiriasi morfologiniais pokyčiais ir genų raiškos aktyvumu, tačiau yra panašios baltymų raiška ir trofinių molekulių sekrecija. Bet verta pastebėti, jog tik polihidramniono mėginių VVKL pasižymėjo uždegimą skatinančio veiksnio TNF $\alpha$  sekrecija, tad svarbu tirti kaip pagerinti tokių ląstelių savybes, kad šio šaltinio kamieninės ląstelės galėtų būti efektyviai pritaikomos regeneracinės medicinos tikslais.

#### 2.4. Mažųjų molekulių poveikių įtaka VVKL savybėms ir nervinės diferenciacijos potencialui

Epigenetiškai aktyvios medžiagos, dar vadinamos mažosiomis molekulėmis, geba aktyvuoti įvairias ląstelių programas, tarp jų ir diferenciaciją ar dediferenciaciją. Tad nusprendėme ištirti, kokį poveikį mažosios molekulės turi sveikų nėštumų VVKL kamieniškumo savybėms. Šiame darbe tyrėme HDAC slopiklius TSA ir NaBut, kurios, kaip anksčiau nustatyta, skatina somatinių ląstelių pluripotentškumo indukciją (Mali ir kt., 2010; Kretsovali ir kt., 2012). Taip pat naudojome įvairiafunkcines biomolekules VitC ir RA. VitC veikdamas kaip TET baltymų ir histonų demetilazių kofaktorius pagerina ląstelių pluripotentškumo indukcijos



efektyvumą (Esteban ir kt., 2010; Wang ir kt., 2011). Taip pat parodyta, kad VitC stimuliuoja kamieninių ląstelių pluripotentiškumo indukciją ir proliferaciją slopinant p53/p21 (Esteban ir kt., 2010; Zhang ir kt., 2016). RA veikimas priklauso nuo naudojamos koncentracijos – nedidelė RA koncentracija (0,5  $\mu$ M) palaiko kamieninių ląstelių pluripotentiškumo programą, o didesnė koncentracija (1,5 ir 4,5  $\mu$ M) skatina diferenciaciją (De Angelis ir kt., 2018). Taip pat parodyta, kad VitC ir RA kombinacija itin efektyviai „ištrina“ ląstelių epigenetinę atmintį ir skatina pluripotentiškumo indukciją (Hore ir kt., 2016). Nors VVKL savybės turi panašumų su PKL, tačiau jos vis tik laikomos multipotentinėmis, o vienas iš būdų pagerinti VVKL plastiškumą – mažųjų molekulių naudojimas.

#### 2.4.1. Mažųjų molekulių poveikių įtaka VVKL genų ir baltymų raiškai

Patikrinome mažųjų molekulių poveikį sveikų nėštumų VVKL gyvybingumui ir nustėme, kad naudotos medžiagų koncentracijos nėra citotoksiškos nei kaip pavienių molekulių poveikiai, nei kaip jų kombinacijos (A kombinacija: VitC, TSA, RA; B kombinacija: VitC, NaBut, RA) (3 publikacija). Toliau tyrėme sudarytų kombinacijų trumpalaikį (24 – 96 val.) poveikį su kamieniškumu susijusių genų ir baltymų, tokių kaip Oct4, Nanog, Sox2, Lin28a, Notch1 ir c-Myc, raiškai. Genų raiškos lygyje pastebėjome tendenciją, jog *OCT4*, *NANOG*, *SOX2*, *NOTCH1* raiška naudojant A kombinaciją labiau padidėja po 24 val. (lyginant su 96 val.), o naudojant B kombinaciją – po 96 val. (lyginant su 24 val.) poveikio. Baltyminiame šių žymenų lygyje nustatėme, jog Oct4, Nanog ir c-Myc kiekis po poveikių pasikeitė labai nežymiai, o Notch1 kiekis reikšmingai sumažėjo. Transkripciniame lygyje tokią skirtingą genų raiškos aktyvaciją galėjo lemti kombinacijose naudoti skirtingi HDAC slopikliai (TSA ir NaBut), kadangi toks efektas buvo parodytas vėžinėse ląstelėse (Kalle ir Wang, 2019).

Ištyrus paviršinių baltymų raiškos pokyčius po 96 val. poveikio A ir B kombinacijomis, parodėme, kad CD44, CD73, CD105, CD117, CD146, SSEA4 raiška reikšmingai sumažėjo po poveikio su VitC, NaBut ir RA, o VitC, TSA ir RA mažosiomis molekulėmis paveiktose sveiko nėštumo VVKL reikšmingai sumažėjo tik CD105 raiška, o CD117 raiška reikšmingai padidėjo (3 publikacija). CD105 raiškos sumažėjimą galėjo lemti sumažėjęs Notch1 kiekis, kadangi parodyta, jog CD105 yra reguliuojamas per Notch signalinį kelią ir Notch slopinimas lemia sumažėjusią CD105 raišką (Na ir kt., 2015).

## 2.4.2. VVKL metabolizmo pokyčiai poveikių mažosiomis molekulėmis metu

Ląstelės metabolizmas yra reikšmingas epigenetinei reguliacijai ir *vice versa*, tuo pačiu žinoma, kad somatinių ląstelių pluripotentiškumo indukcijos metu metabolizmo persitvarkymas ir glikolitinių genų aktyvacija vyksta anksčiau nei kamieniškumo genų aktyvacija (Folmes ir kt., 2011; Cao ir kt., 2015). Atlikę tyrimus nustatėme, jog mažųjų molekulių kombinacijomis paveiktos sveikų nėštumų VVKL tampa energetiškai aktyvesnės, kadangi po 96 val. poveikio mažųjų molekulių kombinacijomis padidėjo tiek oksidacinio fosforilavimo (OxPhos), tiek glikolizės greitis, taip pat tokias tendencijas pastebėjome OxPhos (*NRF1*, *HIF1a*, *PPARGC1A*) ir glikolitinių (*ERRa*, *PKM*, *PKM*, *PKM*, *LDHA*) genų raiškoje (3 publikacija). Literatūriniai duomenys rodo, kad mažosios molekulės pagerina kamieninių ląstelių savybes per metabolinių kelių reguliaciją (Son ir kt., 2018). Taip pat parodyta, kad ląstelių pluripotentiškumo indukcijos iniciacijos fazei būdingas aktyvus OxPhos ir glikolitinis metabolizmas, fenomenas dar vadinamas kaip trumpalaikis hiper energetiškas metabolizmas (angl. *transient hyper-energetic metabolism*), nustatyta, kad šioje pluripotentiškumo indukcijos fazėje metabolinių genų raiška pasiekia savo piką (Cacchiarelli ir kt., 2015).

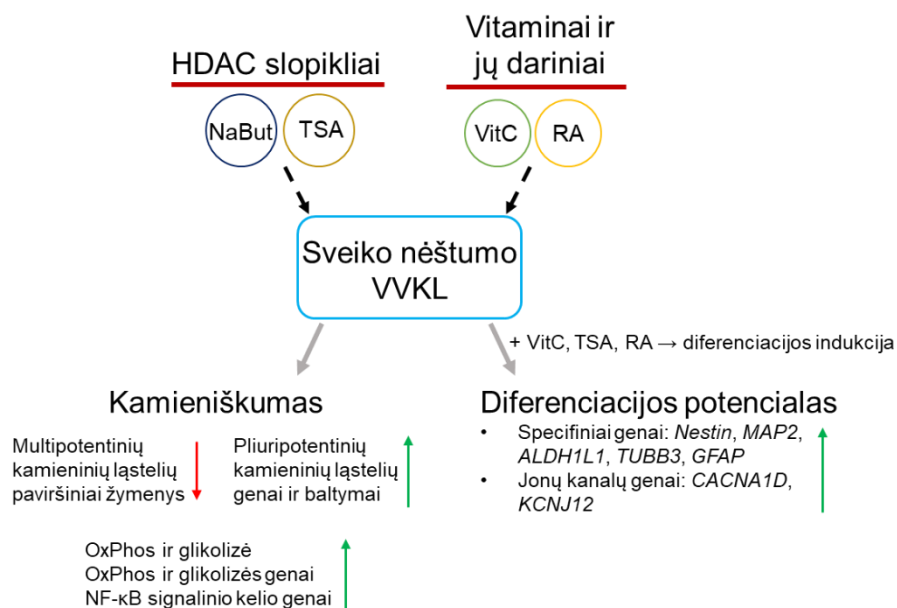
Taip pat tyrinėjome ir NFκB signalinio kelio, susijusio su ląstelių metabolizmu, genų raišką. Nustatėme, kad NFκB signalinio kelio baltymus koduojančių genų *NFKB1*, *NFKB2*, *RELA*, *RELB* ir *REL* raiška reikšmingai padidėja po 96 val. poveikių su mažųjų molekulių kombinacijomis ir stipresnis efektas pastebėtas su A kombinacija (VitC, TSA, RA) (3 publikacija). Kitų mokslininkų darbuose skelbiama, jog RelA (p65) skatina oksidacinį fosforilavimą (Mauro ir kt., 2012), o nuo IKK (NFκB signalinį kelią aktyvuojanti kinazė) ir RelB priklauso mitochondrijų kiekis bei veikla ląstelėse (Bakkar ir kt., 2012). Taip pat parodyta, jog glikolizė stimuliuoja IKK aktyvumą (Kawauchi ir kt., 2008).

Mažųjų molekulių kombinacijomis paveiktos sveikų nėštumų VVKL demonstravo suaktyvėjusį oksidacinį fosforilavimą ir glikolitinį kvėpavimą, su tuo siejama ir padidėjusi genų, siejamų su ląstelių metaboliniais keliais, raiška (6 pav.). VVKL virsmas energetiškai aktyvesnėmis ląstelėmis galėtų būti tapatinamas su ankstyvai ląstelių pluripotentiškumo indukcijos stadijai būdingais pokyčiais.

### 2.4.3. Mažųjų molekulių poveikių įtaka VVKL nervinės diferenciacijos potencialui

Sveikų nėštumų VVKL buvo indukuotos diferencijuoti nervine kryptimi naudojant komercinius priedus N2 ir B27 bei biomolekulę RA, nervinių genų raiška buvo tirta ankstyvuju (7-a diena) ir vėlyvuju (15-a diena), o jonų kanalų genų raiška tirta tik vėlyvuju diferenciacijos laikotarpiu. Taip pat įtraukėme ir trumpą (24 val.) pirminės indukcijos žingsnį su mažųjų molekulių kombinacija A (VitC, TSA, RA), kadangi genų raiškos tyrimuose parodėme *SOX2* ir *NOTCH1* genų raiškos padidėjimą po 24 val. poveikio su šia medžiagų kombinacija. *SOX2* žinomas kaip vienas pagrindinių transkripcijos veiksnių, dalyvaujančių neuroektodermos vystymesi (Sarlak ir Vincent, 2016), o *Notch1* yra svarbus neurogenezės programos signalo perdavimo dalyvis (Lathia ir kt., 2008), tad potencialiai šis pirminės indukcijos žingsnis galėtų pagerinti VVKL diferenciacijos potencialą.

Nervinę diferenciaciją visais naudotais protokolais patvirtinome vertinant ląstelių morfologinius pokyčius bei ištyrus indukuotų VVKL neurotrofinio veiksnio BDNF sekrecijos kiekius. Nustatėme, kad nervinės diferenciacijos metu ląstelės įgauna būdingą formą, vizualizavus ląstelių struktūrinius baltymus  $\beta$ -tubuliną III, vimentiną ir F-aktiną išryškėja pailgėjusi ląstelės forma (3 publikacija). Kaip žinoma, NCAM vaidina labai svarbų vaidmenį neuritų formavimosi procesuose (Kleene ir kt., 2010). Tad mūsų tyrimuose nustatytas NCAM1 kaupimasis ląstelių galuose gali būti siejamas su neuritų formavimusi. Taip pat diferenciacijos metu nustatėme padidėjusią neurotrofinio veiksnio BDNF sekreciją. Mažųjų molekulių kombinacijos poveikis, naudotas kaip pirminės indukcijos žingsnis, atskirais atvejais reikšmingai pagerino astrocitinių ir nervinių genų *Nestin*, *MAP2*, *ALDH1L1*, *TUBB3* ir *GFAP* raišką. Taip pat pagerėjo ir tirtų jonų kanalų genų raiška. Nustatėme, jog mažųjų molekulių poveikis reikšmingai pagerino kalcio jonų kanalo *CACNA1D* bei kalio jonų kanalo *KCNJ12* genų raišką (3 publikacija) (6 pav.).



**6 pav.** Mažųjų molekulių, tokių kaip histonų deacetilazių (HDAC) slopiklių natrio butirato (NaBut) ir trichostatino A (TSA) bei įvairiafunkcinių biomolekulių vitamino C (VitC) ir retinoinės rūgšties (RA), funkcijas ir poveikius sveikų nėštumų VVKL savybėms ir nervinės diferenciacijos potencialui apibendrinanti schema (pagal 3 publikaciją).

Mažųjų molekulių naudojimas norit pagerinti nervinės diferenciacijos efektyvumą gali būti siejamas su signalinių kelių aktyvinimu (Song ir kt., 2018) bei epigenetinės reguliacijos valdymu (Xu ir kt., 2019). Detaliau išaiškinus mažųjų molekulių, jų kombinacijų, koncentracijų ir poveikio trukmės įtaką kamieninių ląstelių savybėms ir diferenciacijos potencialui, būtų suteiktas didžiulia pagreitis platesniam šių ląstelių pritaikymui regeneracinėje medicinoje.

## IŠVADOS

1. Nustatyta, kad antrojo trimestro sveikų nėštumų ir nėštumų su vaisiaus patologija VVKL savybės, kamieniškumo genų bei tirtų mikro RNR raiška nesiskiria. Tuo tarpu trečiojo nėštumo trimestro polihidramniono VVKL skyrėsi nuo sveikų nėštumų VVKL savo morfologija, pasižymėjo didesne *OCT4*, *NOTCH1* ir *MYC* genų raiška, tačiau mažesne paviršinių žymenų CD13, CD73, CD90 ir CD105 raiška. Polihidramniono VVKL būdingas aktyvesnis oksidacinis fosforilinimas, didesnis ATP kiekis, bet mažesnis mitochondrijų membranos potencialas ir reikšmingai didesnė *NRF1* geno raiška, o glikolizės aktyvumas nesiskyrė tarp tirtų VVKL grupių.
2. Įvertinus morfologinius, genų raiškos ir epigenetinės reguliacijos veiksnių raiškos pokyčius nustatyta, kad antrojo nėštumo trimestro sveikų ir nėštumų su vaisiaus patologija VVKL diferencijavo riebaline, kauline, raumenine ir nervine kryptimis su panašiais morfologiniais ir molekuliniais pokyčiais.
3. Parodyta, kad sveikų nėštumų VVKL efektyviau diferencijavo nervine kryptimi nei polihidramniono VVKL. Indukuojant diferenciaciją BDNF, NGF, KCl ir RA medžiagų kombinacija abiejų grupių VVKL padidėja diferenciacijai būdingų viduląstelių ir sekretuojamų baltymų kiekis (Nestin, Musashi1, LIN28a, BDNF, VEGF), o uždegimą skatinančio citokino TNF $\alpha$  sekrecija, kuri sveiko nėštumo VVKL išvis nenustatyta, polihidramniono mėginiuose sumažėja.
4. Nustatyta, jog mažųjų molekulių TSA, NaBut, VitC ir RA kombinacijų poveikiai darė įtaką Oct4, Nanog, Sox2, Lin28a, Notch1 ir c-Myc genų bei baltymų raiškai sveikų nėštumų VVKL, o ląstelės tapo energetiškai aktyvesnės. Nervinės diferenciacijos efektyvumas išaugo naudojant 24 valandų TSA, VitC ir RA poveikį.

## SUMMARY

Alternative sources of potent stem cells are of great interest and human amniotic fluid could be an attractive option. Potentially amniotic fluid stem cells (AFSCs) could be used to treat various congenital anomalies prenatally or neonatally (Di Bernardo et al., 2014; Abe et al., 2019; Shaw et al., 2021), also autoimmune, heart, neurological and other disorders (Gatti et al., 2020; Yang et al., 2021; Fang et al., 2021). Nowadays congenital anomalies could be diagnosed quite early into pregnancy, however, some disorders could develop in later weeks of gestation. One of which is polyhydramnion – a medical condition describing accumulation and excess of amniotic fluid within the amniotic sac (Allaf et al., 2015). Although the etiology of polyhydramnios is unclear in most cases, the majority is linked to congenital anomalies of the fetus such as gastrointestinal abnormalities, central nervous system defects, anomalies of musculoskeletal and airway systems (Kornacki et al., 2017). Thus, AFSCs could prove to be an excellent stem cell source for therapeutic purposes as well as a great tool to research etiology of congenital disorders.

AFSCs has been described to possess several key characteristics that make them an attractive stem cell source. These cells are capable to differentiate towards lineages of all three germ layers (Perin et al., 2008), they also show a great proliferative capacity, are not immunogenic, do not form teratomas *in vivo* and the isolation of AFSCs carries little to no ethical concerns (Trohatou et al., 2013; Gasiunienė et al., 2020). It was also shown that AFSCs are more superior to stem cells derived from other sources, such as bone marrow, umbilical cord blood, placenta (Yan et al., 2013; Jain et al., 2019). The majority of studies investigating the applicability of AFSCs use stem cells isolated from healthy pregnancies and the collected data could be poorly translational and limit the use of AFSCs in clinical setting, as isolated cells from pregnancies with fetal abnormalities could differ in their differentiation potential, stem cell characteristics and other properties. Therefore, studying AFSCs isolated from gestations concomitant with fetal abnormalities is essential in order to successfully use them for therapeutic purposes.

Epigenetic regulation plays a crucial role in stem cell development and differentiation (Wu and Sun, 2006). Epigenetic mechanisms of AFSC differentiation are not well established and even less is known about this regulation in AFSCs isolated from fetus diseased pregnancies. Epigenetically active compounds also known as small molecules can be used to induce and regulate cellular reprogramming, transdifferentiation, and enhance

differentiation potential (Baranek et al., 2017; Kim et al., 2020). A vast selection of small molecules with different functions is available and the amount of possible combinations are innumerable. Thus, investigating epigenetic regulation of AFSCs from healthy and fetus affected gestations, as well as the effects of small molecules on AFSCs could improve the application prospects of these stem cells.

**The aim of this study:** to study molecular (genetic, epigenetic, protein and energetic) alterations in amniotic fluid stem cells of healthy and fetus affected gestations during adipogenic, osteogenic, myogenic and neurogenic differentiation.

**The main tasks:**

1. To characterize AFSCs of healthy and fetus affected pregnancies in terms of surface marker, pluripotency associated gene, and microRNA expression and metabolic profiles.
2. To determine adipogenic, osteogenic, myogenic and neurogenic differentiation potential of AFSCs from both sources according to morphological and molecular changes.
3. To evaluate neurogenic differentiation potential by inducing differentiation with different combinations of agents and assessing morphological, genetic and protein expression changes in AFSCs of healthy and polyhydramnios gestations.
4. To investigate the effects of small molecule treatments on characteristics and neurogenic differentiation potential of AFSCs.

**Scientific novelty**

In this work we studied amniotic fluid stem cells (AFSCs) isolated from healthy and fetus affected pregnancies. By analyzing and comparing cell characteristics and adipogenic, osteogenic, myogenic, neurogenic differentiation potential we determined the existence of phenotypic differences that become more apparent in fetus affected (polyhydramnios) AFSCs of third trimester of pregnancy. Also, we concluded that AFSCs of polyhydramnios gestations are more energetically active as increased oxidative phosphorylation, higher ATP content and elevated ROS levels were observed. We also indicated, that AFSCs of healthy and fetus affected second trimester pregnancies were capable to differentiate towards adipogenic, osteogenic, myogenic and neurogenic lineage with similar efficiency and epigenetic regulation. We were the first to examine neurogenic differentiation

potential in AFSCs of healthy and polyhydramnios samples by inducing differentiation using different signalling and neurotrophic molecules and demonstrated that inflammatory state of polyhydramnios AFSCs was alleviated during neurogenic differentiation, since significant reduction of TNF $\alpha$  was noticed. Finally, we demonstrated that epigenetically active small molecules affect stemness properties in AFSCs and boost their neurogenic differentiation potential.

The acquired results of this work contribute to existing knowledge regarding AFSCs obtained from healthy and fetus affected pregnancies and their characteristics, as well as multilineage differentiation potential. These results could be valuable for future applications of AFSCs in the field of regenerative medicine treating various disorders and congenital anomalies.

### **Propositions**

- AFSCs of second trimester healthy and third trimester fetus affected gestations are different in their morphological, genetic and surface marker expression, and metabolic profile.
- AFSCs are capable to differentiate towards adipogenic, osteogenic, myogenic and neurogenic lineage possessing uniform epigenetic regulation despite the state of second trimester gestation (healthy or fetus affected).
- AFSCs of second trimester healthy pregnancies differentiate towards neurogenic lineage more efficiently when compared to AFSCs of third trimester polyhydramnios gestations.
- Small molecule treatments improve neurogenic differentiation potential in AFSCs.

In this study AFSCs were isolated from amniotic fluid of healthy (2nd trimester) and fetus affected (2nd and 3rd trimester) pregnancies (publications 1-4). The fetal origin of the cells was confirmed by karyotyping AFSCs from gestations with known male fetus and identifying Y chromosome (publication 3). AFSCs from healthy and fetus affected pregnancies of 2nd trimester shared similar spindle shaped morphology (publications 1-2) while AFSCs from polyhydramnios samples (3rd trimester) were rounder in shape (publication 4). We characterized isolated cells by their surface marker expression and found that all AFSCs were negative for hematopoietic and endothelial markers (CD9, CD15, CD31, CD34, CD133, CD309), but were positive for several stem cell surface markers (CD13, CD44, CD56, CD73, CD90, CD105, CD146, CD166), also these cells possess the expression of HLA-ABC (MHC class I), but were negative for HLA-DR (MHC class II) (publications 1-4).



Comparing to AFSCs of healthy gestation the expression of CD90 was downregulated in AFSCs of fetus affected pregnancies (2nd trimester) (publications 1-2), while in polyhydramnios samples the expression of CD13, CD73, CD90 and CD105 was significantly lower (publication 4). We also analyzed and compared the expression of several pluripotency associated gene markers and found that AFSCs express *SOX2*, *OCT4*, *NANOG*, *REX1*, *LIN28A*, *NOTCH1* and *c-MYC* (publications 1-4). The expression of these genes was of similar level between AFSCs of healthy and fetus affected gestations (2nd trimester) (publications 1-2), however, *OCT4*, *NOTCH1* and *c-MYC* were significantly upregulated in AFSCs from polyhydramnios samples (publication 4). Also, we studied AFSCs for their expression patterns of several microRNAs and we found no significant differences in expression levels of miR-17, miR-21, miR-34a and miR-148b between AFSCs of both sources, but some variance was found during stem cell cultivation. We found that levels of miR-17 and miR-21 were downregulated, but miR-34a and miR-148b were upregulated during propagation of AFSC culture (publication 2). In terms of metabolic profiling, we compared AFSCs from healthy and polyhydramnios samples and we determined that polyhydramnios AFSCs could be characterized by higher oxygen consumption rate (linked to oxidative phosphorylation), greater ATP content, lower mitochondrial membrane potential and significantly upregulated expression of *NRF1* gene. Meanwhile, the extracellular acidification rate, which is linked to glycolysis, was similar in both analyzed AFSC groups (publication 4).

In this study, adipogenic, osteogenic, myogenic and neurogenic differentiation potential of healthy and fetus affected AFSCs was tested. Adipogenic differentiation was induced by using a commercially available induction medium and evaluated by positive staining of intracytoplasmic lipids and determining the expression of differentiation genes *PPAR- $\gamma$*  and *Adiponectin*, which was slightly lower in fetus affected AFSCs (publication 2). Osteogenic differentiation was induced by using a commercially available induction medium as well, and assessed by staining calcium deposits. Relative expression of *ALP*, *Osteocalcin* and *Osteopontin* genes was measured and stronger upregulation of *Osteocalcin* was noted in healthy AFSCs (publication 2). We also studied the myogenic differentiation of AFSCs initiated by using media containing low concentration of inactivated horse serum, which stimulated the formation of multinucleated cells and upregulation of myogenic genes *Actinin- $\alpha$* , *Calponin*, *Desmin* and *MRF4*. While the expression of *Calponin* and *Desmin* was similar, AFSCs from healthy samples showed lower levels of *Actinin- $\alpha$* , but *MRF4* was more upregulated when compared to

fetus affected AFSCs (publication 1). Finally, for neurogenic differentiation we applied all-trans retinoic acid (RA) treatment and observed morphological changes, as cells became elongated and formed neurite-like structures. On gene expression level, we determined more intense upregulation of *Nestin* at early phase of differentiation in fetus affected AFSCs, which equalized with healthy AFSCs at later stage. *NSE* expression increased gradually during differentiation and higher expression was observed in fetus affected AFSCs at final phase of neurogenic differentiation (publication 1).

We also studied the changes of epigenetic regulators, such as microRNAs, chromatin modifying proteins, histone modifications and DNA methylation, during induced differentiations of AFSCs obtained from healthy and fetus affected gestations. The obtained data demonstrated that miR-17 was downregulated during all differentiations and it was more downregulated in healthy AFSCs during osteogenic and neurogenic differentiation. miR-21 showed upregulated levels during osteogenic differentiation, with it being more upregulated in healthy AFSCs, during myogenic and neurogenic differentiation the expression level of miR-21 was almost unchanged, but downregulated during adipogenic differentiation (publications 1-2). We also tested miR-34a and miR-146a and determined that these microRNAs were downregulated during adipogenic and osteogenic differentiation (publication 2), but upregulated during myogenic and neurogenic differentiation with stronger upregulation in fetus affected AFSCs (publication 1). We then assessed the expression of different proteins and histone modifications that are involved in epigenetic regulation and found no significant differences between AFSCs of healthy and fetus affected gestations, but changes were observed during investigated differentiations. We found that the levels of all histone modifications associated with transcriptionally active chromatin (H4hiperAc, H3K9ac and H3K4me3) and modification of heterochromatin H3K9me3 were significantly downregulated, but upregulation of repressive modification H3K27me3 was observed during stem cell differentiation (publications 1-2). Next, we investigated the proteins of Polycomb repressive complex 1 and 2 (BMI1, SUZ12, EZH2) and found reduced levels in all differentiations of aforementioned epigenetic factors (publications 1-2). Finally, we studied enzymes of histone deacetylation (HDAC1) and DNA methylation (DNMT1) as well as genes encoding DNMT3a and DNMT3b and found decreased levels of HDAC1 and DNMT1, however we found that myogenic and neurogenic differentiations were followed by upregulation of DNMT3a and DNMT3b genes (publication 1).

In the next phase of this study, we explored neurogenic differentiation potential of AFSCs derived from healthy pregnancies (2nd trimester) and polyhydramnios gestations (3rd trimester). The differentiation was induced using various signaling (8-Br-cAMP, IBMX, RA, KCl) and trophic (BDNF, NGF) molecules and their combinations (publication 4). Firstly, we assessed the differentiation by morphological changes and observed that AFSCs from healthy samples obtained the neural morphology more efficiently (publication 4). Then, we investigated gene expression changes during differentiation induced by all composed induction protocols. We tested various genes of neural progenitor markers (*SOX2*, *NES*, *NEUROD1*, *VIM*), markers of differentiated post-mitotic neural cells (*NSE*, *NCAM1*, *NCAM2*, *GAD1*, *TPH1*, *TPH2*, *MAP2*, *SYP*), glial markers (*GFAP*, *S100B*), genes of (neuro)trophic factors (*BDNF*, *NGF*, *NTF3*, *NTF4*, *VEGFA*, *TGFB1*, *HBEGF*) and their receptor genes (*NTRK1*, *NTRK2*, *NTRK3*, *FGFR1*, *PDGFRA*). From collected data we concluded that AFSCs of healthy pregnancy demonstrated stronger activation of neural gene expression, except for glial markers, since *GFAP* and *S100B* showed higher expression levels in polyhydramnios AFSCs (publication 4). We also noted that AFSCs induced with a combination of BDNF, NGF, KCl and RA (protocol II) showed upregulated gene expression more consistently, so we further analyzed ion channel genes *HCN2* and *KCNJ2* in AFSCs induced to differentiate using the selected protocol and higher expression of both genes was determined in AFSCs of healthy gestation (publication 4). Using differentiation induction protocol II, we then investigated the changes in neuronal differentiation associated proteins Nestin, Musashi1, LIN28a, and TUBB3, as well as changes in secretion of trophic factors BDNF and VEGF, and found more significantly elevated levels of all proteins in AFSCs from healthy gestations when comparing to undifferentiated control, although it is worth to notice that the content of these proteins was more abundant in undifferentiated AFSCs of polyhydramnios samples (publication 4). Apart from trophic factors, we also examined the secretion of several cytokines, such as IL-1 $\beta$ , IL-6, IL-10, and determined that neither AFSCs of healthy gestations, nor AFSCs of polyhydramnios pregnancies secreted proinflammatory cytokine IL-1 $\beta$  or anti-inflammatory cytokine IL-10. But secretion of IL-6 was detected, and subtle changes in levels of IL-6 were observed upon neurogenic induction, as the secretion was downregulated in AFSCs from healthy pregnancies, while slightly upregulated in AFSCs from polyhydramnios, although the differences were not statistically significant (publication 4). Lastly, we noted that only AFSCs from polyhydramnios samples secreted proinflammatory cytokine TNF $\alpha$ ,

which was significantly downregulated upon neural differentiation, also undifferentiated AFSCs from polyhydramnios were more positive for TNFA gene expression, but receptor protein gene TNFR1 was more upregulated in AFSCs from healthy gestations (publication 4).

We also tested several selected epigenetically active compounds, known as small molecules, and their effects on AFSCs from healthy pregnancies. In this study we used histone deacetylase inhibitors trichostatin A (TSA) and sodium butyrate (NaBut), and multifunctional molecules RA and vitamin C (VitC). As we found that these molecules were not cytotoxic to AFSCs at used concentrations or combinations, we proceeded to examine the changes in stemness associated gene and protein expression using treatments with small molecule combinations (combination A: VitC, TSA, RA; combination B: VitC, NaBut, RA). The use of combination A resulted in stronger upregulation of genes *OCT4*, *NANOG*, *SOX2*, *LIN28A*, *NOTCH1*, *c-MYC* after 24 h of treatment (compared to 96 h), while combination B elevated the expression more after 96 h of treatment (compared to 24 h). Corresponding proteins Oct4, Nanog, c-Myc showed negligible changes in their expression after treatments with both combinations, while the levels Notch1 were significantly reduced (publication 3). Small molecules affected surface marker expression, as we found that CD44, CD73, CD105, CD117, CD146, SSEA4 were downregulated after treatment with VitC, NaBut and RA, while VitC, TSA and RA downregulated only CD105, but upregulated levels of CD117 (publication 3). Further, we determined that small molecule combinations affect metabolic activity of AFSCs, as our data demonstrated that 96 h treatments with combination A and B resulted in more energetically active cells with increased oxygen consumption and extracellular acidification rates (oxidative phosphorylation and glycolysis, accordingly). This was also evident on gene expression level, since genes linked to oxidative phosphorylation (*NRF1*, *HIF1 $\alpha$* , *PPARGC1A*), glycolysis (*ERR $\alpha$* , *PKM*, *PDK1*, *LDHA*), and NF $\kappa$ B signaling pathway (*NFKB1*, *NFKB2*, *RELA*, *RELB*, *REL*) were significantly upregulated after 96 h treatments with small molecule combinations (publication 3). AFSCs from healthy pregnancies were induced to differentiate towards neurogenic lineage using two commercially available supplements N2 and B27 combined with RA. Also, we added an additional preinduction step consisting of 24 h treatment with VitC, TSA, RA (small molecule combination A), as upregulation of neurogenesis associated *SOX2* and *NOTCH1* genes was noted at this time point. Neurogenic differentiation of AFSCs was confirmed by significantly increased levels of secreted BDNF and visible morphological changes, when staining TUBB3, NCAM1,

Vimentin and F-actin revealed reorganization of structural cytoskeleton proteins resulting in more elongated cells, and formation of possible neurites, as NCAM1 was more concentrated at the cell ends (publication 3). The small molecule treatment as preinduction step proved to be beneficial for neurogenic differentiation of AFSCs, as we determined boosted expression of neural and astrocytic genes *Nestin*, *MAP2*, *ALDH1L1*, *TUBB3*, *GFAP*, and upregulated expression of ion channel genes *CACNA1D*, *KCNJ12* (publication 3).

### **Conclusions**

1. Significant differences in characteristics, pluripotency gene and microRNA expression were not determined in AFSCs of second trimester healthy and fetus affected pregnancies. Meanwhile, AFSCs of third trimester polyhydramnios gestations possessed different morphology, upregulated expression of *OCT4*, *NOTCH1*, *MYC* genes, but reduced levels of CD13, CD73, CD90, CD105 surface markers. Also, polyhydramnios AFSCs demonstrated more active oxidative phosphorylation, greater ATP content, lower mitochondrial membrane potential and significantly upregulated expression of *NRF1* gene, while glycolysis was of similar level between studied AFSCs groups.
2. Similar morphological and molecular changes were observed in AFSCs of second trimester healthy and fetus affected pregnancies differentiated towards adipogenic, osteogenic, myogenic and neurogenic lineages.
3. AFSCs of healthy pregnancies differentiated towards neurogenic lineage more efficiently than polyhydramnios AFSCs. Using BDNF, NGF, KCl and RA to induce neurogenic differentiation upregulated differentiation specific proteins (*Nestin*, *Musashi 1*, *LIN28a*, *BDNF*, *VEGF*) and reduced  $TNF\alpha$  in polyhydramnios AFSCs, while no secretion of this proinflammatory cytokine was detected in AFSCs of healthy gestations.
4. Treatments with small molecules TSA, NaBut, VitC and RA caused Oct4, Nanog, Sox2, Lin28a, Notch1 and c-Myc expression changes on gene and protein level and metabolic alterations in AFSCs of healthy pregnancies. Short-term treatment with TSA, VitC and RA boosted neurogenic differentiation potential.

## LITERATŪROS SĄRAŠAS/REFERENCES

- Abe Y, Ochiai D, Masuda H, Sato Y, Otani T, Fukutake M, et al. In utero amniotic fluid stem cell therapy protects against myelomeningocele via spinal cord coverage and hepatocyte growth factor secretion. *Stem Cells Transl Med.* 2019. 8(11):1170–1179. doi: 10.1002/sctm.19-0002.
- Alessio N, Pipino C, Mandatori D, Di Tomo P, Ferone A, Marchiso M, et al. Mesenchymal stromal cells from amniotic fluid are less prone to senescence compared to those obtained from bone marrow: an in vitro study. *J Cell Physiol.* 2018. 233(11):8996–9006. doi: 10.1002/jcp.26845.
- Allaf B, Dreux S, Schmitz T, Czerkiewicz I, Le Vaillant C, Benachi A, et al. Amniotic fluid biochemistry in isolated polyhydramnios: a series of 464 cases. *Prenat Diagn.* 2015. 35(13):1331–1335. doi: 10.1002/pd.4700.
- Aranha MM, Santos DM, Solá S, Steer CJ, Rodrigues CM. miR-34a regulates mouse neural stem cell differentiation. *PLoS One.* 2011. 6(8):e21396. doi: 10.1371/journal.pone.0021396.
- Asp P, Blum R, Vethantham V, Parisi F, Micsinai M, Cheng J, et al. Genome-wide remodeling of the epigenetic landscape during myogenic differentiation. *Proc Natl Acad Sci USA.* 2011. 108(22):E149–E158. doi: 10.1073/pnas.1102223108.
- Avgustinova A, Benitah S. Epigenetic control of adult stem cell function. *Nat Rev Mol Cell Biol.* 2016. 17(10):643–658. doi: 10.1038/nrm.2016.76.
- Azargoon A, Negahdari B. Lung regeneration using amniotic fluid mesenchymal stem cells. *Artif Cells Nanomed Biotechnol.* 2018. 46(3):447–451. doi: 10.1080/21691401.2017.1337023.
- Bakkar N, Ladner K, Canan BD, Liyanarachchi S, Bal NC, Pant M, et al. IKK $\alpha$  and alternative NF- $\kappa$ B regulate PGC-1 $\beta$  to promote oxidative muscle metabolism. *J Cell Biol.* 2012. 196(4):497–511. doi: 10.1083/jcb.201108118.
- Baranek M, Belter A, Naskręć-Barciszewska MZ, Stobiecki M, Markiewicz WT, Barciszewski J. Effect of small molecules on cell reprogramming. *Mol Biosyst.* 2017. 13(2):277–313. doi: 10.1039/c6mb00595k.
- Bernal A, Arranz L. Nestin-expressing progenitor cells: function, identity and therapeutic implications. *Cell Mol Life Sci.* 2018. 75(12):2177–2195. doi: 10.1007/s00018-018-2794-z.
- Bonaventura G, Chamayou S, Liprino A, Guglielmino A, Fichera M, Caruso M, et al. Different tissue-derived stem cells: a comparison of neural differentiation capability. *PLoS One.* 2015. 10(10):e0140790. doi: 10.1371/journal.pone.0140790.
- Bossolasco P, Montemurro T, Cova L, Zangrossi S, Calzarossa C, Buiatitot S, et al. Molecular and phenotypic characterization of human amniotic fluid cells and their differentiation potential. *Cell Res.* 2006. 16(4):329–336. doi: 10.1038/sj.cr.7310043.

- Burney MJ, Johnston C, Wong KY, Teng SW, Beglopoulos V, Stanton LW, et al. An epigenetic signature of developmental potential in neural stem cells and early neurons. *Stem Cells*. 2013. 31(9):1868–1880. doi: 10.1002/stem.1431.
- Cacchiarelli D, Trapnell C, Ziller MJ, Soumillon M, Cesana M, Karnik R, et al. Integrative Analyses of Human Reprogramming Reveal Dynamic Nature of Induced Pluripotency. *Cell*. 2015. 162(2):412–424. doi: 10.1016/j.cell.2015.06.016.
- Cadrin C, Golbus MS. Fetal tissue sampling--indications, techniques, complications, and experience with sampling of fetal skin, liver, and muscle. *West J Med*. 1993. 159(3):269–272.
- Cananzi M, Atala A, De Coppi P. Stem cells derived from amniotic fluid: new potentials in regenerative medicine. *Reprod Biomed Online*. 2009. 18(Suppl 1):17–27. doi: 10.1016/s1472-6483(10)60111-3.
- Cao Y, Guo W, Tian S, He X, Wang X, Liu X, et al. miR-290/371-Mbd2-Myc circuit regulates glycolytic metabolism to promote pluripotency. *EMBO J*. 2015. 34(5):609–623. doi: 10.15252/embj.201490441.
- Caretti G, Di Padova M, Micales B, Lyons GE, Sartorelli V. The Polycomb Ezh2 methyltransferase regulates muscle gene expression and skeletal muscle differentiation. *Genes Dev*. 2004. 18(21): 2627–2638. doi: 10.1101/gad.1241904.
- Casciaro F, Beretti F, Zavatti M, McCubrey JA, Ratti S, Marmioli S, et al. Nuclear Nox4 interaction with prelamin A is associated with nuclear redox control of stem cell aging. *Aging (Albany NY)*. 2018. 10(10):2911–2934. doi: 10.18632/aging.101599.
- Castelli V, Antonucci I, d'Angelo M, Tessitore A, Zelli V, Benedetti E, et al. Neuroprotective effects of human amniotic fluid stem cells derived secretome in an ischemia/reperfusion model. *Stem Cells Transl Med*. 2020. 10(2):251–266. doi: 10.1002/sctm.20-0268.
- Chen L, Holmstrøm K, Qiu W, Ditzel N, Shi K, Hokland L, Kassem M. MicroRNA-34a inhibits osteoblast differentiation and in vivo bone formation of human stromal stem cells. *Stem Cells*. 2014. 32(4):902–912. doi: 10.1002/stem.1615.
- Chen YS, Pelekanos RA, Ellis RL, Horne R, Wolvetang EJ, Fisk NM. Small molecule mesengenic induction of human induced pluripotent stem cells to generate mesenchymal stem/stromal cells. *Stem Cells Transl Med*. 2012. 1(2):83–95. doi: 10.5966/sctm.2011-0022.
- Cipriano M, Correia JC, Camões SP, Oliveira NG, Cruz P, Cruz H, et al. The role of epigenetic modifiers in extended cultures of functional hepatocyte-like cells derived from human neonatal mesenchymal stem cells. *Arch Toxicol*. 2017. 91(6):2469–2489. doi: 10.1007/s00204-016-1901-x.
- Corley M, Kroll KL. The roles and regulation of Polycomb complexes in neural development. *Cell Tissue Res*. 2015. 359(1):65–85. doi: 10.1007/s00441-014-2011-9.

- Daum H, Ben David A, Nadjari M, Zenvirt S, Helman S, et al. Role of late amniocentesis in the era of modern genomic technologies. *Ultrasound Obstet Gynecol.* 2019. 53(5):676–685. doi: 10.1002/uog.20113.
- De Angelis MT, Parrotta EI, Santamaria G, Cuda G. Short-term retinoic acid treatment sustains pluripotency and suppresses differentiation of human induced pluripotent stem cells. *Cell Death Dis.* 2018. 9(1):6. doi: 10.1038/s41419-017-0028-1.
- De Coppi P, Bartsch GJr, Siddiqui MM, Xu T, Santos CC, Perin L, et al. Isolation of amniotic stem cell lines with potential for therapy. *Nat. Biotechnol.* 2007. 25:100–106. doi: 10.1038/nbt1274.
- Deng F, Lei H, Hu Y, He L, Fu H, Feng R, et al. Combination of retinoic acid, dimethyl sulfoxide and 5-azacytidine promotes cardiac differentiation of human fetal liver-derived mesenchymal stem cells. *Cell Tissue Bank.* 2016. 17(1):147–159. doi: 10.1007/s10561-015-9514-9.
- Di Bernardo J, Maiden MM, Hershenson MB, Kunisaki SM. Amniotic fluid derived mesenchymal stromal cells augment fetal lung growth in a nitrofen explant model. *J. Pediatr. Surg.* 2014. 49(6):859–865. doi: 10.1016/j.jpedsurg.2014.01.013.
- Ekblad A, Qian H, Westgren M, Le Blanc K, Fossum M, Gotherstrom C. Amniotic fluid—a source for clinical therapeutics in the newborn? *Stem Cells Dev.* 2015. 24(12):1405–1414. doi: 10.1089/scd.2014.0426.
- Esteban MA, Wang T, Qin B, Yang J, Qin D, Cai J, et al. Vitamin C enhances the generation of mouse and human induced pluripotent stem cells. *Cell Stem Cell.* 2010. 6(1):71–79. doi: 10.1016/j.stem.2009.12.001.
- Fang YH., Wang SPH., Chang HY., Yang PJ., Liu PY., Liu YW. Progress and challenges of amniotic fluid derived stem cells in therapy of ischemic heart disease. *Int J Mol Sci.* 2021. 22(1):102. doi: 10.3390/ijms22010102.
- Folmes CD, Nelson TJ, Martinez-Fernandez A, Arrell DK, Lindor JZ, Dzeja PP, et al. Somatic oxidative bioenergetics transitions into pluripotency-dependent glycolysis to facilitate nuclear reprogramming. *Cell Metab.* 2011. 14(2):264–271. doi: 10.1016/j.cmet.2011.06.011.
- Franke J, Abs V, Zizzadoro C, Abraham G. Comparative study of the effects of fetal bovine serum versus horse serum on growth and differentiation of primary equine bronchial fibroblasts. *BMC Vet Res.* 2014. 10:119. doi: 10.1186/1746-6148-10-119.
- Frederiksen LE, Ernst A, Brix N, Braskhøj Lauridsen LL, Roos L, Ramlau-Hansen CH, Ekelund CK. Risk of Adverse Pregnancy Outcomes at Advanced Maternal Age. *Obstet Gynecol.* 2018. 131(3):457–463. doi: 10.1097/AOG.0000000000002504.
- Frid MG, Moiseeva EP, Stenmark KR. Multiple phenotypically distinct smooth muscle cell populations exist in the adult and developing bovine pulmonary arterial media in vivo. *Circ Res.* 1994. 75(4):669–681. doi: 10.1161/01.res.75.4.669.



- Fu Y, Luo N, Klein RL, Garvey WT. Adiponectin promotes adipocyte differentiation, insulin sensitivity, and lipid accumulation. *J Lipid Res.* 2005. 46(7):1369–1379. doi: 10.1194/jlr.M400373-JLR200.
- Gao L, Zhao M, Ye W, Huang J, Chu J, Yan S, et al. Inhibition of glycogen synthase kinase-3 (GSK3) promotes the neural differentiation of full-term amniotic fluid-derived stem cells towards neural progenitor cells. *Tissue Cell.* 2016. 48(4):312–320. doi: 10.1016/j.tice.2016.06.001.
- Gasiūnienė M, Petkus G, Matuzevičius D, Navakauskas D, Navakauskienė R. Angiotensin II and TGF- $\beta$ 1 Induce Alterations in Human Amniotic Fluid-Derived Mesenchymal Stem Cells Leading to Cardiomyogenic Differentiation Initiation. *Int J Stem Cells.* 2019a. 12(2):251–264. doi: 10.15283/ijsc18126.
- Gasiūnienė M, Zentelytė A, Wojtas B, Baronaitė S, Krasovskaja N, Savickienė J, et al. DNMT inhibitors effectively induce gene expression changes suggestive of cardiomyogenic differentiation of human amniotic fluid-derived mesenchymal stem cells via chromatin remodeling. *J Tissue Eng Regen Med.* 2019b. 13(3):469–481. doi: 10.1002/term.2800.
- Gasiūnienė M, Zubova A, Utkus A, Navakauskienė R. Epigenetic and metabolic alterations in human amniotic fluid stem cells induced to cardiomyogenic differentiation by DNA methyltransferases and p53 inhibitors. *J Cell Biochem.* 2019c. 120:8129–8143. doi: 10.1002/jcb.28092.
- Gasiūnienė M, Valatkaitė E, Navakauskienė R. Long-term cultivation of human amniotic fluid stem cells: the impact on proliferative capacity and differentiation potential. *J Cell Biochem.* 2020. 121(7):3491–3501. doi: 10.1002/jcb.29623.
- Gatti M, Zavatti M, Beretti F, Giuliani D, Vandini E, Ottani A, et al. Oxidative stress in Alzheimer's disease: in vitro therapeutic effect of amniotic fluid stem cells extracellular vesicles. *Oxid Med Cell Longev.* 2020. 2020:2785343. doi: 10.1155/2020/2785343.
- George SK, Abolbashari M, Kim TH, Zhang C, Allickson J, Jackson JD, et al. Effect of Human Amniotic Fluid Stem Cells on Kidney Function in a Model of Chronic Kidney Disease. *Tissue Eng Part A.* 2019. 25(21-22):1493-1503. doi: 10.1089/ten.TEA.2018.0371.
- Glemžaitė M, Navakauskienė R. Osteogenic Differentiation Of Human Amniotic Fluid Mesenchymal Stem Cells Is Determined By Epigenetic Changes. *Stem Cells Int.* 2016. 2016:6465307. doi: 10.1155/2016/6465307.
- Hackl M, Brunner S, Fortschegger K, Schreiner C, Micutkova L, Mück C, et al. miR-17, miR-19b, miR-20a, and miR-106a are down-regulated in human aging. *Aging Cell.* 2010. 9(2):291–296. doi: 10.1111/j.1474-9726.2010.00549.x.
- Håkkelien AM, Bryne JC, Harstad KG, Lorenz S, Paulsen J, Sun J, et al. The regulatory landscape of osteogenic differentiation. *Stem Cells.* 2014. 32(10):2780–2793. doi: 10.1002/stem.1759.

- Hamza A, Herr D, Solomayer EF, Meyberg-Solomayer G. Polyhydramnios: Causes, Diagnosis and Therapy. *Geburtshilfe Frauenheilkd.* 2013. 73(12):1241–1246. doi: 10.1055/s-0033-1360163.
- Haque A, Polcyn R, Matzelle D, Banik NL. New Insights into the Role of Neuron-Specific Enolase in Neuro-Inflammation, Neurodegeneration, and Neuroprotection. *Brain Sci.* 2018. 8(2):33. doi: 10.3390/brainsci8020033.
- Hatazawa Y, Ono Y, Hirose Y, Kanai S, Fujii NL, Machida S, et al. Reduced Dnmt3a increases Gdf5 expression with suppressed satellite cell differentiation and impaired skeletal muscle regeneration. *FASEB J.* 2018. 32(3):1452–1467. doi: 10.1096/fj.201700573R.
- Hore TA, von Meyenn F, Ravichandran M, Bachman M, Ficiz G, Oxley D, et al. Retinol and ascorbate drive erasure of epigenetic memory and enhance reprogramming to naïve pluripotency by complementary mechanisms. *Proc Natl Acad Sci U S A.* 2016. 113(43):12202–12207. doi: 10.1073/pnas.1608679113.
- Hu T, Kitano A, Luu V, Dawson B, Hoegenauer KA, Lee BH, Nakada D. Bmi1 Suppresses Adipogenesis in the Hematopoietic Stem Cell Niche. *Stem Cell Rep.* 2019. 13(3):545–558. doi: 10.1016/j.stemcr.2019.05.027.
- Huang J, Ma W, Wei X, Yuan Z. Amniotic fluid mesenchymal stromal cells from early stages of embryonic development have higher selfrenewal potential. *Vitro Cell Dev Biol Anim.* 2020. 56(9):701–714. doi: 10.1007/s11626-020-00511-z.
- Huszar JM, Payne CJ. MIR146A inhibits JMJD3 expression and osteogenic differentiation in human mesenchymal stem cells. *FEBS Lett.* 2014. 588(9):1850–1856. doi: 10.1016/j.febslet.2014.03.057.
- Iampietro C, Grange C, Marozio L, Benedetto C, Perin L, Bussolati B. Full-Term Human Amniotic Fluid Mesenchymal Stem Cells Show Nephroprotective Effect in an Acute Kidney Injury Model. *J Stem Cell Res Dev Ther.* 2020. 6:041. doi: 10.24966/SRDT-2060/100041.
- In 't Anker PS, Scherjon SA, Kleijburg-van der Keur C, Noort WA, Claas FH, Willemze R, et al. Amniotic fluid as a novel source of mesenchymal stem cells for therapeutic transplantation. *Blood.* 2003. 102(4):1548–1549. doi: 10.1182/blood-2003-04-1291 .
- Islam O, Gong X, Rose-John S, Heese K. Interleukin-6 and neural stem cells: more than gliogenesis. *Mol Biol Cell.* 2009. 20(1):188–199. doi: 10.1091/mbc.e08-05-0463.
- Jain M, Minocha E, Tripathy NK, Singh N, Chaturvedi C, Nityanand S. Comparison of the cardiomyogenic potency of human amniotic fluid and bone marrow mesenchymal stem cells. *Int. J. Stem Cells.* 2019. 12(3):449–456. doi: 10.15283/IJSC18087.
- Janesick A, Wu SC, Blumberg B. Retinoic acid signaling and neuronal differentiation. *Cell. Mol. Life Sci.* 2015. 72(8):1559–1576. doi: 10.1007/s00018-014-1815-9.

- Jang S, Jeong HS. Histone deacetylase inhibition-mediated neuronal differentiation via the Wnt signaling pathway in human adipose tissue-derived mesenchymal stem cells. *Neurosci Lett*. 2018. 668:24-30. doi: 10.1016/j.neulet.2018.01.006.
- Joo S, Ko IK, Atala A, Yoo JJ, Lee SJ. Amniotic fluid-derived stem cells in regenerative medicine research. *Arch Pharm Res*. 2012. 35(2):271–280. doi: 10.1007/s12272-012-0207-7.
- Kalle AM, Wang Z. Differential effects of two HDAC inhibitors with distinct concomitant DNA hypermethylation or hypomethylation in breast cancer cells. *Biorxiv*. 2019. [Preprint] doi: 10.1101/578062.
- Kang H, Hata A. The role of microRNAs in cell fate determination of mesenchymal stem cells: balancing adipogenesis and osteogenesis. *BMB Rep*. 2015. 48(6):319–323. doi: 10.5483/BMBRep.2015.48.6.206.
- Kastl L, Sauer SW, Ruppert T, Beissbarth T, Becker MS, Süß D, et al. TNF- $\alpha$  mediates mitochondrial uncoupling and enhances ROS-dependent cell migration via NF- $\kappa$ B activation in liver cells. *FEBS Lett*. 2014. 588(1):175–183. doi: 10.1016/j.febslet.2013.11.033.
- Kaviani A, Guleserian K, Perry TE, Jennings RW, Ziegler MM, Fauza DO. Fetal Tissue Engineering from Amniotic Fluid. *J Am Coll Surg*. 2003. 196(4):592–597. doi: 10.1016/s1072-7515(02)01834-3.
- Kashyap V, Rezende NC, Scotland KB, Shaffer SM, Persson JL, Gudas LJ, Mongan NP. Regulation of stem cell pluripotency and differentiation involves a mutual regulatory circuit of the NANOG, OCT4, and SOX2 pluripotency transcription factors with polycomb repressive complexes and stem cell microRNAs. *Stem Cells Dev*. 2009. 18(7):1093–1108. doi: 10.1089/scd.2009.0113.
- Kawauchi K, Araki K, Tobiume K, Tanaka N. p53 regulates glucose metabolism through an IKK-NF-kappaB pathway and inhibits cell transformation. *Nat Cell Biol*. 2008. 10(5):611–618. doi: 10.1038/ncb1724.
- Kim EY, Lee KB, Kim MK. The potential of mesenchymal stem cells derived from amniotic membrane and amniotic fluid for neuronal regenerative therapy. *BMB Rep*. 2014. 47(3):135–140. doi: 10.5483/bmbrep.2014.47.3.289.
- Kim HM, Haraguchi N, Ishii H, Ohkuma M, Okano M, Mimori K, et al. Increased CD13 expression reduces reactive oxygen species, promoting survival of liver cancer stem cells via an epithelial-mesenchymal transition-like phenomenon. *Ann Surg Oncol*. 2012. 19(3):S539–S548. doi: 10.1245/s10434-011-2040-5.
- Kim H, Jang H, Kim TW, Kang B, Lee S, Jeon Y, et al. Core pluripotency factors directly regulate metabolism in embryonic stem cell to maintain pluripotency. *Stem Cells*. 2015. 33(9):2699–2711. doi: 10.1002/stem.2073.
- Kim Y, Jeong J, Choi D. Small-molecule-mediated reprogramming: a silver lining for regenerative medicine. *Exp Mol Med*. 2020. 52(2):213–226. doi: 10.1038/s12276-020-0383-3.

- Kleene R, Mzoughi M, Joshi G, Kalus I, Bormann U, Schulze C, et al. NCAM-induced neurite outgrowth depends on binding of calmodulin to NCAM and on nuclear import of NCAM and fak fragments. *J Neurosci*. 2010. 30(32):10784–10798. doi: 10.1523/JNEUROSCI.0297-10.2010.
- Kongcharoensombat W, Nakasa T, Ishikawa M, Nakamae A, Deie M, Adachi N, et al. The effect of microRNA-21 on proliferation and matrix synthesis of chondrocytes embedded in atelocollagen gel. *Knee Surg Sports Traumatol Arthrosc*. 2010. 18(12):1679–1684. doi: 10.1007/s00167-010-1111-7.
- Kornacki J, Adameczyk M, Wirstlein P, Osiński M, Wender-Ożegowska E. Polyhydramnios - frequency of congenital anomalies in relation to the value of the amniotic fluid index. *Ginekol Pol*. 2017. 88(8):442–445. doi: 10.5603/GP.a2017.0081.
- Kot M, Baj-Krzyworzeka M, Szatanek R, Musiał-Wysocka A, Suda-Szczurek M, Majka M. The Importance of HLA Assessment in "Off-the-Shelf" Allogeneic Mesenchymal Stem Cells Based-Therapies. *Int J Mol Sci*. 2019. 20(22):5680. doi: 10.3390/ijms20225680.
- Kouamé N, N'goan-Domoua AM, Nikiéma Z, Konan AN, N'guessan KE, Sétchéou A, et al. Polyhydramnios: a warning sign in the prenatal ultrasound diagnosis of foetal malformation? *Diagn Interv Imaging*. 2013. 94(4):433-437. doi: 10.1016/j.diii.2013.01.002.
- Kretsovali A, Hadjimichael C, Charmpilas N. Histone Deacetylase Inhibitors in Cell Pluripotency, Differentiation, and Reprogramming. *Stem Cells Int*. 2012. 2012:184154. doi: 10.1155/2012/184154.
- Kunisaki SM. Amniotic fluid stem cells for the treatment of surgical disorders in the fetus and neonate. *Stem Cells Transl. Med*. 2018. 7(11):767–773. doi: 10.1002/sctm.18-0018.
- Kunisaki SM, Fuchs JR, Steigman SA, Fauza DO. A comparative analysis of cartilage engineered from different perinatal mesenchymal progenitor cells. *Tissue Eng*. 2007. 13(11):2633–2644. doi: 10.1089/ten.2006.0407.
- Laker RC, Ryall JG. DNA methylation in skeletal muscle stem cell specification, proliferation, and differentiation. *Stem Cells Int*. 2016. 2016:5725927. doi: 10.1155/2016/5725927.
- Lathia JD, Mattson MP, Cheng A. Notch: from neural development to neurological disorders. *J Neurochem*. 2008. 107(6):1471–1481. doi: 10.1111/j.1471-4159.2008.05715.x.
- Lazure F, Blackburn DM, Corchado AH, Sahinyan K, Karam N, Sharanek A, et al. Myf6/MRF4 is a myogenic niche regulator required for the maintenance of the muscle stem cell pool. *EMBO Rep*. 2020. 21(12):e49499. doi: 10.15252/embr.201949499.
- Lee HW, Suh JH, Kim AY, Lee YS, Park SY, Kim JB. Histone deacetylase 1-mediated histone modification regulates osteoblast differentiation. *Mol Endocrinol*. 2006. 20(10):2432–2443. doi: 10.1210/me.2006-0061.

- Li Z, Yang CS, Nakashima K, Rana TM. Small RNA-mediated regulation of iPS cell generation. *EMBO J*. 2011. 30(5):823–834. doi: 10.1038/emboj.2011.2.
- Lim JY, Park SI, Oh JH, Kim SM, Jeong CH, Jun JA, et al. Brain-derived neurotrophic factor stimulates the neural differentiation of human umbilical cord blood-derived mesenchymal stem cells and survival of differentiated cells through MAPK/ERK and PI3K/Akt-dependent signaling pathways. *J Neurosci Res*. 2008. 86(10):2168–2178. doi: 10.1002/jnr.21669.
- Liu T, Zhou Y, Ko KS, Yang H. Interactions between Myc and Mediators of Inflammation in Chronic Liver Diseases. *Mediators Inflamm*. 2015. 2015:276850. doi: 10.1155/2015/276850.
- Loukogeorgakis SP, De Coppi P. Concise Review: Amniotic Fluid Stem Cells: The Known, the Unknown, and Potential Regenerative Medicine Applications. *Stem Cells*. 2017. 35(7):1663–1673. doi: 10.1002/stem.2553.
- Ma X, Kong L, Zhu S. Reprogramming cell fates by small molecules. *Protein Cell*. 2017. 8(5):328–348. doi: 10.1007/s13238-016-0362-6.
- Maguire CT, Demarest BL, Hill JT, Palmer JD, Brothman AR, Yost HJ, Condic ML. Genome-wide analysis reveals the unique stem cell identity of human amniocytes. *PLoS ONE*. 2013. 8(1):e53372. doi: 10.1371/journal.pone.0053372.
- Maioli M, Contini G, Santaniello S, Bandiera P, Pigliaru G, Sanna R, et al. Amniotic fluid stem cells morph into a cardiovascular lineage: analysis of a chemically induced cardiac and vascular commitment. *Drug Des Devel Ther*. 2013. 7:1063–1073. doi: 10.2147/DDDT.S44706.
- Mali P, Chou BK, Yen J, Ye Z, Zou J, Dowey S, et al. Butyrate greatly enhances derivation of human induced pluripotent stem cells by promoting epigenetic remodeling and the expression of pluripotency-associated genes. *Stem Cells*. 2010. 28(4):713–720. doi: 10.1002/stem.402.
- Martorana F, Gaglio D, Bianco MR, Aprea F, Virtuoso A, Bonanomi M, et al. Differentiation by nerve growth factor (NGF) involves mechanisms of crosstalk between energy homeostasis and mitochondrial remodeling. *Cell Death Dis*. 2018. 9(3):391. doi: 10.1038/s41419-018-0429-9.
- Mauro C, Leow S, Anso E, Rocha S, Thotakura A, Tornatore L, et al. NF- $\kappa$ B controls energy homeostasis and metabolic adaptation by upregulating mitochondrial respiration. *Nat Cell Biol*. 2011. 13(10):1272–1279. doi: 10.1038/ncb2324.
- Miron RJ, Zhang YF. Osteoinduction: a review of old concepts with new standards. *J Dent Res*. 2012. 91(8):736–744. doi: 10.1177/0022034511435260.
- Moraghebi R, Kirkeby A, Chaves P, Rönn RE, Sitnicka E, Parmar M, et al. Term amniotic fluid: an unexploited reserve of mesenchymal stromal cells for reprogramming and potential cell therapy applications. *Stem Cell Res Ther*. 2017. 8(1):190. doi: 10.1186/s13287-017-0582-6.
- Morris JK, Springett AL, Greenlees R, Loane M, Addor MC, Arriola L, et al. Trends in congenital anomalies in Europe from 1980 to 2012. *PLoS One*. 2018.13(4):e0194986. doi: 10.1371/journal.pone.0194986.

- Musri MM, Corominola H, Casamitjana R, Gomis R, Parrizas M. Histone H3 lysine 4 dimethylation signals the transcriptional competence of the adiponectin promoter in preadipocytes. *J Biol Chem.* 2006. 281(25):17180–17188. doi: 10.1074/jbc.M601295200.
- Na T, Liu J, Zhang K, Ding M, Yuan BZ. The notch signaling regulates CD105 expression, osteogenic differentiation and immunomodulation of human umbilical cord mesenchymal stem cells. *PLoS One.* 2015. 10(2):e0118168. doi: 10.1371/journal.pone.0118168.
- Nguyen LS, Fregeac J, Bole-Feysot C, Cagnard N, Iyer A, Anink J, et al. Role of miR-146a in neural stem cell differentiation and neural lineage determination: relevance for neurodevelopmental disorders. *Mol Autism.* 2018. 9:38. doi: 10.1186/s13229-018-0219-3.
- Nicholls DG. Mitochondrial membrane potential and aging. *Aging Cell.* 2004. 3(1):35–40. doi: 10.1111/j.1474-9728.2003.00079.x.
- Noer A, Lindeman LC, Collas P. Histone H3 modifications associated with differentiation and long-term culture of mesenchymal adipose stem cells. *Stem Cells Dev.* 2009. 18(5):725–736. doi: 10.1089/scd.2008.0189.
- Osborne JK, Larsen JE, Shields MD, Gonzales JX, Shames DS, Sato M, et al. NeuroD1 regulates survival and migration of neuroendocrine lung carcinomas via signaling molecules TrkB and NCAM. *Proc Natl Acad Sci U S A.* 2013. 110(16):6524–6529. doi: 10.1073/pnas.1303932110.
- Ozkul Y, Galderisi U. The Impact of Epigenetics on Mesenchymal Stem Cell Biology. *J Cell Physiol.* 2016. 231(11):2393–2401. doi: 10.1002/jcp.25371.
- Pataskar A, Jung J, Smialowski P, Noack F, Calegari F, Straub T, Tiwari VK. NeuroD1 reprograms chromatin and transcription factor landscapes to induce the neuronal program. *EMBO J.* 2016. 35(1):24–45. doi: 10.15252/embj.201591206.
- Perin L, Sedrakyan S, Da Sacco S, De Filippo R. Characterization of human amniotic fluid stem cells and their pluripotential capability. *Methods Cell Biol.* 2008. 86:85–99. doi: 10.1016/S0091-679X(08)00005-8.
- Prusa AR, Hengstschläger M. Amniotic fluid cells and human stem cell research – a new connection. *Med Sci Monit.* 2002. 8(11):RA253–257. doi: 10.1155/2012/741810.
- Prusa AR, Marton E, Rosner M, Bernaschek G, Hengstschläger M. Oct-4-expressing cells in human amniotic fluid: a new source for stem cell research? *Human Reprod.* 2003. 18(7):1489–1493. doi: 10.1093/humrep/deg279.
- Puchtler H, Meloan SN, Terry MS. On the history and mechanism of alizarin and alizarin red S stains for calcium. *J Histochem Cytochem.* 1969. 17(2):110–124. doi: 10.1177/17.2.110.
- Ramasamy TS, Velaithan V, Yeow Y, Sarkar FH. Stem cells derived from amniotic fluid: a potential pluripotent-like cell source for cellular therapy? *Curr Stem Cell Res Ther.* 2018. 13(4):252–264. doi: 10.2174/1574888x13666180115093800.

- Ramírez-Zacarias JL, Castro-Muñozledo F, Kuri-Harcuch W. Quantitation of adipose conversion and triglycerides by staining intracytoplasmic lipids with Oil red O. *Histochemistry*. 1992. 97(6):493–497. doi: 10.1007/BF00316069.
- Richly H, Aloia L, Di Croce L. Roles of the Polycomb group proteins in stem cells and cancer. *Cell Death Dis*. 2011. 2(9):e204. doi: 10.1038/cddis.2011.84.
- Rienecker KDA, Poston RG, Saha RN. Merits and Limitations of Studying Neuronal Depolarization-Dependent Processes Using Elevated External Potassium. *ASN Neuro*. 2020. 12:1759091420974807. doi: 10.1177/1759091420974807.
- Rizk F, Salameh P, Hamadé A. Congenital Anomalies: Prevalence and Risk Factors. *Universal Journal of Public Health*. 2014. 2(2):58 – 63. doi: 10.13189/ujph.2014.020204.
- Roubelakis MG, Pappa KI, Bitsika V, Zagoura D, Vlahou A, Papadaki HA, et al. Molecular and proteomic characterization of human mesenchymal stem cells derived from amniotic fluid: Comparison to bone marrow mesenchymal stem cells. *Stem Cells Dev*. 2007. 16(6):931–952. doi: 10.1089/scd.2007.0036.
- Saini A, Rullman E, Lilja M, Mandić M, Melin M, Olsson K, Gustafsson T. Asymmetric cellular responses in primary human myoblasts using sera of different origin and specification. *PLoS One*. 2018. 13(2):e0192384. doi:10.1371/journal.pone.0192384.
- Sarlak G, Vincent B. The Roles of the Stem Cell-Controlling Sox2 Transcription Factor: from Neuroectoderm Development to Alzheimer's Disease? *Mol Neurobiol*. 2016. 53(3):1679–1698. doi: 10.1007/s12035-015-9123-4.
- Sato F, Tsuchiya S, Meltzer SJ, Shimizu K. MicroRNAs and epigenetics. *FEBS J*. 2011. 278(10):1598–1609. doi: 10.1111/j.1742-4658.2011.08089.x.
- Sato Y, Ochiai D, Abe Y, Masuda H, Fukutake M, Ikenoue S. Prophylactic therapy with human amniotic fluid stem cells improved survival in a rat model of lipopolysaccharide-induced neonatal sepsis through immunomodulation via aggregates with peritoneal macrophages. *Stem Cell Res Ther*. 2020. 11(1):300. doi: 10.1186/s13287-020-01809-1.
- Savickienė J, Baronaitė S, Zentelytė A, Treigyte G, Navakauskienė R. Senescence-Associated Molecular and Epigenetic Alterations in Mesenchymal Stem Cell Cultures from Amniotic Fluid of Normal and Fetus-Affected Pregnancy. *Stem Cells Int*. 2016. 2016:2019498. doi: 10.1155/2016/2019498.
- Savickiene J, Treigyte G, Baronaite S, Valiulienė G, Kaupinis A, Valius M, et al. Human Amniotic Fluid Mesenchymal Stem Cells from Second- and Third-Trimester Amniocentesis: Differentiation Potential, Molecular Signature, and Proteome Analysis. *Stem Cells Int*. 2015. 2015:319238. doi: 10.1155/2015/319238.
- Schieke SM, Ma M, Cao L, McCoy JP, Liu C, Hensel N, et al. Mitochondrial metabolism modulates differentiation and teratoma formation capacity in mouse embryonic stem cells. *J Biol Chem*. 2008. 283(42):28506–28512. doi: 10.1074/jbc.M802763200.

- Shahbazi A, Safa M, Alikarami F, Kargozar S, Asadi MH, Joghataei MT, Soleimani M. Rapid Induction of Neural Differentiation in Human Umbilical Cord Matrix Mesenchymal Stem Cells by cAMP-elevating Agents. *Int J Mol Cell Med*. 2016. 5(3):167–177.
- Shan Y, Liang Z, Xing Q, Zhang T, Wang B, Tian S, et al. PRC2 specifies ectoderm lineages and maintains pluripotency in primed but not naive ESCs. *Nat Commun*. 2017. 8(1):672. doi: 10.1038/s41467-017-00668-4.
- Shaw SWS, Cheng PJ, Chang YL, Chao A, Wang T, Chang S, et al. Human amniotic fluid stem cells have better potential in early second trimester of pregnancy and can be reprogrammed to iPS. *Taiwan J Obstet Gynecol*. 2017. 56(6):770–774. doi: 10.1016/j.tjog.2017.10.012.
- Shaw SW, Peng SY, Liang CC, Lin T, Cheng P, Hsieh T, et al. Prenatal transplantation of human amniotic fluid stem cell could improve clinical outcome of type III spinal muscular atrophy in mice. *Sci Rep*. 2021. 11(1):9158. doi: 10.1038/s41598-021-88559-z.
- Shin MH, Lee EG, Lee SH, Lee YS, Son H. Neural cell adhesion molecule (NCAM) promotes the differentiation of hippocampal precursor cells to a neuronal lineage, especially to a glutamatergic neural cell type. *Exp Mol Med*. 2002. 34(6):401–410. doi: 10.1038/emmm.2002.57.
- Siegel N, Rosner M, Hanneder M, Valli A, Hengstschläger M. Stem cells in amniotic fluid as new tools to study human genetic diseases. *Stem Cell Rev*. 2007. 3(4):256–264. doi: 10.1007/s12015-007-9003-z.
- Sincennes MC, Brun CE, Rudnicki MA. Concise review: epigenetic regulation of myogenesis in health and disease. *Stem Cells Transl Med*. 2016. 5(3):282–290. doi: 10.5966/sctm.2015-0266.
- Sjöblom B, Salmazo A, Djinović-Carugo K. Alpha-actinin structure and regulation. *Cell Mol Life Sci*. 2008. 65(17):2688–2701. doi: 10.1007/s00018-008-8080-8.
- Son M, Jeong J, Kwon Y, Ryu J, Mun S, Kim H, et al. A novel and safe small molecule enhances hair follicle regeneration by facilitating metabolic reprogramming. *Exp Mol Med*. 2018. 50(12):1–15. doi: 10.1038/s12276-018-0185-z.
- Song Y, Lee S, Jho EH. Enhancement of neuronal differentiation by using small molecules modulating Nodal/Smad, Wnt/ $\beta$ -catenin, and FGF signaling. *Biochem Biophys Res Commun*. 2018. 503(1):352–358. doi: 10.1016/j.bbrc.2018.06.033.
- Spitzhorn LS, Rahman MS, Schwindt L, Ho HT, Wruck W, Bohndorf M, et al. Isolation and Molecular Characterization of Amniotic Fluid-Derived Mesenchymal Stem Cells Obtained from Caesarean Sections. *Stem Cells Int*. 2017. 2017:5932706. doi: 10.1155/2017/5932706.
- Sun Y, Xu L, Huang S, Hou Y, Liu Y, Chan KM, et al. mir-21 overexpressing mesenchymal stem cells accelerate fracture healing in a rat closed femur fracture model. *Biomed Res Int*. 2015. 2015:412327. doi: 10.1155/2015/412327.



- Tan J, Lu J, Huang W, Dong Z, Kong C, Li L, et al. Genome-wide analysis of histone H3 lysine9 modifications in human mesenchymal stem cell osteogenic differentiation. *PLoS One*. 2009. 4(8):e6792. doi: 10.1371/journal.pone.0006792.
- Tontonoz P, Hu E, Spiegelman BM. Stimulation of adipogenesis in fibroblasts by PPAR gamma 2, a lipid-activated transcription factor. *Cell*. 1994. 79(7):1147–1156. doi: 10.1016/0092-8674(94)90006-x.
- Trohatou O, Anagnou NP, Roubelakis MG. Human amniotic fluid stem cells as an attractive tool for clinical applications. *Curr Stem Cell Res Ther*. 2013. 8(2):125–132. doi: 10.2174/1574888x11308020003.
- Tsogtbaatar E, Landin C, Minter-Dykhouse K, Folmes CDL. Energy metabolism regulates stem cell pluripotency. *Front Cell Dev Biol*. 2020. 8:87. doi: 10.3389/fcell.2020.00087.
- Vadasz S, Jensen T, Moncada C, Girard E, Zhang F, Blanchette A, Finck C. Second and third trimester amniotic fluid mesenchymal stem cells can repopulate a decellularized lung scaffold and express lung markers. *J Pediatr Surg*. 2014. 49(11):1554–1563. doi: 10.1016/j.jpedsurg.2014.04.006.
- Wang T, Chen K, Zeng X, Yang J, Wu Y, Shi X, et al. The histone demethylases Jhdmla/1b enhance somatic cell reprogramming in a vitamin-C-dependent manner. *Cell Stem Cell*. 2011. 9(6):575–587. doi: 10.1016/j.stem.2011.10.005.
- Watanabe D, Uchiyama K, Hanaoka K. Transition of mouse de novo methyltransferases expression from Dnmt3b to Dnmt3a during neural progenitor cell development. *Neuroscience*. 2006. 142(3):727–737. doi: 10.1016/j.neuroscience.2006.07.053.
- Wei Y, Chen YH, Li LY, Lang J, Yeh SP, Shi B, et al. CDK1-dependent phosphorylation of EZH2 suppresses methylation of H3K27 and promotes osteogenic differentiation of human mesenchymal stem cells. *Nat Cell Biol*. 2011. 13(1):87–94. doi: 10.1038/ncb2139.
- Wu H, Sun Y. Epigenetic Regulation of Stem Cell Differentiation. *Pediatr Res*. 2006. 59(4 Pt 2):21R–25R. doi: 10.1203/01.pdr.0000203565.76028.2a.
- Xu G, Wu F, Gu X, Zhang J, You K, Chen Y, et al. Direct Conversion of Human Urine Cells to Neurons by Small Molecules. *Sci Rep*. 2019. 9(1):16707. doi: 10.1038/s41598-019-53007-6.
- Yaffe D, Saxel O. A myogenic cell line with altered serum requirements for differentiation. *Differentiation*. 1977. 7(3):159–166. doi: 10.1111/j.1432-0436.1977.tb01507.x.
- Yan ZJ, Hu YQ, Zhang HT, Zhang P, Xiao Z, Sun X, et al. Comparison of the neural differentiation potential of human mesenchymal stem cells from amniotic fluid and adult bone marrow. *Cell Mol Neurobiol*. 2013. 33(4):465–475. doi: 10.1007/s10571-013-9922-y.
- Yang C, Wu M, You M, Chen Y, Luo M, Chen Q. The therapeutic applications of mesenchymal stromal cells from human perinatal tissues in autoimmune diseases. *Stem Cell Res Ther*. 2021. 12(1):103. doi: 10.1186/s13287-021-02158-3.

- Yoo EJ, Chung JJ, Choe SS, Kim KH, Kim JB. Down-regulation of histone deacetylases stimulates adipocyte differentiation. *J Biol Chem.* 2006. 281(10):6608–6615. doi: 10.1074/jbc.M508982200.
- Yu L, Ji KY, Zhang J, Xu Y, Ying Y, Mai T, et al. Core pluripotency factors promote glycolysis of human embryonic stem cells by activating GLUT1 enhancer. *Protein Cell.* 2019. 10(9):668–680. doi: 10.1007/s13238-019-0637-9.
- Yu NH, Chun SY, Ha YS, Kim HT, Lih E, Kim DH, et al. In Vivo Safety and Regeneration of Long-Term Transported Amniotic Fluid Stem Cells for Renal Regeneration. *Tissue Eng Regen Med.* 2019. 16(1):81–92. doi: 10.1007/s13770-018-0162-6.
- Yu S, Levi L, Siegel R, Noy N. Retinoic acid induces neurogenesis by activating both retinoic acid receptors (RARs) and peroxisome proliferator-activated receptor  $\beta/\delta$  (PPAR $\beta/\delta$ ). *J Biol Chem.* 2012. 287(50):42195–42205. doi: 10.1074/jbc.M112.410381.
- Yuan J, Zhang S, Zhang Y. Nrf1 is paved as a new strategic avenue to prevent and treat cancer, neurodegenerative and other diseases. *Toxicol Appl Pharmacol.* 2018. 360:273–283. doi: 10.1016/j.taap.2018.09.037.
- Zammit PS. Function of the myogenic regulatory factors Myf5, MyoD, Myogenin and MRF4 in skeletal muscle, satellite cells and regenerative myogenesis. *Semin Cell Dev Biol.* 2017. 72:19–32. doi: 10.1016/j.semcdb.2017.11.011.
- Zhang F, Cui J, Liu X, Lv B, Liu X, Xie Z, Yu B. Roles of microRNA-34a targeting SIRT1 in mesenchymal stem cells. *Stem Cell Res Ther.* 2015. 6:195. doi: 10.1186/s13287-015-0187-x.
- Zhang JG, Shi Y, Hong DF, Song M, Huang D, Wang CY, Zhao G. MiR-148b suppresses cell proliferation and invasion in hepatocellular carcinoma by targeting WNT1/ $\beta$ -catenin pathway. *Sci Rep.* 2017. 7:46886. doi: 10.1038/srep46886.
- Zhang L, Seitz LC, Abramczyk AM, Liu L, Chan C. cAMP initiates early phase neuron-like morphology changes and late phase neural differentiation in mesenchymal stem cells. *Cell Mol Life Sci.* 2011. 68(5):863–876. doi: 10.1007/s00018-010-0497-1.
- Zhang P, Li J, Qi Y, Zou Y, Liu L, Tang X, et al. Vitamin C promotes the proliferation of human adipose-derived stem cells via p53-p21 pathway. *Organogenesis.* 2016. 12(3):143–51. doi: 10.1080/15476278.2016.1194148.

Internetinēs svetainēs:

who.int [internetinē svetainē]. Congenital anomalies [žiūrēta 2021-10-20]. Adresas: <https://www.who.int/health-topics/congenital-anomalies>

Elektroninēs knygos:

Cheng EY. „Avery’s Diseases of the Newborn (10th Edition)“. Skyrius „Prenatal Diagnosis“. Leidējas Elsevier Inc.; 2018. ISBN: 978-0-323-40139-5.

## REZULTATŲ VIEŠINIMAS

### Žodiniai pranešimai:

1. **A. Zentelytė**, E. Beržanskytė, G. Valiulienė, R. Navakauskienė. Neurogenic Differentiation of Human Amniotic Fluid Stem Cells from Healthy and Fetus Affected Pregnancies. Open Readings, Vilnius, Lithuania, 2021.

2. **A. Zentelytė**, V.V. Borutinskaitė, R. Navakauskienė. Amniotic fluid – the untapped source of stem cells. The Coins, Vilnius, Lithuania. 2020.

### Stendiniai pranešimai:

1. E. Beržanskytė, **A. Zentelytė**, G. Valiulienė, R. Navakauskienė. Neural Differentiation and Neuron-Type Specific Marker Expression of Human Amniotic Fluid-Derived Stem Cells Grown In 3D Cultures. The Coins, Vilnius, Lithuania, 2021.

2. E. Beržanskytė, **A. Zentelytė**, G. Valiulienė, R. Navakauskienė. Neural Gene Expression Patterns Of Differentiated Human Amniotic Fluid Stem Cells. Open Readings, Vilnius, Lietuva, 2020.

3. E. Beržanskytė, **A. Zentelytė**, G. Valiulienė, R. Navakauskienė. Neural differentiation and neuron-type specific markers expression of human amniotic fluid-derived stem cells. Vita Scientia, Vilnius, Lithuania, 2020.

4. **A. Zentelytė**, D. Žukauskaitė, V. Borutinskaitė, R. Navakauskienė. Neural differentiation and gene expression of human amniotic fluid stem cells derived from healthy and foetus Down syndrome pregnancies. 3rd International Conference on Stem Cells, Chania, Crete, Greece, 2019.

5. **A. Zentelytė**, G. Treigytė, S. Baronaitė, N. Krasovskaja, J. Savickienė, V. Borutinskaitė, R. Navakauskienė. Epigenetics of adipogenic and osteogenic differentiation of MSCs isolated from amniotic fluid of healthy and fetus-affected pregnancies. Cambridge International Stem Cell Symposium, Cambridge, United Kingdom, 2018.

6. **A. Zentelytė**, S. Baronaitė, N. Krasovskaja, J. Savickienė, R. Navakauskienė. Characteristics and differentiation profiles of human stem cells isolated from amniotic fluid of healthy and pathological pregnancies. XVth International Conference of the Lithuanian Biochemical Society, Dubingiai, Lithuania, 2018.

## PADĖKA

Norėčiau nuoširdžiai padėkoti savo mokslinio darbo vadovėms dr. Veronikai Borutinskaitei ir prof. dr. Rūtai Navakauskienei už suteiktą galimybę studijuoti doktorantūrą ir atlikti mokslinius tyrimus Ląstelės molekulinės biologijos skyriuje. Dėkoju už tikėjimą manimi, suteiktas žinias, padaršinimą ir paskatinimą vis žengti pirmyn. Jūsų dėka galėjau tobulėti ir augti ne tik kaip mokslininkė, bet ir kaip žmogus.

Taip pat labai norėčiau padėkoti Ląstelės molekulinės biologijos skyriaus esamiems ir buvusiems kolegoms už šiltą priėmimą, visokeriopą pagalbą, palaikymą ir smagius pokalbius. Ypatingai ačiū dr. Giedrei Valiulienei, dr. Aidai Vitkevičienei, dr. Monikai Gasiūnienei, dr. Sandrai Baronaitei, Deimantei Žukauskaitei, Giedrei Skliutei ir Elvinai Valatkaitei už puikią atmosferą, už juoką, už pasidalijimą džiaugsmiais ir vargais, o svarbiausia už draugystę.

Esu dėkinga magistro ir bakalauro studijų studentėms Ievai Jacerytei ir Elizabet Beržanskytei, kurios savo darbais svariai prisidėjo prie šioje disertacijoje aptariamų rezultatų, o vadovaujant jų baigiamiesiems darbams pati daug mokiausi ir tobulėjau.

Didžiausias ačiū patiems artimiausiems už palaikymą, motyvaciją, tikėjimą manimi, labai tai vertinu ir labai jus branginu. Ačiū tėveliams, ačiū Žygimantui ir Pronto, ačiū Viktorijai už palaikymą, kai buvo sunku, už paskatinimą, kai abejojau savimi, už buvimą šalia, kai man to reikėjo. Esu be galo dėkinga ir labai jus visus myliu.

## CURRICULUM VITAE

**Vardas, Pavardė:** Aistė Zentelytė

### **Išsilavinimas:**

- 2017-2021: Biochemijos mokslo krypties doktorantūra; Vilniaus universitetas, Lietuva
- 2014-2016: Biotechnologijų magistras (Nanobiotechnologijos); Vilniaus Gedimino technikos universitetas, Lietuva
- 2010-2014: Biotechnologijų bakalauras (Bioinžinerija); Vilniaus Gedimino technikos universitetas, Lietuva

### **Darbo patirtis:**

- 2015-dabar: Specialistė / Jaunesnioji mokslo darbuotoja, Vilniaus universitetas, Gyvybės mokslų centras, Vilnius, Lietuva
- 2019-2021: Jaunesnioji mokslo darbuotoja; UAB Nanodiagnostika, Antezeriai, Lietuva

### **Dalyvavimas moksliniuose projektuose**

- Inovatyvių terapijų ir prognostinių įrankių, skirtų chemoterapijai atsparios ūminės mieloleukemijos gydymui, sukūrimas. Projekto Nr. S-SEN-20-2
- Pažangios technologijos inovatyviam nevaisingumo gydymui. Projekto Nr. 01.2.2-MITA-K702-12-0004
- Gydymui atsparios depresijos fiziologinių požymių ir dinamikos tyrimas: biožymenų paieška. Projekto Nr. MSF-LMT-6
- Mezenchiminių kamieninių ląstelių egzosomų panaudojimo medikamentams atsparios depresijos gydymui įvertinimas. Projekto Nr. MSF-LMT-3/2020
- Žmogaus vaisiaus vandenų kamieninių ląstelių nervinės diferenciacijos tyrimas. Projekto Nr. MSF-JM-4
- Nevaisingumo gydymo panaudojant kamienines ląsteles technologijos modelio kūrimas". Projekto Nr. S-J05-LVPA-K-04-0028
- Hematologinės sistemos molekuliniai veiksniai ir jų vaidmuo žmogaus ląstelių senėjimo, diferenciacijos ir regeneracijos sankirtoje. Projekto Nr. SEN-12/2015
- Epigenetinių veiksnių ir mikro RNR vaidmuo vaisiaus vandenų kamieninių ląstelių funkcionavime“. Projekto Nr. MIP-57/2015
- Biotechnologija ir biofarmacija: fundamentiniai ir taikomieji tyrimai. Projekto Nr. VP1-3.1-ŠMM-08-K-01-005

## PRIEDAI

**Priedas Nr.1** Tyrimuose naudoti prietaisai, reagentai ir komerciniai rinkiniai.

<b>Prietaisas</b>	<b>Gamintojas</b>	
Seahorse XFp Extracellular Flux Analyzer	<i>Agilent Technologies, JAV</i>	
BD FACSCanto™ II	<i>BD Biosciences, JAV</i>	
Rotor-Gene™ 6000	<i>Corbett Life Science, Australija</i>	
Guava® easyCyte 8HT	<i>Millipore, JAV</i>	
ECLIPSE E200	<i>Nikon, Japonija</i>	
Infinite M200 Pro	<i>Tecan, Šveicarija</i>	
EVOS FL	<i>Thermo Fisher Scientific, JAV</i>	
Varioskan Flash Multimode Reader		
Zeiss Axio Observer	<i>Zeiss, Vokietija</i>	
<b>Reagentai</b>	<b>Gamintojas</b>	
Chemiluminescence Detection Kit	<i>Amersham Pharmacia, Švedija</i>	
Vitaminas C	<i>Armila, Lietuva</i>	
NutriStem® hPSC XF terpė	<i>Biological Industries, Izraelis</i>	
AmnioMAX™ C-100 bazinė terpė	<i>Gibco, Thermo Fisher Scientific, JAV</i>	
AmnioMAX™ C-100 priedas		
DMEM/F12 su GlutaMax™		
DMEM (4,5 g/l gliukozės)		
DMEM (1 g/l gliukozės)		
FBS		
Arklis serumas		
N2 priedas		
B27 priedas		
100 U/ml penicilino ir 100 µg/ml streptomicino tirpalas		<i>Gibco, Thermo Fisher Scientific, JAV</i> <i>Genaxxon bioscience, Vokietija</i>
TRIzol®	<i>Invitrogen, Thermo Fisher Scientific, JAV</i>	
DAPI		
Alexa Fluor® 594 Phalloidin		
Giemsas dažai	<i>Merck, JAV</i>	
Trihostatinas A	<i>Sigma-Aldrich, JAV</i>	
Natrio butiratas		
retinoinė rūgštis		
MTT		
KCl		
NeuroCult™		<i>STEMCELL Technologies, Kanada</i>
BrainPhys™		
8-Br-cAMP		<i>PeproTech, JAV</i>
IBMX		
BDNF		
NGF		
FGF		
EGF		

Priedas Nr.1 tęsinys		
<b>Komerciniai rinkiniai</b>		<b>Gamintojas</b>
Glycolysis Assay		<i>Abcam, JK</i>
Extracellular O <sub>2</sub> Consumption Assay		
TMRE Mitochondrial Membrane Potential Assay		
Luminescent ATP Detection Assay		
DCFDA Cellular ROS Detection Assay Kit		
Cell Energy Phenotype Test Kit		<i>Agilent Technologies, JAV</i>
SensiFAST™ cDNA Synthesis Kit		<i>Bioline, JK</i>
SensiFAST™ SYBR® No-ROX Kit		
StemPro™ Adipogenesis Differentiation Kit		<i>Gibco, Thermo Fisher Scientific, JAV</i>
StemPro™ Osteogenesis Differentiation Kit		
BDNF, VEGF, TNFα, IL-1β, IL-6, IL-10 ELISA Kits		<i>R&amp;D Systems, JAV</i>
TaqMan™ MicroRNA Reverse Transcription Kit		<i>Thermo Fisher Scientific, JAV</i>
TaqMan™ MicroRNA Assay		
TaqMan™ Universal PCR Master Mix II, no UNG		
Maxima First Strand cDNA Synthesis Kit		<i>Thermo Scientific, Lietuva</i>
Maxima SYBR Green qPCR Master Mix		
<b>Antikūnas</b>	<b>Fluoroforas</b>	<b>Gamintojas</b>
anti-TUBB3	FITC	<i>Abcam, JK</i>
anti-Vimentin	Alexa Fluor® 488	
anti-NCAM	-	
anti- GAPDH	-	<i>Biolgend, JAV</i>
anti-CD105	PE	
anti-CD166		
anti-Notch1		
anti-CD31	Alexa Fluor® 488	
anti-HLA-ABC		
anti-HLA-DR		
anti-Sox2		
anti-CD34	FITC	
anti-CD90		
anti-CD44		
anti-CD56		
anti-CD117		
anti-CD133	APC	
anti-CD146		
anti-CD309		
anti-CD338		
anti-SSEA4		
anti-Nanog	Alexa Fluor® 647	
anti-Oct4		
anti-Lin28a	-	
anti-c-Myc		

Priedas Nr.1 tęsinys		
Antikūnas	Fluoroforas	Gamintojas
anti- EZH2	-	<i>Cell Signaling Technology, JAV</i>
anti- SUZ12		
anti-CD15	PE	<i>Exbio, Čekija</i>
anti-CD9	FITC	
anti-CD73	APC	
anti-CD13		
anti-CD90		
anti-CD117		
anti-CD105	PE	
anti-TRA-1-60	FITC	
anti-CD44		
anti-TRA-1-81	APC	
anti- H3K4me3	-	<i>Millipore, JAV</i>
anti- H3K9me3		
anti- H3K27me3		
anti- BMI1		
anti- H4hyperAc		
anti-CD34	FITC	<i>Miltenyi Biotec, Vokietija</i>
anti-CD90	FITC	<i>Molecular Probes, Thermo Fisher Scientific, JAV</i>
anti-Nestin	-	<i>Novus Biologicals, JAV</i>
anti-Musashi1		
anti-DNMT1	-	<i>Santa Cruz Biotechnology, JAV</i>
anti-HDAC1		



## PUBLIKACIJŲ KOPIJOS

1 publikacija / publication 1

M. Gasiūnienė, **A. Zentelytė**, G. Treigytė, S. Baronaitė, J. Savickienė, A. Utkus, R. Navakauskienė

Epigenetic alterations in amniotic fluid mesenchymal stem cells derived from normal and fetus-affected gestations: a focus on myogenic and neural differentiations

2019; *Cell Biology International*, 43:299-312

doi: 10.1002/cbin.11099


Copyright © 2019 International Federation for Cell Biology

Perspausdinta su John Wiley and Sons leidimu (licencijos nr. 5181881162115)

Reproduced with John Wiley and Sons permission (license no. 5181881162115)

RESEARCH ARTICLE

# Epigenetic alterations in amniotic fluid mesenchymal stem cells derived from normal and fetus-affected gestations: A focus on myogenic and neural differentiations

Monika Gasiūnienė <sup>1\*</sup>, Aistė Zentelytė<sup>1</sup>, Gražina Treigyte<sup>1</sup>, Sandra Baronaitė<sup>1</sup>, Jūratė Savickienė<sup>1</sup>, Algirdas Utkus<sup>2</sup> and Rūta Navakauskienė<sup>1</sup>

<sup>1</sup> Department of Molecular Cell Biology, Institute of Biochemistry, Life Sciences Center, Vilnius University, Sauletekio av. 7, Vilnius LT-10257, Lithuania  
<sup>2</sup> Department of Human and Medical Genetics, Faculty of Medicine, Vilnius University, M. K. Ciurlionio st. 21, Vilnius LT-03101, Lithuania

## Abstract

Amniotic fluid-derived mesenchymal stem cells (AF-MSCs) are autologous to the fetus and represent a potential alternative source for the regenerative medicine and treatment of perinatal disorders. To date, AF-MSCs differentiation capacity to non-mesodermal lineages and epigenetic regulation are still poorly characterized. The present study investigated the differentiation potential of AF-MSCs toward neural-like cells in comparison to the mesodermal myogenic lineage and assessed epigenetic factors involved in tissue-specific differentiation. Myogenic and neural differentiation assays were performed by the incubation with specific induction media. Typical MSCs markers were determined by flow cytometry, the expression of lineage-specific genes, microRNAs and chromatin modifying proteins were examined by RT-qPCR and Western blot, respectively. AF-MSCs of normal and fetus-affected gestations had similar stem cells characteristics and two-lineage potential, as characterized by cell morphology and the expression of myogenic and neural markers. Two-lineage differentiation process was associated with the down-regulation of miR-17 and miR-21, the up-regulation of miR-34a, miR-146a and *DNMT3a/DNMT3b* along with the gradual decrease in the levels of DNMT1, HDAC1, active marks of chromatin (H4hyperAc, H3K9ac, H3K4me3) and the repressive H3K9me3 mark. Differentiation was accompanied by the down-regulation of PRC1/2 proteins (BMI1/SUZ12, EZH2) and the retention of the repressive H3K27me3 mark. We report that both AF-MSCs of normal and fetus-affected gestations possess differentiation capacity toward myogenic and neural lineages through rather similar epigenetic mechanisms that may provide potential applications for further investigation of the molecular basis of prenatal diseases and for the future autologous therapy.

**Keywords:** chromatin remodeling; histone modifications; microRNA; polycomb repressive complex 1/2

## Introduction

Human amniotic fluid (AF) contains mesenchymal stem cells (MSC) possessing a multi-lineage differentiation potential, low immune response, non-tumorigenicity and minimal ethical problems (Bossolasco et al., 2006; Perin et al., 2008). Therefore, AF-MSCs may be employed as a tool for basic research, in regenerative medicine and clinical applications for degenerative diseases (Da Sacco et al., 2011; Joo et al., 2012;

Trohatou et al., 2013; Kim et al., 2014) as well as for the neonatal cell therapy (Ekblad et al., 2015). These prenatal state stem cells can be considered as “young” and, isolated from different donors at the similar time of pregnancies, have the same “gestational age” and properties. However, AF-MSCs from different gestational ages are marked by variability in their features (Maguire et al., 2013) similarly to adipose tissue-derived MSCs that have differences in growth kinetics, morphology, differentiation potential and senescence

\*Corresponding author: e-mail: monika.gasiuniene@gmc.vu.lt

Conflict of interest: None.

**Abbreviations:** AF-MSCs, amniotic fluid mesenchymal stem cells; BMI1, B lymphoma Mo-MLV insertion region 1; EED, embryonic ectoderm development; EZH2, enhancer of zeste 2; PPAR- $\gamma$ , peroxisome proliferator-activated receptor-gamma; PRC 1/2, polycomb repressive complex 1/2; Sox2, Sry-related HMG-box 2; SUZ12, suppressor of zeste 12

dependent on the donor age (Kornicka et al., 2015; Maređziak et al., 2016). In addition, AF-MSCs possess better expansion, yield, recovery properties than amniotic epithelial cells obtained from placenta (Di Germanio et al., 2016). We have reported that MSCs derived from AF of a normal gestation have a potential to differentiate into both mesodermal and neuroectodermal lineages (Savickiene et al., 2015; Glemzaite and Navakauskiene, 2016). However, no evidence exists that AF-MSCs from AF of fetus-diseased gestations have the capability to neural or myogenic differentiation. Recent studies have shown that MSCs isolated from perinatal tissues can differentiate into cells of neuroectodermal lineage (Tamagawa et al., 2008; Kwon et al., 2016). MSCs derived from AF or amniotic membrane generated terminally differentiated neural cells expressing neurotransmitters, brain-derived and nerve growth factors, which lead to bio-delivery and regeneration of the damaged tissue (Pan et al., 2006; Yan et al., 2013; Kim et al., 2014; Maraldi et al., 2014). Therefore, these properties made them suitable for novel approaches for stem cell therapy in neurodegenerative disorders. To date, the epigenetic differentiation mechanisms underlying AF-MSCs mesodermal and ectodermal lineage differentiation are not fully understood. It has been suggested that epigenetic factors, such as histone modifications, Polycomb group (PcG) proteins and chromatin epigenetic modifiers, could contribute to these processes. PcG proteins comprise two Polycomb repressive complexes, PRC1 and PRC2, containing intrinsic histone modifying activities. EZH2 containing PRC2, which also requires SUZ12 and EED, initiates transcription repression maintained by PRC1 (Schwartz and Pirrotta, 2008). Additionally, the pluripotency transcription factors, Oct4, Nanog and Sox2, are responsible for the self-renewal simultaneously repressing genes that mediate the differentiation and determination of the state during ESCs differentiation (Kashyap et al., 2009). Among epigenetic modifiers, microRNAs are known as regulators of neurogenesis and skeletal myogenesis (Liu and Zhao, 2009; Ge and Chen, 2011). Myogenesis process that involves myogenic lineage commitment, differentiation to myoblasts and formation of multi-nucleated myotubes undergoes a complex of morphological and molecular changes and is regulated by a family of myogenic regulatory factors (MRFs) required for the lineage determination and terminal differentiation (Shimokawa et al., 1998; Blais et al., 2005) in collaboration with histone modifying enzymes, including histone acetylation for activation of muscle-specific genes and histone H3K27 methylation for their selective repression. Furthermore, PRC2 complexes play an important role in the regulation of terminal muscle differentiation (Caretti et al., 2004; Cao et al., 2010). Despite a large amount of information, AF-MSCs myogenic differentiation is not comprehensively studied in terms of dynamic changes in histone modifications and PcG proteins.

Our study demonstrates that AF-MSCs isolated from amniocentesis samples of normal gestations and those with fetal abnormalities have similar ability to differentiate into myogenic and neural lineages and reveals molecular mechanisms at the gene expression and epigenetic levels involved in lineage-specific differentiation.

## Materials and methods

### Isolation of MSCs from amniotic fluid and their cultivation

AF samples (about 5 mL) were obtained by biopsy (amniocentesis) from mid second trimester (17–20 week) or late third trimester (31–32 week) pregnant women who needed prenatal diagnostics using protocols approved by the Ethics Committee of Biomedical Researches of Vilnius District No 158200-123-428-122. Samples ( $n = 3$  from healthy donors [N] and  $n = 6$  from pathological gestations [Pat]) were maintained at the room temperature for about 4 h prior to the isolation of amniotic cells using a two-stage protocol (Tsai et al., 2004; Savickiene et al., 2015). It is based on different adherence properties of stem cells and other (mainly epithelial) cells residing in amniotic fluid. Briefly, the washed cell pellets were suspended in the growth medium (AmnioMAX<sup>TM</sup>-C100 basal medium with AmnioMAX<sup>TM</sup>-C100 supplement, 100 U/mL penicillin and 100  $\mu$ g/mL streptomycin [Gibco, Thermo Fisher Scientific, USA]) and plated in a 25-cm<sup>2</sup> culture flask (TPP, Switzerland). After 10–15 days the first colonies appeared (epithelial cells, first stage) and the cells that did not adhere yet (AF-MSCs) were collected and plated in a new culture flask. These cells attached to the flask later (second stage). Cells were subcultured at approximately 80% confluence with 0.05% trypsin-EDTA (Gibco, Thermo Fisher Scientific, USA).

### Flow cytometric analysis

For identification of the phenotype of AF-MSCs from passages 4–5, cells were collected by centrifugation at 600g for 6 min, washed once in phosphate buffered saline (PBS) with 0.2% fetal calf serum (FCS), and centrifuged again. A total of  $5 \times 10^5$  cells were resuspended in 50  $\mu$ L of PBS with 1% BSA and incubated with fluorescein isothiocyanate (FITC)-conjugated mouse anti-human antibodies against CD44 (Invitrogen, Thermo Fisher Scientific, USA), CD34 (Miltenyi Biotec, Germany), CD90 (Molecular Probes, Thermo Fisher Scientific, USA) or phycoerythrin (PE)-labelled CD105 (Invitrogen, Thermo Fisher Scientific, USA) and appropriate isotype controls—mouse IgG2A-FITC (Miltenyi Biotec, Germany), IgG1-FITC, IgG2B-FITC (Invitrogen, Thermo Fisher Scientific, USA) or IgG1-PE (Molecular Probes, Thermo Fisher Scientific, USA). Samples were incubated in the dark at 4°C for 30 min and finally

analyzed with the Millipore Guava<sup>®</sup> easyCyte 8HT flow cytometer, using the InCyte 2.2.2 software. Ten thousand events were collected for each sample.

### Differentiation assays

To confirm AF-MSCs differentiation potential into three lineages *in vitro*, STEMPro Differentiation media (Gibco, Thermo Fisher Scientific, USA) were used as described in our previous paper (Savickiene et al., 2015). For adipogenic differentiation, cells were cultured at 80% confluence and differentiation was induced with STEMPro Adipogenic Differentiation medium. After 12 days of differentiation, the formed lipid droplets were stained using Oil Red O solution (freshly diluted in distilled water at a ratio 3:2). For osteogenic differentiation, cells were cultured similarly and differentiated using STEMPro Osteogenic Differentiation medium. After 12 days of differentiation, a calcified extracellular matrix was stained with 2 % Alizarin Red solution (in deionized water). For chondrogenic differentiation, micromass cultures of AF-MSCs were generated and differentiated using STEMPro Chondrogenic Differentiation medium. Chondrogenic pellets were determined by staining with 1 % Alcian Blue (in 3% acetic acid).

For the myogenic differentiation, cells were plated at  $1 \times 10^4$  cells/cm<sup>2</sup> and cultured at 80% confluence, then washed with PBS before the incubation in DMEM containing 100 U/mL penicillin and 100 µg/mL streptomycin and 2% of horse serum (Gibco, Thermo Fisher Scientific, USA) for 12 days with low serum media changes every 2–3 days (Lin et al., 2014). Multinucleated cells were visualized by a phase contrast microscope (Nikon Eclipse TS100) after staining with 0.1% Crystal violet solution in 20% ethanol, followed by washes with water. For the neural differentiation, the induction medium (Park et al., 2007) containing 1.5 µM all-*trans* retinoic acid (RA) (Sigma, Germany) in DMEM/F12 with GlutaMax<sup>™</sup> and N2 supplement (Gibco, Thermo Fisher Scientific, USA) was used after culturing cells at 60% confluence. A morphologic change to neuron-like cells with axonal outgrowth was visualized by a phase contrast microscope after staining with 0.1% Crystal violet solution.

### RNA isolation and RT-qPCR

MSCs from AF samples of normal gestation and with fetus abnormalities were cultured up to four passages and analyzed for stem cell-specific genes-markers. Total RNA was extracted using TRIzol (Invitrogen, Thermo Fisher Scientific, USA), as recommended by the manufacturer, and then reverse transcribed into cDNA using Maxima First Strand cDNA Synthesis Kit for RT-qPCR (Thermo Scientific, Lithuania). Quantitative real-time-PCR (RT-qPCR) was performed with Maxima<sup>®</sup> SYBR Green qPCR

Master Mix (Thermo Scientific, Lithuania) on the Rotor-Gene 6000 system (Corbett Life Science).

Forward (F) and reverse (R) primers (5'-3') used in RT-qPCR were as follows:

OCT4 – F: CGAGAAGGATGTGGTCCGAG; R: CAGAGG AAAGGACACTGGTC

NANOG – F: AGATGCCTCACACGGAGACT; R: GTTTG CCTTTGGGACTGGTG

SOX2 – F: TGGACAGTTACGCGCACAT; R: CGAGTAG GACATGCTGTAGGT

REX1 – F: GCCTTATGTGATGGCTATGTGT; R: ACCCC TTATGACGCATTCTATGT

Nestin – F: CTGCTACCCTTGAGACACCTG; R: GGGCT CTGATCTCTGCATCTAC

NSE – F: CCCACTGATCCTTCCCAGATACAT; R: CCGAT CTGGTTGACCTTGAGCA

Actinin-α – F: CGAGCGCCATGAACCAGATA; R: GTGG AACCGCATTTTTCCCC

Calponin – F: TCCAAATATGACCCCCAGAA; R: CCCAC TCTCAAACAGGTCGT

Desmin – F: CCTACTCTGCCCTCAACTTC; R: AGTAT CCCAACACCCCTGCTC

MRF4 – F: AATCTTGAGGGTGCGGATTTTC; R: CTTAG CCGTTATACGAGCCC

DNMT3a – F: CAGCGTCACACAGAAGCATATCC; R: G GTCCTCACITTTGCTGAACCTGG

DNMT3b: – F: CCTGCTGAATTACTACGCCCC; R: GT CTGTGTAGTGACAGGAAA

GAPDH – F: TCCATGACAACITTTGGTATCG; R: TGTA GCCAAATTCGTTGTCA

The amount of mRNA was normalized to GAPDH. The relative difference in the expression level was calculated by a comparative threshold cycle delta-delta Ct method. The data is presented from at least three independent biological repeats each assayed in triplicate.

### MicroRNAs expression analysis

The expression of target miRNAs in AF-MSC samples was evaluated by RT-qPCR analysis using probe-based TaqMan MicroRNA Assays. Reverse transcription was performed using TaqMan<sup>®</sup> MicroRNA Reverse Transcription Kit (Thermo Fisher Scientific, USA), amplification was performed using Taqman<sup>®</sup> MicroRNA Assay and Taqman<sup>®</sup> Universal PCR Master Mix II, no UNG (Thermo Fisher Scientific, USA) according to the manufacturer's recommendations. Reactions were conducted in Arktik Thermocycler (Finnzymes) with a program as follows: 16°C for 30 min, 42°C for 30 min, 85°C for 5 min. The synthesized cDNA of each reaction was used as a template for qPCR. RT-qPCR was carried out in a Rotor-Gene 6000 system (Corbett Life Science). RNU 48 gene was used as a reference gene to normalize all experimental data. All reactions were performed

in triplicate, and relative expression of miRNA was calculated by a comparative threshold cycle delta-delta Ct method.

### Preparation of proteins and Western blotting

AF-MSCs (about  $5 \times 10^5$ ) were harvested by centrifugation (500g, 6 min) after trypsinization with 0.05 % trypsin-EDTA, washed twice in ice-cold PBS and resuspended in 10 volumes of lysis solution (62.5 mM Tris, pH 6.8, 100 mM DTT and 2% SDS, 10% glycerol, traces of bromphenol blue). Benzonase (Pure Grade, Merck) was added to give a final concentration of 2.5 units/ml. The cell lysate was prepared by homogenization through the needle No 21 on the ice and then centrifuged at 20,000g for 10 min, 4°C. The supernatants were immediately subjected to electrophoresis or frozen at -76°C. The lysates were separated on a 7–15% polyacrylamide gradient gel and then transferred onto the PVDF membrane. Membranes were incubated with primary antibodies according to the manufacturer's recommendations, and then with horseradish peroxidase-conjugated (HPR) secondary antibodies at room temperature for 1 h. The bands were developed using enhanced chemiluminescence detection (Amersham Pharmacia) according to the manufacturer instruction. The following primary antibodies were used: goat anti-DNMT1 and mouse anti-HDAC1 was from Santa Cruz Biotechnology; rabbit anti-EZH2 and SUZ12 were from Cell Signalling; rabbit anti-H3K4me3, H3K9me3, H3K27me3 and mouse anti-BMI1 were from Merck-Millipore; rabbit anti-H4hyperAc (penta acetyl) was from Upstate; mouse anti-GAPDH was from Abcam; goat anti-rabbit or rabbit anti-goat HPR-linked secondary antibodies were from Dako Cytomation A/S. The intensity of each band was quantified by densitometric analysis using ImageJ 1.45 S software (NIH, USA). Data from blots of MSCs samples from experimental groups were normalized to GAPDH (for DNMT1, HDAC1, EZH2, SUZ12, and BMI1 proteins) or H4 (for modified histones) loading controls and the relative fold change over control was calculated.

### Statistical analysis

All values of flow cytometry, RT-qPCR and Western blot analysis are expressed as mean  $\pm$  SD. One-way ANOVA with Tukey test was performed for data comparison, \* $P < 0.05$ , \*\* $P < 0.01$  and \*\*\* $P < 0.001$  were considered statistically significant.

## Results

### Characterization of AF-MSCs from normal gestations and those with fetal abnormalities

MSCs of healthy donors were isolated from AF at mid-second (17–20 weeks) trimester of gestation. AF-MSCs from

fetus-affected pregnancies included samples from donors carrying different fetal abnormalities: P1–dilated brain ventricles and fetal central nervous system pathology (17–20 week); P2–heart defect and flefotaxia (17–20 week); P3–Down syndrome—chromosome 21 trisomy (17–20 week); P4–multiple malformations and the universal fetus hydrocephalus (31–32 week); P5–nonimmune fetal hydrocephalus and anemia (17–20 week); P6–twin to twin transfusion syndrome (17–20 week). AF-MSCs from amniocentesis samples of normal (N) and fetus-affected (Pat) pregnancies were successfully isolated by a two-step protocol. A morphologically homogeneous population of spindle-shaped (mesenchymal-type) cells (Figure 1A) obtained after two rounds of subculture were typical both for normal and pathological pregnancies and they were used for experiments after 4–5 passages. AF-MSCs cultures that showed typical growth pattern expressed high levels of cell surface markers, such as CD44, CD90 and CD105, but did not express hematopoietic lineage marker CD34 when analyzed by flow cytometry (Figure 1B, AF-MSCs from healthy and representative pathology P4 pregnancies are shown). The comparison of AF-MSCs from N samples ( $n = 3$  donors) and Pat samples ( $n = 6$ , P1–P6 donors) demonstrated rather similar phenotypic characteristics maintaining the original CD44 and CD105 expression profile but with less portion of CD90 positive cells in Pat samples (Figures 1B and 1C). Also, AF-MSCs from healthy and fetus-affected gestations possessed differentiation potential into three lineages—adipogenic, osteogenic and neurogenic as determined by specific staining with Oil Red O, Alizarin Red and Alcian Blue, respectively (Figure 1D). Thus these stem cells from amniotic fluid were fully characterized as MSCs. In addition, RT-qPCR analysis showed that AF-MSCs from N and Pat samples expressed typical markers of pluripotency and self-renewal, such as *OCT4*, *NANOG*, *SOX2* and *REX1*. The expressional levels of those transcription factors did not differ significantly (Figure 1E) but varied more in pathological gestation samples, apparent from bigger standard deviation than in healthy gestations samples.

### Changes in the expression of differentiation-specific markers in AF-MSCs from normal and fetus-pathological gestations undergoing myogenic and neural differentiation

To investigate whether MSCs from two AF sources show the myogenic differentiation potential, MSCs were cultured for 5–12 days in myogenesis induction medium. No morphological differences were visible between AF-MSCs derived from N and Pat samples during myogenic differentiation, which was obvious at the 12th day of post-induction by the presence of multinucleated cells determined by phase contrast microscope after staining with 0.1 % Crystal violet

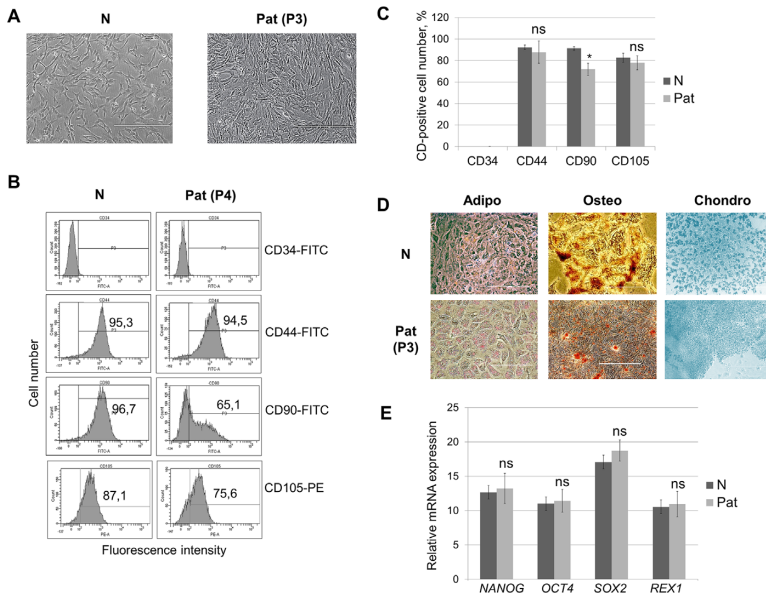


**Figure 1** Characterization of MSCs derived from AF of normal and fetus-affected gestations. (A) Morphology of spindle-shaped AF-MS cells from a healthy donor (N) and pathological (Pat (P3), Down syndrome) amniocentesis samples, representative images (scale bar = 400 μm). (B) The immunophenotypical characteristics of representative samples of MSCs from AF of a healthy (N) donor and a donor carrying multiple fetal malformations (Pat, P4) determined by flow cytometric analysis after incubation with fluorescent-conjugated antibodies against cell surface antigens CD44, CD90, CD105 and CD34. (C) The percentages of each surface marker of AF-MSCs of normal (N, n = 3) and fetus-affected (Pat, n = 6, P1–P6) gestations are shown as mean ± SD. (D) In vitro differentiation potential of AF-MSCs from a healthy donor (N) and a donor with Down syndrome (Pat, P3) into adipogenic (stained with Oil Red O), osteogenic (stained with Alizarin Red) and chondrogenic (stained with Alcian Blue) lineages, representative images (scale bar = 400 μm). (E) RT-qPCR analysis of pluripotency genes-markers in samples of AF-MSCs of normal (N, n = 3) and fetus-pathological (Pat, n = 6, P1–P6) gestations. mRNA expression levels were compared after normalization to *GAPDH* and presented as mean ± SD. \**P* < 0.05 indicates significant changes between N and Pat samples, ns, non-significant changes between N and Pat samples.

(Figure 2A, representative images for N and Pat samples) and the expression of myoblast-specific genes, such as *Calponin* and *Desmin* (both smooth muscle markers) and *Actinin-α* (skeletal muscle marker) as well as *MRF4* (myogenic regulatory factor 4). Relative mRNA expression of all genes was up-regulated in differentiated myoblasts from both N and Pat samples compared to undifferentiated control and no significant differences between N and Pat were detected in the levels of *Calponin* and *Desmin*, while *Actinin-α* expression was significantly higher in Pat samples (Figure 2B). On the contrary, the expression of *MRF4* that is required for the formation of myotubes was higher in differentiated cells from N samples. The obtained difference in the levels of expression of myogenic markers may be due to the differences in cell sources and their potency to myogenic differentiation.

To evaluate the neuro-ectodermal differentiation ability of AF-MSCs, cells were treated with RA containing neural differentiation medium. The early morphological changes were observed after 5 days of treatment, and typical

morphologies of neurons, such as elongated bodies, the presence of neurite-like projections and cell extensions, were observed after 12 days by phase contrast microscopy in differentiated cells from both N and Pat samples (Figure 3A, representative images for N and Pat samples). There were no obvious morphological differences between differentiating AF-MSCs of normal gestations and those with fetal abnormalities. Both morphological characteristics and gene expression pattern, confirmed by RT-qPCR, demonstrated the neural differentiation of AF-MSCs. As shown in Figure 3B, undifferentiated AF-MSCs were positive for *Nestin* (neural stem cell marker)—that is an indication of the neural potential of AF-MSCs. *Nestin* expression significantly increased during neural differentiation for 5–12 days but varied among individual N and Pat samples. The expression of this marker was significantly higher on the 5th day in Pat samples than in N samples and reached the same levels in both samples on the 12th day of differentiation (Figure 3B). The expression of *NSE* (neuron-specific enolase) gene gradually increased

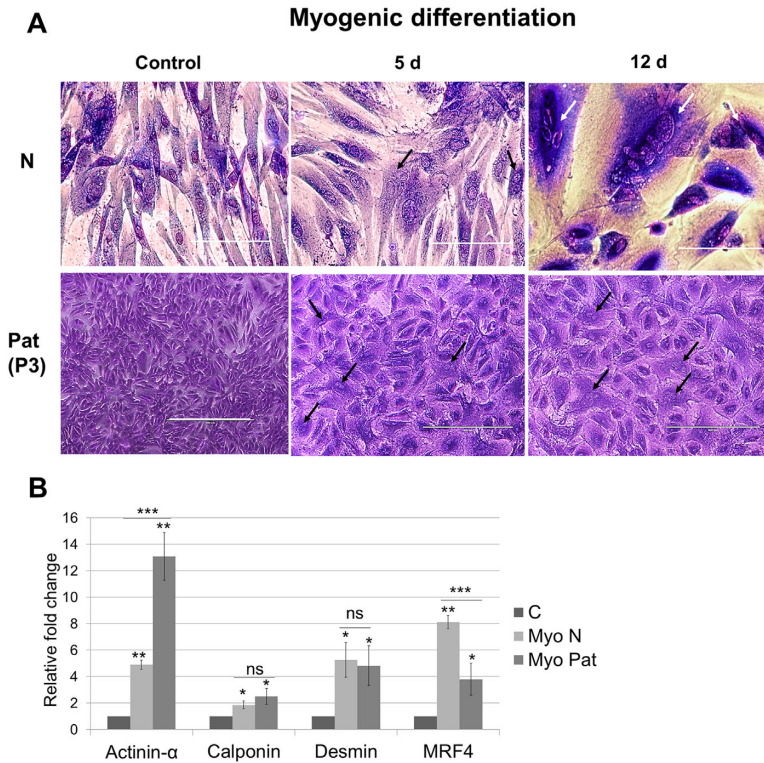


**Figure 2** Myogenic differentiation of MSCs derived from AF of normal and fetus-affected gestations. (A) Representative images of undifferentiated AF-MSCs and upon exposure to myogenic differentiation medium for 5 and 12 days (scale bars = 400 μm). AF-MSCs were from a normal (N) and fetus-pathological gestations (Pat [P3], Down syndrome). Multinucleated cells were visualized after staining with 0.1 % Crystal violet solution. (B) RT-qPCR analysis of myogenic genes-markers was performed using samples of AF-MSCs of normal (N, n = 3) and fetus-pathological (Pat, n = 4) gestations at the Day 12. Relative mRNA levels were calculated as a fold change of differentiated AF-MSCs relative to undifferentiated control (C) using a comparative threshold cycle delta-delta Ct method. All transcripts were normalized to *GAPDH*. The data are presented as mean ± SD. \* $P \leq 0.05$ , \*\* $P \leq 0.01$  and \*\*\* $P \leq 0.001$  were considered significant, ns, non-significant changes.

during neural differentiation (until the 12th day) being higher in neuron-like cells from Pat samples compared to N samples, implying that AF-MSCs were activated for the neural lineage but to the different extent, dependently on the source of AF-MSCs.

**Differential miRNAs expression in AF-MSCs undergoing myogenic and neural differentiation**

The miRNAs expression was investigated in MSCs derived from AF of normal pregnancies and carrying fetal abnormalities with the aim to reveal some differences regarding their functions related to induced differentiation to myocytes-like and neural-like cells. We performed RT-qPCR analysis for selected miRNAs, such as hsa-miR-17, hsa-miR-21, hsa-miR-34a and hsa-miR-146a that are implicated in the regulation of MSCs proliferation or

lineage-specific differentiation (Foshay and Gallicano, 2009; Krichevsky and Gabriely, 2009; Huszar and Payne, 2014; Park et al., 2015). A significant decrease in miR-17 expression was detected in AF-MSCs from both N and Pat samples differentiated into myoblasts and neural cells compared with undifferentiated control (Figures 4A and 4B). Expressional changes of miR-21 were minimal for those samples while the expression of miR-34a was up-regulated in both myocytes-like and neural cells but with a higher increase in Pat samples compared to N samples. Similarly, the levels of miR-146a were up-regulated in both types of differentiated cells from N and Pat samples compared to undifferentiated control. In addition, levels of miR-146a also increased more in differentiated Pat AF-MSCs in comparison to differentiated N AF-MSCs in both types of differentiation. Our results demonstrate that the differences in miRNAs expression during myogenic and neuronal



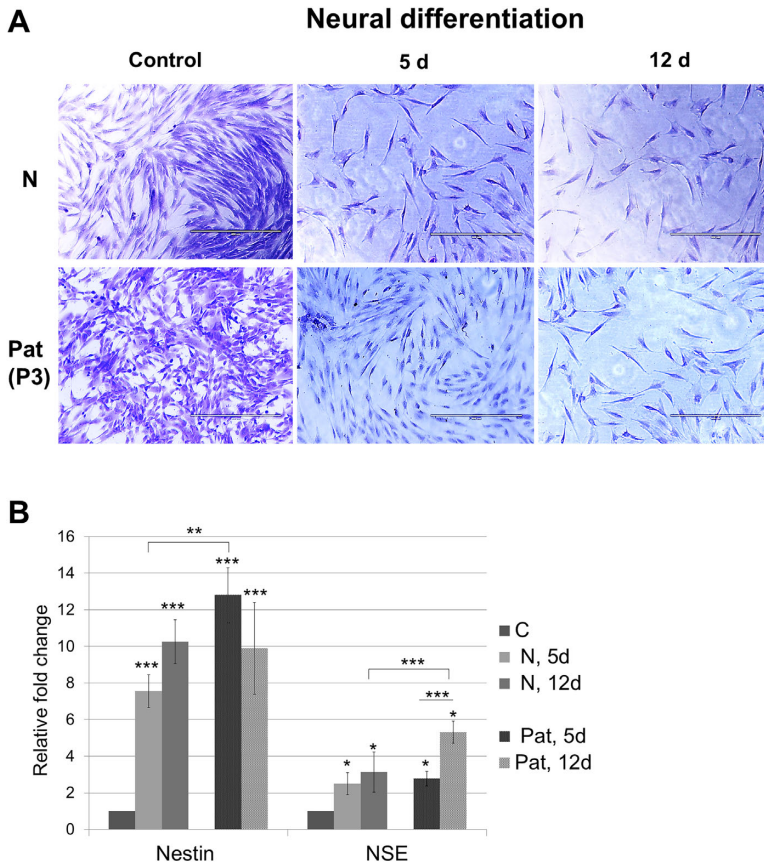


**Figure 3** Neural differentiation of MSCs derived from AF of normal and fetus-affected gestations. (A) Representative images of undifferentiated AF-MSCs and upon exposure to differentiation medium containing 1,5  $\mu$ M all-*trans* retinoic acid for 5 and 12 days (scale bars = 400  $\mu$ m). AF-MSCs were from a normal (N) and fetus-pathological gestations (Pat (P3), Down syndrome). A morphologic feature of neuronal cells with elongated bodies and their branched form was visualized after staining with 0.1 % Crystal violet solution. (B) RT-qPCR analysis of neuronal genes-markers was performed using samples of AF-MSCs of normal (N, n = 3) and fetus-pathological (Pat, n = 4) gestations at 5 and 12 days of differentiation. Relative mRNA levels were calculated as a fold change of differentiated AF-MSCs relative to undifferentiated control (C) using a comparative threshold cycle delta-delta Ct method. All transcripts were normalized to *GAPDH*. The data are presented as mean  $\pm$  SD. \* $P \leq 0.05$ , \*\* $P \leq 0.01$  and \*\*\* $P \leq 0.001$  were considered as significant changes.

differentiation exist in MSCs derived from AF at normal and fetus-affected conditions.

#### Epigenetic state alterations during myogenic and neural differentiation of AF-MSCs

To define the epigenetic environment of AF-MSCs, the core histone modifications, PcG proteins and DNA modifiers were analyzed at the global level. The comparison of the expression of histone modifications during myogenic and neural differentiation was performed using AF samples of normal pregnancy and those

with fetal abnormalities upon differentiation induction at the days 5 and 12. Figure 5A presents the representative Western blots of proteins from a healthy donor (N) and a donor carrying 21-trisomy-Down syndrome (P3, Pat). Quantified data from blots (Figures 5B and 5C) is presented as the average of calculations from both N and Pat samples as no significant differences were obtained between the levels of modified histones or proteins in N and Pat differentiated cells (separate calculations for N and Pat samples are not shown). Myogenic and neural differentiation was linked with the gradual decrease in the levels of chromatin activating histone modifications



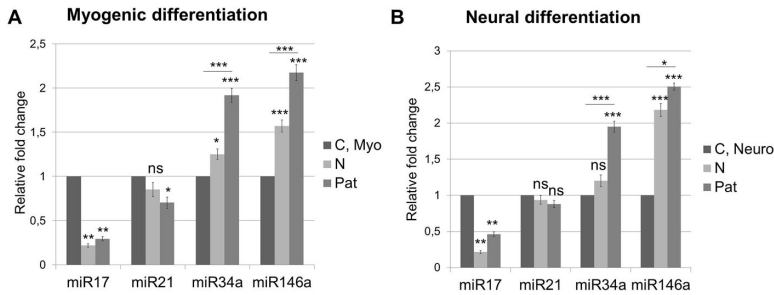


**Figure 4** Differentiation-induced changes in miRNAs expression in AF-MSCs undergoing myogenic and neural differentiation. miRNAs expression in AF-MSCs undergoing (A) myogenic and (B) neural differentiation (at the end of a 12-day period) in AF-MSCs of normal (N, n = 3) and fetus-pathological (Pat, n = 3) gestations was determined by RT-qPCR. miRNAs expression was normalized to RNU48 and the relative fold change between differentiated and undifferentiated (control, C) cells was calculated using a comparative threshold cycle delta-delta Ct method. Data are presented as mean  $\pm$  SD. \* $P \leq 0.05$ , \*\* $P \leq 0.01$  and \*\*\* $P \leq 0.001$  were considered as significant changes, ns, non-significant changes.

(H4hyperAc, H3K9ac, H3K4me3) and H3K9me3, the inactivating mark of heterochromatin. Conversely, the levels of the repressive H3K27me3 modification were increased in differentiated myocytes and neural cells at Day 12 compared to decreased levels of this mark after 5 days of differentiation induction. However, the expression of EZH2, which directly methylate H3K27me3, declined during myogenic and neural differentiation. Two-lineage differentiation process was also accompanied by the global decrease in the levels of HDAC1, DNMT1 and PRC2 protein SUZ12 (required for methyltransferase activity of EZH2 and histone H3K27 methylation) (Figures 6A and 6B). The expression of PRC1 protein BMI1 which maintains the repressive chromatin state also decreased but to a smaller extent during both types of differentiation (Figures 6A and 6B). Despite the fact that levels of chromatin remodeling proteins and histone modifications were rather similar in healthy and pathological samples, some differences in the relative *DNMT3a/DNMT3b* gene expression were detected between N and Pat differentiated AF-MSCs. RT-qPCR analysis demonstrated that myogenic differentiation was associated with a time-dependent increase in the expression of de novo methyltransferases genes, *DNMT3a/DNMT3b*, (Figure 6C) with higher expressional levels in differentiating AF-MSCs from Pat samples compared to N samples. Similarly, in cells, differentiated toward neural lineage, the increase in the expression of *DNMT3a/DNMT3b* genes was observed with the same tendency for *DNMT3a*. However, *DNMT3b* expression was upregulated more in differentiated N samples. Thus, PcG proteins, histone modifications and fluctuations in their global levels are implicated in the epigenetic mechanism of AF-MSCs differentiation into myogenic and neural

lineages and cell maintenance in the differentiated state at normal and fetus-diseased conditions.

## Discussion

In this study, we characterized MSCs from amniotic fluid by assessing the fibroblastic-like morphological features, the expression of a classical set of surface proteins and three-lineage differentiation potential in vitro according to the MSCs identification criteria proposed by the International Society for Cellular Therapy (Dominici et al., 2006). What is more, AF-MSCs have the capability of myogenic and neural differentiation as demonstrated in this study. These findings suggest that MSCs from amniotic fluid could occupy the niche in the stem cells hierarchy between pluripotent stem cells having the ability to differentiate into cells from all three germ layers (meso-, ecto- and endoderm) as well as into germline cells and more committed multipotent stem cells able to give rise to two germ layers (Ratajczak et al., 2014). Our study shows that AF-MSCs from normal and fetus-affected gestations did not differ significantly from each other in terms of morphology, phenotypic and pluripotency markers and their differentiation potential. However, we have observed the lower expression of the cell surface marker CD90 and variable levels of pluripotency markers, such as *NANOG*, *OCT4*, *SOX2* and *REX1*, in some fetus-pathological samples. It is important to take into account that amniocytes from multiple patients are marked by variability in the pluripotency markers expression and their genome-wide profiles are distinct at different gestational ages (Maguire et al., 2013), however, AF-MSCs used in this study were at the similar gestational age.

Myogenic differentiation was previously studied in MSCs from an adipose connective tissue, bone marrow and skeletal muscle tissue that exhibited the highest rate of myogenic

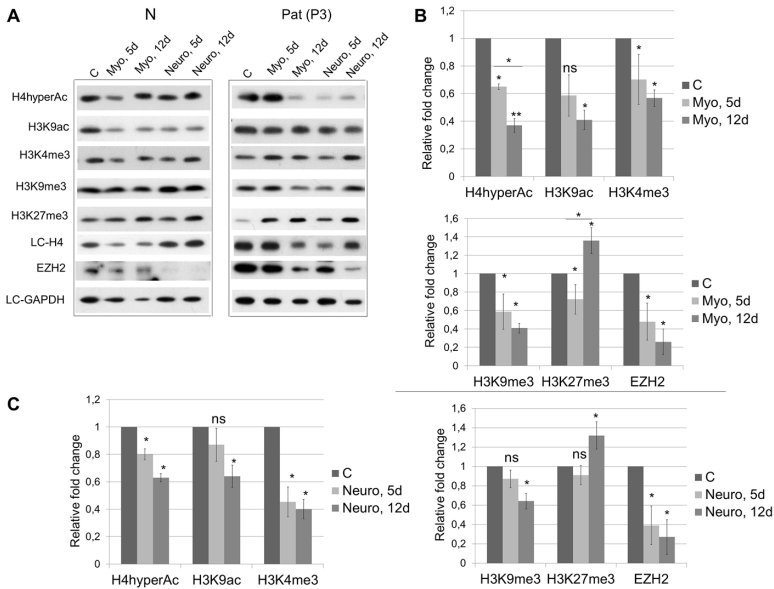


**Figure 5** Histone modifications pattern in MSCs from AF of normal and fetus-affected gestations during two-lineage differentiation. Lysates from cell samples were subjected to Western blot analysis to monitor the expression of proteins using the indicated antibodies after 5 and 12 days of differentiation induction. (A) Representative blots of proteins from AF of normal gestation (N) and a donor with fetal abnormalities (P3—Down syndrome) (Pat) undergoing myogenic and neural differentiation. The intensity of each protein band was normalized against loading control (LC—histone H4 for modified histones or GAPDH for EZH2) after scanning densitometry. The normalized values of active and repressive marks of chromatin were used to calculate the relative fold change in the expression between undifferentiated cells (control, C) and differentiated toward myogenic (B) and neural (C) lineage. The data is from at least four gels of samples (N, n = 2 and Pat, n = 2) and the differences, detected between these samples, were insignificant thus the relative fold change, presented as mean ± SD, is from both types of samples in one graph. \* $P < 0.05$  and \*\* $P < 0.01$  were considered as significant changes, ns, non-significant changes.

differentiation potential (Meligy et al., 2012; Kalvelyte et al., 2013). For myogenic differentiation induction, we used horse serum that is low in growth-promoting factors and slows down the proliferation of cells as well as promotes differentiation (Franke et al., 2014; Lin et al., 2014). In addition, without growth factors, MyoD family of muscle-specific transcription factors that inhibit division and cause differentiation of cells is activated (Olson 1992) so the replacement of fetal bovine serum into horse serum initiates myogenic differentiation. Our previous (Savickiene et al., 2015) and the present study demonstrated that AF-MSCs differentiate into myoblasts at normal and fetus-diseased conditions but exhibit different levels of myogenic markers, such as *Actinin-α* and *MRF4*, suggesting that donor individuality may influence differential gene activation in differentiating myoblasts and during the formation of myotubes. Additionally, according to our proteomic analysis data (Savickiene et al., 2015), differentiated myoblasts from AF-MSCs expressed high levels of myogenic markers (Integrin alpha 5, Caveolin 1), smooth muscle markers (Desmin, Calponin 1, Transgelin 3, Caldesmon) and muscle

cell structural proteins involved in the regulation of actin filaments.

Our findings establish that AF-MSCs from two AF sources differentiate into neuron-like cells with typical morphological changes, showing trans-differentiation potential from a mesenchymal to neural lineage despite the fact that MSCs are considered being distant from neural cells. This observation is consistent with the results from the previous studies using MSCs from prenatal tissues and amniotic fluid (Prusa et al., 2004; Chen et al., 2016; Kwon et al., 2016). The spontaneous expression of several neural markers (including *Nestin*) in undifferentiated MSCs from various sources has been considered as an evidence of the cell predisposition to differentiate toward neural lineages (Foudah et al., 2014). In our study, AF-MSCs already express *Nestin*, and increased expression of this marker as well as *NSE* is related to their function in the neural differentiation. Also, according to our proteomic analysis data (Savickiene et al., 2015), AF-MSCs, differentiated to neural lineage, expressed proteins associated with the mature neuronal phenotype and nervous system development, such as

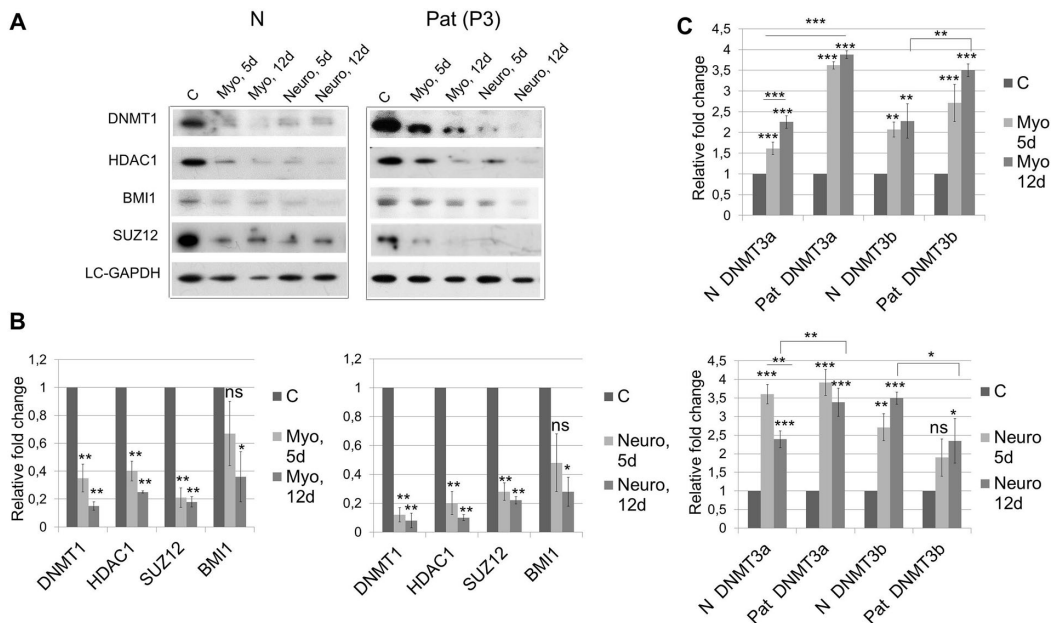


**Figure 6** Chromatin modifying proteins pattern in MSCs cultures from AF of normal and fetus-affected gestations during myogenic and neural differentiation. (A) Representative Western blots of chromatin remodeling proteins after 5 and 12 days of myogenic or neural differentiation of MSCs from AF of normal gestation (N) and a donor with fetal abnormalities (P3–Down syndrome, Pat). (B) The intensity of each protein band was normalized against loading control (LC–GAPDH) after scanning densitometry, and the normalized values of proteins were used to calculate the relative fold change in the expression between undifferentiated (control, C) and differentiated cells. The data is from at least four gels of samples (N,  $n = 2$  and Pat,  $n = 2$ ) and the differences, detected between these samples, were insignificant thus the relative fold change, presented as mean  $\pm$  SD, is from both types of samples in one graph. (C) Relative levels of *DNMT3a*/*DNMT3b* genes in AF–MSCs during myogenic and neural differentiation as determined by RT–qPCR, normalized to *GAPDH* and calculated using a comparative threshold cycle delta–delta Ct method. The data are presented as mean  $\pm$  SD ( $n = 3$ ), \* $P \leq 0.05$ , \*\* $P \leq 0.01$  and \*\*\* $P \leq 0.001$  were considered as significant changes, ns, non-significant changes.

Retinoic acid binding protein 2, Tubulin  $\alpha 8$ , Integrin  $\alpha 8$ , Tenascin and Nestin. Several studies demonstrate that MSCs displayed functional hallmarks of neurons and expressed high levels of ionic channel genes, which are important in the neural function (Jang et al., 2010; Shabhazi et al., 2016). For the induction of neural differentiation of AF–MSCs, we used neural differentiation medium containing retinoic acid (RA), known as a signaling molecule, involved in neural development, differentiation and axon outgrowth (Maden, 2007). Recently, some researchers showed that RA itself as well as combined with chemical agents (IBMX, BDNF, Forskolin) and growth factors (NGF, EGF, bFGF) may improve the functional efficiency of neuronal differentiation of MSCs (Jin et al., 2015; Rafieemehr et al., 2015). This demonstrates that RA might play an important role in MSCs fate decision compared to other neuronal inducers. The evidence that AF–MSCs are able to differentiate and integrate into nervous tissue (Maraldi et al., 2014) opens up the possibility to use AF–MSCs for neural repair.

In this work, we also compared the epigenetic landscape of MSCs derived from AF of normal and fetus-diseased gestations undergoing two-lineage differentiation. Myogenic differentiation was associated with the global differentiation-dependent decrease in acetylation of histones H4 and H3K9, methylation of H3K4me3 and H3K9me3, and global reduction of HDAC1 and DNMT1. Despite the differences in several myogenic genes–markers expression, epigenetic changes in differentiated AF–MSCs from N and Pat gestations were similar. Our results are in agreement with previous reports showing that the activation of muscle-specific genes is accompanied by the loss of EZH2 and HDAC1, demethylation of H3K9, hypomethylation of H3K27 and the subsequent engagement of positive muscle transcription regulators as well as the downregulation of DNMT1 (Caretta et al., 2004; Verrier et al., 2011; Laker and Ryall, 2016; Sincennes et al., 2016). Here, we found that myogenic differentiation was associated with a significant reduction in PRC1/2 proteins (BMI1/SUZ12 and EZH2)

levels and the retention of the H3K27me3 mark. Previous studies indicated the distinct roles of Polycomb complexes in muscle differentiation (Caretti et al., 2004; Asp et al., 2011). If PRC2 protein EZH2 is required for the determination of myogenic differentiation, overexpression of EZH2 prevents terminal muscle differentiation. PRC1, which causes long-term transcriptional repression of lineage commitment genes stabilizing H3K27me3, helps retention of H3K27me3 on genes that must be silenced when the level of SUZ12 (essential for PRC2 activity) declines and even disappears in myotubes. Furthermore, PRC1 protein BMI1 concentrates on genes of non-muscle lineages helping to retain H3K27me3 in the face of declining EZH2 activity in differentiating cells (Asp et al., 2011). In this study, we also detected the upregulation of *DNMT3a/3b* genes during myogenic differentiation. DNMT3b may be involved in controlling histone modification patterns by regulating PRC1 function (Jin et al., 2009). It is possible that DNMT3a/3b might have varied functions for different cell types and processes (Tadokoro et al., 2007).

To date, epigenetic mechanisms underlying the AF-MSCs differentiation to the neural lineage are still poorly understood. Evidence exists that bivalent modifications (H3K4me3 and H3K27me3) are essential for the differentiation toward the neuronal fate (Mikkelsen et al., 2007). The current data indicate that the removal of the epigenetic suppression of genes by the decrease in a high profile of H4hyperAc, H3K4me3, H3K27me3 modifications and changes in DNA methylation marks (5-MeCyt, DNMT1, DNMT3a/3b) are required for neuronal stem cell restriction into neural differentiation (Singh et al., 2009). Here we demonstrated the differentiation-dependent decrease in the global levels of activating histone modifications (H3K4me3, H4hyperAc) and also H3K9ac that is involved in the neural commitment of ESCs and activation of multiple neurodevelopmental genes (Krejčí et al., 2009; Qiao et al., 2015) leading to the progression to a more compact, repressive chromatin state. We obtained that changes in the epigenetic modifications were rather similar in healthy and fetus-affected AF-MSCs differentiated toward neural lineage despite differences in the expression of differentiation-specific genes. Polycomb complexes (PRC1/2) have also been described to be highly involved in neural development by maintaining the repression of inactive genes at different neural differentiation stages (Corley and Kroll, 2015) and EZH2 is one of the main regulators of human ESCs differentiation into neural ectoderm lineages (Shan et al., 2017). Our data are in agreement with this because the levels of SUZ12, EZH2 and BMI1 decreased compared to undifferentiated control as neurogenic differentiation proceeded. DNMT1 and HDAC1 that play a critical role in regulating neurogenesis (Noguchi et al., 2016) were expressed in undifferentiated

AF-MSCs but diminished during neural differentiation. As was suggested, DNMT3b is required for the initial steps of the neuronal cell differentiation and DNMT3a is essential for maturation processes and the inhibition of reversibility of the cell differentiation by fixing chromatin structures of differentiated cells (Watanabe et al., 2006). Our study identifies a positive involvement of DNMT3a/3b in AF-MSCs neural differentiation as well. Overall, our observation in the epigenetic environment of MSCs from AF of normal and fetus-affected gestations did not show apparent specific differences between cells differentiated toward myogenic and neural lineages. Our results are in agreement with the suggestions that temporal phases and the temporal interplay of various epigenetic factors regulating gene expression during the process of lineage-specific differentiation exist (Lee et al., 2007).

Moreover, we have studied the involvement of selected miRNAs in AF-MSCs undergoing myogenic and neural differentiation. miRNAs, a family of protein non-coding transcripts of ~20–25 nucleotides, are responsible for changes in the cell epigenome because of their ability to influence the gene expression post-transcriptionally and control the expression of important epigenetic regulators, such as DNMTs, HDACs and Polycomb complex genes (Sato et al., 2011). Several reports described the changes in the pattern of the miRNAs expression during the lineage-specific differentiation (Lakshminpathy et al., 2008; Ge and Chen, 2011). Recently, miR-21 and miR-17 were shown to have a critical role in the regulation of MSCs proliferation, three-lineage differentiation and control of various processes involved in maintaining health and disease (Mei et al., 2013; Kang and Hata, 2015). miR-21 expression was also increased during adipogenesis and osteogenesis (Mei et al., 2013). In this study, we determined an only slight decrease in miR-21 expression and a great reduction in the expression of miR-17 in differentiated myocytes and neural-like cells while miR-34a was significantly up-regulated. As it was previously reported, miR-34a is involved in MSCs proliferation by regulating cell cycle control genes and also in osteoblastic differentiation while miR-146a plays a role in regulating adipogenic and osteogenic differentiation (Chen et al., 2014; Huszar and Payne, 2014). Here we demonstrated that miR-146a is also involved and up-regulated in both myogenic and neural differentiation of AF-MSCs. The obtained results suggest that functions of miRNAs used in this study are universal rather than unique to myoblasts or neural-like cells. To date, there is evidence of coordinated actions of miRNAs and epigenetic mechanisms mediated by the PRC complex, DNA methylation and pluripotency factors, such as Oct4, Nanog, Sox2 (Fouse et al., 2008; Bianchi et al., 2017), depicting a more complex gene regulation mechanisms in MSCs.

## Conclusions

Epigenetic status is one of the key-players in stem cells differentiation and renewal. We demonstrated that the regulation of chromatin remodeling during lineage-specific differentiation into myogenic and neurogenic cells occurring via epigenetic mechanisms is rather similar in AF-MSCs from normal and fetus-affected gestations. This is the first study in which the epigenetic landscape of AF-MSCs undergoing two-lineage differentiation has been compared improving current understanding of epigenetic regulatory mechanisms in AF-MSCs function at physiological and pathological gestation conditions.

## Acknowledgments and funding

The authors thank all subjects who participated in this study. This work was supported by the Research Council of Lithuania (project MIP-057/2015).

## References

- Asp P, Blum R, Vethantham V, Parisi F, Micsinai M, Cheng J, Bowman C, Kluger Y, Dynlacht BD (2011) Genome-wide remodeling of the epigenetic landscape during myogenic differentiation. *Proc Natl Acad Sci U S A* 108: E149–58.
- Bianchi M, Renzini A, Adamo S, Moresi V (2017) Coordinated actions of microRNAs with other epigenetic factors regulate skeletal muscle development and adaptation. *Int J Mol Sci* 18(4): E840.
- Blais A, Tsikitis M, Acosta-Alvear D, Sharan R, Kluger Y, Dynlacht BD (2005) An initial blueprint for myogenic differentiation. *Genes Dev* 19(5): 553–69.
- Bossolasco P, Montemurro T, Cova L, Zangrossi S, Calzarossa C, Buiatitios S, Soligo D, Bosari S, Silani V, Delilieri GL, Rebulla P, Lazzari I (2006) Molecular and phenotypic characterization of human amniotic fluid cells and their differentiation potential. *Cell Res* 16(4): 329–36.
- Cao Y, Yao Z, Sarkar D, Lawrence M, Sanchez GJ, Parker MH, MacQuarrie KL, Davison J, Morgan MT, Ruzzo WL, Gentleman RC, Tapscott SJ (2010) Genome-wide MyoD binding in skeletal muscle cells: a potential for broad cellular reprogramming. *Dev Cell* 18: 662–74.
- Caretto G, Di Padova M, Micales B, Lyons GE, Sartorelli V (2004) The Polycomb Ezh2 methyltransferase regulates muscle gene expression and skeletal muscle differentiation. *Genes Dev* 18(21): 2627–38.
- Chen L, Holmström K, Qiu W, Ditzel N, Shi K, Hokland L, Kassem M (2014) MicroRNA-34a inhibits osteoblast differentiation and in vivo bone formation of human stromal stem cells. *Stem Cells* 32: 902–12.
- Chen S, Zhang W, Wang JM, Duan HT, Kong JH, Wang YX, Dong M, Bi X, Song J (2016) Differentiation of isolated human umbilical cord mesenchymal stem cells into neural stem cells. *Int J Ophthalmol* 9: 41–7.
- Corley M, Kroll KL (2015) The roles and regulation of Polycomb complexes in neural development. *Cell Tissue Res* 359(1): 65–85.
- Da Sacco S, De Filippo RE, Perin L (2011) Amniotic fluid as a source of pluripotent and multipotent stem cells for organ regeneration. *Curr Opin Organ Transplant* 16: 101–5.
- Di Germanio C, Bernier M, de Cabo R, Barboni B (2016) Amniotic epithelial cells: a new tool to combat aging and age-related diseases? *Front Cell Dev Biol* 4: 135.
- Dominici M, Le Blanc K, Mueller I, Slaper-Cortenbach I, Marini F, Krause D, Deans R, Keating A, Prockop DJ, Horwitz E (2006) Minimal criteria for defining multipotent mesenchymal stromal cells. The International Society for Cellular Therapy position statement. *Cytotherapy* 8(4): 315–7.
- Ekblad A, Qian H, Westgren M, Le Blanc K, Fossum M, Gotherstrom C (2015) Amniotic fluid—a source for clinical therapeutics in the newborn? *Stem Cells Dev* 24(12): 1405–14.
- Foshay KM, Gallicano GI (2009) MiR-17 family miRNAs are expressed during early mammalian development and regulate stem cell differentiation. *Dev Biol* 326: 431–43.
- Foudah D, Monfrini M, Donzelli E, Niada S, Brini AT, Orciani M, Tredici G, Miloso M (2014) Expression of neural markers by undifferentiated mesenchymal-like stem cells from different sources. *J Immunol Res* 2014: 987678.
- Fouse SD, Shen Y, Pellegrini M, Cole S, Meissner A, Van Neste L, Jaenisch R, Fan G (2008) Promoter CpG methylation contributes to ES cell gene regulation in parallel with Oct4/Nanog, PcG complex, and histone H3 K4/K27 trimethylation. *Cell Stem Cell* 2: 160–9.
- Franke J, Abs V, Zizzadoro C, Abraham G (2014) Comparative study of the effects of fetal bovine serum versus horse serum on growth and differentiation of primary equine bronchial fibroblasts. *BMC Vet Res* 10: 119.
- Ge Y, Chen J (2011) MicroRNAs in skeletal myogenesis. *Cell Cycle* 10: 441–8.
- Glemzaitė M, Navakauskienė R (2016) Osteogenic differentiation of human amniotic fluid mesenchymal stem cells is determined by epigenetic changes. *Stem Cells Int* 2016: 6465307.
- Huszar JM, Payne CJ (2014) MIR146A inhibits JMJD3 expression and osteogenic differentiation in human mesenchymal stem cells. *FEBS Lett* 588: 1850–6.
- Jang S, Cho HH, Cho YB, Park JS, Jeong HS (2010) Functional neural differentiation of human adipose tissue-derived stem cells using bFGF and forskolin. *BMC Cell Biol* 11: 25.
- Jin B, Yao B, Li JL, Fields CR, Delmas AL, Fields CR, Delmas AL, Liu C, Robertson KD (2009) DNMT1 and DNMT3B modulate distinct polycomb-mediated histone modifications in colon cancer. *Cancer Res* 69: 7412–21.
- Jin W, Xu YP, Yang AH, Xing YQ (2015) In vitro induction and differentiation of umbilical cord mesenchymal stem cells into neuron-like cells by all-trans retinoic acid. *Int J Ophthalmol* 8: 250–6.
- Joo S, Ko IK, Atala A, Yoo JJ, Lee SJ (2012) Amniotic fluid-derived stem cells in regenerative medicine research. *Arch Pharm Res* 35: 271–80.

- Kalvelyte A, Krestnikova N, Stulpinas A, Bukelskiene V, Bironaite D, Baltruikiene D, Imbrasaitė A (2013) Long-term muscle-derived cell culture: multipotency and susceptibility to cell death stimuli. *Cell Biol Int* 37: 292–304.
- Kang H, Hata A (2015) The role of microRNAs in cell fate determination of mesenchymal stem cells: balancing adipogenesis and osteogenesis. *BMB Rep* 48: 319–23.
- Kashyap V, Rezende NC, Scotland KB, Shaffer SM, Persson JL, Gudas LJ, Mongan NP (2009) Regulation of stem cell pluripotency and differentiation involves a mutual regulatory circuit of the NANOG, OCT4, and SOX2 pluripotency transcription factors with polycomb repressive complexes and stem cell microRNAs. *Stem Cells Dev* 18(7): 1093–108.
- Kim EY, Lee KB, Kim MK (2014) The potential of mesenchymal stem cells derived from amniotic membrane and amniotic fluid for neuronal regenerative therapy. *BMB Rep* 47: 135–40.
- Kornicka K, Marycz K, Tomaszewski KA, Marędzia M, Śmieszek A (2015) The effect of age on osteogenic and adipogenic differentiation potential of human adipose derived stromal stem cells (hASCs) and the impact of stress factors in the course of the differentiation process. *Oxid Med Cell Longev* 2015: 309169.
- Krejčí J, Uhlířová R, Galiová G, Kozubek S, Smigová J, Bártová E (2009) Genome-wide reduction in H3K9 acetylation during human embryonic stem cell differentiation. *J Cell Physiol* 219: 677–87.
- Krichevsky AM, Gabrieli G (2009) MiR-21: a small multi-faceted RNA. *J Cell Mol Med* 13: 39–53.
- Kwon A, Kim Y, Kim M, Kim J, Choi H, Jekarl DW, Lee S, Kim JM, Shin JC, Park IY (2016) Tissue-specific differentiation potency of mesenchymal stromal cells from perinatal tissues. *Sci Rep* 6: 23544.
- Laker RC, Ryall JG (2016) DNA methylation in skeletal muscle stem cell specification, proliferation, and differentiation. *Stem Cells Int* 2016: 5725927.
- Lakshminpathy U, Love B, Goff LA, Jornsten R, Graichen R, Hart RP, Chesnut JD (2008) MicroRNA expression pattern of undifferentiated and differentiated human embryonic stem cells. *Stem Cells Dev* 16: 1003–16.
- Lee ER, Murdoch FE, Fritsch MK (2007) High histone acetylation and decreased polycomb repressive complex 2 member levels regulate gene specific transcriptional changes during early embryonic stem cell differentiation induced by retinoic acid. *Stem Cells* 25: 2191–9.
- Lin Y, Zhao Y, Li R, Jiaqi G, Yucai Z, Wang Y (2014) PGC-1 $\alpha$  is associated with C2C12 Myoblast differentiation. *Cent Eur J Biol* 9: 1030–6.
- Liu C, Zhao X (2009) MicroRNAs in adult and embryonic neurogenesis. *Neuromolecular Med* 11: 141–52.
- Maden M (2007) Retinoic acid in the development, regeneration and maintenance of the nervous system. *Nat Rev Neurosci* 8: 755–65.
- Maguire CT, Demarest BL, Hill JT, Palmer JD, Brothman AR, Yost HJ, Condic ML (2013) Genome-wide analysis reveals the unique stem cell identity of human amniocytes. *PLoS ONE* 8(1): e53372.
- Maraldi T, Bertoni L, Riccio M, Zavatti M, Carnevale G, Resca E, Guida M, Beretti F, La Sala GB, De Pol A (2014) Human amniotic fluid stem cells: neural differentiation in vitro and in vivo. *Cell Tissue Res* 357: 1–3.
- Marędzia M, Marycz K, Tomaszewski KA, Kornicka K, Henry BM (2016) The influence of aging on the regenerative potential of human adipose derived mesenchymal stem cells. *Stem Cells Int* 2016: 2152435.
- Mei Y, Bian C, Li J, Du Z, Zhou H, Yang Z, Zhao RC (2013) MiR-21 modulates the ERK-MAPK signaling pathway by regulating SPRY2 expression during human mesenchymal stem cell differentiation. *J Cell Biochem* 114: 1374–84.
- Meligy FY, Shigemura K, Behnsawy HM, Fujisawa M, Kawabata M, Shirakawa T (2012) The efficiency of in vitro isolation and myogenic differentiation of MSCs derived from adipose connective tissue, bone marrow, and skeletal muscle tissue. *In Vitro Cell Dev Biol Anim* 48: 203–15.
- Mikkelsen TS, Ku M, Jaffe DB, Issac B, Lieberman E, Giannoukos G, Alvarez P, Brockman W, Kim TK, Koche RP, Lee W, Mendenhall E, O'Donovan A, Presser A, Russ C, Xie X, Meissner A, Wernig M, Jaenisch R, Nusbaum C, Lander ES, Bernstein BE (2007) Genome-wide maps of chromatin state in pluripotent and lineage-committed cells. *Nature* 448(7153): 553–60.
- Noguchi H, Kimura A, Murao N, Namihira M, Nakashima K (2016) Prenatal deletion of DNA methyltransferase 1 in neural stem cells impairs neurogenesis and causes anxiety-like behavior in adulthood. *Neurogenesis (Austin)* 3(1): e1232679.
- Olson E (1992) Interplay between proliferation and differentiation within the myogenic lineage. *Dev Biol* 154(2): 261–72.
- Pan HC, Yang DY, Chiu YT, Lai SZ, Wang YC, Chang MH, Cheng FC (2006) Enhanced regeneration in injured sciatic nerve by human amniotic mesenchymal stem cell. *J Clin Neurosci* 13: 570–5.
- Park H, Park H, Pak HJ, Yang DY, Kim YH, Choi WJ, Park SJ, Cho JA, Lee KW (2015) MiR-34a inhibits differentiation of human adipose tissue-derived stem cells by regulating cell cycle and senescence induction. *Differentiation* 90: 91–100.
- Park JS, Kim S, Han DK, Lee JY, Ghil SH (2007) Isolation of neural precursor cells from skeletal muscle tissues and their differentiation into neuron-like cells. *Exp Mol Med* 39: 483–90.
- Perin L, Sedrakyan S, Da Sacco S, De Filippo R (2008) Characterization of human amniotic fluid stem cells and their pluripotential capability. *Methods Cell Biol* 86: 85–99.
- Prusa AR, Marton E, Rosner M, Bettelheim D, Lubec G, Pollack A, Bernaschek G, Hengstschlagger M (2004) Neurogenic cells in human amniotic fluid. *Am J Obstet Gynecol* 191: 309–14.
- Qiao Y, Wang R, Yang X, Tang K, Jing N (2015) Dual roles of histone H3 lysine 9 acetylation in human embryonic stem cell pluripotency and neural differentiation. *J Biol Chem* 290: 2508–20.
- Rafeemehr H, Kheirandish M, Soleimani M (2015) Improving the neuronal differentiation efficiency of umbilical cord blood-

- derived mesenchymal stem cells cultivated under appropriate conditions. *Iran J Basic Med Sci* 18: 1100–6.
- Ratajczak MZ, Marycz K, Poniewierska-Baran A, Fiedorowicz K, Zbucka-Kretowska M, Moniuszko M (2014) Very small embryonic-like stem cells as a novel developmental concept and the hierarchy of the stem cell compartment. *Adv Med Sci* 59(2): 273–80.
- Sato F, Tsuchiya S, Meltzer SJ, Shimizu K (2011) MicroRNAs and epigenetics. *FEBS J* 278: 1598–609.
- Savickiene J, Treigyte G, Baronaite S, Valiuliene G, Kaupinis A, Valius M, Arlauskienė A, Navakauskienė R (2015) Human amniotic fluid mesenchymal stem cells from second- and third-trimester amniocentesis: differentiation potential, molecular signature, and proteome analysis. *Stem Cells Int* 2015: 319238.
- Schwartz YB, Pirrotta V (2008) Polycomb complexes and epigenetic states. *Curr Opin Cell Biol* 20: 266–73.
- Shahbazi A, Safa M, Alikarami F, Kargozar S, Asadi MH, Joghataei MT, Soleimani M (2016) Rapid induction of neural differentiation in human umbilical cord matrix mesenchymal stem cells by cAMP-elevating agents. *Int J Mol Cell Med* 5: 167–77.
- Shan Y, Liang Z, Xing Q, Zhang T, Wang B, Tian S, Huang W, Zhang Y, Yao J, Zhu Y, Huang K, Liu Y, Wang X, Chen Q, Zhang J, Shang B, Li S, Shi X, Liao B, Zhang C, Lai K, Zhong X, Shu X, Wang J, Yao H, Chen J, Pei D, Pan G (2017) PRC2 specifies ectoderm lineages and maintains pluripotency in primed but not naïve ESCs. *Nat Commun* 8(1): 672.
- Shimokawa T, Kato M, Ezaki O, Hashimoto S (1998) Transcriptional regulation of muscle-specific genes during myoblast differentiation. *Biochem Biophys Res Commun* 246: 287–92.
- Sincennes MC, Brun CE, Rudnicki MA (2016) Concise review: epigenetic regulation of myogenesis in health and disease. *Stem Cells Transl Med* 5: 282–90.
- Singh RP, Shiue K, Schomberg D, Zhou FC (2009) Cellular epigenetic modifications of neural stem cell differentiation. *Cell Transplant* 18: 1197–211.
- Tadokoro Y, Ema H, Okano M, Li E, Nakauchi H (2007) De novo DNA methyltransferase is essential for self-renewal, but not for differentiation, in hematopoietic stem cells. *J Exp Med* 204: 715–22.
- Tamagawa T, Ishiwata I, Ishikawa H, Nakamura Y (2008) Induced in vitro differentiation of neural-like cells from human amnion derived fibroblast-like cells. *Hum Cell* 21: 38–45.
- Trohatou O, Anagnou NP, Roubelakis MG (2013) Human amniotic fluid stem cells as an attractive tool for clinical applications. *Curr Stem Cell Res Ther* 8: 125–32.
- Tsai MS, Lee JL, Chang YJ, Hwang SM (2004) Isolation of human multipotent mesenchymal stem cells from second-trimester amniotic fluid using a novel two-stage culture protocol. *Hum Reprod* 19: 1450–6.
- Verrier L, Escaffit F, Chailleux C, Trouche D, Vandromme M (2011) A new isoform of the histone demethylase JMJD2A/KDM4A is required for skeletal muscle differentiation. *PLoS Genet* 7(6): e1001390.
- Watanabe D, Uchiyama K, Hanaoka K (2006) Transition of mouse de novo methyltransferases expression from Dnmt3b to Dnmt3a during neural progenitor cell development. *Neuroscience* 142: 727–37.
- Yan ZJ, Hu YQ, Zhang HT, Zhang P, Xiao ZY, Sun XL, Cai YQ, Hu CC, Xu RX (2013) Comparison of the neural differentiation potential of human mesenchymal stem cells from amniotic fluid and adult bone marrow. *Cell Mol Neurobiol* 33: 465–75.

Received 25 September 2018; accepted 5 January 2019.  
Final version published online 28 January 2019.

### Supporting Information

Additional supporting information may be found online in the Supporting Information section at the end of the article.

2 publikacija / publication 2

**A. Zentelytė, M. Gasiūnienė, G. Treigyte, S. Baronaitė, J. Savickienė, V. Borutinskaitė, R. Navakauskienė**

Epigenetic Regulation of Amniotic Fluid Mesenchymal Stem Cell  
Differentiation to the Mesodermal Lineages at Normal and Fetus-Diseased  
Gestation

2020, *Journal of Cellular Biochemistry*, 121:1811-1822

doi: 10.1002/jcb.29416

Copyright © 2019 Wiley Periodicals, Inc.

Perspausdinta su John Wiley and Sons leidimu (licencijos nr.  
5181891304399)

Reproduced with John Wiley and Sons permission (license no.  
5181891304399)



## RESEARCH ARTICLE

# Epigenetic regulation of amniotic fluid mesenchymal stem cell differentiation to the mesodermal lineages at normal and fetus-diseased gestation

Aistė Zentelytė | Monika Gasiūnienė  | Gražina Treigyte | Sandra Baronaitė | Jūratė Savickienė | Veronika Borutinskaitė | Rūta Navakauskienė 

Department of Molecular Cell Biology,  
Institute of Biochemistry, Life Sciences  
Center, Vilnius University, Vilnius,  
Lithuania

**Correspondence**

Ruta Navakauskiene, Department of  
Molecular Cell Biology, Institute of  
Biochemistry, Life Sciences Center, Vilnius  
University, Sauletekio av. 7, LT-10257  
Vilnius, Lithuania.  
Email: ruta.navakauskiene@bchi.vu.lt

**Funding information**

Research Council of Lithuania, Grant/  
Award Number: project No. MIP-057/  
2015

**Abstract**

Human mesenchymal stem cells isolated from amniotic fluid (AF-MSCs) demonstrate the potency for self-renewal and multidifferentiation, and can, therefore, be a potential alternative source of stem cells adapted for therapeutic purposes. The object of this study is to evaluate the efficacy of MSCs from AF when the pregnancy is normal or when the fetus is affected during pregnancy to differentiate into mesodermal lineage tissues and to elucidate epigenetic states responsible for terminal adipogenic and osteogenic differentiation. The morphology of AF-MSCs from two cell sources and the expression of the cell surface-specific (CD44, CD90, and CD105) markers and pluripotency (Oct4, Nanog, Sox2, and Rex1) genes were quite similar and underwent mesodermal lineage differentiation because this is shown by the typical cell morphology and of genes' expression specific for adipogenic (peroxisome proliferator-activated receptor- $\gamma$ , adiponectin) and osteoblastic (alkaline phosphatase, osteopontin, and osteocalcin) differentiation. Terminal lineage-specific differentiation was related to differential expression of miR-17, miR-21, miR-34a, and miR-146a, decreased levels of acetylated H4 and H3K9, trimethylated H3K4 and H3K9, and the retention of H3K27me3 along with a reduction in the levels of HDAC1, DNMT1, and PRC1/2 proteins (BMI1/SUZ12). No significant distinction could be identified in the levels of expression of all epigenetic or pluripotency markers between undifferentiated MSCs isolated from AF of normal gestation and pregnancy where the fetus was damaged and between those differentiated toward adipocytes or osteoblasts. The expressional changes of those marks and microRNAs that occurred during terminal differentiation to mesodermal tissues indicate subtle epigenetic regulation in AF-MSCs when the condition of the fetus is healthy normal or diseased. More detailed studies of epigenetic

**Abbreviations:** AF-MSC, amniotic fluid-derived mesenchymal stem cells; ALP, alkaline phosphatase; BMI1, B lymphoma Mo-MLV insertion region 1; EED, embryonic ectoderm development; EZH2e, enhancer of zeste histone H3K27 methyltransferase; GAPDH, glyceraldehyde-3-phosphate dehydrogenase; Oct4, octamer-binding transcription factor 4; PPAR- $\gamma$ , peroxisome proliferator-activated receptor-gamma; Rex1, (Zfp42) zinc finger protein; RT-qPCR, quantitative real-time polymerase chain reaction; Sox2, sex determining region Y-box 2; SUZ12, suppressor of zeste 12.

mechanisms may offer a better understanding of AF-MSCs differentiation in fetus-diseased conditions and their usage in an autologous therapeutic application and prenatal disease research.

#### KEYWORDS

amniotic fluid stem cells, differentiation, epigenetics, histone modifications, miRNA

## 1 | INTRODUCTION

Mesenchymal stem cells (MSCs) are the stromal stem cells that are able to self-renew themselves and differentiate into multiple tissues.<sup>1</sup> Human amniotic fluid (AF) is an alternative source for derivation of MSCs that are easily isolated and demonstrate a great proliferative capacity, no tumorigenicity, low immunogenicity, anti-inflammatory properties, and do not raise ethical problems, so they become great assistants in regenerative medicine.<sup>2,3</sup> AF-MSCs have the potency for multilineage differentiation, counting the mesodermal lineage, namely osteocytes, adipocytes, and chondrocytes. Thus, treating complicated bone defects, human obesity, and related diseases, it can help greatly. In particular, AF-MSCs are autogenous to the fetus and can make a significant contribution to the treatment of perinatal genetic disorders as well.<sup>4</sup> Moreover, AF-MSCs are semiallogeneic to each parent, so it can possibly benefit other family members.<sup>5</sup> However, to use clinically AF-MSCs, for regenerative medicine based on MSC, it is important to understand the molecular mechanisms of cell differentiation. In our study, we have used MSC which was obtained from AF in gestations with healthy and diseased fetus differentiated to adipocytes and osteocytes to examine the pattern of polycomb group (PcG) proteins and peculiar histone modifications that define changes in gene expression related to the terminal differentiation.

Tissue-specific transcriptional regulators and chromatin states greatly influence the regulation of phenotypic gene expression in settings of lineage commitment.<sup>6,7</sup> It is known that epigenetic mechanisms with DNA and histone modifications and small noncoding RNAs are crucial to regulating MSCs differentiation.<sup>7-9</sup> The PcG proteins involved in the development of “bivalent” chromatin domains of lineage-specific genes, which are methylated at H3K4 (an active mark) and at H3K27 (a repressive mark), repress the early differentiation genes to keep the pluripotency of embryonic stem cells.<sup>10</sup> Most PcG target developmental genes are activated through differentiation and at the same time lose the repressive H3K27me3 mark. The polycomb repressive complex 2 (PRC2) proteins<sup>11</sup> cooperate and repress the promoter/regulatory domains of genes that participate in decisions

of differentiation and cell fate. Enhancer of zeste histone H3K27 methyltransferase (EZH2), suppressor of zeste 12 (SUZ12), and embryonic ectoderm development containing PRC2 repression is maintained by PRC1, a large multisubunit complex that contains chromodomain proteins (BMI1, CBC2/4/8, Ring1 A/B ubiquitin-ligase). It was as well estimated that a key modulator of MSC lineage specification is histone methylation/acetylation state.<sup>6</sup> However, the exact role of specific histone modifications and PcG proteins that control phenotypic gene expression through AF-MSCs differentiation to specific-cell lineages is not currently well understood.

The comprehensive studies of osteogenic and adipogenic differentiation of MSCs have been carried out. Osteogenesis is a highly regulated program of stem cells differentiation into immature preosteoblasts, which evolve into mature osteoblasts. This process involves proliferation, maturation, matrix synthesis, and bone matrix mineralization,<sup>12</sup> which is regarded as a criterion of the final phase of osteogenic differentiation. The differentiation process is tightly controlled by the expression of osteogenesis-related genes, which include osteocalcin (OCN), runt-related transcription factor 2 (RUNX2), alkaline phosphatase (ALP), and osterix.<sup>13</sup> Adipogenesis includes determination phase in which multipotent MSCs bring to the adipocyte lineage and the terminal differentiation phase when preadipocytes develop into adipocytes and gain new functions, for example lipid synthesis, storage, and protein production specific to adipocytes.<sup>14</sup> The contemporary regulation of gene expression is needed for adipogenic differentiation by various molecular factors, including PPAR- $\gamma$  and C/EBP $\alpha$  which roles are the most important to control most of the downstream adipogenic genes.<sup>15</sup>

An inverted connection exists between the commitment and differentiation of MSC toward osteogenic or adipogenic lineage, which allows us to suggest a switch between the two aforementioned processes. The multiple signaling pathways ( $\beta$ -catenin dependent Wnt signaling, Hedgehog, and NELL-1 signaling) govern this balance with pro-osteogenic/antiadipogenic stimuli.<sup>16</sup> The two main transcription factors are involved in this inverse balance: the master regulatory gene of osteogenesis Runx2 and the master regulatory gene of adipogenesis

PPAR- $\gamma$  having antiosteoblastogenic effects. The switch between osteogenesis and adipogenesis is epigenetically governed by differential involvement H3K27me3 methyltransferase activity of EZH2.<sup>17</sup> In addition, several microRNAs (miRNAs) may act as switches through both adipogenic and osteogenic differentiation of MSCs when there is an inverse expression pattern between osteogenesis and adipogenesis.<sup>18</sup> However, the estimation of peculiar miRNAs and their regulatory importance in AF-MSCs differentiation still need to be elucidated. In this study, the authors questioned which epigenetic modifiers and miRNAs describe terminal adipogenic and osteogenic differentiation of MSCs obtained from the AF of gestations with the healthy and diseased fetus. This study will deepen our understanding to the epigenetic mechanisms of AF-MSCs differentiation and promote future autologous therapy.

## 2 | MATERIAL AND METHODS

### 2.1 | AF-MSC isolation and cultivation

AF specimens (about 3-5 mL) were collected using a method of biopsy (amniocentesis) from pregnant women during midsecond (16-24 weeks) or third (28-34 weeks) trimester. These women required prenatal diagnosis, and it was conducted using protocols that are approved by the Ethics Committee of Biomedical Research of Vilnius District No 158200-123-428-122. The specimens were kept at ordinary temperature for about 4 hours. AF-MSCs from fetus-affected pregnancies included samples from donors carrying different fetal abnormalities: P1—dilated brain ventricles and fetal central nervous system pathology; P2—heart defect and fletotaxia; P3—18 trisomy-Down's syndrome; P4—multiple malformations and the universal fetus hydrocephalus; P5—nonimmune fetal hydrocephalus and anemia; P6—twin-to-twin transfusion syndrome. AF-MSCs were isolated according to the two-stage protocol as described earlier.<sup>19</sup> To observe cell morphology, phase contrast microscope (Nikon Eclipse TS100) was used.

### 2.2 | Adipogenic and osteogenic differentiation

To carry out adipogenic differentiation, AF-MSCs were induced to differentiation with STEMPro Adipogenic differentiation medium at 37°C in 5% CO<sub>2</sub> for 9 days, according to the instructions of the manufacturer. The differentiation was inspected by Oil Red O staining. PPAR- $\gamma$  and adiponectin expression were defined by the quantitative real-time polymerase chain reaction (RT-qPCR).

To perform osteogenic differentiation, AF-MSCs were cultivated in STEMPro osteogenic differentiation medium

at 37°C in 5% CO<sub>2</sub> for 9 days. Osteogenic differentiation was defined by Alizarin red S staining. ALP, osteopontin, and OCN expression was estimated by RT-qPCR.

### 2.3 | Flow cytometry

For AF-MSCs, phenotype identification cells were analyzed with fluorescein isothiocyanate (FITC)-conjugated mouse anti-human antibodies against CD44 (Invitrogen), CD34 (Miltenyi Biotech), CD90 (Molecular probes, Life technologies) or phycoerythrin (PE)-labeled CD105 (Invitrogen), and appropriate isotype control—mouse IgG2A-FITC (Miltenyi Biotech) or IgG1-PE (Molecular probes, Life Technologies). Specimens were analyzed with the BD FACS Canto II (Becton and Dickinson) flow cytometer, using FACSDiva software. Ten thousand events were assembled for each sample.

### 2.4 | RNA and miRNA expression analysis

AF-MSCs from normal and fetus-diseased gestation were cultivated up to passage 5, then RNA was isolated for genes and miRNA expression analysis by RT-qPCR as described earlier.<sup>20</sup> To normalize all experimental data, as reference genes GAPDH and RNU 48 were used.

The following forward (F) and reverse (R) primers (5'-3') were used for RT-qPCR:

Oct4 - F: CGAGAAGGATGTGGTCCGAG; R: CAGAGG AAAGGACACTGGTC

Nanog - F: AGATGCCTCACACGGAGACT; R: GTTTGC CTTTGGGACTGGTG

Sox2 - F: TGGACAGTTACGCGCACAT; R: CGAGTA GGACATGCTGTAGTG

Rex1 - F: GCCTTATGTGATGGCTATGTGT; R: ACCCC TTATGACGCATTCTATGT

Osteopontin - F: GTCCAGTCTTACCTCTCAAACCT; R: ATGTGGTCAGCCAGCTCGTC

Osteocalcin - F: CACTCCTCGCCCTATTGGC; R: CCTT CCTGCTTGACACAAAG

Adiponectin - F: TGCTGGGAGCTGTCTACTG; R: TAC TCCGGTTTACCAGATGC

PPAR- $\gamma$  - F: CGACCAGCTGAATCCAGAGT; R: TTGCC AAGTCGCTGTCATCT

ALP - F: AGCCCTTCACTGCCATCCTGT; R: ATTCT CTCGTTACC GCCCCAC

GAPDH - F: AGTCCCTGCCACACTCAG; R: TACTTT ATTGATGGTACATGACAAGG

All reactions were conducted in triplicate, and relative quantification of miRNA was estimated through the use of the comparative threshold cycle delta-delta Ct method.

## 2.5 | Protein isolation and immunoanalysis

Total proteins were isolated from AF-MSCs (about  $5 \times 10^5$ ) after trypsinization with 0.05% trypsin-EDTA in 10 volumes of lysis solution (62.5 mM Tris, pH 6.8, 100 mM DTT and 2% SDS, 10% glycerol). Benzonase (Pure Grade, Merck) was supplemented to make a final concentration of 2.5 units/mL. The measurements of protein concentrations were taken through the use of commercial RC DC protein Assay (Bio-Rad). The isolated total proteins were separated on a 7% to 15% polyacrylamide gradient SDS-PAGE gel and afterward transferred to a PVDF membrane. The filters were incubated with the primary antibody: DNMT1 was from Santa Cruz Biotechnology; H3K4me3, H3K9me3, H3K27me3, and BMI1 were from Millipore; H4 (penta) was from Upstate; EZH2, SUZ12, and HDAC1 were from Cell Signaling; GAPDH was from Abcam; goat anti-rabbit or rabbit anti-goat horseradish peroxidase-linked secondary antibodies were from Dako Cytomation A/S. Band intensity of Western blots was evaluated by densitometric analysis by the use of ImageJ 1.45S software.

## 2.6 | Statistics

All the values of RT-qPCR, flow cytometry, and immunoanalysis are presented as mean  $\pm$  SD. The Student's paired *t* test was carried out to compare the data of paired samples, and the values \**P* < .05, \*\**P* < .01, and \*\*\**P* < .001 were recognized as statistically significant.

## 3 | RESULTS

### 3.1 | Characteristics of AF-MSC and differentiation potential to mesodermal tissues

MSCs of healthy donors (about 39 years old) were isolated from AF at second (16–24 weeks) trimester of pregnancy. AF-MSCs from fetus-diseased gestations enfolded specimens from donors that had different abnormalities of fetus: P1—21 trisomy-Down's syndrome; P2—multiple fetal malformations and the universal fetus hydrocephalus; P3—heart defect and Russell-Silver syndrome; P4—central nervous system pathology and dilated brain ventricles; P5—nonimmune fetal hydrocephalus and anemia; and P6—twin-to-twin transfusion syndrome. Stem cells from AF amniocentesis samples of normal (N) and fetus-affected gestations (Pat) were efficiently isolated and morphologically homogeneous population of spindle-shaped (mesenchymal-type) cells was collected (Figure 1A). Undifferentiated AF-MSCs from both sources showed similar fibroblast-like morphology with

differentiation potential to mesodermal lineage, that is adipocytes and osteoblasts. As the criterion to identify stem cells, established mesenchymal (CD90, CD105) and surface adhesion (CD44) markers were defined through the use of flow cytometry analysis. AF-MSCs of normal pregnancies were positive for CD105, CD90, and CD44 antigen and negative for hematopoietic marker CD34 (Figure 1B). No significant differences were identified in phenotype during flow cytometry between MSCs cultures which were obtained from AF of normal gestations (N) and diseased fetus pregnancies (Pat) maintaining the original CD44 and CD105 expression profile, but there was a smaller amount of CD90 positive cells in Pat samples in comparison with normal samples (Figure 1C). To confirm stem cell origin in normal and fetus-diseased samples, the authors conducted RT-qPCR analysis of transcription factors, Nanog, Oct4, Sox2, and Rex1, which account for the maintenance of multipotency and self-renewal of MSCs. The data shown in Figure 2A demonstrated more or less similar levels of pluripotency markers expression, and among Pat samples there were nonsignificant variations (Figure 2B). The variable messenger RNA (mRNA) levels of Nanog were observed in different fetus-pathological samples that may be due with the different extent of proliferation potential of such MSCs cultures.

To better appreciate the adipogenic and osteogenic potential, we compared differentiation properties of MSCs obtained from AF of healthy fetus gestations and pregnancies with the diseased fetus. AF-MSCs from both cell sources cultured in adipogenic medium for 9 days accumulated lipid vacuoles and demonstrated intensive staining with Oil Red O (Figure 3A). The presence of adipocyte-specific PPAR- $\gamma$ , a transcription factor that regulates genes for induction and progression of adipogenesis, confirmed the adipogenic differentiation, and adiponectin was expressed during the late stages of differentiation. The RT-qPCR analysis showed low expressional levels of early marker PPAR- $\gamma$  and marked upregulation of adiponectin at ninth day of adipogenic differentiation (Figure 3B). The adipogenic potential of AF-MSCs of normal gestations was slightly greater than that of fetus-pathological samples, as evaluated by higher levels of adiponectin at the same time upon adipogenic induction.

After the stage in which AF-MSCs were cultured in osteogenic medium for 9 days, most of them demonstrated extracellular matrix mineralization, which was detected by Alizarin red S staining (Figure 3C). The osteogenic potential was confirmed by the expression of osteogenic markers, which includes ALP, a phosphatase associated with matrix production, and proteins produced by osteoblasts, osteopontin, or OCN, which are the common markers of bone formation (Figure 3D). AF-MSCs showed the increased expression of osteopontin,

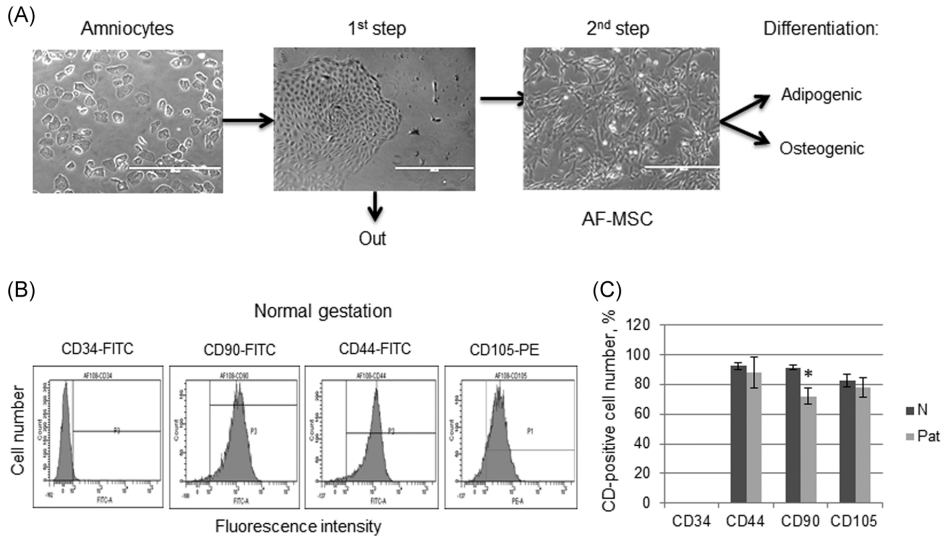


**FIGURE 1** Identification and characterization of AF-MSCs isolated from AF of normal and fetus-diseased gestations. A, Morphology of cells from amniocentesis samples: amniocytes, epithelial-like cell colonies at first stage (E-MSC) and spindle-shaped AF-MSC at second stage of isolation. B, Immunophenotypic profile of AF-MSCs from normal gestation determined by flow cytometric analysis against cell surface antigens CD44, CD90, CD105, and CD34. C, The percentages of positive surface marker of AF-MSCs of normal (N, n = 4) and fetus-affected (Pat, n = 6) gestations are shown as mean ± SD. \* $P \leq .05$  were considered as significant changes, ns—nonsignificant changes between N and Pat samples. AF-MSCs, amniotic fluid-derived mesenchymal stem cells

elevated levels of OCN, and a significant increase in ALP expression over the 9 days in culture. Of note, AF-MSCs derived from fetus-pathological samples exhibited quite similar osteogenic differentiation potential compared with the samples of normal gestations but exhibited lower levels of OCN that may be due with lower differentiation extent or MSCs intrinsic state of needing additional time for terminal differentiation.

### 3.2 | Differential miRNA expression in AF-MSCs subjected to adipogenic and osteogenic differentiation

The miRNA expression was analyzed in AF-MSCs' cultures obtained from donors who had healthy fetus or they had fetus-diseased gestations. It was expected that the comparison of these populations will show up several differences regarding miRNAs functions connected to

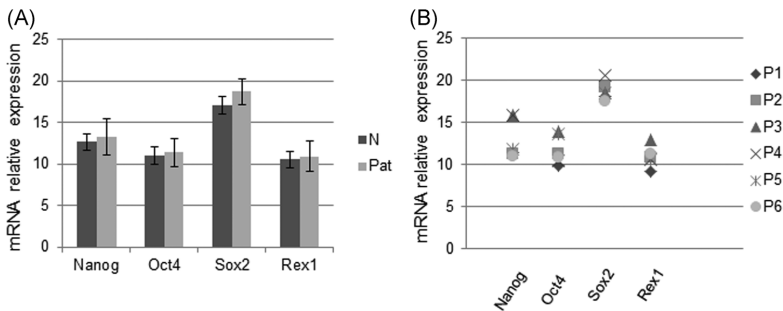


**FIGURE 2** Characteristics of pluripotency transcription factors in AF-MSCs representing normal and fetus-affected gestations. A, Relative mRNA expression of stemness markers in AF-MSCs of normal (N, n = 3) and fetus-affected gestations (Pat, n = 6) at passage 5 determined by RT-qPCR. B, mRNA expression of stemness markers in AF-MSCs from individual donors carrying fetal abnormalities (P1-P6). mRNA expression levels were compared after normalization to endogenous GAPDH. Data are presented as the mean ± SD showing nonsignificant changes between N and Pat samples. AF-MSCs, amniotic fluid-derived mesenchymal stem cells; mRNA, messenger RNA

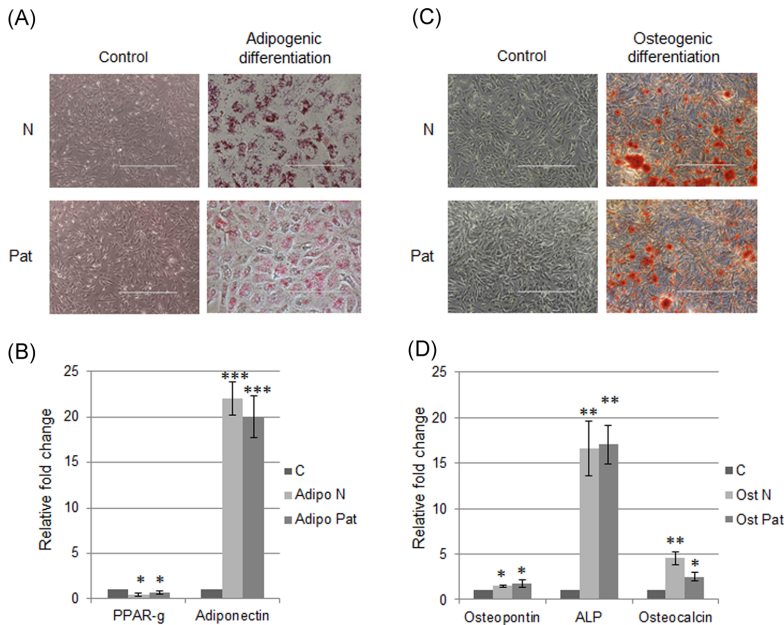


**FIGURE 3** AF-MSCs differentiation potential to mesodermal lineages. A, Representative image of Oil Red O-stained lipids produced in AF-MSCs of normal (N,  $n = 3$ ) and fetus-affected gestations (Pat,  $n = 6$ ) cultured for 9 days in adipogenic medium. C, Representative image of Alizarine red S stained minerals upon exposure of AF-MSCs of normal (N,  $n = 3$ ) and fetus-affected gestations (Pat,  $n = 6$ ) to osteogenic differentiation medium for 9 days (scale bar =  $400 \mu\text{m}$ ). B, Gene expression levels for adipogenic markers (PPAR- $\gamma$  and adiponectin) and D, osteogenic markers (ALP, osteopontin, osteocalcin) in MSCs derived from AF of normal ( $n = 4$ ) and fetus-affected ( $n = 6$ ) gestations at the ninth day of differentiation by RT-qPCR. All data are presented as the mean  $\pm$  SD; \* $P \leq .05$ ; \*\* $P \leq .01$ ; \*\*\* $P \leq .001$  were considered as significant changes. AF-MSCs, amniotic fluid-derived mesenchymal stem cells; ALP, alkaline phosphatase; PPAR- $\gamma$ , peroxisome proliferator-activated receptor-gamma; RT-qPCR, quantitative real-time polymerase chain reaction

AF-MSCs proliferation and adipogenic/osteogenic differentiation. The authors carried out RT-qPCR analysis for chosen miRNAs, such as hsa-miR-21, which acts as a regulator of clonogenic potential, proliferation and stem cell differentiation,<sup>21</sup> hsa-miR-17, hsa-miR-34a, and hsa-miR-146a/148b, which take part in regulation of lineage-specific differentiation.<sup>22-24</sup> As shown in Figure 4A, the expression of selected miRNAs (miR-17, miR-21, miR-34a, and miR-148b) during cultivation of undifferentiated AF-MSCs from both sources during early, intermediate, and late passages showed that miR-17 and miR-21 levels significantly decreased during passaging (from intermediate to late passage) while the levels of miR-34a and miR-148b increased as compared with early passage. Differentially expressed miRNAs in AF-MSCs cultures at intermediate passage between healthy donors and carrying fetal abnormalities are shown in Figure 4B, where all miRNAs were present at relatively lower levels in samples with fetal abnormalities than those of healthy donors.

To additionally investigate the role of miRNAs in differentiation toward distinct mesodermal tissues, the authors estimated the expression levels of four selected miRNAs in normal and fetus-pathological samples undergoing terminal adipogenic/osteogenic differentiation. A strong decrease in miR-17 and miR-21 expression was noticed in AF-MSCs from normal and fetus-affected gestations after 9 days of adipogenic induction compared with undifferentiated control (Figure 4C). Osteogenic differentiation at day 9 was associated with a downregulation of miR-17 but an upregulation of miR-21 (Figure 4D) while miR-34a and miR-146a expression was apparently downregulated in both adipocytes and osteoblasts with lower expressional changes in fetus-pathological samples. Thus, the results make it clear that the differences in miRNAs expression and their regulated functions during cultivation and differentiation to mesodermal lineage tissues exist in MSCs obtained from AF with fetal abnormalities.



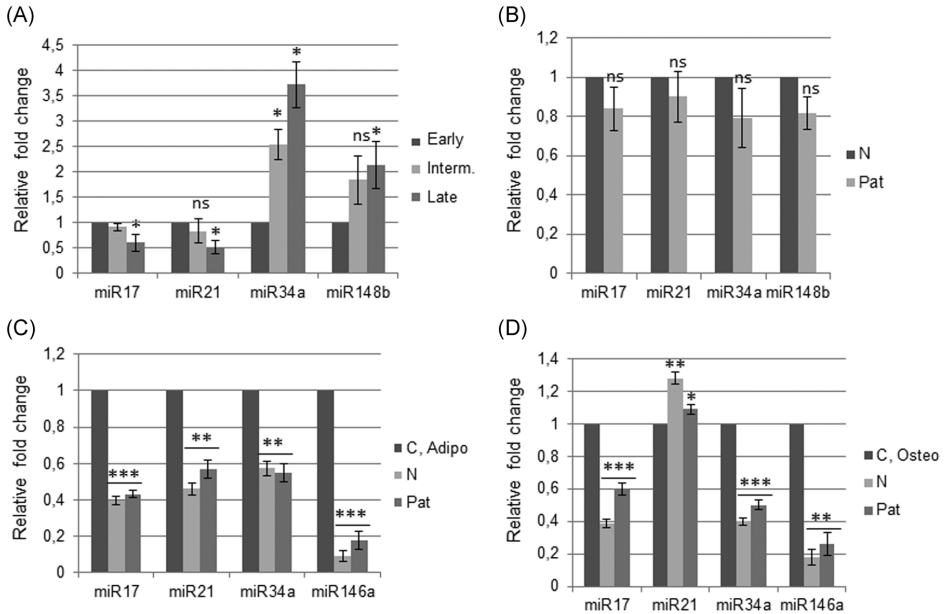


**FIGURE 4** Differential expression of miRNAs during passing and adipogenic/osteogenic differentiation of MSCs-derived AF of normal and fetus-pathological gestations. A, miRNA expression during passing (at early, intermediate [interm.], and late passages) of AF-MSCs and B, at intermediate passage of normal (N,  $n = 4$ ) and fetus-pathological samples (Pat,  $n = 6$ ). The fold change in miRNAs levels following C, adipogenic and D, osteogenic differentiation (ninth day). The relative expression levels were determined by the comparative threshold cycle delta-delta Ct method. All values are presented as the mean  $\pm$  SD; \* $P \leq .05$ ; \*\* $P \leq .01$ ; \*\*\* $P \leq .001$  were considered as significant changes versus control, ns—nonsignificant changes

### 3.3 | Epigenetic alterations associated with adipogenic and osteogenic differentiation of AF-MSC

Considering the fact that histone modifications are fundamentally involved in differentiation processes, the authors used Western blot analysis and in such way examined the state of core histone modifications and PcG proteins at the global level. The authors were interested in the comparison of the expression of histone modifications in AF samples of normal pregnancy (N) and fetus-diseased gestation (Pat) occurring at the terminal stage of osteogenic and adipogenic differentiation when most of the cells showed typical morphological changes (Figure 3). The authors found that at day 9 of adipogenic and osteogenic differentiation, the levels of active marks of chromatin, H4ac, H3K9ac, and “bivalent” mark H3K4me3 were decreased (Figure 5A,B). The terminal stage was related with a decrease in the levels of H3K9me3, a mark of heterochromatin, and EZH2, but the accumulation of a repressive H3K27me3 mark (Figures 5A and 5C). Both adipogenic and osteogenic differentiation were characterized by the strong decline in the levels of chromatin modifiers, DNMT1, and HDAC1, PRC2 protein SUZ12, and PRC1 protein BMI1 that maintain the repressive chromatin

state (Figure 6A,B). Figure 7 summarizes the epigenetic landscape of AF-MSCs in relation to terminal adipogenic and osteogenic differentiation. Overall, there were nonsignificant differences between MSCs from AF of normal and fetus-defected pregnancies in the expression of all epigenetic marks, indicating that various histone modifications and PcG proteins are involved similarly in chromatin reorganization for cell maintenance at the terminal stage of adipogenic and osteogenic differentiation of AF-MSCs at normal gestation and a pregnancy with fetus abnormalities.

## 4 | DISCUSSION

The question that the authors addressed in this study is whether MSCs isolated from AF of fetus-diseased gestations have the same potential to differentiate toward mesodermal lineage tissues. Our previous studies<sup>25,26</sup> reported the ability of second- and third-trimester AF-MSCs of healthy gestation to differentiate into adipogenic, osteogenic, and chondrogenic lineages. Consistent with this finding, this study demonstrates that MSCs from AF of pregnancies with fetus abnormalities had the same differentiation potential toward

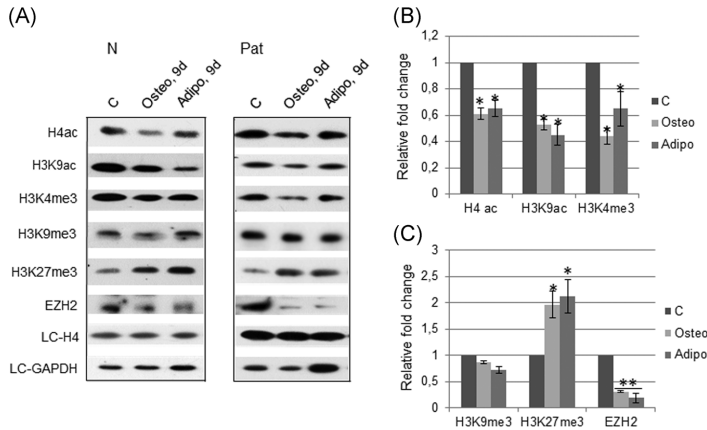


**FIGURE 5** The changes in histone modifications patterns in MSCs cultures from AF of normal and fetus-pathological gestations undergoing terminal differentiation to mesodermal lineages. Total proteins isolated after 9 days of differentiation induction. A, Representative Western blots of proteins from AF of normal gestation (N) and from individual donor carrying multiple fetal malformations (Pat). Histone H4 or GAPDH (as a loading control, [LC]) were used for normalization of each protein band. The normalized values of B, active marks and C, repressive marks of chromatin were used to calculate the fold change in the expression between undifferentiated and differentiated AF-MSCs. The data are from at least four gels of N and Pat samples showing similar results. All values are presented as the mean  $\pm$  SD; \* $P \leq .05$ ; \*\* $P \leq .01$  were considered as significant changes. AF-MSC, amniotic fluid-derived mesenchymal stem cells; EZH2: enhancer of Zeste histone H3K27 methyltransferase; GAPDH, glyceraldehyde-3-phosphate dehydrogenase

adipocytes and osteoblasts as was characterized by the characteristic features of cell phenotype and upregulation of lineage-specific markers' expression. However, some dissimilarity between samples may be due to the differences in the donor individuality, gestational time, or a state of cultured cells. This study also depicts some molecular features that influence the fate of MSCs from both cell sources. Here, the expressional level of transcription factors (Nanog, Oct4, Sox2, and Rex1) was studied as those factors that form a self-reinforcing and interconnected network are important not only to keep pluripotency and self-renewal, but to regulate the state of differentiation of stem cells as well.<sup>27</sup>

The expressional pattern of miRNAs has a major impact on MSCs differentiation by negatively regulating several transcription factors and key signaling molecules or targeting regulators of osteogenesis or adipogenesis.<sup>28,29</sup> To identify similarities or differences in the expression of miRNAs between cultured AF-MSCs obtained from two fetal sources and differentiated to adipocytes or osteoblasts, the authors defined selected miRNAs with predicted targets enriched in genes involved in Wnt, MAPK, or TGF $\beta$  signaling pathways.<sup>30</sup> Specifically, miR-21 was shown as a differentiation-associated miRNA in MSCs with an inverse expression pattern between adipogenesis and osteogenesis.<sup>21,31</sup> Our results also defined such correlation between decreased miR-21 expression leading to adipogenic differentiation and conversely, elevated expression of miR-21 during osteogenic differentiation of AF-MSCs derived from two fetal sources.

miR-17 is also involved in the balance between osteogenic and adipogenic differentiation by directly targeting BMP2 (bone morphogenetic protein 2) decreasing early osteogenic genes (TAZ, MSX2, and Runx2) and increasing adipogenic C/EBP $\alpha$  and PPAR- $\gamma$ , and, conversely, inhibition of miR-17 increases BMP2 expression promoting adipocyte differentiation and suppressing osteogenesis.<sup>32</sup> In this study, the authors found decreased levels of miR-17 in both adipocytes and osteoblasts that led to suggest that miR-17 is commonly implicated in the differentiation process of AF-MSCs under normal or diseased gestation conditions. According to the earlier data of the authors,<sup>33</sup> decreased expression of miR-21 and miR-17 during cell cultivation may be associated with the decrease in their proliferation potential. miR-34a had a dual regulatory nature controlling MSCs proliferation and osteoblast differentiation through targeting of Notch signaling where overexpression of miR-34a inhibited early commitment and late osteogenic differentiation, and conversely, inhibition of miR-34a improved these processes.<sup>29,34</sup> In this study, miR-34a expression grew along with the passage number of cultivated AF-MSCs, but terminal osteogenic and adipogenic differentiation was characterized by the decrease in the levels of miR-34a along with a significant downregulation of miR-146a. miR-146a has previously been shown<sup>23</sup> to be highly expressed in multiple types of adult stem cells and may be linked to osteogenic differentiation by its downregulation, but the role of miR-146a in adipogenic differentiation of AF-MSCs has not been



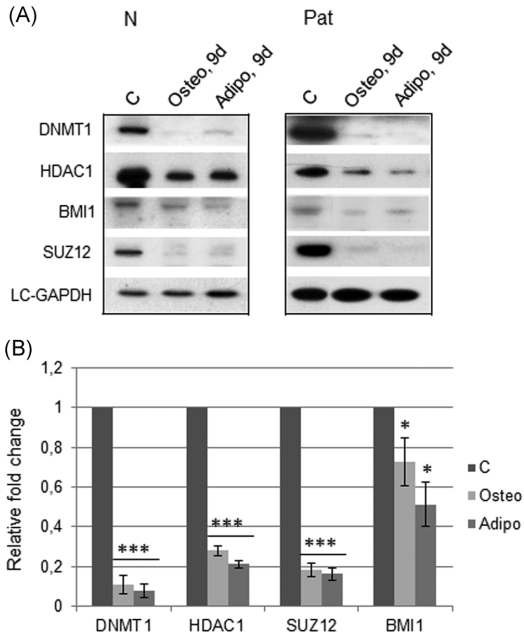


**FIGURE 6** Expression profile of chromatin modifiers in AF-MSCs from normal and fetus-pathological gestations undergoing terminal adipogenic and osteogenic differentiation. A, Representative immunoanalysis of chromatin proteins after 9 days of differentiation from AF of normal gestation (N) and individual donor carrying multiple fetal malformations (Pat). B, Quantification of Western blot analysis data in Fig. A. Protein levels in each gel after scanning densitometry was normalized to corresponding loading control (LC-GAPDH). The data are from at least four gels of N and Pat samples showing similar results. All values are presented as the mean  $\pm$  SD, \* $P \leq .05$ ; \*\*\* $P \leq .001$  were considered as significant changes. AF-MSC, amniotic fluid-derived mesenchymal stem cells; GAPDH, glyceraldehyde-3-phosphate dehydrogenase

elucidated. These and our previous observations<sup>25</sup> led to gain a better knowledge of the miRNAs that are characteristic of AF-MSCs from various sources and may be essential in determining MSCs proliferation and differentiation.

The key aspect of MSCs differentiation is the extensive chromatin remodeling which happens in consequence of cell commitment to differentiate. It was shown that the dynamical change of gene expression during differentiation happens because of cooperation between PcG proteins and histone modifications, and the chromatin structure is regulated by regulating the chromatin structure.<sup>35</sup> So far, there is no large amount of data available on such cooperation in undifferentiated AF-MSCs and differentiated toward specific-cell lineages. Here, we have analyzed histone modifications and PcG proteins involved in AF-MSCs

terminal differentiation to mesodermal tissues. As shown in Figure 7, decrease in chromatin active marks levels was indicated after this process (H4ac, H3K9ac, and H3K4me3), the repressive mark H3K9me3, SUZ12 (which methylate H3K9 and function to silent the EZH2 complex), and also BMI1, which keeps the repressive chromatin state.<sup>36</sup> Conversely, increased level of H3K27me3 but decreased expression of EZH2 was determined in the terminal stage of adipogenic and osteogenic differentiation as compared with undifferentiated control. It has been shown that different histone modifications are integral to chromatin reorganization and regulation of gene transcription upon adipogenic differentiation of MSCs.<sup>37,38</sup> The activation of adipogenesis was shown to be accompanied by the downregulation of HDAC1, demethylation of H3K27me3 in addition to increased acetylation of H3K9.<sup>39,40</sup> The previous research<sup>9</sup> demonstrated that core histone modifications are constant at global levels, but highly dynamic at the level of specific genes during adipogenic differentiation, suggesting that the alterations specific to genes in histone modification states occur also because of their fluctuation at the global level.

The role of PcG proteins and histone methylation in regulating osteogenic differentiation was also described.<sup>41,42</sup> In human MSCs, induction of osteogenic differentiation has been shown to be associated with acetylation of H4, H3K9, and H3K9 dimethylation for osteogenic-specific gene activation.<sup>43,44</sup> Upon MSCs osteogenic differentiation, H3K9ac decreased and H3K9me2 increased globally while total levels of "bivalent" marks, H3K4me3, and H3K27me3 remained mostly unchanged during differentiation.<sup>42,45</sup> Here, we provide evidence that terminal osteogenic differentiation was related to the decrease in active H3K4me3 mark and the accumulation of H3K27me3 along with a loss of PRC1/2 proteins that may be due to derepression of the late differentiation marker genes.<sup>11,46</sup> By a proposed mechanism, PRC2 is in a definite way recruited to target genes for the repression of transcription upon induction of differentiation or enables activation of target genes for the following differentiation, and SUZ12 is necessary for the establishment of particular expression programs of differentiation. PRC1 (includes BMI1) can be recruited to target genes, in case there is no functional PRC2 complex, and regardless of H3K27me3.<sup>47</sup> In addition, EZH2 may have self-sufficient functions that do not include H3K27 methylation.<sup>48</sup> Recent research works announce that it is possible to regulate epigenetically the switch between adipogenesis and osteogenesis, while involving EZH2 and demethylase KDM6A, determining MSCs differentiation toward adipocytes and osteocytes, respectively.<sup>49</sup> Mechanistically, EZH2 stimulates adipogenesis by destroying the Wnt/ $\beta$ -catenin signaling through direct binding to the promoters of Wnt genes to repress their expression. On the contrary, the suppression of

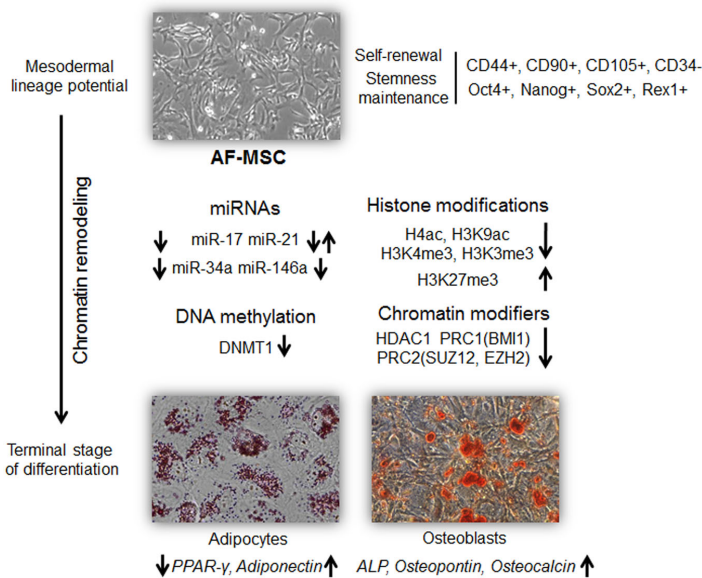


**FIGURE 7** Schematic illustration of the changes in expression patterns of selected miRNAs, epigenetic histone modifications, and chromatin-modifying proteins at the terminal stage of adipogenic and osteogenic differentiation of MSCs derived from AF of normal gestations and those with fetal abnormalities. AF, amniotic fluid; miRNA, micro RNA; MSC, mesenchymal stem cell

EZH2 results in differentiation into osteoblasts.<sup>17</sup> According to our data, PRC1/2 proteins (BMI1/EZH2, SUZ12), which participate in the determination of lineage-specific differentiation in AF-MSCs, are similarly involved in the regulation of genes that mediate terminal differentiation and the progression to a more solid, repressive chromatin state.

## 5 | CONCLUSION

AF-MSCs from healthy pregnancies and fetus-diseased gestations represent a population of stem cells, the origin of which is mesenchymal and which have quite similar expression profile of cell surface and pluripotency markers and share the similar differentiation potential through rather similar epigenetic mechanisms regulating chromatin modifications during terminal stage of their differentiation to mesodermal lineage tissues and cell maintenance in the differentiated state. This could direct that AF-MSCs may be a significant alternative for patient-specific therapy.

## ACKNOWLEDGMENTS

This work was supported by the Research Council of Lithuania (Project No. MIP-057/2015). The authors would like to thank Natalija Krasovskaja for the sample collecting and the subjects whose participation made this study possible.

## CONFLICT OF INTERESTS

The authors declare that there are no conflict of interests.

## AUTHOR CONTRIBUTIONS

AZ performed experiments and analyzed the data and contributed in writing a manuscript; MG performed experiments and data interpretations; GT performed experiments and analyzed the data; SB performed experiments and analyzed the data; JS contributed in writing a manuscript and performed data interpretations; VB performed data analysis; RN designed the research study, performed data interpretations, and revised the manuscript.

## ORCID

Monika Gasiūnienė <http://orcid.org/0000-0001-5997-1088>

Rūta Navakauskienė <http://orcid.org/0000-0002-1077-9439>

## REFERENCES

- Bianco P, Robey PG, Simmons PJ. Mesenchymal stem cells: revisiting history, concepts, and assays. *Cell Stem Cell*. 2008;2: 313-319.
- Trohatou O, P. Anagnou N, Roubelakis GM. Human amniotic fluid stem cells as an attractive tool for clinical applications. *Curr Stem Cell Res Ther*. 2013;8:125-132.

3. Da Sacco S, De Filippo RE, Perin L. Amniotic fluid as a source of pluripotent and multipotent stem cells for organ regeneration. *Curr Opin Organ Transplant*. 2011;16:101-105.
4. Siegel N, Rosner M, Hanneder M, Valli A, Hengstschläger M. Stem cells in amniotic fluid as new tools to study human genetic diseases. *Stem Cell Rev*. 2007;3:256-264.
5. Cananzi M, Atala A, De Coppi P. Stem cells derived from amniotic fluid: new potentials in regenerative medicine. *Reprod Biomed Online*. 2009;18(Suppl 1):17-27.
6. Teven CM, Liu X, Hu N, et al. Epigenetic regulation of mesenchymal stem cells: a focus on osteogenic and adipogenic differentiation. *Stem Cells Int*. 2011;2011:1-18.
7. Wu H, Gordon JAR, Whitfield TW, et al. Chromatin dynamics regulate mesenchymal stem cell lineage specification and differentiation to osteogenesis. *Biochimica et Biophysica Acta—Gene Regul Mech*. 2017;1860:438-449.
8. Deng P, Chen Q-M, Hong C, Wang C-Y. Histone methyltransferases and demethylases: regulators in balancing osteogenic and adipogenic differentiation of mesenchymal stem cells. *Int J Oral Sci*. 2015;7:197-204.
9. Zhang Q, Ramlee MK, Brunmeir R, Villanueva CJ, Halperin D, Xu F. Dynamic and distinct histone modifications modulate the expression of key adipogenesis regulatory genes. *Cell Cycle*. 2012;11:4310-4322.
10. Bernstein BE, Mikkelsen TS, Xie X, et al. A bivalent chromatin structure marks key developmental genes in embryonic stem cells. *Cell*. 2006;125:315-326.
11. Schuettengruber B, Cavalli G. Recruitment of Polycomb group complexes and their role in the dynamic regulation of cell fate choice. *Development*. 2009;136:3531-3542.
12. Neve ACorrado, Cantatore FP. Osteoblast physiology in normal and pathological conditions. *Cell Tissue Res*. 2011;343:289-302.
13. Stein GS, Lian JB, Wijnen AJ, et al. Runx2 control of organization, assembly and activity of the regulatory machinery for skeletal gene expression. *Oncogene*. 2004;23:4315-4329.
14. Rosen ED, MacDougald OA. Adipocyte differentiation from the inside out. *Nat Rev Mol Cell Biol*. 2006;7:885-896.
15. Farmer SR. Transcriptional control of adipocyte formation. *Cell Metab*. 2006;4:263-273.
16. D'Alimonte I, Lannutti A, Pipino C, et al. Wnt signaling behaves as a “master regulator” in the osteogenic and adipogenic commitment of human amniotic fluid mesenchymal stem cells. *Stem Cell Rev Rep*. 2013;9:642-654.
17. Wang L, Jin Q, Lee JE, Su I, Ge K. Histone H3K27 methyltransferase Ezh2 represses Wnt genes to facilitate adipogenesis. *Proc Natl Acad Sci USA*. 2010;107:7317-7322.
18. Kang H, Hata A. The role of microRNAs in cell fate determination of mesenchymal stem cells: balancing adipogenesis and osteogenesis. *BMB Rep*. 2015;48:319-323.
19. Tsai MS, Lee JL, Chang YJ, Hwang SM. Isolation of human multipotent mesenchymal stem cells from second-trimester amniotic fluid using a novel two-stage culture protocol. *Hum Reprod*. 2004;19:1450-1456.
20. Gasiūnienė M, Zentelytė A, Treigytė G, et al. Epigenetic alterations in amniotic fluid mesenchymal stem cells derived from normal and fetus-affected gestations: a focus on myogenic and neural differentiations. *Cell Biol Int*. 2019;43:299-312.
21. Krichevsky AM, Gabrieli G. miR-21: a small multi-faceted RNA. *J Cell Mol Med*. 2009;13:39-53.
22. Foshay KM, Gallicano GI. miR-17 family miRNAs are expressed during early mammalian development and regulate stem cell differentiation. *Dev Biol*. 2009;326:431-443.
23. Huszar JM, Payne CJ. MIR146A inhibits JMJD3 expression and osteogenic differentiation in human mesenchymal stem cells. *FEBS Lett*. 2014;588:1850-1856.
24. Park H, Park H, Pak HJ, et al. miR-34a inhibits differentiation of human adipose tissue-derived stem cells by regulating cell cycle and senescence induction. *Differentiation*. 2015;90:91-100.
25. Glemžaitė M, Navakauskienė R. Osteogenic differentiation of human amniotic fluid mesenchymal stem cells is determined by epigenetic changes. *Stem Cells Int*. 2016;2016:1-10.
26. Savickienė J, Treigytė G, Baronaite S, et al. Human amniotic fluid mesenchymal stem cells from second- and third-trimester amniocentesis: differentiation potential, molecular signature, and proteome analysis. *Stem Cells Int*. 2015;2015:1-15.
27. Boyer LA, Lee TI, Cole MF, et al. Core transcriptional regulatory circuitry in human embryonic stem cells. *Cell*. 2005;122:947-956.
28. Gao J, Yang T, Han J, et al. MicroRNA expression during osteogenic differentiation of human multipotent mesenchymal stromal cells from bone marrow. *J Cell Biochem*. 2011;112:1844-1856.
29. Chen L, Holmström K, Qiu W, et al. MicroRNA-34a inhibits osteoblast differentiation and in vivo bone formation of human stromal stem cells. *Stem Cells*. 2014;32:902-912.
30. Lazzarini R, Olivieri F, Ferretti C, Mattioli-Belmonte M, Di Primio R, Orciani M. mRNAs and miRNAs profiling of mesenchymal stem cells derived from amniotic fluid and skin: the double face of the coin. *Cell Tissue Res*. 2014;355:121-130.
31. Trohatou O, Zagoura D, Bitsika V, et al. Sox2 suppression by miR-21 governs human mesenchymal stem cell properties. *Stem Cells Transl Med*. 2014;3:54-68.
32. Li H, Li T, Wang S, et al. miR-17-5p and miR-106a are involved in the balance between osteogenic and adipogenic differentiation of adipose-derived mesenchymal stem cells. *Stem Cell Res*. 2013;10:313-324.
33. Savickienė J, Baronaite S, Zentelytė A, Treigytė G, Navakauskienė R. Senescence-associated molecular and epigenetic alterations in mesenchymal stem cell cultures from amniotic fluid of normal and fetus-affected pregnancy. *Stem Cells Int*. 2016;2016:1-13.
34. Chen F, Hu S-J. Effect of microRNA-34a in cell cycle, differentiation, and apoptosis: a review. *J Biochem Mol Toxicol*. 2012;26:79-86.
35. Ku M, Koche RP, Rheinbay E, et al. Genome-wide analysis of PRC1 and PRC2 occupancy identifies two classes of bivalent domains. *PLoS Genet*. 2008;4:e1000242.
36. Cao R, Zhang Y. SUZ12 is required for both the histone methyltransferase activity and the silencing function of the EED-EZH2 complex. *Mol Cell*. 2004;15:57-67.
37. Huang B, Li G, Jiang XH. Fate determination in mesenchymal stem cells: a perspective from histone-modifying enzymes. *Stem Cell Res Ther*. 2015;6:35.
38. Musri MM, Gomis R, Párrizas M. Chromatin and chromatin-modifying proteins in adipogenesis. *Biochem Cell Biol*. 2007;85:397-410.
39. Noer A, Lindeman LC, Collas P. Histone H3 modifications associated with differentiation and long-term culture of mesenchymal adipose stem cells. *Stem Cells Dev*. 2009;18:725-736.

40. Yoo EJ, Chung JJ, Choe SS, Kim KH, Kim JB. Down-regulation of histone deacetylases stimulates adipocyte differentiation. *J Biol Chem*. 2006;281:6608-6615.
41. Fakhry M, Hamade E, Badran B, Buchet R, Magne D. Molecular mechanisms of mesenchymal stem cell differentiation towards osteoblasts. *World J Stem Cells*. 2013;5:136-148.
42. Wei Y, Chen YH, Li LY, et al. CDK1-dependent phosphorylation of EZH2 suppresses methylation of H3K27 and promotes osteogenic differentiation of human mesenchymal stem cells. *Nat Cell Biol*. 2011;13:87-94.
43. Lee HW, Suh JH, Kim AY, Lee YS, Park SY, Kim JB. Histone deacetylase 1-mediated histone modification regulates osteoblast differentiation. *Mol Endocrinol*. 2006;20:2432-2443.
44. Tan J, Lu J, Huang W, et al. Genome-wide analysis of histone H3 lysine9 modifications in human mesenchymal stem cell osteogenic differentiation. *PLoS One*. 2009;4:e6792.
45. Häkkelien AM, Bryne JC, Harstad KG, et al. The regulatory landscape of osteogenic differentiation. *Stem Cells*. 2014;32:2780-2793.
46. Pietersen AM, van Lohuizen M. Stem cell regulation by polycomb repressors: postponing commitment. *Curr Opin Cell Biol*. 2008;20:201-207.
47. Pasini D, Bracken AP, Hansen JB, Capillo M, Helin K. The polycomb group protein Suz12 is required for embryonic stem cell differentiation. *Mol Cell Biol*. 2007;27:3769-3779.
48. Margueron R, Li G, Sarma K, et al. Ezh1 and Ezh2 maintain repressive chromatin through different mechanisms. *Mol Cell*. 2008;32(4):503-518.
49. Hemming S, Cakouros D, Isenmann S, et al. EZH2 and KDM6A act as an epigenetic switch to regulate mesenchymal stem cell lineage specification. *Stem Cells*. 2014;32:802-815.

**How to cite this article:** Zentelytė A, Gasiūnienė M, Treigytyė G, et al. Epigenetic regulation of amniotic fluid mesenchymal stem cell differentiation to the mesodermal lineages at normal and fetus-diseased gestation. *J Cell Biochem*. 2020;121:1811–1822. <https://doi.org/10.1002/jcb.29416>

3 publikacija / publication 3

**A. Zentelytė, D. Žukauskaitė, I. Jacerytė, V.V. Borutinskaitė, R. Navakauskienė**

Small Molecule Treatments Improve Differentiation Potential of Human Amniotic Fluid Stem Cells

2021, *Frontiers in Bioengineering and Biotechnology*, 9:623886  
doi: 10.3389/fbioe.2021.623886

Copyright © 2021 Zentelytė, Žukauskaitė, Jacerytė, Borutinskaitė, Navakauskienė

Atviros prieigos publikacija platinama pagal „Creative Commons“ priskyrimo licenciją (CC BY). Publikacijos naudojimas, platinimas ar atgaminimas kituose forumuose yra leidžiamas su sąlyga, kad pirminis(-iai) autorius(-iai) ir autorių teisių savininkas(-ai) yra nurodytas ir šio žurnalo publikacija yra cituojama laikantis priimtų akademinės praktikos normų.

This is an open-access article distributed under the terms of the Creative Commons Attribution License (CC BY). The use, distribution or reproduction in other forums is permitted, provided the original author(s) and the copyright owner(s) are credited and that the original publication in this journal is cited, in accordance with accepted academic practice.



# Small Molecule Treatments Improve Differentiation Potential of Human Amniotic Fluid Stem Cells

Aisté Zentelytė\*, Deimantė Žukauskaitė, Ieva Jacerytė, Veronika V. Borutinskaitė and Rūta Navakauskienė

Department of Molecular Cell Biology, Life Sciences Center, Institute of Biochemistry, Vilnius University, Vilnius, Lithuania

## OPEN ACCESS

### Edited by:

Antonietta Rosa Silini,  
Fondazione Poliambulanza Istituto  
Ospedaliero, Italy

### Reviewed by:

Sveva Bollini,  
University of Genoa, Italy  
Tullia Maraldi,  
University of Modena and Reggio  
Emilia, Italy

### \*Correspondence:

Aisté Zentelytė  
aiste.zentelyte@bchi.vu.lt

### Specialty section:

This article was submitted to  
Tissue Engineering and Regenerative  
Medicine,  
a section of the journal  
Frontiers in Bioengineering and  
Biotechnology

**Received:** 30 October 2020

**Accepted:** 02 February 2021

**Published:** 22 February 2021

### Citation:

Zentelytė A, Žukauskaitė D,  
Jacerytė I, Borutinskaitė VV and  
Navakauskienė R (2021) Small  
Molecule Treatments Improve  
Differentiation Potential of Human  
Amniotic Fluid Stem Cells.  
Front. Bioeng. Biotechnol. 9:623886.  
doi: 10.3389/fbioe.2021.623886

Human amniotic fluid stem cells (AFSC) are an exciting and very promising source of stem cells for therapeutic applications. In this study we investigated the effects of short-term treatments of small molecules to improve stem cell properties and differentiation capability. For this purpose, we used epigenetically active compounds, such as histone deacetylase inhibitors Trichostatin A (TSA) and sodium butyrate (NaBut), as well as multifunctional molecules of natural origin, such as retinoic acid (RA) and vitamin C (vitC). We observed that combinations of these compounds triggered upregulation of genes involved in pluripotency (*KLF4*, *OCT4*, *NOTCH1*, *SOX2*, *NANOG*, *LIN28a*, *CMYC*), but expression changes of these proteins were mild with only significant downregulation of Notch1. Also, some alterations in cell surface marker expression was established by flow cytometry with the most explicit changes in the expression of CD105 and CD117. Analysis of cellular energetics performed using Seahorse analyzer and assessment of gene expression related to cell metabolism and respiration (*NRF1*, *HIF1 $\alpha$* , *PPARGC1A*, *ERR $\alpha$* , *PKM*, *PDK1*, *LDHA*, *NFKB1*, *NFKB2*, *RELA*, *RELB*, *REL*) revealed that small molecule treatments stimulate AFSCs toward a more energetically active phenotype. To induce cells to differentiate toward neurogenic lineage several different protocols including commercial supplements N2 and B27 together with RA were used and compared to the same differentiation protocols with the addition of a pre-induction step consisting of a combination of small molecules (vitC, TSA and RA). During differentiation the expression of several neural marker genes was analyzed (*Nestin*, *MAP2*, *TUBB3*, *ALDH1L1*, *GFAP*, *CACNA1D*, *KCNJ12*, *KCNJ2*, *KCNH2*) and the beneficial effect of small molecule treatment on differentiation potential was observed with upregulated gene expression. Differentiation was also confirmed by staining TUBB3, NCAM1, and Vimentin and assessed by secretion of BDNF. The results of this study provide valuable insights for the potential use of short-term small molecule treatments to improve stem cell characteristics and boost differentiation potential of AFSCs.

**Keywords:** amniotic fluid stem cells, neurogenic differentiation, small molecules, trichostatin A, vitamin C, retinoic acid



## INTRODUCTION

Nowadays, alternative sources of potent stem cells are of great interest and human amniotic fluid could be an attractive option. Stem cells isolated from amniotic fluid display several key characteristics that are essential for therapeutic applications. Amniotic fluid stem cells (AFSC) possess the ability to self-renew, differentiate into cell lineages from all three germ layers, they do not form teratomas *in vivo* and have low immunogenicity (Bossolasco et al., 2006; De Coppi et al., 2007; Roubelakis et al., 2007; Da Sacco et al., 2011). These cells are autogenous to the fetus and semiallogenic to each parent and are said to be more potent than stem cells from other sources, such as bone marrow, umbilical cord blood, endometrium and other (Yan et al., 2013; Bonaventura et al., 2015; Alessio et al., 2018). Although AFSCs are somewhat similar to pluripotent stem cells, they are still considered as multipotent stem cells, and one approach to improve the plasticity and applicability of AFSCs could be by using small molecules. The use of small molecules is a relatively new technique of cell reprogramming and transdifferentiation (Kim et al., 2020). Nuclear transfer, transcription factor transfection, mRNA based reprogramming methods face many challenges in time and yield efficiency, complexity of delivery and the risk of integrating exogenous genetic material. Meanwhile, small molecules are inexpensive and easy to apply and control time, concentration and combination wise, they usually easy to manufacture and have a long shelf life. In addition, small molecules are cell permeable, non-immunogenic and can be prescribed to patients as drugs to promote endogenous cell repair and regeneration (Baranek et al., 2017; Ma et al., 2017). Our study was designed to determine how our selected epigenetically active compounds affect stem cell characteristics, such as surface marker and pluripotency associated gene expression, as well as what effect small molecules of interest have on metabolic phenotype and neurogenic differentiation of AFSCs. The aim of this study was to investigate whether uncomplicated and short-term treatments with small molecules improve stem cell characteristics and also provide an improved differentiation efficiency of AFSCs toward neurogenic lineage. We investigated the impact of the following small molecules on primary stem cell lines: HDAC inhibitors trichostatin A (TSA), sodium butyrate (NaBut) and multifunctional molecules of natural origin retinoic acid (RA) and vitamin C (vitC). We demonstrated that the concentrations and combinations of small molecules do not have a cytotoxic effect on AFSCs, but they do affect gene expression patterns with an increased expression of pluripotency markers and neurogenesis associated transcription factors (*OCT4*, *NANOG*, *LIN28a*, *CMYC*, *NOTCH1*, *SOX2*), although at protein level the changes are mild except for significant downregulation of Notch1. Also, small molecules affect the expression of surface markers (SSEA4, CD117, TRA-1-81, CD105). Treated stem cells with combinations of small molecules showed altered metabolic profile as evident by the changes in mitochondrial and glycolytic activity and expression of genes involved in cellular metabolism (*NRF1*, *HIF1 $\alpha$* , *PPARGC1A*, *ERR $\alpha$* , *PKM*, *PDK1*, and *LDHA*) and NF- $\kappa$ B pathway (*NFKB1*, *NFKB2*, *RELA*, *RELB*, *REL*). To

test the small molecule combination treatments, we examined the neurogenic differentiation potential of AFSCs and showed that adding a pre-induction step of small molecule treatment improved secretion levels of BDNF and the expression of tested neurogenic genes (*Nestin*, *MAP2*, *TUBB3*, *ALDH1L1*, *GFAP*) and genes of several ion channels (*CACNA1D*, *KCNJ12*, *KCNJ2*, *KCNH2*). In summary, this study demonstrates that short treatments with small molecule combinations could be used as pre-induction steps to improve differentiation efficiency.

## MATERIALS AND METHODS

### Isolation and Expansion of Human Amniotic Fluid Stem Cells

Human amniotic fluid samples were obtained by amniocentesis from healthy women (age average—39 years) who needed prenatal diagnostics, but no abnormalities were detected by genetic and karyotype analysis (protocols approved by the Ethics Committee of Biomedical Research of Vilnius District, No 158200-123-428-122). AFSC were isolated using two-step isolation protocol as previously described (Tsai et al., 2004; Savickiene et al., 2015). Isolated cells were maintained in DMEM media, supplemented with 10% fetal bovine serum (FBS), 100 U/ml penicillin and 100  $\mu$ g/ml streptomycin (Gibco, Thermo Fisher Scientific). To observe cells in culture, phase contrast microscope (Nicon Eclipse TS100) was used.

### Flow Cytometry Analysis

AFSCs were characterized by the expression of their surface markers. Cells were collected and washed twice with phosphate buffered saline (PBS) with 1% bovine serum albumin (BSA). A total of  $6 \cdot 10^4$  cells/sample were resuspended in 50  $\mu$ l of PBS with 1% BSA and incubated with the following mouse anti-human antibodies: phycoerythrin (PE) conjugated CD166 (Biolegend) TRA-1-60 (Invitrogen), fluorescein isothiocyanate (FITC) conjugated CD34, CD73, CD90, CD105 (Biolegend), Alexa Fluor<sup>®</sup> 488 conjugated CD31, HLA-ABC, HLA-DR (Biolegend), allophycocyanin (APC) conjugated CD44, CD117, CD146, SSEA4 (Biolegend), TRA-1-81 (Invitrogen). Appropriate mouse isotype controls were used, such as IgG1-PE (Biolegend), IgM-PE (Invitrogen), IgG1-FITC, IgG2a-FITC (Biolegend), IgG1-Alexa Fluor<sup>®</sup> 488, IgG2a-Alexa Fluor<sup>®</sup> 488 (Biolegend), IgG1-APC, IgG3-APC (Biolegend), IgM-APC (Invitrogen). Labeled cells were incubated in the dark at 4°C for 30 min, then washed twice with PBS with 1% BSA and then analyzed. For intracellular staining cells were washed with PBS and fixed using 2% paraformaldehyde at RT for 10 min. After washing step cells were permeabilized with 0.1% Triton X-100 in PBS/1% BSA solution at RT for 15 min. After centrifugation cells were resuspended in permeabilization solution and incubated for 30 min at 4°C in the dark with the following mouse anti-human antibodies: Alexa Fluor<sup>®</sup> 488 conjugated Sox2 (Biolegend), Alexa Fluor<sup>®</sup> 647 conjugated Nanog, Oct4 (Biolegend), unconjugated Lin28a and c-Myc. Goat anti-mouse IgG (H + L) Highly Cross-Absorbed Alexa Fluor<sup>®</sup> 488 (Invitrogen) conjugated secondary antibodies were used to label Lin28a and c-Myc samples for

another 30 min at 4°C in the dark. After incubations cells were washed with PBS/1% BSA and analyzed. The measurements were performed using BD FACSCanto™ II flow cytometer with BD FACSDIVA™ software (BD Biosciences). Ten thousand events were collected for each sample.

## Karyotyping AFSCs

To determine origin of AFSCs, karyotype analysis was performed and only samples with confirmed male fetus were chosen. AFSCs were treated with 0.6 µg/ml of colchicine for 3 h, then cells were collected by trypsinization and incubated with pre-warmed hypotonic 0.55% KCl solution for 30 min. at 37°C. The cells were fixed with fixation solution consisting of methanol and glacial acetic acid (3:1) at -20°C for 30 min., centrifuged and fixation repeated two more times. A few drops of cell suspension were transferred on a microscope slide and stained with 5% Giemsa (Merck) solution in Sorensen's phosphate buffer for 5 min. Slides were analyzed at a magnification of 1,000× (Nikon ECLIPSE E200). Only well-spread metaphases with 42 ± 1 chromosomes were used for the analysis.

## Treatment With Agents and MTT Assay

Cells were seeded into 48-well plates and treated with different concentrations and combinations of epigenetically active compounds [Decitabine, Trichostatin A (TSA), Sodium butyrate (NaBut), Retinoic acid (RA) and Vitamin C (VitC)], three replicates each. After incubation periods the medium was removed from the cells and to measure cell viability 100 µl of 0.2 mg/ml MTT reagent in PBS (Sigma-Aldrich) was added to each well and then incubated for 1.5 h at 37°C. The precipitate was dissolved in 200 µl 96% ethanol and optical density (OD) of each well was measured using spectrophotometer Infinite M200 Pro (Tecan) at 570 and 630 nm wavelength. Cell viability (in percent) was calculated as the ratio between ODs (570 and 630 nm) of treated samples and untreated control.

## Neurogenic Differentiation

To differentiate AFSCs toward neurogenic lineage, several induction protocols were used. Induction medias consisted of DMEM/F12 with GlutaMax™, 3 µM of RA (Sigma-Aldrich), 100 U/ml penicillin and 100 µg/ml streptomycin and either 1% of N2 supplement, 2% B27 supplement or their combination (Gibco, Thermo Fisher Scientific). Cells were induced to differentiate at 40–60% confluence with media changes every 3 days. To test the effect of epigenetically active molecules, a pre-treatment step was added. AFSCs were treated for 24 h with 25 µg/ml VitC, 20 nM TSA, 0.1 µM RA in DMEM/F12 supplemented with 5% FBS and 100 U/ml penicillin and 100 µg/ml streptomycin. Then the pretreatment media was changed to differentiation medias. I—1% of N2 and 3 µM of RA, II—2% B27 and 3 µM of RA, III—1% of N2, 2% B27 and 3 µM of RA, VI—preinduction, then 1% of N2 and 3 µM of RA, V—preinduction, then 2% B27 and 3 µM of RA, VI—preinduction, then 1% of N2, 2% B27 and 3 µM of RA. Morphological changes were observed with phase contrast microscopy. More information on optimization of neurogenic differentiation media and differentiation induction design is provided in **Supplementary Figures 1, 2**.

## Gene Expression Analysis

Total RNA from AFSCs was isolated using TRIzol® reagent (Applied Biosystems) as recommended by the manufacturer. For the gene expression analysis, cDNA synthesis was performed using SensiFAST™ cDNA Synthesis Kit (Bioline). RT-qPCR was performed with SensiFAST™ SYBR® No-ROX Kit (Bioline) on the Rotor-Gene 6000 thermocycler with Rotor-Gene 6000 series software (Corbett Life Science). *GAPDH* gene was used for normalization of the mRNA amount and the relative gene expression was calculated using  $\Delta\Delta C_t$  method (compared to untreated or undifferentiated control). The list of primers (Metabion International AG, Planegg-Steinkirchen, Germany) is provided in **Supplementary Material**.

## Extracellular Flux Analysis

Control and treated cells were characterized by their energetic profile which was determined using Seahorse XFp Extracellular Flux Analyzer and Cell Energy Phenotype Test Kit (Agilent Technologies, CA, United States). Oxygen consumption rate (OCR) and extracellular acidification rate (ECAR) were measured simultaneously firstly without inhibitors (the baseline), and then after the addition of oligomycin and FCCP (inhibitors of the electron transfer chain). After the measurements cell protein lysates were obtained using RIPA buffer (150 mM NaCl, 10 mM EDTA, pH 8.0, 10 mM Tris, pH 7.4, 0.1% SDS, 1% deoxycholate, 1% NP-40 in PBS, pH 7.6) and protein concentrations were measured with spectrophotometer Infinite M200 Pro (Tecan, Switzerland) using DC Protein Assay (Bio-Rad Laboratories, CA, United States). OCR and ECAR values were normalized to the total amount of protein in each well. Cell energy phenotype as the ratio of normalized OCR to normalized ECAR (OCR/ECAR) and the metabolic potential as the percentage increase of stressed OCR over baseline OCR and stressed ECAR over baseline ECAR, were assessed from Cell Energy Phenotype Test data using Seahorse Wave Desktop Software.

## Immunofluorescence Analysis

To assess neurogenic differentiation, AFSCs were seeded on coverslips and cultivated as undifferentiated control or differentiated toward neurogenic lineage using I-VI protocols for 14 days. Cells were with 4% paraformaldehyde for 15 min at RT and permeabilized using 0.2% Triton X-100 in PBS for 20 min. at RT. After washing with PBS, cells were blocked using 1% BSA/10% goat serum/PBS for 30 min at 37°C. Detection of NCAM: cells were incubated with primary mouse antibodies against NCAM1 (15 µg/ml) (Abcam) and secondary goat anti-mouse IgG (H + L) Highly Cross-Adsorbed, Alexa Fluor® 594 antibodies (1:400) (Invitrogen) for 1 h each at 37°C in a humid chamber. Detection of TUBB3 and Vimentin: cells were incubated with FITC conjugated rabbit anti-beta III tubulin antibodies (1:100) (Abcam) or Alexa Fluor® 488 conjugated rabbit anti-Vimentin antibodies (1:150) (Abcam) for 1 h at 37°C in a humid chamber. F-actin was labeled with Alexa Fluor® 594 Phalloidin (Thermo Fisher Scientific) for 30 min RT. After each incubation coverslips were washed several times with PBS/1% BSA. Nuclei were stained using 300 nM



DAPI solution (Invitrogen) for 10 min RT. Coverslips were mounted using Dako Fluorescent Mounting Medium (Agilent Technologies) and analyzed using Zeiss Axio Observer (Zeiss) fluorescent microscope,  $\times 63$  magnification with immersion oil and Zen BLUE software.

## Enzyme-Linked Immunosorbent Assay of BDNF

ELISA method was used to determine the secreted levels of BDNF in conditioned media of control AFSCs and AFSCs differentiated toward neurogenic lineage. Cells were seeded in wells of 6-well plates and were cultivated as control or induced to differentiate toward neurogenic lineage using I-VI protocols. Cells were washed with PBS and NutriStem<sup>®</sup> hPSC XF medium (Biological Industries) was added for 3 days, after which both the cells and the media were collected separately. BDNF detection kit was purchased from R&D Systems and all procedures were carried out according to the manufacturer instructions. Plates were read with spectrophotometer Infinite M200 Pro (Tecan). AFSC protein lysates were obtained using RIPA buffer (150 mM NaCl, 10 mM EDTA, pH 8.0, 10 mM Tris, pH 7.4, 0.1% SDS, 1% deoxycholate,

1% NP-40 in PBS, pH 7.6) and protein concentrations were measured with Infinite M200 Pro using DC Protein Assay (BioRad Laboratories). BDNF values were normalized to total amount of cell protein.

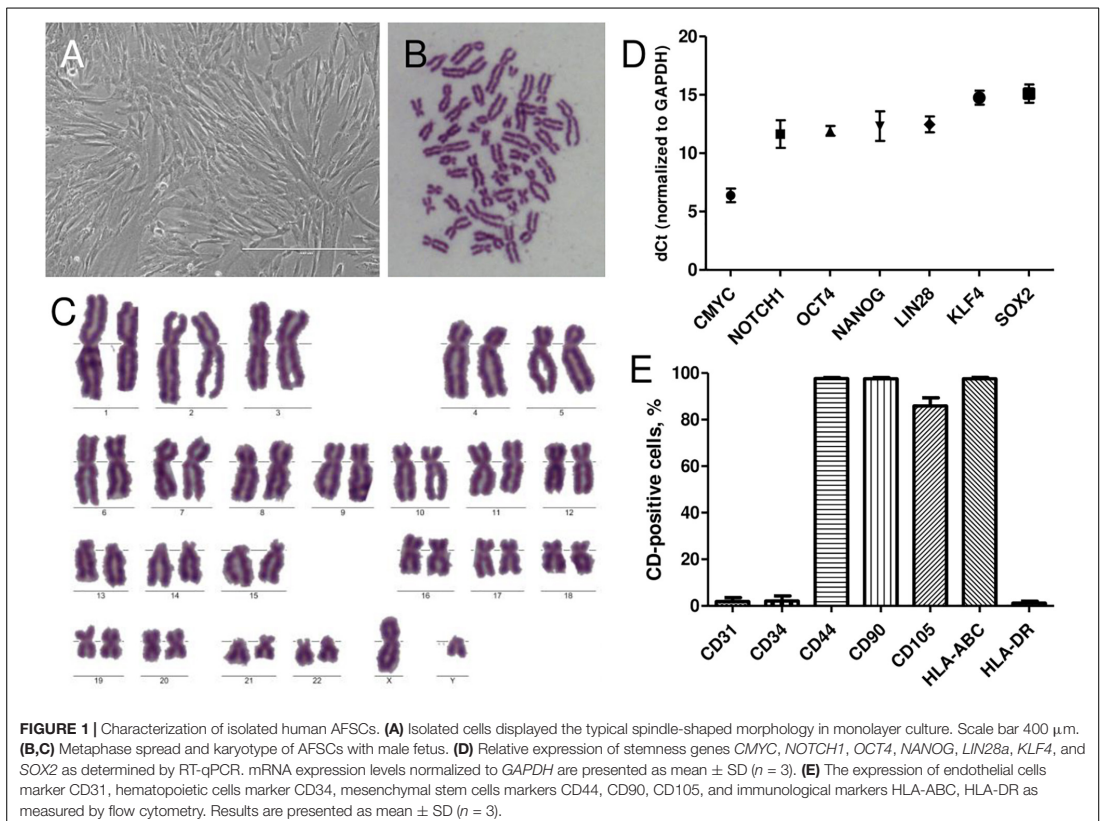
## Statistical Analysis

All experiments were repeated at least 3 times (three independent experiments). Data were expressed as mean values with SDs. For statistical analysis, repeated measures analysis of variance with Tukey's multiple comparison test or two-way analysis of variance with Bonferroni post-test in the GraphPad Prism Software (La Jolla, CA) was used.

## RESULTS

### Characterization of Isolated AFSCs

AFSCs were isolated from amniocentesis samples of healthy donors at midsecond (17–20 weeks) trimester of gestation. Stem cells were successfully isolated by a two-step protocol and when grown in culture demonstrated spindle-shaped morphology (Figure 1A). To confirm the fetal origin of the cells karyotype



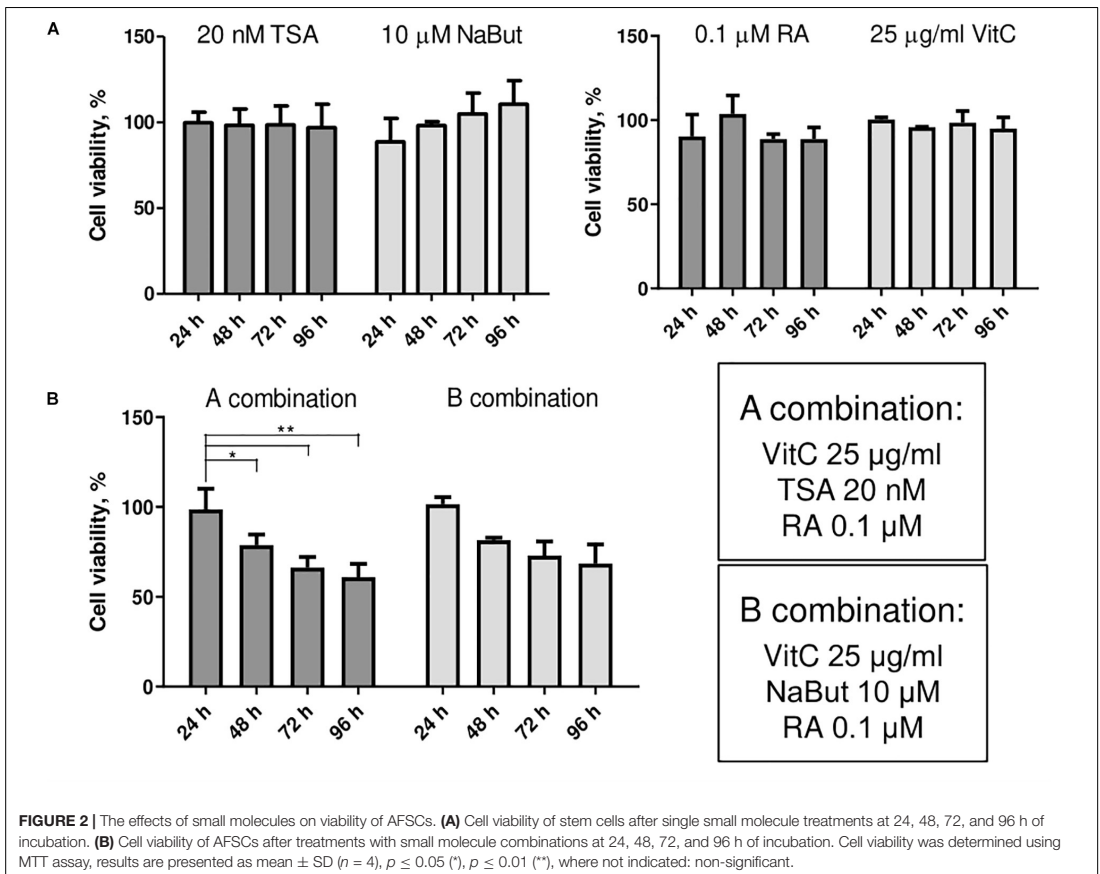
analysis was performed (Figures 1B,C). Only the samples with male fetus were chosen and Y chromosome was present in all instances. Relative expression of stemness markers *CMYC*, *NOTCH1*, *OCT4*, *NANOG*, *LIN28a*, *KLF4*, and *SOX2* was also detected by RT-qPCR (Figure 1D). AFSCs were strongly positive (over 90%) for mesenchymal cell surface markers, such as CD44, CD90, and CD105 and immunological marker HLA-ABC, negative (<5%) for hematopoietic marker CD34, endothelial marker CD31 and immunological marker HLA-DR (Figure 1E) as measured by flow cytometry.

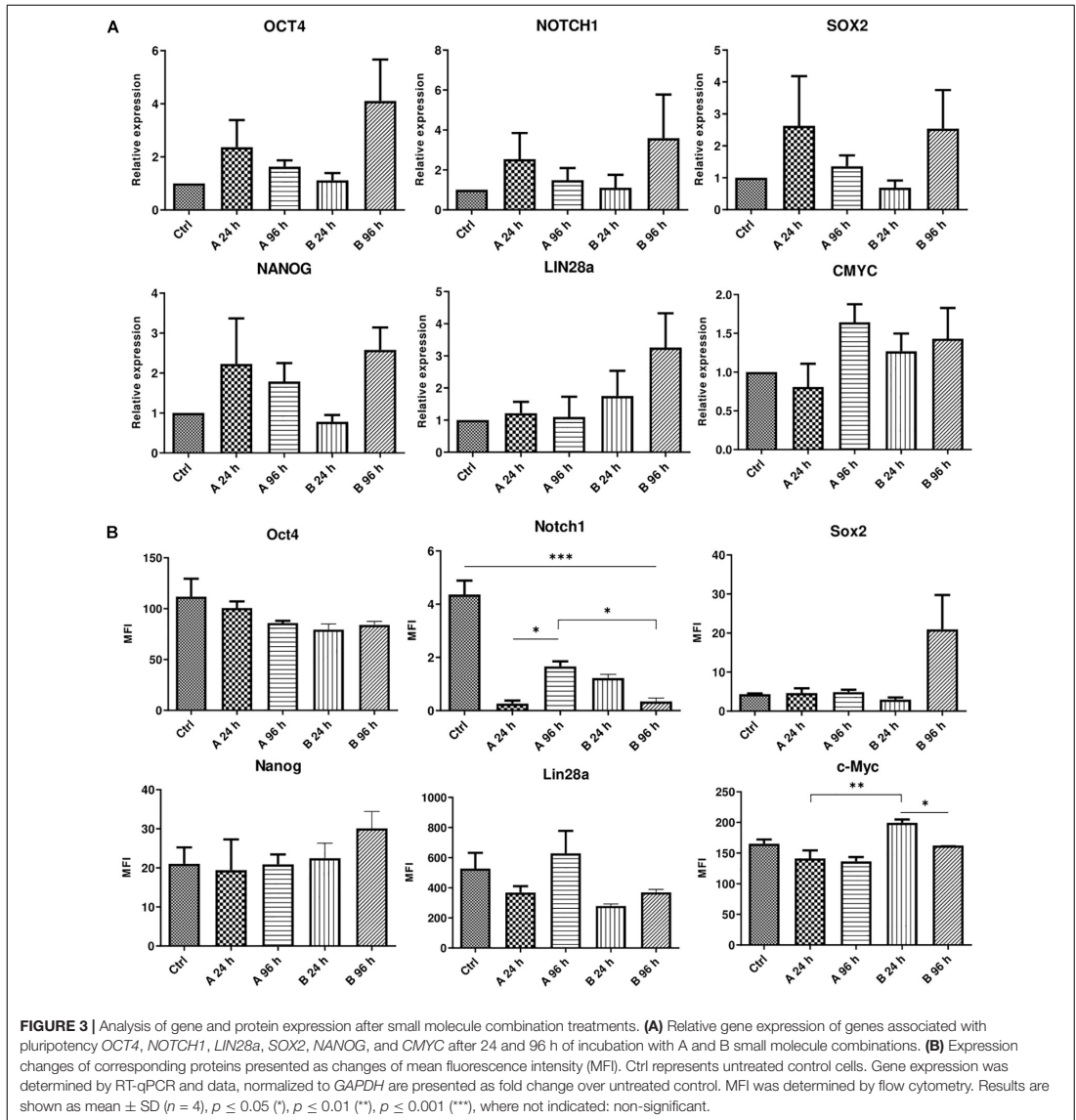
## Evaluation of Small Molecule Effects on AFSCs

Small molecule treatments were tested for their toxicity as single molecules (Figure 2A) and in combinations (Figure 2B) using MTT assay. We investigated the effects of HDAC inhibitors TSA and NaBut, and multifunctional molecules RA and vitC on cell viability of AFSCs every 24 h for 4 days. The concentrations for used small molecules were chosen regarding previous studies

(Huangfu et al., 2008; Esteban et al., 2010; Han et al., 2010; Hou et al., 2013). The results revealed that these compounds affect cell viability but do not induce cellular cytotoxicity at given concentrations and combinations. When treated with small molecule compounds separately cell viability did not decrease lower than 90% and treatment with NaBut even stimulated cell proliferation since cell viability improved during treatment time. After treating AFSCs with small molecule combinations a gradual decrease in cell viability was observed and after 4 days it reached around 65–75%. We also tested the effects of DNMT inhibitor decitabine (Supplementary Figure 4) as a single compound and in combinations with other small molecules. However, due to insufficient efficacy, we did not use these combinations in further studies.

AFSCs were treated with combination A (25 µg/mL vitC, 20 nM TSA, 0.1 µM RA) and B (25 µg/mL vitC, 10 µM NaBut, 0.1 µM RA) for 24 and 96 h and some variations in the expression of genes and corresponding proteins that are involved in maintaining pluripotency was observed (Figure 3). Incubation with small molecule combinations induced changes of gene





expression in an adversative manner (Figure 3A). Expression levels of *OCT4*, *NOTCH1*, *SOX2*, and *NANOG* were higher with combination A after 24 h when compared to 96 h of incubation and combination B shows upregulated expression after 96 h of treatment. Expression of *LIN28a* increased only with combination B and *CMYC* showed slight upregulation with A combination after 96 h and with combination B at both time points. This indicates that even though these combinations differ by only one substance with similar function

(TSA in combination A and NaBut in combination B), it can influence the cellular response and gene expression activation differently. The results of protein expression changes induced by combination A and B treatments reveal different response to small molecule stimulation. The changes in expression level of Oct4, Nanog and c-Myc are quite mild with only c-Myc displaying significant decrease with combination B after 96 h treatments when comparing to 24 h incubation. Sox2 is upregulated only with B combination after 96 h of treatments

and Lin28a is downregulated except for combination A treatment after 96 h, although these expression changes are insignificant. Notch1 is significantly downregulated with both combination treatments at both time points. Differences in gene and protein expression patterns after small molecule treatments show that stimulation of gene transcription and protein translation are regulated differently.

The effect of A and B combinations on typical mesenchymal and pluripotent stem cell surface marker and MHC class I and II surface receptor expression were tested by flow cytometry (Figure 4). After 96 h of treatment with small molecule combinations A and B the expression of CD90, CD166, HLA-ABC, TRA-1-61, and TRA-1-81 surface markers remained similar to untreated control. Compared to control cells, treatment with combination A did not have much effect on the expression of CD44, CD73, CD146, SSEA4, and HLA-DR, while with combination B the expression level of these markers decreased 10–15%, except for HLA-DR when a slight increase of approximately 10% was noted. The expression of CD105 decreased when cells were treated with both combinations and the expression of CD117 decreased with combination B, but an increase of 10% was observed with combination A.

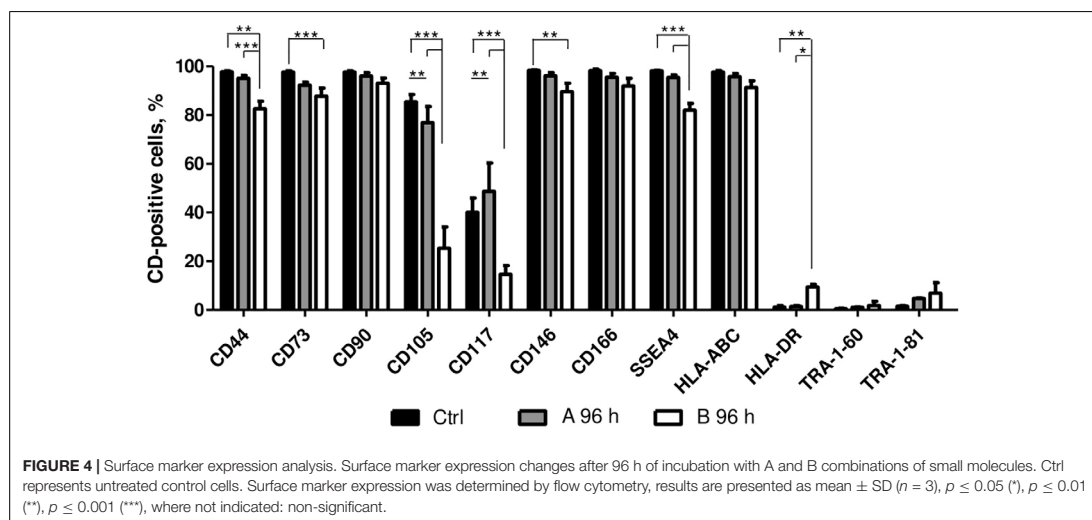
## Changes in Metabolic Phenotype

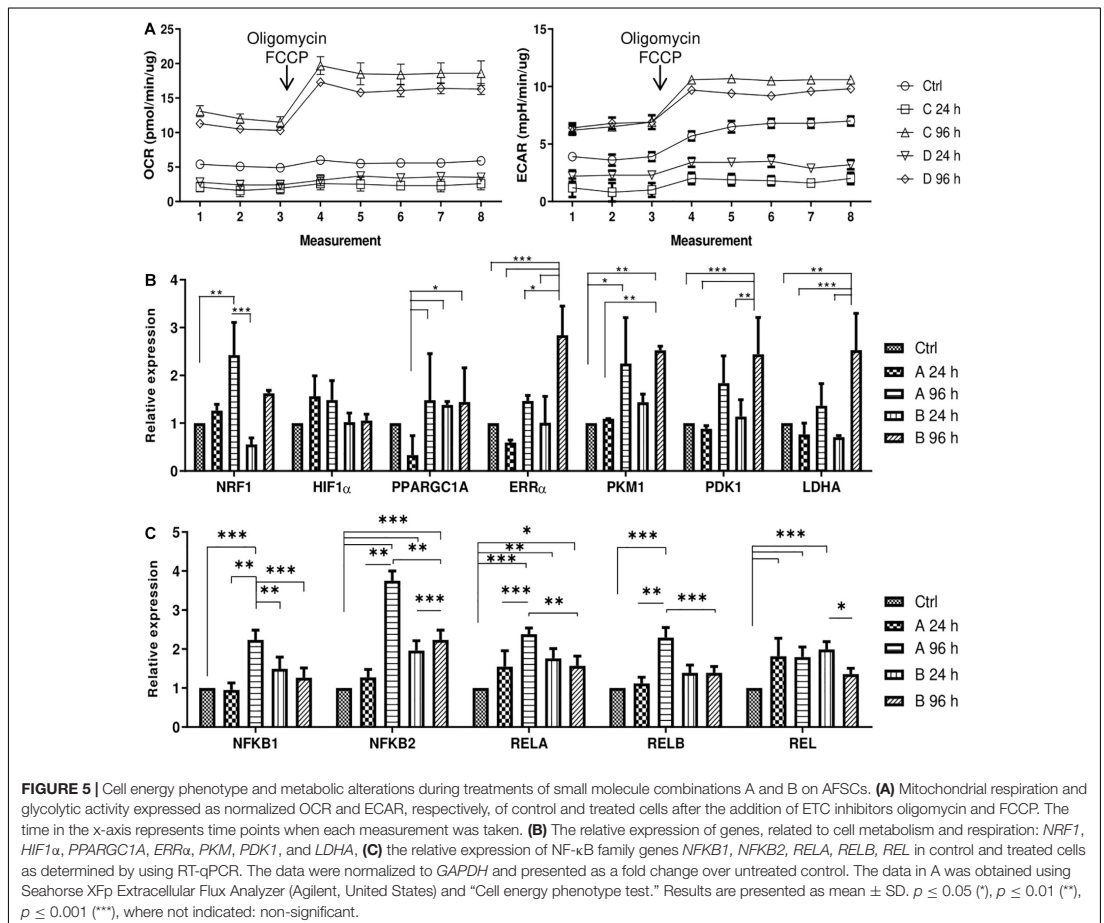
After the effects of small molecule treatments were established, the changes in metabolic profile of AFSCs were determined. AFSCs were treated with combinations A and B for 24 and 96 h and their mitochondrial and glycolytic activity was assessed using Seahorse extracellular flux analyzer and expression of genes associated with mitochondrial respiration, glycolysis and cellular metabolism was examined (Figure 5). The rates of oxygen consumption (OCR) and extracellular acidification (ECAR) were measured simultaneously under basal and induced stressed (after addition of electron transport chain (ETC) inhibitors

oligomycin and FCCP) conditions (Figure 5A). The data suggest that 96 h treatments result in more energetically active cells compared to untreated cells or 24 h incubations with small molecule combinations. Analysis of gene expression (Figure 5B) reveal that genes related to glycolysis (*ERRα*, *PKM*, *PDK1*, *LDHA*) are upregulated more significantly than genes linked to mitochondrial respiration (*NRF1*, *HIF1α*, *PPARGC1A*) and after 96 h treatments. Also, genes encoding transcription factors of NF-κB signaling pathway (*NFKB1*, *NFKB2*, *RELA*, *RELB*, *REL*) were examined (Figure 5C) and upregulated expression after treatments with both combinations was registered, especially with combination A after 96 h of treatment. The functional analysis and gene expression results suggest that small molecule combination treatments stimulate AFSCs to enter a more energetically active state.

## Assessment of Neurogenic Differentiation

AFSCs were induced to differentiate toward neurogenic lineage and gene expression was analyzed at early (day 7) and late (day 15) differentiation stages (Figure 6). Several differentiation medias were used containing such supplements as 1% N2 with 3 μM RA (I), 2% B27 with 3 μM RA (II) or their combination with 3 μM RA (III). Taking into account that combination C stimulates *SOX2* and *NOTCH1* expression after 24 h of treatment and other investigated genes are upregulated (except for *CMYC*) at given time point, we selected A combination and 24 h treatment for the preinduction step, especially since *SOX2* and *NOTCH1* are associated with neurogenesis. After 24 h the media with preinduction compounds was changed to differentiation medias with 1% N2 with 3 μM RA (IV), 2% B27 with 3 μM RA (V) and N2/B27 combination with 3 μM RA (VI). Morphological (Supplementary Figure 3) and gene expression changes under different conditions were observed.



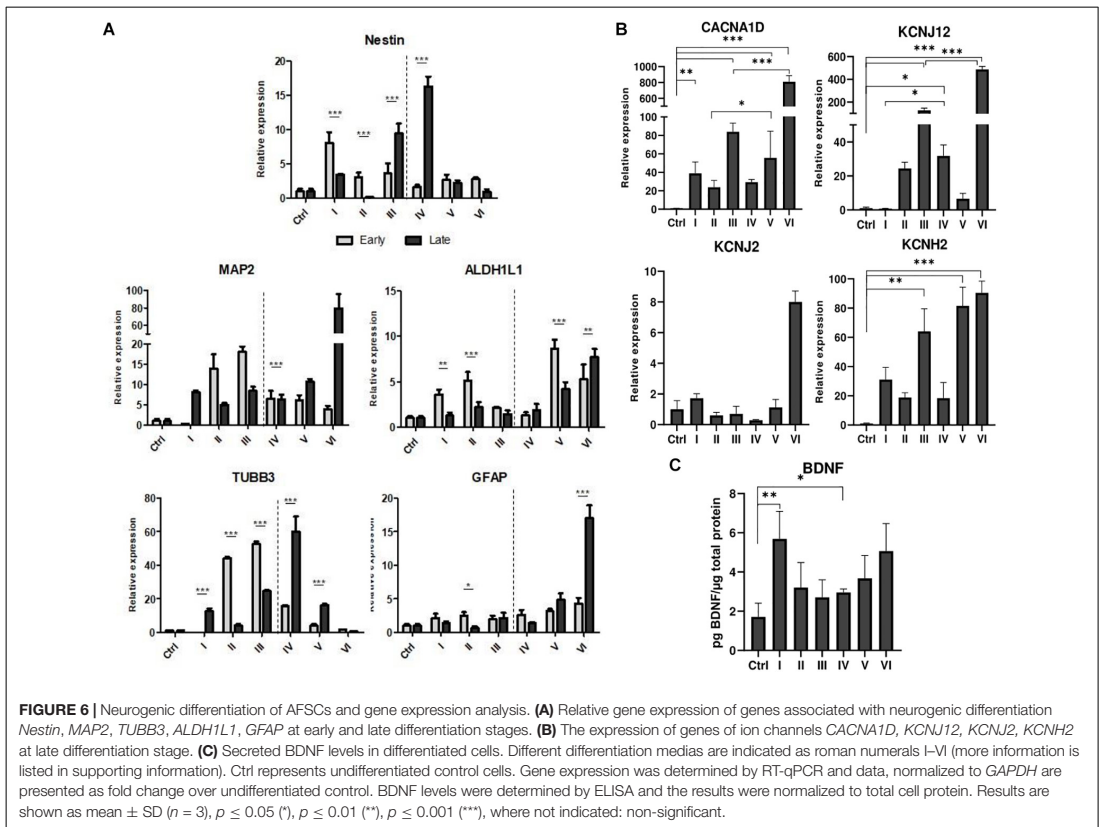


A preinduction step upregulated expression of astrocyte markers *ALDH1L1* and *GFAP* when compared to differentiations without preinduction step. Neural markers *MAP2* and *TUBB3* reveals varied expressional changes, when VI protocol was favorable for *MAP2* expression and IV protocol improved *TUBB3* expression (Figure 6A). Differentiation was also assessed by examining gene expression of ion channels *CACNA1D*, *KCNJ12*, *KCNJ2*, and *KCNH2* at late differentiation stage (Figure 6B). Comparing the gene expression between differentiation protocols with and without pretreatment step, the expression level of calcium ion channel *CACNA1D* was significantly upregulated when comparing protocol II and V, and protocol III and VI. Potassium ion channel *KCNJ12* also showed great upregulation when preinduction stem was added to differentiation protocol, since expression level significantly increased comparing protocols I and IV, and protocols III and VI. Secretion of BDNF was analyzed at late differentiation stage (Figure 6C) and significant increase of BDNF can be observed with protocol I and

IV when comparing to undifferentiated control. Neurogenic differentiation was confirmed by staining *TUBB3*, *NCAM1*, and Vimentin (Figure 7). Differentiated cells acquire more elongated morphology which is highlighted by reorganization of *TUBB3*, Vimentin and F-actin, and begin to form neurite growths with *NCAM1* becoming more concentrated at the cell ends. Upregulation of neural marker genes and ion channel genes suggest the beneficial effect of adding small molecule treatment step to differentiation induction protocol.

## DISCUSSION

Ever since Takahashi and Yamanaka in 2006 discovered and developed iPSC technology (Takahashi and Yamanaka, 2006) alternative cell reprogramming approaches has been of great interest. Small molecules and their role in modifying cell fate is a rapidly developing field of study and they are

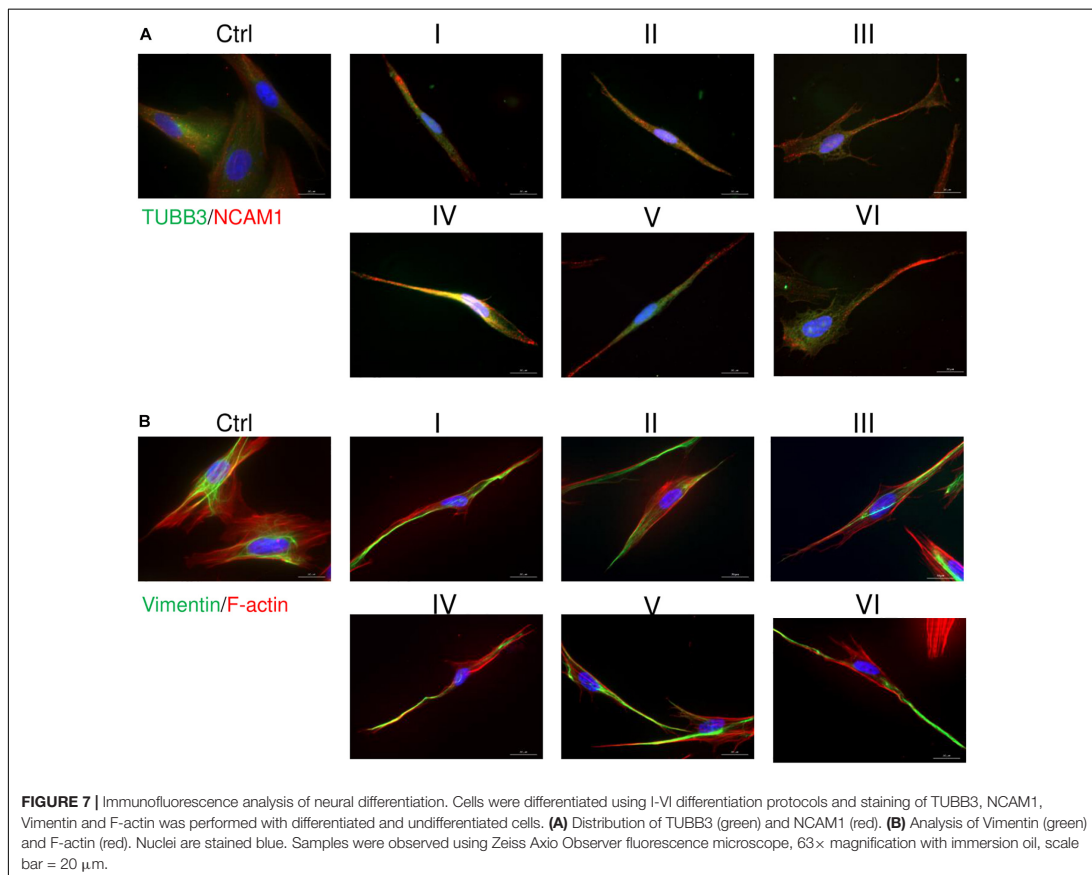


an attractive alternative to viral and non-viral vectors for cellular reprogramming. One of the benefits of small molecules is their fast and mostly reversible effects that allows easy manipulation of cell treatment conditions. A vast assortment of different small molecules exists and their combination options are immeasurable.

Small molecules have been widely used for differentiation induction of stem cells from various tissues of origin. Maioli et al. (2013) achieved cardiovascular phenotype of human AFSCs by using a mixture of hyaluronic, butyric, and retinoic acids. Another study used 5-azacytidine (AZA), RA, and dimethyl sulfoxide (DMSO) to induce cardiomyogenic differentiation of fetal liver-derived MSCs (Deng et al., 2016). Small molecules are also reported to facilitate transdifferentiation. TSA and AZA was used to induce hepatic differentiation with DMSO (Cipriano et al., 2017) or to enhance differentiation (Kim et al., 2016). Also, small molecules can be used to generate more specialized stem cells, such as MSCs from iPSCs or ESCs. In the study by Chen et al. (2012) used TGF- $\beta$  inhibitor SB431542 to initiate mesengenic differentiation and obtain MSCs. Results of previous studies reveal the broad potential of small molecules for applications in stem cell research.

In this study, AFSCs were treated with several selected small molecules and their combinations (Zhang et al., 2012; Qin et al., 2017; Yoshida and Yamanaka, 2017; De Angelis et al., 2018) and changes in cell and stem cell characteristics were observed. The tested combinations include HDAC inhibitors trichostatin A (TSA) and sodium butyrate (NaBut) that are shown to promote somatic cell reprogramming (Mali et al., 2010; Huang et al., 2011). It was proposed that HDAC inhibitors could replace CMYC and KLF4 factors during induction of pluripotency (Kretsovali et al., 2012). Vitamin C (vitC) was chosen based on evidence suggesting its role in DNA demethylation as a cofactor of Ten-Eleven Translocation (TET) enzymes (Esteban and Pei, 2012; Stadtfeld et al., 2012). By enhancing TET1 activity, vitC was found to indirectly promote reprogramming efficiency (Esteban et al., 2010; Blaschke et al., 2013). Retinoic acid (RA) signaling was linked to pluripotency reprogramming when enhancing effect of overexpression of RA receptor  $\alpha$  (RAR $\alpha$ ) and  $\gamma$  (RAR $\gamma$ ) was observed in iPSC derived using Yamanaka factors (Wang et al., 2011). And it has been demonstrated that the effects of RA are tightly related to used concentration. De Angelis et al. (2018) concluded that low concentrations of RA (0.5  $\mu$ M) positively affected





pluripotency state of hiPSCs while higher concentrations of RA (1.5 and 4.5 μM) promoted differentiation and downregulation of pluripotency markers OCT4, NANOG, and REX1. It was also demonstrated that a combination of retinoic acid and vitamin C act synergistically and boost cell reprogramming to pluripotency (Alexander et al., 2016).

Our study was focused on short-term treatments with small molecules on AFSCs. When cells were treated with small molecules individually, stable or upregulated cell viability was observed. Many papers report tendencies that agree with our results with decitabine (Pang et al., 2019), TSA (Han et al., 2013), NaBut (Panta et al., 2019), RA (Pourjafar et al., 2017), vitC (Markmee et al., 2019). Decitabine is a well-known hypomethylating agent which incorporates itself into host DNA, but is used as a drug to treat myelodysplastic syndrome and acute myeloid leukemia. And even though Öz et al. (2014) demonstrated that incorporation rates of decitabine at 100 nM are not genotoxic in myeloid leukemia cells, the effects of higher concentrations of decitabine and how its incorporation affect healthy cells are still unknown. Taking that

into consideration, combinations with decitabine were excluded from further experiments.

Certain gene expression and surface marker expression are an important characteristic of stem cells. In our experiments we obtained an interesting pattern of gene expression after treatment with small molecule combinations A (vitC, TSA, RA) and B (vitC, NaBut, RA). The obtained results show that combination C leads to more upregulated expression levels of *OCT4*, *NOTCH1*, *SOX2*, and *NANOG* after 24 h compared to 96 h treatments, while combination B promote higher upregulation after 96 h when compared to 24 h treatments. Increased gene expression of *LIN28a* and was observed with combination B and *CMYC* displayed slight upregulation with combination A after 96 h and combination B at both time points. Such differences in gene expression upregulation could be linked with different HDAC inhibitors present in used combinations of small molecules. Differential effects of TSA and NaBut were reported in breast cancer cells (Kalle and Wang, 2019), but more information on how these molecules influence pluripotency associated gene activation is lacking. At protein level investigated markers show

different response to small molecule treatments. Oct4, Nanog, and c-Myc show minor changes in the expression levels with significant decrease of c-Myc with combination B comparing 96–24 h treatment and significant downregulation of Notch1 is induced by small molecule treatments.

A set of surface markers related with multipotent mesenchymal stem cells were examined. The most profound effect was noted after 96 h incubation with B combination when significant decrease of CD positive cells were observed for such markers as CD44, CD73, CD105, CD117, CD146, SSEA4. Na et al. (2015) report that CD105 expression is regulated by Notch signaling pathway. They demonstrate that inhibition of Notch signaling leads to reduction of CD105 expression, in contrast, our results show *NOTCH1* upregulation after 96 h with B combination, thus meaning that other mechanisms are in play of regulating the expression of this surface marker. One more factor that can influence expression of CD105 is the concentration of serum in culture media. A study by Mark et al. (2013) demonstrated that only 50% of bone marrow stem cells cultured under serum-free conditions were positive for CD105, when nearly 100% of cells cultured in media containing serum were positive for CD105.

Cellular metabolism and metabolites are closely involved in regulating epigenetic state of the cell and epigenetics have a crucial role in regulating metabolic profile of the cell. Also, it has been established that during somatic cell reprogramming upregulation of genes associated with glycolytic metabolism occurs even before the expression of pluripotency genes (Folmes et al., 2011; Cao et al., 2015). In our experiment treatment with small molecule combinations result in more energetically active cells as evident by increased oxygen consumption (OCR) and extracellular acidification (ECAR) rates after 4 days. Also, both oxidative phosphorylation (*NRF1*, *HIF1 $\alpha$* , *PPARGC1A*) and glycolytic (*ERR $\alpha$* , *PKM*, *PDK1*, *LDHA*) genes are upregulated after 96 h treatments. Small molecules are known to improve stem cell function by regulation of cellular metabolism (Son et al., 2018). And several studies suggest that the initiation phase of cell reprogramming could be characterized by a phenomenon called transient hyper-energetic metabolism, which is a hybrid of high OxPhos and high glycolysis. Cacchiarelli et al. (2015) report metabolism-related genes show peak levels of expression at an early stage of reprogramming. Also, Kida et al. (2015) have linked *ERR $\alpha$*  and *ERR $\gamma$*  expression to iPSC generation. Their study identified transient upregulation of *ERR $\alpha$*  and *ERR $\gamma$* , which are typically expressed in oxidative tissues, in the early stages of reprogramming and showed that the transient OxPhos burst and increased glycolysis are essential for reprogramming (Kida et al., 2015). Additionally, we examined gene expression of NF- $\kappa$ B family, since it has been associated with cellular metabolism. It was shown that depletion of *IKK $\alpha$*  or *RelB*, which are important components of NF- $\kappa$ B signaling pathway, resulted in reduced mitochondrial content and function (Bakkar et al., 2012). Also, it was determined that p65 or *RelA*, another protein of NF- $\kappa$ B family, promotes the mitochondrial expression of cytochrome c oxidase 2 assembly factor and oxidative phosphorylation (Mauro et al., 2012). It was also proposed that glycolysis stimulates *IKK/NF- $\kappa$ B* activity, as revealed by reduced *IKK*

activity in the presence of a glycolytic inhibitor and increased *IKK* activity after *GLUT3* expression (Kawauchi et al., 2008). Increased levels of OCR and ECAR as well as upregulated expression of genes associated with cellular metabolism would suggest that small molecule treatments increase energetic needs of AFSCs, which could be similar to those linked to early reprogramming stages.

Because of an increase in *SOX2* and *NOTCH1* expression, A combination was chosen for a preinduction step in neurogenic differentiation induction. *SOX2* is a transcription factor known for its role in neuroectoderm development (Sarlak and Vincent, 2016) and *NOTCH1* is a receptor and its signaling is crucial in neurogenesis (Lathia et al., 2008), thus the upregulation of these genes could potentially promote neurogenic differentiation of AFSCs. To test this theory, neurogenic differentiation was induced by using two commercially available supplements N2 and B27 and with the addition of RA (Janesick et al., 2015), without a preinduction step and with a 24 h preinduction, then expression of neurogenic differentiation associated genes was analyzed. In our experiment small molecule pretreatment improved the expression of astrocytic genes *ALDH1L1* and *GFAP*, neural markers *MAP2* benefited from preinduction step when induced with N2/B27 supplements and *TUBB3* showed increased expression after small molecule treatment when induced using N2 supplement. Also, the preinduction step proved to benefit the expression levels of ion channel genes. Small molecule treatment boosted expression of calcium ion channel *CACNA1D* when differentiation was induced with B27 and N2/B27 supplements. While potassium ion channel gene *KCNJ12* showed an increase in expression when N2 and N2/B27 supplements were used for neurogenic differentiation. Neurogenic differentiation was confirmed by significantly increased levels of secreted BDNF when using N2 supplement alone or with the preinduction step. Also, morphological changes were visualized by staining *TUBB3*, *NCAM1*, *Vimentin* and F-actin. Differentiated AFSCs become more elongated as evident by reorganization of structural cytoskeleton proteins *TUBB3*, *Vimentin* and F-actin, and possible neurites begin to form as *NCAM1* is becoming more concentrated at the cell ends. Using small molecules to improve neurogenic differentiation by targeting signaling pathways (Song et al., 2018) or epigenetic regulation (Xu et al., 2019) has been reported, but evidence of similar effect when using the same small molecules as used in this study is scarce.

## CONCLUSION

To conclude, small molecules are an important tool in cell biology, cancer research, they are investigated as potential drugs for many disorders. Also, small molecules can be used to enhance cellular properties of stem cells. Our investigated small molecule combinations upregulated genes related to pluripotency, treatments lead to more energetically active cells, and pretreatment step deemed beneficial for neurogenic differentiation. A vast selection of small molecules exists and many different combinations could lead to different effects. Many



studies are focused on establishing these effects and bringing small molecules closer to clinical use.

## DATA AVAILABILITY STATEMENT

The raw data supporting the conclusions of this article will be made available by the authors, without undue reservation.

## ETHICS STATEMENT

The studies involving human participants were reviewed and approved by the Ethics Committee of Biomedical Research of Vilnius District. The patients/participants provided their written informed consent to participate in this study.

## AUTHOR CONTRIBUTIONS

AZ, VB, and RN: conception and design, collection of data, analysis, and interpretation, and writing original draft of manuscript. DŽ and IJ: data collection and interpretation.

## REFERENCES

- Alessio, N., Pipino, C., Mandatori, D., Di Tomo, P., Ferone, A., Marchiso, M., et al. (2018). Mesenchymal stromal cells from amniotic fluid are less prone to senescence compared to those obtained from bone marrow: An in vitro study. *J. Cell Physiol.* 233, 8996–9006. doi: 10.1002/jcp.26845
- Alexander, T., Von Meyenn, F., Ravichandran, M., Bachman, M., and Ficiz, G. (2016). Retinol and ascorbate drive erasure of epigenetic memory and enhance reprogramming to naïve pluripotency by complementary mechanisms. *Proc. Natl. Acad. Sci. USA.* 113, 12202–12207. doi: 10.1073/pnas.1608679113
- Bakkar, N., Ladner, K., Canan, B. D., Liyanarachchi, S., Bal, N. C., Pant, M., et al. (2012). IKK $\alpha$  and alternative NF- $\kappa$ B regulate PGC-1 $\beta$  to promote oxidative muscle metabolism. *J. Cell Biol.* 196, 497–511. doi: 10.1083/jcb.201108118
- Baranek, M., Belter, A., Naskręć-Barciszewska, M. Z., Stobiecki, M., Markiewicz, W. T., and Barciszewska, J. (2017). Effect of small molecules on cell reprogramming. *Mol. Biosyst.* 13, 277–313. doi: 10.1039/c6mb00595k
- Blaschke, K., Ebata, K. T., Karimi, M. M., Zepeda-Martinez, J. A., Goyal, P., Mahapatra, S., et al. (2013). Vitamin C induces Tet-dependent DNA demethylation and a blastocyst-like state in ES cells. *Nature* 500, 222–226. doi: 10.1038/nature12362
- Bonaventura, G., Chamayou, S., Liprino, A., Guglielmino, A., Fichera, M., Caruso, M., et al. (2015). Different Tissue-Derived Stem Cells: A Comparison of Neural Differentiation Capability. *PLoS One.* 10:e0140790. doi: 10.1371/journal.pone.0140790
- Bossolasco, P., Montemurro, T., Cova, L., Zangrossi, S., Calzarossa, C., Buiatiotis, S., et al. (2006). Molecular and phenotypic characterization of human amniotic fluid cells and their differentiation potential. *Cell Res.* 16, 329–336. doi: 10.1038/sj.cr.7310043
- Cacchiarelli, D., Trapnell, C., Ziller, M. J., Soumillon, M., Cesana, M., Karnik, R., et al. (2015). Integrative analyses of human reprogramming reveal dynamic nature of induced pluripotency. *Cell* 162, 412–424. doi: 10.1016/j.cell.2015.06.016
- Cao, Y., Guo, W. T., Tian, S., He, X., Wang, X. W., Liu, W., et al. (2015). miR-290/371–Mbd2–Myc circuit regulates glycolytic metabolism to promote pluripotency. *EMBO J.* 34, 609–623. doi: 10.15252/emj.201490441
- Chen, Y. S., Pelekanos, R. A., Ellis, R. L., Horne, R., Wolvetang, E. J., and Fisk, N. M. (2012). Small Molecule Mesengenic Induction of Human Induced Pluripotent

All authors contributed to the article and approved the submitted version.

## ACKNOWLEDGMENTS

We thank Natalija Krasovskaja (Vilnius University, Faculty of Medicine) for providing samples of human amniotic fluid and Veronika Dedonytė (Vilnius University, Life Sciences Center) for assistance in karyotype analysis. We acknowledge the COST Action CA17116 International Network for Translating Research on Perinatal Derivatives into Therapeutic Approaches (SPRINT), supported by COST (European Cooperation in Science and Technology) for the development of ideas and valuable discussions in scientific research in the field of perinatal derivatives.

## SUPPLEMENTARY MATERIAL

The Supplementary Material for this article can be found online at: <https://www.frontiersin.org/articles/10.3389/fbioe.2021.623886/full#supplementary-material>

- Stem Cells to Generate Mesenchymal Stem/Stromal Cells. *Stem Cells Transl. Med.* 1, 83–95. doi: 10.5966/sctm.2011-0022
- Cipriano, M., Correia, J. C., Camões, S. P., Oliveira, N. G., Cruz, P., Cruz, H., et al. (2017). The role of epigenetic modifiers in extended cultures of functional hepatocyte-like cells derived from human neonatal mesenchymal stem cells. *Arch. Toxicol.* 91, 2469–2489. doi: 10.1007/s00204-016-1901-x
- Da Sacco, S., De Filippo, R. E., and Perin, L. (2011). Amniotic fluid as a source of pluripotent and multipotent stem cells for organ regeneration. *Curr. Opin. Organ Transplant.* 16, 101–105. doi: 10.1097/MOT.0b013e3283424f6e
- De Angelis, M. T., Parrotta, E. I., Santamaria, G., and Cuda, G. (2018). Short-term retinoic acid treatment sustains pluripotency and suppresses differentiation of human induced pluripotent stem cells. *Cell Death Dis.* 9:6. doi: 10.1038/s41419-017-0028-1
- De Coppi, P., Bartsch, G. Jr., Siddiqui, M. M., Xu, T., Santos, C. C., Perin, L., et al. (2007). Isolation of amniotic stem cell lines with potential for therapy. *Nat. Biotechnol.* 25, 100–106. doi: 10.1038/nbt1274
- Deng, F., Lei, H., Hu, Y., He, L., Fu, H., Feng, R., et al. (2016). Combination of retinoic acid, dimethyl sulfoxide and 5-azacytidine promotes cardiac differentiation of human fetal liver-derived mesenchymal stem cells. *Cell Tissue Bank.* 17, 147–159. doi: 10.1007/s10561-015-9514-9
- Esteban, M. A., Wang, T., Qin, B., Yang, J., Qin, D., Cai, J., et al. (2010). Vitamin C enhances the generation of mouse and human induced pluripotent stem cells. *Cell Stem Cell.* 6, 71–79. doi: 10.1016/j.stem.2009.12.001
- Esteban, M. A., and Pei, D. (2012). Vitamin C improves the quality of somatic cell reprogramming. *Nat. Genet.* 44, 366–367. doi: 10.1038/ng.2222
- Folmes, C. D. L., Nelson, T. J., Martinez-Fernandez, A., Arrell, D. K., Zlatkovic Lindor, J., Dzeja, P. P., et al. (2011). Somatic oxidative bioenergetics transitions into pluripotency-dependent glycolysis to facilitate nuclear reprogramming. *Cell Metab.* 14, 264–271. doi: 10.1016/j.cmet.2011.06.011
- Han, B., Li, J., Li, Z., Guo, L., Wang, S., Liu, P., et al. (2013). Trichostatin A Stabilizes the Expression of Pluripotent Genes in Human Mesenchymal Stem Cells during Ex Vivo Expansion. *PLoS One.* 8:e81781. doi: 10.1371/journal.pone.0081781
- Han, J., Sachdev, P. S., and Sidhu, K. S. (2010). A combined epigenetic and non-genetic approach for reprogramming human somatic cells. *PLoS One.* 5:e12297. doi: 10.1371/journal.pone.0012297
- Hou, P., Li, Y., Zhang, X., Liu, C., Guan, J., Li, H., et al. (2013). Pluripotent stem cells induced from mouse somatic cells by small-molecule compounds. *Science* 341, 651–654. doi: 10.1126/science.1239278

- Huang, P., He, Z., Ji, S., Sun, H., Xiang, D., Liu, C., et al. (2011). Induction of functional hepatocyte-like cells from mouse fibroblasts by defined factors. *Nature* 475, 386–389. doi: 10.1038/nature10116
- Huangfu, D., Maehr, R., Guo, W., Eijkelenboom, A., Snitow, M., Chen, A. E., et al. (2008). Induction of pluripotent stem cells by defined factors is greatly improved by small molecule compounds. *Nat. Biotechnol.* 26, 795–797. doi: 10.1038/nbt1418
- Janesick, A., Wu, S. C., and Blumberg, B. (2015). Retinoic acid signaling and neuronal differentiation. *Cell Mol. Life Sci.* 72, 1559–1576. doi: 10.1007/s00018-014-1815-9
- Kalle, A. M., and Wang, Z. (2019). Differential effects of two HDAC inhibitors with distinct concomitant DNA hypermethylation or hypomethylation in breast cancer cells. *Biorxiv [Preprint]* doi: 10.1101/578062
- Kawauchi, K., Araki, K., Tobiume, K., and Tanaka, N. (2008). p53 regulates glucose metabolism through an IKK-NF-kappaB pathway and inhibits cell transformation. *Nat. Cell Biol.* 10, 611–618. doi: 10.1038/ncb1724
- Kida, Y. S., Kawamura, T., Wei, Z., Sogo, T., Jacinto, S., Shigeno-Kamitsuji, A., et al. (2015). ERRs Mediate a Metabolic Switch Required for Somatic Cell Reprogramming to Pluripotency. *Cell Stem Cell* 16, 547–555. doi: 10.1016/j.stem.2015.03.001
- Kim, H. J., Kwon, Y. R., Bae, Y. J., and Kim, Y. J. (2016). Enhancement of human mesenchymal stem cell differentiation by combination treatment with 5-azacytidine and trichostatin A. *Biotechnol. Lett.* 38, 167–174. doi: 10.1007/s10529-015-1949-3
- Kim, Y., Jeong, J., and Choi, D. (2020). Small-molecule-mediated reprogramming: a silver lining for regenerative medicine. *Exp. Mol. Med.* 52, 213–226. doi: 10.1038/s12276-020-0383-3
- Kretsovali, A., Hadjimihael, C., and Charmpilas, N. (2012). Histone Deacetylase Inhibitors in Cell Pluripotency, Differentiation, and Reprogramming. *Stem Cells Int.* 2012:184154. doi: 10.1155/2012/184154
- Lathia, J. D., Mattson, M. P., and Cheng, A. (2008). Notch: From Neural Development to Neurological Disorders. *J. Neurochem.* 107, 1471–1481. doi: 10.1111/j.1471-4159.2008.05715.x
- Ma, X., Kong, L., and Zhu, S. (2017). Reprogramming cell fates by small molecules. *Protein Cell.* 8, 328–348. doi: 10.1007/s13238-016-0362-6
- Maioli, M., Contini, G., Santaniello, S., Bandiera, P., Pigliaru, G., Sanna, R., et al. (2013). Amniotic fluid stem cells morph into a cardiovascular lineage: analysis of a chemically induced cardiac and vascular commitment. *Drug Des. Devel. Ther.* 7, 1063–1073. doi: 10.2147/DDDT.S44706
- Mali, P., Chou, B. K., Yen, J., Ye, Z., Zou, J., Dowey, S., et al. (2010). Butyrate greatly enhances derivation of human induced pluripotent stem cells by promoting epigenetic remodeling and the expression of pluripotency-associated genes. *Stem Cells* 28, 713–720. doi: 10.1002/stem.402
- Mark, P., Kleinsorge, M., Gaebel, R., Lux, C. A., Toelk, A., Pittermann, E., et al. (2013). Human Mesenchymal Stem Cells Display Reduced Expression of CD105 after Culture in Serum-Free Medium. *Stem Cells Int.* 2013:698076. doi: 10.1155/2013/698076
- Markmee, R., Aungsuchawan, S., Pothacharon, P., Tancharoen, W., Narakornsak, S., Laowanitwattana, T., et al. (2019). Effect of ascorbic acid on differentiation of human amniotic fluid mesenchymal stem cells into cardiomyocyte-like cells. *Heliyon.* 5:e02018. doi: 10.1016/j.heliyon.2019.e02018
- Mauro, C., Leow, S. C., Anso, E., Rocha, S., Thotakura, A. K., Tornatore, L., et al. (2012). NF- $\kappa$ B controls energy homeostasis and metabolic adaptation by upregulating mitochondrial respiration. *Nat. Cell Biol.* 13, 1272–1279. doi: 10.1038/ncb2324
- Na, T., Liu, J., Zhang, K., Ding, M., and Yuan, B. Z. (2015). The Notch Signaling Regulates CD105 Expression, Osteogenic Differentiation and Immunomodulation of Human Umbilical Cord Mesenchymal Stem Cells. *PLoS One.* 10:e0118168. doi: 10.1371/journal.pone.0118168
- Oz, S., Raddatz, G., Rius, M., Blagitko-Dorfs, N., Lübbert, M., Maercker, C., et al. (2014). Quantitative determination of decitabine incorporation into DNA and its effect on mutation rates in human cancer cells. *Nucleic Acids Res.* 42:e152. doi: 10.1093/nar/gku775
- Pang, Y., Geng, S., Zhang, H., Lai, P., Liao, P., Zeng, L., et al. (2019). Phenotype of mesenchymal stem cells from patients with myelodysplastic syndrome may be partly modulated by decitabine. *Oncol. Lett.* 18, 4457–4466. doi: 10.3892/ol.2019.10788
- Panta, W., Imsoonthornruksa, S., Yoisungnern, T., Suksaweang, S., Ketudat-Cairns, M., and Parnpai, R. (2019). Enhanced Hepatogenic Differentiation of Human Wharton's Jelly-Derived Mesenchymal Stem Cells by Using Three-Step Protocol. *Int. J. Mol. Sci.* 20:3016. doi: 10.3390/ijms20123016
- Pourjafar, M., Saidijam, M., Mansouri, K., Ghasemibasis, H., Karimi Dermani, F., and Najafi, R. (2017). All-trans retinoic acid preconditioning enhances proliferation, angiogenesis and migration of mesenchymal stem cell in vitro and enhances wound repair in vivo. *Cell Prolif.* 50:e12315. doi: 10.1111/cpr.12315
- Qin, H., Zhao, A., and Fu, X. (2017). Small molecules for reprogramming and transdifferentiation. *Cell. Mol. Life Sci.* 74, 3553–3575. doi: 10.1007/s00018-017-2586-x
- Roubelakis, M. G., Pappa, K. I., Bitsika, V., Zagoura, D., Vlahou, A., Papadaki, H. A., et al. (2007). Molecular and proteomic characterization of human mesenchymal stem cells derived from amniotic fluid: Comparison to bone marrow mesenchymal stem cells. *Stem Cells Dev.* 16, 931–952. doi: 10.1089/scd.2007.0036
- Sarlak, G., and Vincent, B. (2016). The Roles of the Stem Cell-Controlling Sox2 Transcription Factor: from Neuroectoderm Development to Alzheimer's Disease? *Mol. Neurobiol.* 53, 1679–1698. doi: 10.1007/s12035-015-9123-4
- Savickiene, J., Treigyte, G., Baronaite, S., Valiulienė, G., Kaupinis, A., Valius, M., et al. (2015). Human amniotic fluid mesenchymal stem cells from second- and third trimester amniocentesis: differentiation potential, molecular signature, and proteome analysis. *Stem Cells Int.* 2015:319238. doi: 10.1155/2015/319238
- Son, M. J., Jeong, J. K., Kwon, Y., Ryu, J. S., Mun, S. J., Kim, H. J., et al. (2018). A novel and safe small molecule enhances hair follicle regeneration by facilitating metabolic reprogramming. *Exp. Mol. Med.* 50, 1–15. doi: 10.1038/s12276-018-0185-z
- Song, Y., Lee, S., and Jho, E. H. (2018). Enhancement of neuronal differentiation by using small molecules modulating Nodal/Smad, Wnt/ $\beta$ -catenin, and FGF signaling. *Biochem. Biophys. Res. Commun.* 503, 352–358. doi: 10.1016/j.bbrc.2018.06.033
- Stadtfeld, M., Apostolou, E., Ferrari, F., Choi, J., Walsh, R. M., Chen, T., et al. (2012). Ascorbic acid prevents loss of Dlk1-Dio3 imprinting and facilitates generation of all-iPS cell mice from terminally differentiated B cells. *Nat. Genet.* 44, 398–405. doi: 10.1038/ng.1110
- Takahashi, K., and Yamanaka, S. (2006). Induction of Pluripotent Stem Cells from Mouse Embryonic and Adult Fibroblast Cultures by Defined Factors. *Cell* 126, 663–676. doi: 10.1016/j.cell.2006.07.024
- Tsai, M. S., Lee, J. L., Chang, Y. J., and Hwang, S. M. (2004). Isolation of human multipotent mesenchymal stem cells from second-trimester amniotic fluid using a novel two-stage culture protocol. *Hum. Reprod.* 19, 1450–1456. doi: 10.1093/humrep/deh279
- Yan, Z. J., Hu, Y. Q., Zhang, H. T., Zhang, P., Xiao, Z. Y., Sun, X. L., et al. (2013). Comparison of the neural differentiation potential of human mesenchymal stem cells from amniotic fluid and adult bone marrow. *Cell. Mol. Neurobiol.* 33, 465–475. doi: 10.1007/s10571-013-9922-y
- Yoshida, Y., and Yamanaka, S. (2017). Induced Pluripotent Stem Cells 10 Years Later. *Circ. Res.* 120, 1958–1968. doi: 10.1161/CIRCRESAHA.117.311080
- Wang, W., Yang, J., Liu, H., Lu, D., Chen, X., Zenonos, Z., et al. (2011). Rapid and efficient reprogramming of somatic cells to induced pluripotent stem cells by retinoic acid receptor gamma and liver receptor homolog 1. *Proc. Natl. Acad. Sci. USA.* 108, 18283–18288. doi: 10.1073/pnas.1100893108
- Xu, G., Wu, F., Gu, X., Zhang, J., You, K., Chen, Y., et al. (2019). Direct Conversion of Human Urine Cells to Neurons by Small Molecules. *Sci. Rep.* 9:16707. doi: 10.1038/s41598-019-53007-6
- Zhang, Y., Li, W., Laurent, T., and Ding, S. (2012). Small molecules, big roles - the chemical manipulation of stem cell fate and somatic cell reprogramming. *J. Cell Sci.* 125, 5609–5620. doi: 10.1242/jcs.096032

**Conflict of Interest:** The authors declare that the research was conducted in the absence of any commercial or financial relationships that could be construed as a potential conflict of interest.

Copyright © 2021 Zentelytė, Žukauskaitė, Jacerytė, Borutinskaitė and Navakauskienė. This is an open-access article distributed under the terms of the Creative Commons Attribution License (CC BY). The use, distribution or reproduction in other forums is permitted, provided the original author(s) and the copyright owner(s) are credited and that the original publication in this journal is cited, in accordance with accepted academic practice. No use, distribution or reproduction is permitted which does not comply with these terms.

4 publikacija / publication 4

G. Valiulienė, **A. Zentelytė**, E. Beržanskytė, and R. Navakauskienė

Metabolic Profile and Neurogenic Potential of Human Amniotic Fluid  
Stem Cells from Normal vs. Fetus-Affected Gestations

2021, *Frontiers in Cell and Developmental Biology*, 9:700634

doi: 10.3389/fcell.2021.700634

Copyright © 2021 Valiulienė, Zentelytė, Beržanskytė, Navakauskienė

Atviros prieigos publikacija platinama pagal „Creative Commons“ priskyrimo licenciją (CC BY). Publikacijos naudojimas, platinimas ar atgaminimas kituose forumuose yra leidžiamas su sąlyga, kad pirminis(-iai) autorius(-iai) ir autorinių teisių savininkas(-ai) yra nurodytas ir šio žurnalo publikacija yra cituojama laikantis priimtų akademinės praktikos normų.

This is an open-access article distributed under the terms of the Creative Commons Attribution License (CC BY). The use, distribution or reproduction in other forums is permitted, provided the original author(s) and the copyright owner(s) are credited and that the original publication in this journal is cited, in accordance with accepted academic practice



# Metabolic Profile and Neurogenic Potential of Human Amniotic Fluid Stem Cells From Normal vs. Fetus-Affected Gestations

Giedrė Valiulienė\*, Aistė Zentelytė, Elizabet Beržanskytė and Rūta Navakauskienė

Department of Molecular Cell Biology, Institute of Biochemistry, Life Sciences Center, Vilnius University, Vilnius, Lithuania

## OPEN ACCESS

### Edited by:

Vivian Capilla-González,  
Andalusian Center of Molecular  
Biology and Regenerative Medicine  
(CABIMER), Spain

### Reviewed by:

Shaun Kunisaki,  
Johns Hopkins Children's Center,  
United States  
Vahideh Assadolahi,  
Kurdistan University of Medical  
Sciences, Iran  
Sveva Bollini,  
University of Genoa, Italy

### \*Correspondence:

Giedrė Valiulienė  
giedre.valiuliene@bchi.vu.lt

### Specialty section:

This article was submitted to  
Stem Cell Research,  
a section of the journal  
Frontiers in Cell and Developmental  
Biology

**Received:** 26 April 2021

**Accepted:** 21 June 2021

**Published:** 16 July 2021

### Citation:

Valiulienė G, Zentelytė A,  
Beržanskytė E and Navakauskienė R  
(2021) Metabolic Profile  
and Neurogenic Potential of Human  
Amniotic Fluid Stem Cells From  
Normal vs. Fetus-Affected Gestations.  
Front. Cell Dev. Biol. 9:700634.  
doi: 10.3389/fcell.2021.700634

Human amniotic fluid stem cells (hAFSCs) possess some characteristics with mesenchymal stem cells (MSCs) and embryonic stem cells and have a broader differentiation potential compared to MSCs derived from other sources. Although hAFSCs are widely researched, their analysis mainly involves stem cells (SCs) obtained from normal, fetus-unaffected gestations. However, in clinical settings, knowledge about hAFSCs from normal gestations could be poorly translational, as hAFSCs from healthy and fetus-diseased gestations may differ in their differentiation and metabolic potential. Therefore, a more thorough investigation of hAFSCs derived from pathological gestations would provide researchers with the knowledge about the general characteristics of these cells that could be valuable for further scientific investigations and possible future clinical applicability. The goal of this study was to look into the neurogenic and metabolic potential of hAFSCs derived from diseased fetuses, when gestations were concomitant with polyhydramnios and compare them to hAFSCs derived from normal fetuses. Results demonstrated that these cells are similar in gene expression levels of stemness markers (*SOX2*, *NANOG*, *LIN28A*, etc.). However, they differ in expression of CD13, CD73, CD90, and CD105, as flow cytometry analysis revealed higher expression in hAFSCs from unaffected gestations. Furthermore, hAFSCs from “Normal” and “Pathology” groups were different in oxidative phosphorylation rate, as well as level of ATP and reactive oxygen species production. Although the secretion of neurotrophic factors BDNF and VEGF was of comparable degree, as evaluated with enzyme-linked immunosorbent assay (ELISA) test, hAFSCs from normal gestations were found to be more prone to neurogenic differentiation, compared to hAFSCs from polyhydramnios. Furthermore, hAFSCs from polyhydramnios were distinguished by higher secretion of pro-inflammatory cytokine  $TNF\alpha$ , which was significantly downregulated in differentiated cells. Overall, these observations show that hAFSCs from pathological gestations with polyhydramnios differ in metabolic and inflammatory status and also possess lower neurogenic potential compared to hAFSCs from normal gestations. Therefore, further *in vitro* and *in vivo* studies are necessary to dissect the potential of hAFSCs from polyhydramnios in stem cell-based therapies. Future studies should also search for strategies that could improve the characteristics of hAFSCs derived from diseased fetuses in order for those cells to be successfully applied for regenerative medicine purposes.

**Keywords:** mesenchymal stem cells, polyhydramnios, cell differentiation, energy metabolism, neurogenesis

## INTRODUCTION

Since the discovery that human amniotic fluid stem cells (hAFSCs) have a broader differentiation potential compared to mesenchymal stem cells (MSCs), obtained from other sources (e.g., bone marrow) (Yan et al., 2013; Bonaventura et al., 2015; Jain et al., 2019), hAFSC therapy has emerged as a new and promising approach in the field of regenerative medicine (Ramasamy et al., 2018). In general, MSCs, especially those obtained from birth-associated or perinatal tissues, are a promising strategy for the treatment of various prenatal and neonatal disorders with complex multifactorial etiologies, such as bronchopulmonary dysplasia, congenital heart disease, intraventricular hemorrhage, and even type III spinal muscular atrophy (Nitkin et al., 2020; Ahn et al., 2021; Shaw et al., 2021).

In addition, hAFSCs show only minimal replicative senescence (Alessio et al., 2018; Gasiūnienė et al., 2020), which makes amniotic fluid an especially attractive stem cell source. Considering the fact that amniotic fluid may be obtained *via* routine prenatal diagnostics, with minimal invasiveness and minimal ethical issues, this source of stem cells is of particular importance for the treatment of newborns. This is especially relevant considering the cases of polyhydramnios, when excessive accumulation of amniotic fluid occurs and amniocentesis (amniotic fluid reduction) is inevitable (Kleine et al., 2016). In such cases, hAFSCs could be proliferated and modulated *ex vivo* to be further used for autologous stem cell therapy.

According to literature, polyhydramnios complicates between 0.5 and 2% of all pregnancies. Several possible causes may lead to polyhydramnios, such as maternal diabetes, rhesus isoimmunization, fetal chromosome abnormalities (e.g., Down syndrome and Edward's syndrome), and malformations of the gastrointestinal tract (e.g., fetal gastric atony and esophageal atresia) or the central nervous system (Yefet and Daniel-Spiegel, 2016). Sadly, in the case of polyhydramnios, abnormalities of the central nervous system, such as neural tube defects (e.g., *spina bifida occulta*, meningocele, and myelomeningocele), are the most common cause of malformation (Kouamé et al., 2013). Recently, amniotic fluid stem cell therapy *in utero* emerged as a promising strategy for myelomeningocele (MMC) treatment (Abe et al., 2019). The aforementioned study showed that in the retinoic acid-induced rat MMC model, treatment with hAFSCs reduced neuronal damage and induced neuro-regeneration in a hepatocyte growth factor-dependent manner. In addition, studies demonstrated that hAFSCs may suppress neuronal inflammation and restore neuronal cells; therefore, in the future, hAFSCs could possibly be applied for the treatment of perinatal neurological diseases (Abe et al., 2021).

Although promising, the field of hAFSC cellular therapy for treating neonatal birth defects is still in its infancy. Studies that have evaluated hAFSC applicability to treat neural tube defects (Abe et al., 2019) examined the applicability of hAFSCs obtained *via* amniocentesis from the pregnancies without fetal abnormalities. For preclinical studies of other conditions such as congenital heart disease, respiratory tract anomalies, and perinatal gastrointestinal disorders, hAFSCs from healthy

gestations were also used (Kunisaki, 2018). However, in real clinical settings when autologous hAFSC transplantation would be desirable, the knowledge obtained while investigating hAFSCs from healthy gestations may be poorly translational, as hAFSCs from normal and fetus-affected gestations could possibly differ in their metabolic status and consequently in their differentiation and trophic potential. It should be emphasized that the aforementioned potential may also be affected by the gestational age at which hAFSCs are obtained, as some studies showed that hAFSCs obtained from early second trimester of gestation are more potent compared to hAFSCs obtained at a later gestational age (Shaw et al., 2017). However, in the case of polyhydramnios, hAFSCs may be acquired only when the polyhydramnios condition occurs (in most cases, polyhydramnios develops late in the second or in the third trimester of pregnancy) (Ursachen and Therapie, 2013). It should also be emphasized that scientific data about hAFSCs derived from fetus-affected gestations are very limited. Our group previously showed that hAFSCs from normal and fetus-affected gestations had similar stem cell characteristics and potential to differentiate toward mesodermal (adipogenic, osteogenic, chondrogenic, and myogenic) as well as ectodermal (neurogenic) lineages (Gasiūnienė et al., 2019b; Zentelytė et al., 2020). However, no scientific data exist on the metabolic characteristics of these two types of hAFSCs, nor are there any data on the neurogenic and neurotrophic potential of hAFSCs obtained exclusively from polyhydramnios samples. Therefore, it is crucial to describe the basic characteristics and determine the potential of hAFSCs derived from fetus-diseased gestations concomitant with polyhydramnios in order to explore their future therapeutic applicability in averting highly debilitating pregnancy complications.

Consequently, the main objective of this study was to evaluate the general metabolic and inflammatory characteristics, as well as the neurogenic and neurotrophic potential of hAFSCs, obtained from fetus-affected gestations with polyhydramnios, in comparison with normal fetus-unaffected gestations. Therefore, we examined the cellular energy flux of tested hAFSCs and assessed their total ATP production, as well as the mitochondrial membrane potential and quantities of intracellular reactive oxygen species (ROS). For neurogenic induction, several different chemical cocktails were used, and their effect on neurite formation and the gene expression of the main neural differentiation-associated factors (e.g., *NCAM1-2*, *NSE*, *NES*, *TUBB3*, *NEUROD1*, *SYP*, *MAP2*, *BDNF*, and *NGF*) were evaluated. In addition, expression of intracellular neural proteins (Nestin, Musashi, Lin28a and  $\beta$ -tubulin) and secretion of certain trophic and inflammatory factors (BDNF, VEGF, TNF $\alpha$ , and IL-6) were also examined.

On the whole, the results of our study expand the knowledge about the general properties and differences of hAFSCs, obtained from the third-trimester fetus-affected gestations concomitant with polyhydramnios in comparison to hAFSCs derived from the second-trimester normal gestations. Data show that tested hAFSCs from pathological and normal gestations differ in their phenotypic and inflammatory characteristics, as well as neurogenic potential. Therefore, future studies should address further functional investigations, as well as the

modulation of hAFSCs from pathological gestations obtained from polyhydramnios samples *ex vivo*, in order for these cells to be successfully used for autologous stem cell therapies in treating neonatal conditions.

## MATERIALS AND METHODS

### Isolation of hAFSCs

Amniotic fluid samples were obtained by amniocentesis from mid-second-trimester pregnancies (16–17 weeks of gestation; patient age:  $39 \pm 2.1$  years) from healthy women who needed prenatal diagnostics but in whom no genetic abnormalities were detected and from specimens of polyhydramnios, when amnioreduction was needed at the third trimester of gestation (32 weeks; patient age:  $27.7 \pm 7.4$  years). No aneuploidies were detected during clinical diagnostics in samples from both groups. hAFSCs ( $n = 3$  samples from healthy gestations and  $n = 3$  samples from pathological gestations concomitant with polyhydramnios ([Pat1: diagnosed with fetal gastric atony], [Pat2: diagnosed with fetal esophageal atresia], [Pat3: diagnosed with Treacher Collins syndrome])) were isolated using a two-stage protocol as described in Gasiūnienė et al. (2019b) (protocol approved by the Vilnius Regional Biomedical Research Ethics Committee, No. 158200-18/7-1049-550, version No. 1). Briefly, samples were centrifuged at  $500 \times g$  for 20 min, supernatant was removed, and cell pellets were washed once with PBS. After centrifugation, cells were resuspended in complete growth medium consisting of DMEM with 10% FBS (Gibco, Thermo Fisher Scientific), 100 U/ml penicillin, and 100  $\mu$ g/ml streptomycin (Gennaxxon bioscience) and plated in culture flasks. First, cell colonies (mostly of epithelial morphology, first stage) appeared after 10–15 days, and the non-adhering cells were collected and transferred to new culture flasks. After the appearance of cell colonies (hAFSCs, second stage), growth medium was changed every 3 days.

All patients involved in this study signed a written consent. The personal patient data were encrypted before handing over to researchers.

### Cultivation of Isolated hAFSCs

Isolated hAFSCs were maintained in complete growth medium and subcultured at approximately 80% confluence using 0.05% trypsin-EDTA solution (Gennaxxon bioscience), and the cells were reseeded at a density of  $1 \times 10^4$  cells/cm<sup>2</sup>.

All experiments were performed at five to seven passages. During cultivation, the cell population doubling time (in days) was calculated using the following formula:  $DT = \text{time(days)} \times \log(2)/\log(c2/c1)$ , where  $c1$  is the number of seeded cells and  $c2$  is the number of collected cells (Roth, 2006).<sup>1</sup>

### Flow Cytometry Analysis

Human amniotic fluid stem cells were characterized by surface marker expression. Cells were collected and washed twice with phosphate buffered saline (PBS) with 1% bovine serum albumin (BSA). A total of  $6 \times 10^4$  cells/sample were resuspended in 50  $\mu$ l of 1% BSA/PBS and incubated with mouse anti-human antibodies for CD9, CD13, CD15, CD31, CD34, CD44, CD56, CD73, CD90, CD105, CD117, CD133, CD146, CD166, CD309, CD338, HLA-ABC, and HLA-DR. Cells were incubated with antibodies in the dark at +4°C for 30 min, washed twice with 1% BSA/PBS, and then analyzed. For intracellular flow cytometry staining, cells were washed with PBS, fixed with 2% paraformaldehyde at RT for 10 min, and then permeabilized using 0.1% Triton X-100 in PBS/1% BSA solution at RT for 15 min. After centrifugation, cells were resuspended in PBS/BSA/Triton X-100 solution and incubated for 30 min at 4°C in the dark with mouse anti-human or rabbit anti-human antibodies for Nestin, Musashi 1, LIN28a, and TUBB3. Goat anti-mouse or goat anti-rabbit IgG (H + L) Highly Cross-Absorbed Alexa Fluor<sup>®</sup> 488 (Invitrogen) conjugated secondary antibodies were used to label Nestin, MSI1, and LIN28a for another 30 min at 4°C in the dark (fluorophore and manufacturer information is listed in **Supplementary Table 1**). After incubation, cells were washed twice with PBS/1% BSA and analyzed. The measurements were carried out using a Millipore Guava<sup>®</sup> easyCyte 8HT flow cytometer, using the InCyte 2.2.2 software. Ten thousand events were collected for each sample.

### Differentiation Assay

Neurogenic differentiation of hAFSCs was induced using four different chemical cocktails (**Table 1**). Cells were seeded to culture dishes, and when the confluency reached 60%, growth media was removed, cell monolayer was washed with PBS, and pre-induction (for protocols I, II, and III) or differentiation (protocol IV) media was applied. After 24 h of pre-induction

<sup>1</sup><http://www.doubling-time.com/compute.php>

**TABLE 1** | Neurogenic differentiation conditions.

Protocol	Preinduction (24 h)	Differentiation media (72 h)
I	DMEM (low glucose) 10% heat-inactivated FBS	BrainPhys <sup>TM</sup> , 100 U/ml penicillin and 100 $\mu$ g/ml streptomycin, 1% NeuroCult <sup>TM</sup> , 1 mM 8-Bromo-cAMP, 0.3 mM IBMX, 5 mM KCl, 2 $\mu$ M RA
II	100 U/ml penicillin 100 $\mu$ g/ml streptomycin	BrainPhys <sup>TM</sup> , 100 U/ml penicillin and 100 $\mu$ g/ml streptomycin, 1% NeuroCult <sup>TM</sup> , 50 ng/ml BDNF, 100 ng/ml NGF, 5 mM KCl, 2 $\mu$ M RA
III	20 ng/ml FGF 20 ng/ml EGF	BrainPhys <sup>TM</sup> , 100 U/ml penicillin and 100 $\mu$ g/ml streptomycin, 1% NeuroCult <sup>TM</sup> , 1 mM 8-Bromo-cAMP, 0.3 mM IBMX, 50 ng/ml BDNF, 100 ng/ml NGF, 5 mM KCl, 2 $\mu$ M RA
IV	-	DMEM/F12, 100 U/ml penicillin and 100 $\mu$ g/ml streptomycin, 1% N2 Supplement, 2 $\mu$ M RA



(for protocols I, II, and III), cells were washed with PBS and differentiation media was applied. hAFSCs were further differentiated for 72 h. Neural differentiation was assessed by neurite formation and a total of >1,000 cells were examined in each sample. Neurite length was measured with NIH ImageJ using the NeuronJ plugin.

## Immunofluorescence Analysis

For immunofluorescence, hAFSCs were seeded in Lab-Tek Chamber slides (Thermo Fisher Scientific), cultivated as control, or differentiated (with III protocol) toward neurogenic lineage and then fixed with 4% formaldehyde for 15 min at RT, washed with PBS, and then permeabilized with 10% Triton X-100/PBS for 20 min at RT. After washing with PBS, cells were blocked using 1% BSA/10% goat serum/PBS for 30 min at 37°C. For detection of NCAM1, cells were incubated with primary mouse antibodies against NCAM1 (15 µg/ml) (Abcam) for 1 h at 37°C, followed by incubation with secondary goat anti-mouse IgG (H + L) Highly Cross-Adsorbed, Alexa Fluor® 594 antibodies (1:400) (Invitrogen) for 1 h at 37°C. For detection of TUBB3 and Vimentin, cells were incubated with FITC-conjugated rabbit anti-beta III tubulin antibodies (1:100) (Abcam) or Alexa Fluor® 488-conjugated rabbit anti-Vimentin antibodies (1:150) (Abcam) for 1 h at 37°C. F-actin was detected using Alexa Fluor® 594 Phalloidin (Thermo Fisher Scientific) for 30 min at RT. Cells were washed several times with 1% BSA/PBS after each incubation. Nuclei were stained using 300 nM DAPI solution (Invitrogen) for 10 min at RT and slides were mounted with Dako Fluorescent Mounting Medium (Agilent Technologies). Labeled cells were analyzed using a Zeiss Axio Observer (Zeiss) fluorescent microscope, 63 × objective magnification with immersion oil and Zen BLUE software.

## RNA Isolation and RT-qPCR

Total RNA from hAFSCs was isolated using TRIzol® reagent (Applied Biosystems) as recommended by the manufacturer. For the gene expression analysis, cDNA synthesis was performed using SensiFAST™ cDNA Synthesis Kit (Bioline). RT-qPCR was performed with SensiFAST™ SYBR® No-ROX Kit (Bioline) on the Rotor-Gene 6000 thermocycler with Rotor-Gene 6000 series software (Corbett Life Science). *GAPDH* and *RPL13A* genes (geometric mean of their Ct values) were used for normalization of the mRNA and the relative gene expression was calculated using the  $\Delta\Delta C_t$  method (compared to undifferentiated control). The list of primers (Metabion International AG) is provided in **Supplementary Table 2**.

## BDNF, VEGF, TNF $\alpha$ , IL-1 $\beta$ , IL-6, and IL-10 Quantification in Conditioned Media

Enzyme-linked immunosorbent assay (ELISA) was used to determine the secreted levels of BDNF, VEGF, TNF $\alpha$ , IL-1 $\beta$ , IL-6, and IL-10 in conditioned media of control and differentiated hAFSCs. For this purpose, cells were seeded in culture flasks and were cultivated for 3 days as control (untreated) cells or cells induced to differentiate toward neurogenic lineage using

II differentiation protocol. Then, control and differentiated hAFSCs were washed thoroughly with PBS and cell media was changed to NutriStem® hPSC XF medium (Biological Industries) for 3 days, after which both the cells and the media were collected separately. All ELISA detection kits were purchased from R&D Systems and all procedures were carried out according to the manufacturer's instructions and plates were read with spectrophotometer Infinite M200 Pro (Tecan). For a blank control, NutriStem® hPSC XF medium was used. hAFSC protein lysates were obtained using RIPA buffer (150 mM NaCl, 10 mM EDTA, pH 8.0, 10 mM Tris, pH 7.4, 0.1% SDS, 1% deoxycholate, and 1% NP-40 in PBS, pH 7.6). Cell protein concentrations and conditioned media concentrations were measured with Infinite M200 Pro using DC Protein Assay (BioRad Laboratories) according to the manufacturer's instructions. BDNF, VEGF, TNF $\alpha$ , and IL-6 values as well as protein yield in conditioned media were normalized to the total amount of cell protein.

## Energetic Profile Analysis

Metabolic activity of hAFSCs was measured using Abcam Extracellular O<sub>2</sub> Consumption Assay (ab197243), TMRE-Mitochondrial Membrane Potential Assay (ab113852), Glycolysis Assay (ab197244), and Luminescent ATP Detection Assay (ab113849). All procedures were carried out following the manufacturer's instructions. Shortly, for Extracellular O<sub>2</sub> Consumption Assay,  $5 \times 10^5$  of trypsinized cells were resuspended in 150 µl of fresh media and transferred to a 96-well plate, and 10 µl of Extracellular O<sub>2</sub> Consumption Reagent was added to each well. A few drops of mineral oil were added to cover the well and prevent evaporation. The plate was read using a Varioskan Flash multimode reader (Thermo Fisher Scientific) at 37°C for 3 h at 2-min intervals at Ex/Em = 380/650 nm. For TMRE-Mitochondrial Membrane Potential Assay,  $1 \times 10^5$  of hAFSCs were resuspended in PBS/0.2% BSA and incubated with 400 nM TMRE for 30 min at 37°C. Samples were analyzed with a Millipore Guava® easyCyte 8HT flow cytometer, using the InCyte 2.2.2 software. Ten thousand events were collected for each sample. For Glycolysis Assay,  $5 \times 10^5$  of trypsinized cells per sample were washed with Respiration Buffer and transferred to a 96-well plate. Ten microliters of Glycolysis Assay Reagent was added to each sample well, and the plate was read with a Varioskan Flash multimode reader at 37°C for 3 h at 1.5-min intervals at Ex/Em = 380/615 nm. For ATP Detection Assay,  $5 \times 10^4$  cells were seeded into a white 96-well plate; the next day, 50 µl of detergent was added into each well and the plate was placed on a shaker for 5 min at 600–700 rpm. Then, 50 µl of Substrate Solution was added to each well and the plate was again placed on a shaker for 5 min at 600–700 rpm. The plate was dark adapted by covering it for 10 min and then luminescence was measured by using a Varioskan Flash multimode reader.

## Evaluation of ROS Levels

Cellular ROS of hAFSCs were determined using the DCFDA Cellular ROS Detection Assay Kit (ab113851, Abcam) and all procedures were carried out according to

the manufacturer's instructions. In brief,  $2.5 \times 10^4$  cells were incubated with  $25 \mu\text{M}$  of 2',7'-dichlorofluorescein diacetate (DCFDA) for 30 min at  $37^\circ\text{C}$  and then analyzed using a Millipore Guava® easyCyte 8HT flow cytometer with InCyte 2.2.2 software. Ten thousand events were collected for each sample. For fluorescence microscopy,  $1.5 \times 10^4$  cells per well were seeded in a 48-well plate and incubated with  $25 \mu\text{M}$  DCFDA for 45 min at  $37^\circ\text{C}$  and then observed using an EVOS FL microscope (Thermo Fisher Scientific).

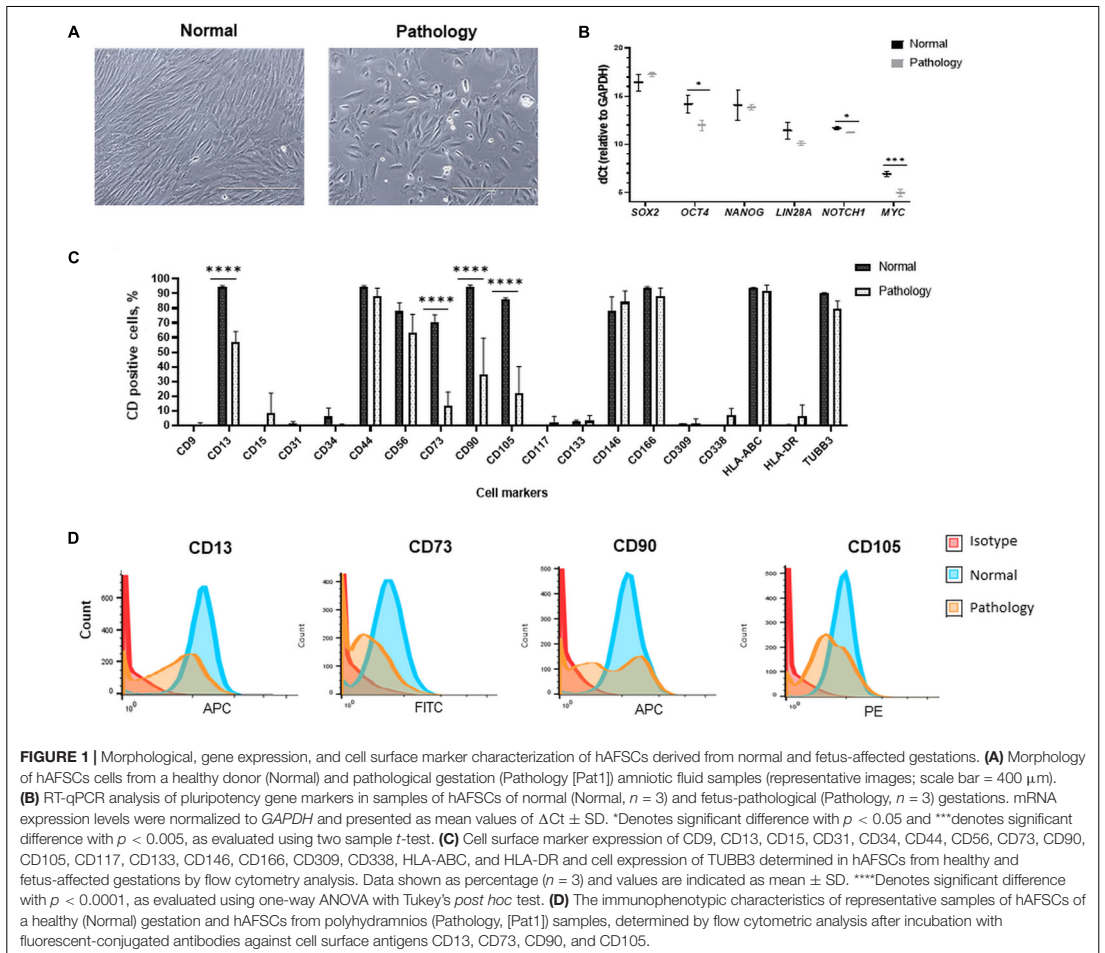
## Statistical Analysis

All experiments were performed in triplicate; data were expressed as the mean  $\pm$  SD. Statistical analysis was conducted using Student's *t*-test and one-way ANOVA with Tukey's *post hoc* test in GraphPad Prism software.

## RESULTS

### Characterization of Human AFSCs From Fetus-Unaffected and Fetus-Affected Gestations

In this study, human amniotic fluid-derived stem cells, obtained from the amniotic fluid of the second-trimester fetus-unaffected pregnancies (in figures denoted as "Normal"), as well as cells obtained *via* amnioreduction procedures from the third trimester of fetus-affected gestations (in figures denoted as "Pathology") were used. Stem cells from normal gestations had typical elongated spindle-shaped morphology, whereas hAFSCs obtained from polyhydramnios were distinguished by their round-shaped appearance (Figure 1A). Cells from fetus-unaffected and fetus-affected gestations also differed by their doubling time in early passages (p1–p5): as hAFSCs doubling





time was  $2.20 \pm 0.45$  days for the “Normal” group and  $2.67 \pm 0.47$  days for the “Pathology” group, differences were not statistically significant [calculated according to Roth, 2006 (see text footnote 1); data not shown].

In addition, differences in expression of mesenchymal cell surface markers were also observed between studied groups: expression of CD13 (membrane ananyl aminopeptidase), CD73 (5'-nucleotidase), CD90 (thymocyte differentiation antigen 1), and CD105 (endoglin) were significantly more pronounced (up to 96%,  $p < 0.0001$ ) in hAFSCs from fetus-affected gestations (Figures 1C,D). However, expression of CD44 (homing cell adhesion molecule), CD56 (neural cell adhesion molecule 1, NCAM1), CD146 (melanoma cell adhesion molecule), and CD166 (activated leukocyte cell adhesion molecule) mesenchymal cell surface markers were of comparable magnitude (Figure 1C). Both studied groups of hAFSCs had low expression (less than 10%) of hematopoietic and endothelial cell marker CD15 (Lewis X antigen), CD31 (platelet endothelial cell adhesion molecule), CD34 (hematopoietic progenitor cell antigen), CD133 (prominin-1), and CD309 (fetal liver kinase 1), as well as negligible expression of other stem cell markers, such as CD9 (tetraspin) and CD117 (proto-oncogene c-kit). It should be noticed that both hAFSCs from fetus-affected gestations and fetus-unaffected gestations were highly positive for  $\beta$ -tubulin protein expression (Figure 1C), which is known to be a marker of neural cells.

Furthermore, RT-qPCR gene expression analysis revealed that hAFSCs from fetus-unaffected gestations and hAFSCs from fetus-affected gestations are positive for pluripotency gene markers, such as *SOX2*, *OCT4*, *NANOG*, *LIN28A*, *NOTCH1*, and *MYC* (Figure 1B). Interestingly, evidently higher expression of *OCT4* (up to 4.6-fold,  $p < 0.05$ ) and *MYC* (up to 3.8-fold,  $p < 0.005$ ) were observed in hAFSCs from polyhydramnios specimens.

## Assessment of Metabolic Differences Between hAFSCs From Fetus-Affected and Fetus-Unaffected Gestations

The metabolic potential of hAFSCs obtained from fetus-unaffected gestations, as well as hAFSCs obtained via amnioreduction procedures from the fetus-affected gestations, was determined. Firstly, oxygen consumption rate was evaluated and compared between the study groups. Analysis revealed statistically significant ( $p < 0.05$ ) differences between hAFSCs from normal and fetus-affected gestations, as hAFSCs obtained from polyhydramnios samples were respiring more efficiently (oxygen consumption rate was approximately two-fold higher in the “Pathology” group in comparison to the “Normal” group; Figure 2A). However, extracellular acidification rate (Figure 2A), which resembles the intensity of glycolysis, was of comparable degree in both “Normal” and “Pathology” groups of hAFSCs.

Secondly, we compared the relative mitochondrial membrane potential values between the study groups using the TMRE accumulation test. Obtained data showed that TMRE median fluorescence intensity was approximately 1.69-fold higher ( $p < 0.05$ ) in hAFSCs from fetus-unaffected gestations compared

to hAFSCs from polyhydramnios samples (Figure 2B). In accordance with glycolysis and oxidative phosphorylation analysis results, assessment of total ATP content confirmed that hAFSCs from polyhydramnios are more energetic, as their ATP content, measured by the luminescent counts per  $5 \times 10^4$  cells, was approximately 1.4-fold higher ( $p < 0.05$ ) compared to hAFSCs from fetus-unaffected gestations (Figure 2C).

Because of the variance in mitochondrial oxidative phosphorylation rate and mitochondrial membrane potential values among hAFSCs obtained from fetus-unaffected vs. fetus-affected gestations, we performed more thorough investigation of additional parameters, associated with cellular bioenergetics. Estimation of ROS production revealed that hAFSCs obtained from polyhydramnios generate higher levels of ROS, which was demonstrated by increased median fluorescence intensity of 2',7'-dichlorofluorescein (DCF) [highly fluorescent DCF is formed upon oxidation of 2',7'-dichlorofluorescein diacetate (DCFDA) by ROS]. In hAFSCs from polyhydramnios, DCF signal was 1.66-fold higher ( $p = 0.054$ ) in comparison to hAFSCs from normal gestations (Figures 2D–F).

In addition, gene expression analysis (Figure 2G) revealed that hAFSCs obtained from polyhydramnios samples can be characterized by higher expression of the *NRF1* (nuclear respiratory factor 1) gene, which acts as a transcription factor regulating some key metabolic genes required for respiration (Yuan et al., 2018). However, no significant differences between groups were detected regarding gene expression of other genes related to cell metabolism and respiration: *HIF1A* (hypoxia-inducible factor 1-alpha), *PPARGC1A* (peroxisome proliferator-activated receptor gamma coactivator 1 alpha), *ERRA* (estrogen related receptor alpha), *PKM* (pyruvate kinase), *LDHA* (lactate dehydrogenase A), and *PKD1* (pyruvate dehydrogenase kinase 1), as well as genes involved in antioxidant defense: *CAT1* (catalase 1), *SOD2* (superoxide dismutase 2), or *GPX1* (glutathione peroxidase 1).

## Morphological Changes of hAFSCs From Fetus-Affected vs. Fetus-Unaffected Gestations Upon Neurogenic Induction

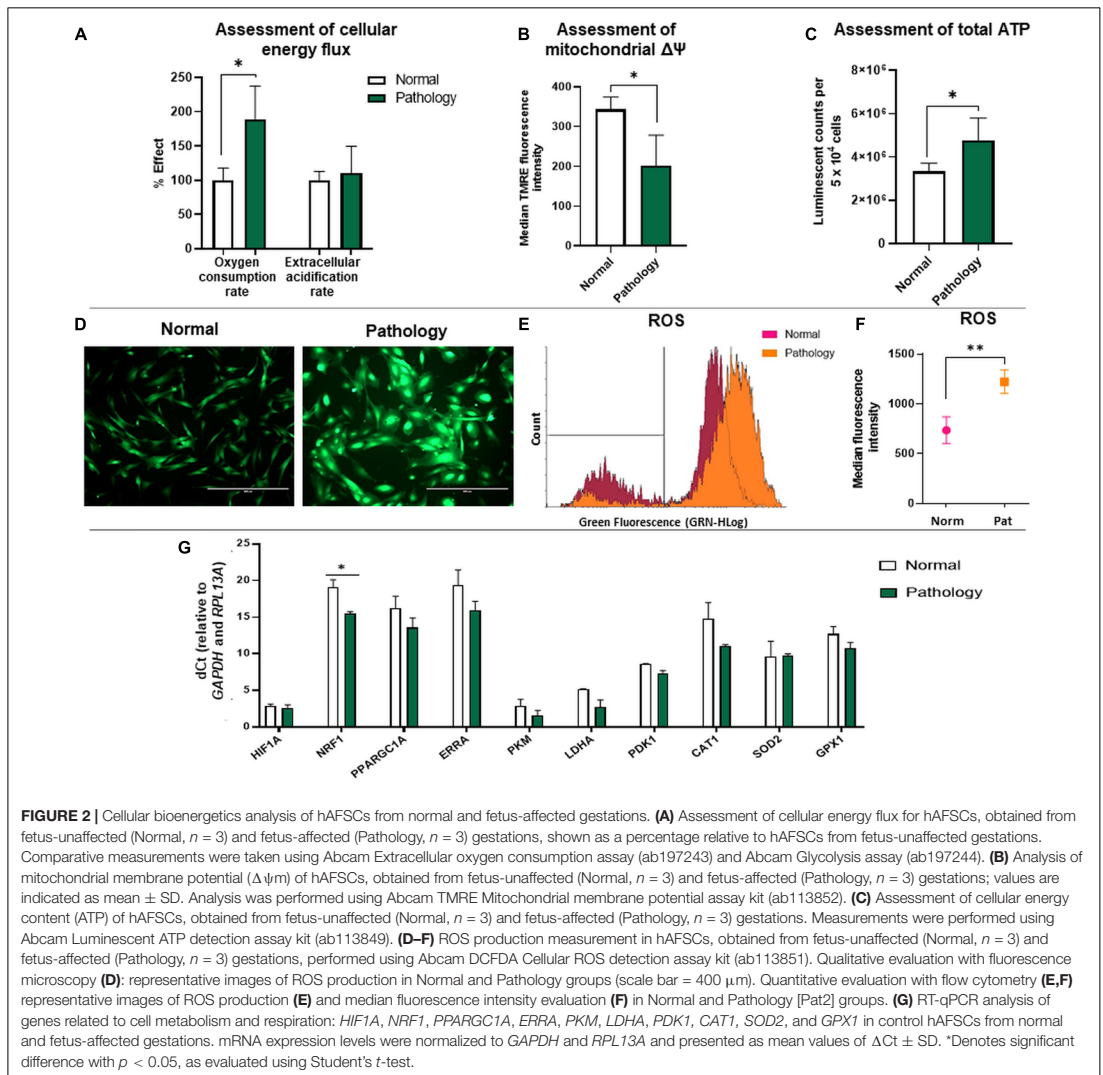
Results of differentiation analysis demonstrated that hAFSCs from fetus-unaffected gestations were more susceptible to neurogenic differentiation induction (Figure 3). All four neurogenic differentiation induction strategies (chemical cocktail Nos. I–IV) after 72-h treatment induced visible morphological changes in hAFSCs, obtained from fetus-unaffected gestations (“Normal” group). However, morphological alterations in hAFSCs from the “Pathology” group upon neurogenic differentiation induction was only modest (Figure 3A). In order to quantitatively evaluate the neurogenic differentiation in hAFSCs from fetus-affected vs. fetus-unaffected gestations, neurite length (Figure 3B) and neurite-to-cell ratio (Figure 3C) were counted. Results indicated that hAFSCs from normal gestations generated the longest neurites (median value:  $78.695 \mu\text{m}$ ) upon treatment with cAMP + IBMX + RA + KCl (induction cocktail No. I). However, the highest neurite-to-cell ratio (0.95/1) was observed in hAFSCs from

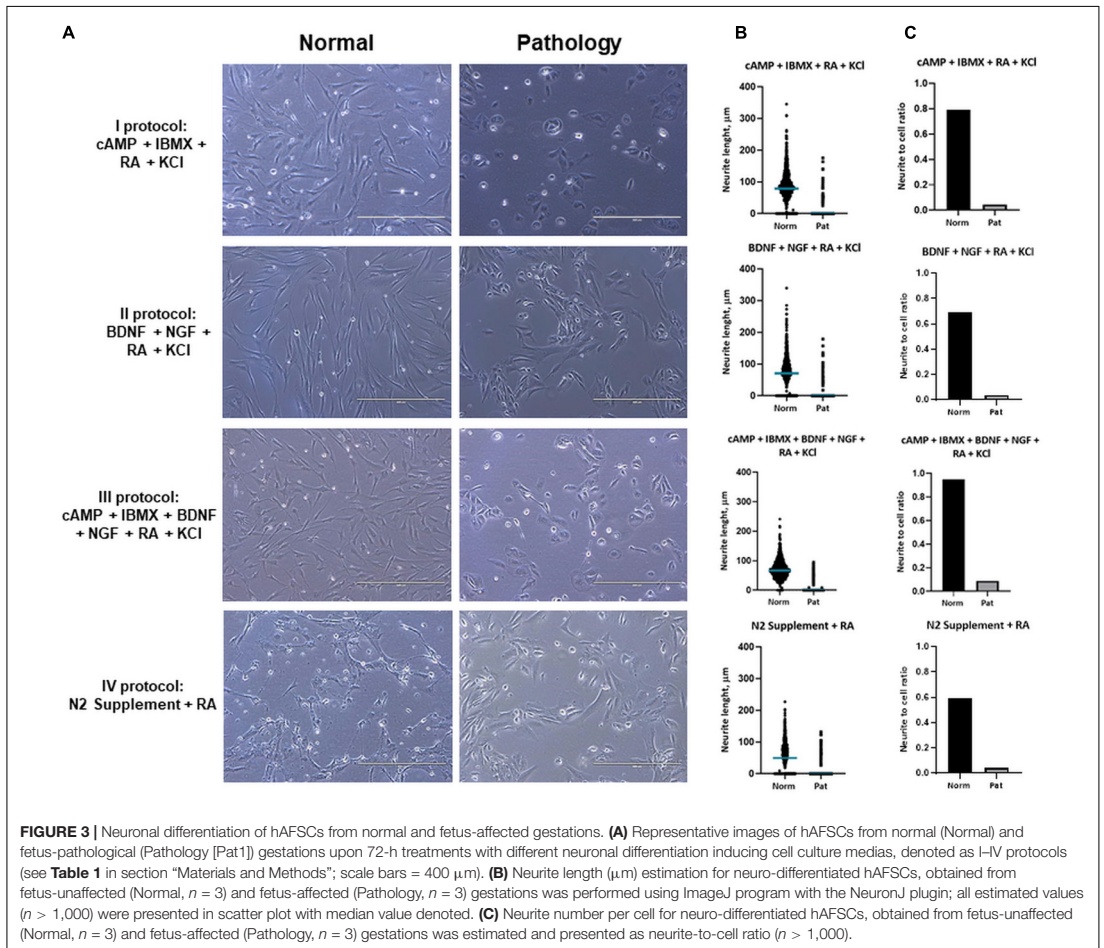
normal gestations, when treated with the combination cAMP + IBMX + BDNF + NGF + RA + KCl (induction cocktail No. III).

Furthermore, we noticed that upon treatment with the combination of cAMP + IBMX + BDNF + NGF + RA + KCl, both “Normal” and “Pathology” group hAFSCs acquired neural-like morphology very fast—even after 3-h treatment, neural-like cells in hAFSC cultures could be detected (Figure 4). Immunofluorescence analysis of these neuro-induced cells revealed drastic reorganization of hAFSC cytoskeleton (realignment of  $\beta$ -tubulin, vimentin, and F-actin), as well as redistribution of neural marker NCAM1 (Figure 4).

## Evaluation of Neural Gene Expression in Neuro-Induced hAFSCs From Fetus-Affected vs. Fetus-Unaffected Gestations

The RT-qPCR technique was used to evaluate the effect of neural differentiation induction protocols on hAFSC gene expression of neural progenitor cell markers (*SOX2*, *NES*, *NEUROD1*, *VIM*, and *TUBB3*), markers of differentiated post-mitotic neural cells (*NSE*, *NCAM1-2*, *GAD1*, *TPH1*, *TPH2*, *MAP2*, and *SYP*), glial markers (*GFAP* and *S100B*), oligodendrocyte precursor cell markers (*PDGFRA*), and genes of (neuro)trophic factors (*BDNF*,





*NGF*, *NTF3*, *NTF4*, *VEGFA*, *TGFB1*, and *HBEGF*), as well as expression of (neuro)trophic factor receptors (*NTRK1*, *NTRK2*, *NTRK3*, and *FGFR1*).

Results revealed that upon 72-h neural differentiation induction in hAFSCs, obtained from fetus-unaffected gestations, *NCAM1* gene expression was profoundly upregulated, whereas in hAFSCs from polyhydramnios, changes in *NCAM1* gene expression were negligible (**Figure 5A**). In hAFSCs from normal gestations, the strongest *NCAM1* expression (increase by 3,376-fold,  $p < 0.0001$ ) was induced when using the combination N2 Supplement + RA (induction cocktail No. IV). However, the strongest effect on *NCAM2* and *NES* gene expression (approximately sevenfold and threefold, respectively; NS) was observed upon treatment with a combination of BDNF + NGF + RA + KCl (induction cocktail No. II) (**Figures 5A,B**). In addition, treatment with BDNF + NGF + RA + KCl had the greatest impact on

gene expression of transcription factor *SOX2* (approximately 5-fold; NS; **Figure 6A**), as well as on expression of the neuron-specific cytoskeletal protein *MAP2* gene (approximately 12-fold,  $p < 0.0001$ ; **Figure 6B**). Furthermore, in hAFSCs obtained from fetus-unaffected gestations, 72-h treatment with BDNF + NGF + RA + KCl enhanced gene expression of neurotrophic factors *BDNF* and *NTF4* (**Figure 7C**), though increase was moderate (accordingly: 1.8- and 3.2-fold; NS). This treatment also upregulated gene expression of other trophic factors (**Figure 7B**), such as *VEGFA* (up to 5-fold,  $p = 0.001$ ) and expression of cytokine *TGFB1* (up to 2.7-fold; NS).

We have also evaluated the effect that neural differentiation-inducing treatments have on gene expression of neurotransmitter-producing enzyme genes, such as tryptophan hydroxylase 1 and 2 (*TPH1* and *TPH2*) and the gene of glutamate decarboxylase1 (*GAD1*). Gene expression of *TPH1* and *GAD1* was induced in hAFSCs from normal gestations after treatment

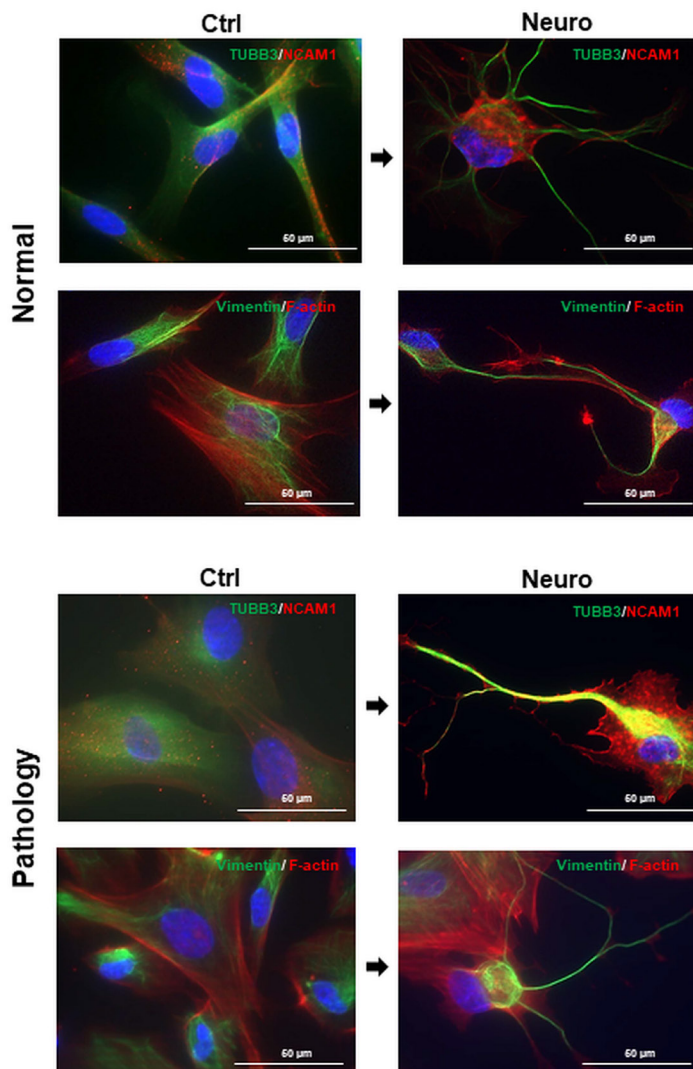
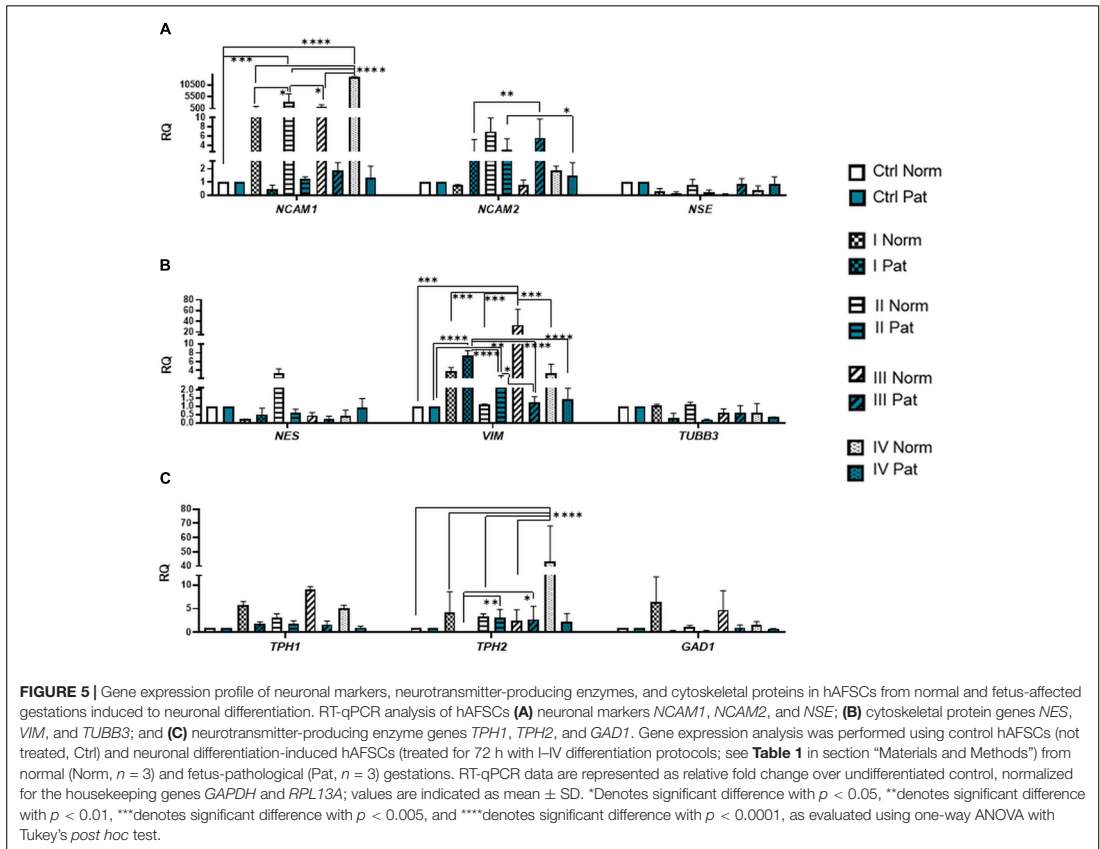


**FIGURE 4 |** Cytoskeletal reorganization and neural marker expression of control and neural differentiation-induced hAFSCs derived from normal and fetus-affected gestations. Representative images of healthy hAFSCs (Normal) and fetus-affected gestations (Pathology [Pat3]) shown. Neural differentiation was induced after 24-h exposure to pre-induction media, enriched with 20 ng/ml FGF and 20 ng/ml EGF, and further 3-h treatment with neuronal differentiation-inducing cell culture media, supplemented with 1 mM 8-Bromo-cAMP, 0.3 mM IBMX, 50 ng/ml BDNF, 100 ng/ml NGF, 5 mM KCl, and 2  $\mu$ M RA (see III protocol in section "Materials and Methods," **Table 1**). Immunofluorescence analysis of hAFSCs showing positive cells for neural marker TUBB3 and cytoskeletal protein Vimentin (green) as well as neural marker NCAM1 and cytoskeletal protein F-actin (red). Nuclei were counterstained with DAPI (blue); scale bar = 50  $\mu$ m.

with cAMP + IBMX + RA + KCl and after treatment with cAMP + IBMX + BDNF + NGF + RA + KCl (approximately by 5- to 9-fold, NS), whereas *TPH2* gene expression was upregulated the most strongly upon treatment with N2 Supplement + RA (approximately 44-fold,  $p < 0.0001$ ; **Figure 5C**). In addition,

all neural differentiation induction schemes used profoundly increased gene expression of key neuronal differentiation transcription factor *NEUROD1* (**Figure 6A**). However, the greatest increase in *NEUROD1* gene expression (up to 277,473-fold,  $p < 0.01$ ) was observed after combined treatment with



cAMP + IBMX + BDNF + NGF + RA + KCl. In hAFSCs from normal gestations, this treatment scheme also had the strongest effect on cytoskeletal protein Vimentin gene expression (increase up to 33-fold,  $p < 0.005$ ; **Figure 5B**) and the receptor of PDGF gene expression (increase up to 17.6-fold,  $p < 0.0001$ ; **Figure 7A**).

As it is evident from the gene expression data, hAFSCs obtained from polyhydramnios samples were much less inducible to neural differentiation, compared to hAFSCs from normal gestations. However, gene expression of glial marker *GFAP* (**Figure 6C**; “Pat” vs. “Norm” when treated with protocol I differed 39-fold,  $p = 0.13$ ), as well as expression of neurotrophic receptor genes, was upregulated more intensely in hAFSCs from fetus-affected gestations [“Pat” vs. “Norm” when treated with protocol III differed in the *NTRK1* gene expression approximately 335,000-fold ( $p < 0.01$ ), *NTRK2* 15.5-fold ( $p = 0.096$ ), *NTRK3* 21-fold ( $p = 0.251$ ); **Figure 7D**].

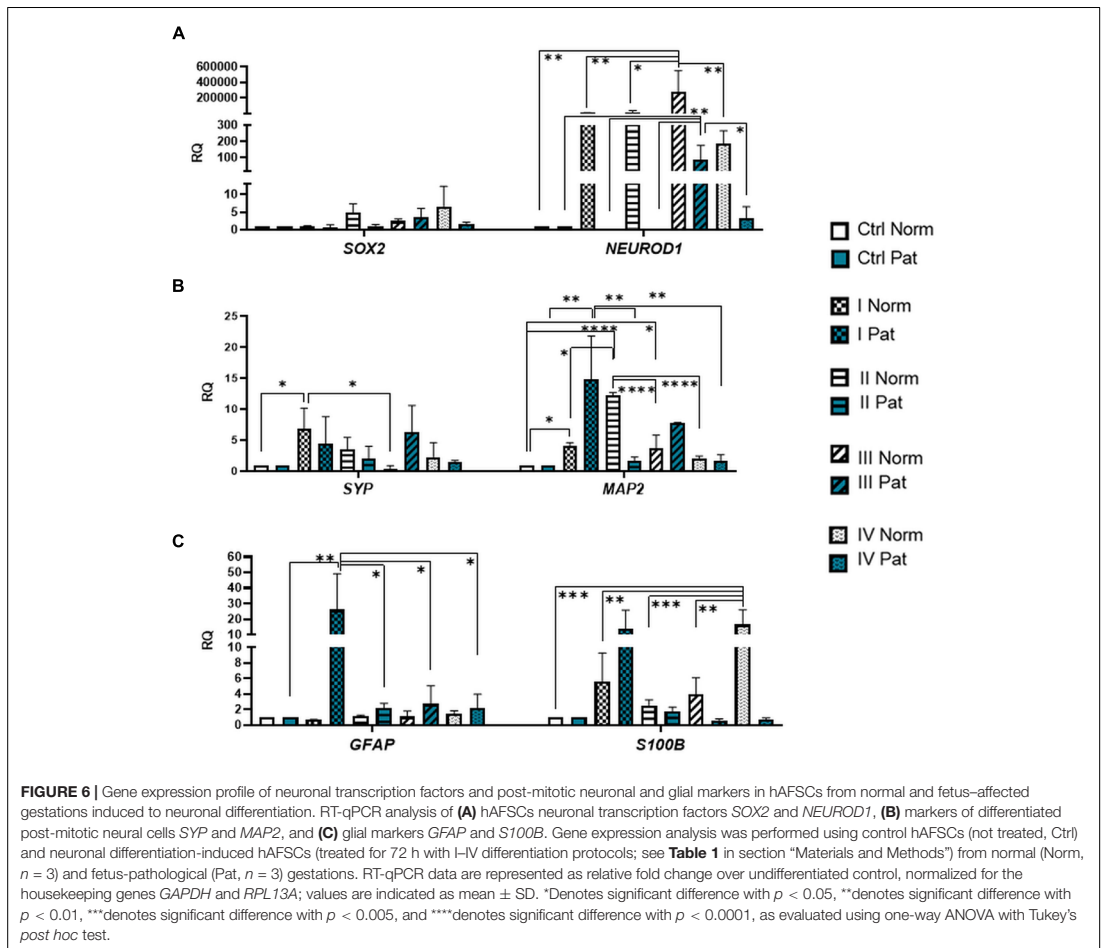
Considering the fact that the most effective in neural marker induction was the chemical cocktail consisting of BDNF + NGF + RA + KCl, we additionally tested its effect on neural ion channel gene expression (**Figure 8B**).

RT-qPCR analysis revealed that upon neurogenic induction, gene expression of *HCN2* (Hyperpolarization activated cyclic nucleotide gated potassium and sodium channel) and *KCNJ2* (Potassium inwardly rectifying channel subfamily member 2) ion channels was more strongly upregulated in hAFSCs from healthy gestations (37-fold and 4.3-fold respectively, although differences were not statistically significant). Consequently, these results support our observation that hAFSCs from healthy gestations are more susceptible to neural differentiation in comparison to hAFSCs from fetus-affected gestations with polyhydramnios.

### Protein Expression Analysis of Neuro-Induced hAFSCs From Fetus-Affected vs. Fetus-Unaffected Gestations

Expression of neuronal differentiation-associated proteins Nestin, Musashi 1, LIN28a, and neuronal-specific *TUBB3* was evaluated flow cytometrically by measuring the mean fluorescence intensity in control and 72-h differentiated hAFSCs from normal and pathological gestations (**Figure 8A**). For

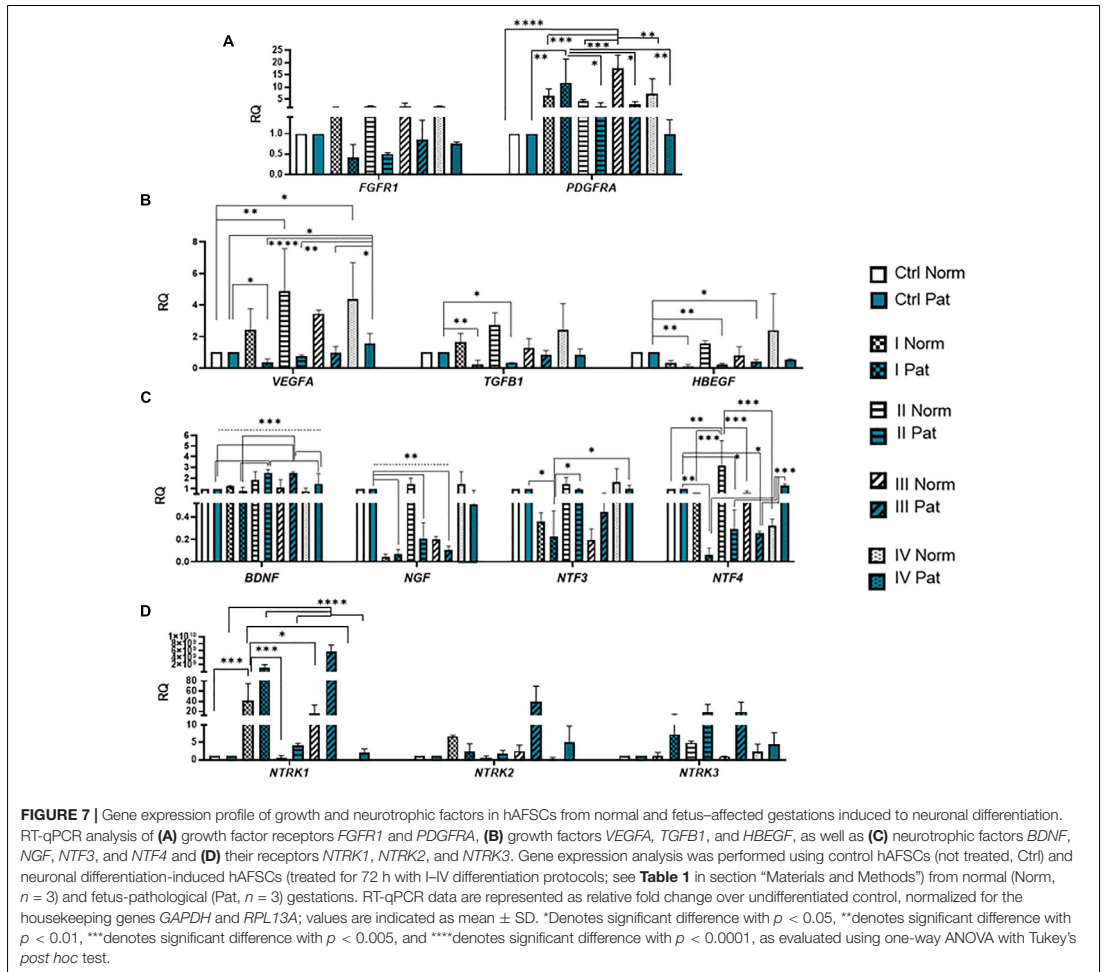




hAFSCs, neurogenic induction chemical cocktail consisting of 50 ng/ml BDNF + 100 ng/ml NGF + 2  $\mu$ M RA + 5 mM KCl (II protocol) was used. Data of protein expression analysis demonstrated that protein expression of intermediate filament Nestin was significantly upregulated upon neurogenic differentiation induction in both hAFSCs from healthy gestations and gestations with polyhydramnios ( $p < 0.005$ ), though a greater increase was observed in hAFSCs from polyhydramnios samples ( $p < 0.01$ ). Protein expression of stem cell and neural progenitor marker Musashi 1 was also activated by neurogenic induction media. However, only in hAFSCs from normal gestations was this augmentation statistically significant ( $p < 0.01$ ). Similarly to the pattern of protein expression of Nestin, expression of transcription factor LIN28a was also upregulated more profoundly in neuro-differentiated hAFSCs from polyhydramnios samples ( $p < 0.05$ ).

In order to evaluate the secretion of BDNF, VEGF, IL-1 $\beta$ , IL-6, IL-10, and TNF $\alpha$  by untreated and neuro-differentiated hAFSCs, obtained from normal and fetus-affected gestations, we performed ELISA-based analysis and compared secretion of aforementioned trophic and pro-inflammatory factors between study groups. In this case, for neurogenic differentiation induction, the same treatment with 50 ng/ml BDNF, 100 ng/ml NGF, 5 mM KCl, and 2  $\mu$ M RA (protocol No. II) has been chosen. The yield of secretome fractions was determined based on protein enrichment, as evaluated by BCA assay. The resulting values of micrograms of secreted proteins per microgram of total cell protein were as follows: "Normal" control  $75.39 \pm 0.18$ , "Pathology" control  $64.33 \pm 3.86$ , "Normal" differentiation  $61.72 \pm 2.4$ , and "Pathology" differentiation  $95.52 \pm 30.14$ .

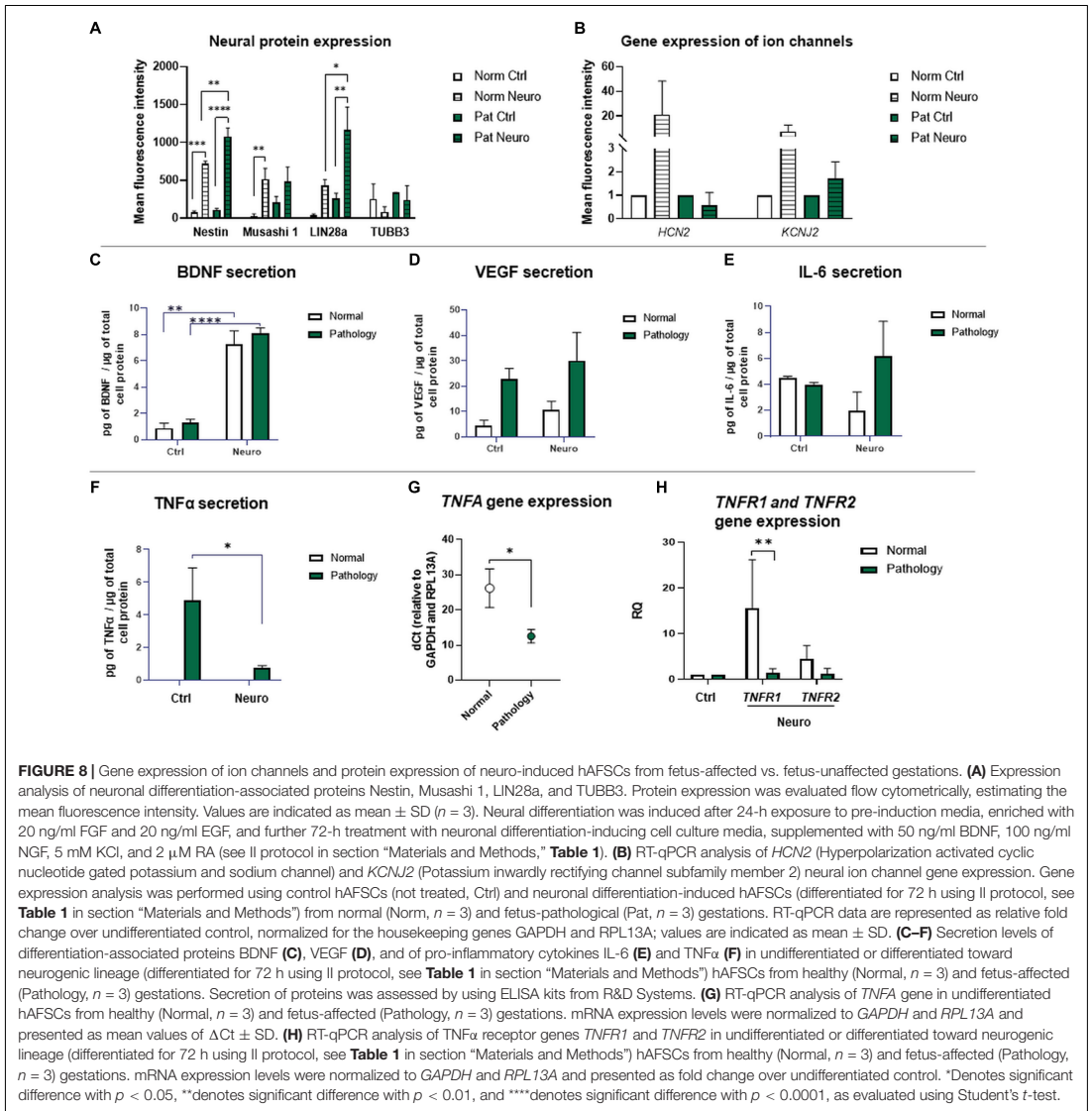
The results of our study revealed that secretion of neurotrophic factor BDNF was significantly increased after



72 h of neurogenic differentiation induction in both hAFSCs from the “Normal” and “Pathology” groups to 8.3-fold ( $p < 0.01$ ) and 6.2-fold ( $p < 0.0001$ ), respectively (Figure 8C). In addition, in both cell types, in hAFSCs from normal gestations and gestations with polyhydramnios, secretion of trophic factor VEGF was also increased upon neurogenic differentiation induction approximately by 2.2- and 1.3-fold, respectively (Figure 8D). It is worth to mention that before neurogenic differentiation induction, both BDNF and VEGF secretion was higher in hAFSCs, obtained from gestations concomitant with polyhydramnios (Figures 8C,D).

Interestingly, ELISA analysis demonstrated that studied hAFSCs, obtained from different sources, do differ in pro-inflammatory cytokine  $TNF\alpha$  secretion—hAFSCs from the “Pathology” group secreted approximately 4.9 pg of  $TNF\alpha/\mu g$  of total cell protein, whereas no secretion of  $TNF\alpha$  was detected

in hAFSCs from normal gestations (Figure 8F). It should be emphasized that after 72 h of neurogenic differentiation induction,  $TNF\alpha$  secretion by hAFSCs from polyhydramnios was reduced by 6.6-fold ( $p < 0.05$ ). Furthermore, we have evaluated the gene expression of *TNFA* and its receptors *TNFR1* and *TNFR2*. RT-qPCR analysis revealed that control, untreated, hAFSCs from healthy gestations have lower *TNFA* expression (dCt value higher by 13.7 points, which means approximately 13,170-fold difference;  $p < 0.05$ ) compared to control hAFSCs from polyhydramnios (Figure 8G). Though gene expression of  $TNF\alpha$  receptor gene *TNFR2* was of comparable degree between control hAFSCs from “Normal” and “Pathology” groups, *TNFR1* gene expression was significantly upregulated in hAFSCs from normal gestations after neuronal differentiation induction ( $p < 0.01$ ; Figure 8H).



In addition, we also evaluated hAFSC secretion of other inflammation-associated cytokines IL-1 $\beta$ , IL-6, and IL-10. ELISA analysis revealed that hAFSCs, either from healthy or pathological gestations, do not secrete pro-inflammatory cytokine IL-1 $\beta$ . Secretion of anti-inflammatory cytokine IL-10 was also not detected (data not shown). However, secretion analysis of IL-6 indicated that both types of tested hAFSCs (groups "Norm" and "Pat") were comparable in the level of secretion of this pro-inflammatory cytokine (**Figure 8E**). Although subtle changes in IL-6 secretion were observed

upon hAFSC neurogenic induction (in hAFSCs from healthy gestations, secretion was downregulated, while in hAFSCs from polyhydramnios, it was slightly upregulated), observed differences were not statistically significant.

Collectively, these data show that despite having a lower neurogenic potential, when evaluated morphologically (**Figure 3**), hAFSCs from gestations with polyhydramnios do hold similar or even greater capacity of producing neural proteins intracellularly. They also have the ability to secrete neurotrophic factors extracellularly, such as BDNF and VEGF, in comparable



amounts to hAFSCs from healthy gestations. However, it should also be mentioned that hAFSCs from pathological gestations with polyhydramnios do exhibit different inflammatory phenotypes in comparison to hAFSCs from normal pregnancies, as secretion of pro-inflammatory cytokine TNF $\alpha$  was detected only from hAFSCs, obtained from polyhydramnios samples.

## DISCUSSION

Amniotic fluid-derived stem cells are considered as a new and potential experimental approach toward improving various conditions, such as autoimmune diseases (Yang et al., 2021), ischemic heart disease (Fang et al., 2021), and Alzheimer's disease (Gatti et al., 2020). They are also suggested to help to suppress cancer (Jafari et al., 2021) or even improve spermatogenesis (Mobarak et al., 2021). However, the main interest goes to treating congenital anomalies such as *spina bifida*, congenital diaphragmatic hernia, and congenital heart disease (Di Bernardo et al., 2014; Kunisaki, 2018; Abe et al., 2019). Although advances in the medical field provide some level of treatment for patients who have been prenatally diagnosed with these anomalies, they continue to burden pediatric care and account for a significant part of infant mortality, morbidity, and hospitalization days worldwide.

The use of hAFSCs for therapeutic applications presents both logical and practical choice for a number of reasons. Stem cell harvesting can be performed prior to delivery by amniocentesis, during which a small sample of amniotic fluid is aspirated from the amniotic sac. Since amniocentesis is a routine tool for diagnostic purposes (sampling amniotic cells for aneuploidies and genetic abnormalities), it is considered as a safe procedure performed with needle aspiration under ultrasound guidance (Daum et al., 2019). Amniotic fluid is an easily accessible source rich with potent cells and even small volumes of sample can produce an abundant quantity of amniocytes and amniotic fluid stem cells (Gasiūnienė et al., 2020). On the contrary, isolating stem cells from other prenatal tissues such as chorionic villi, umbilical cord blood (cordocentesis), fetal skin, liver, or muscle is more technically challenging (Cadrin and Golbus, 1993; Cheng, 2018). In addition, hAFSCs have a robust proliferation rate that exceeds MSCs from other sources when expanded under identical conditions (Kunisaki et al., 2007). Therefore, once the prenatal diagnosis is complete, hAFSCs can be easily propagated *in vitro* for therapeutic purposes. Furthermore, amniotic fluid stem cells originate from the fetus, thus enabling autologous therapeutic applications without concern for immunological rejection upon delivery either prenatally or during the postnatal period (Abe et al., 2021).

While there is a potential for hAFSCs to be a tool in regenerative medicine-based approaches, there is a relative shortage of information on disease-specific amniotic fluid stem cells. A major portion of conducted studies investigated only the benefits of hAFSCs isolated from healthy pregnancies. The results of these studies could cause some limitations on the application of stem cells derived from fetus-affected gestations to be used in clinical settings due to possible key differences in

stem cell characteristics between stem cells of these two sources (healthy and fetus-affected gestations). It should be emphasized that there is no scientific data on metabolic characteristics of hAFSCs obtained from fetus-diseased gestations, nor are there any data on the neurogenic and neurotrophic potential of hAFSCs obtained, for example, from polyhydramnios samples. Therefore, it is crucial to describe the general characteristics and determine the potential of hAFSCs derived from fetus-diseased gestations concomitant with polyhydramnios in order to test their future therapeutic applicability in treating highly devastating pregnancy complications. Previous studies of our research group demonstrated that undifferentiated hAFSCs from normal gestations may produce ATP either *via* a tricarboxylic acid cycle or anaerobic glycolysis (both pathways almost equally active) (Gasiūnienė et al., 2019a). However, there were still no scientific data on the respiratory potential and metabolic activity of hAFSCs obtained from polyhydramnios. Increasing knowledge supports the idea that the status of stem cells' bioenergetic metabolism is intrinsically regulated by pluripotency factors and in turn metabolites can regulate some epigenetic machinery that may affect the state of pluripotency (Tsogtbaatar et al., 2020). Consequently, in order for hAFSCs from fetus-affected gestations to be successfully applied in clinical practice, first, the state of their metabolism must be elucidated. In addition, for the neuro-therapeutic approach, hAFSC neurogenic potential should also be evaluated.

Therefore, in this study, we compared the bioenergetic/metabolic and neurogenic characteristics of hAFSCs, obtained from normal and fetus-affected gestations. Results of our analysis demonstrated that hAFSCs from polyhydramnios samples were exploiting oxidative phosphorylation approximately twice as efficiently as hAFSCs from normal gestations (Figure 2A). In accordance to OXPHOS, hAFSCs from polyhydramnios were noticed to have higher levels of intracellular ATP (Figure 2C), as well as higher expression of *NR1F1* gene (Figure 2G), which is known as one of the main mitochondrial respiratory function regulators (Yuan et al., 2018). Not surprisingly, mitochondrial membrane potential was registered to be higher in hAFSCs from normal gestations in comparison to hAFSCs from polyhydramnios (Figure 2B), as it is widely accepted that mitochondrial membrane potential drops in the state of active respiration (Nicholls, 2004). In addition, our study demonstrated that hAFSCs from healthy pregnancies were significantly more prone to neurogenic differentiation induction compared to hAFSCs from polyhydramnios (Figure 3). Furthermore, hAFSCs from normal pregnancies were more positive for stemness markers, such as CD73, CD90, and CD105 (Figure 1D). Aforementioned differences could possibly be explained by considering the gestational age of investigated cells, as in our study, hAFSCs were obtained from 16 to 17 weeks of normal gestations, whereas hAFSCs from polyhydramnios were obtained at 32 weeks. Although some studies, also including our previous research, showed that hAFSCs may be comparably potent in their ability to differentiate to certain lineages despite their differences in gestational age (Hamid et al., 2017; Gasiūnienė et al., 2019b; Zentelytė et al., 2020), other studies contradict this notion

(Shaw et al., 2017; Huang et al., 2020). Furthermore, it is argued that pluripotent SCs typically have a lower rate of OXPHOS and maintain higher mitochondrial membrane potential in comparison to more differentiated SCs (Tsogtbaatar et al., 2020). In addition, research with mouse embryonic SCs (Schieke et al., 2008) revealed that SCs with high mitochondrial membrane potential may differentiate into all three germ layers, whereas SCs with lower mitochondrial membrane potential are restricted only to the mesodermal lineage. Therefore, results obtained in our study would suggest that hAFSCs from polyhydramnios samples have lower neurogenic differentiation potential due to the gestational age-determined changes in metabolic status.

On the other hand, it should be emphasized that hAFSCs from normal and pathological pregnancies were comparable in glycolysis rate (Figure 2A), as well as gene and protein expression of certain pluripotency-associated factors, which are known to directly regulate glycolysis in pluripotent SCs, such as LIN28A (Figures 1B, 8A; Tsogtbaatar et al., 2020). However, gene expression of other pluripotency-associated factors that are involved in glycolysis regulation of OCT4 and MYC was significantly higher in hAFSCs from polyhydramnios samples compared to hAFSCs from normal gestations (Figure 1B). It should be stressed out that transcription factor OCT4 is known for the direct modulation of pyruvate kinase M2 (PKM) gene expression (Kim et al., 2015). In addition, it was also demonstrated to upregulate GLUT1 expression via binding to the GLUT1 enhancer site (Yu et al., 2019). Similarly, c-MYC regulates transcription of PKM and LDHA (Cao et al., 2015), which in our study was also more pronounced in hAFSCs from polyhydramnios (Figure 2G). On the other hand, c-MYC itself is involved in transcriptional regulation of certain stem cell marker proteins, such as SOX2 and OCT4 (Sisodiya et al., 2012). Moreover, c-MYC was shown to upregulate expression of TNF $\alpha$  (Liu et al., 2015), which in our study was also significantly higher expressed and secreted by hAFSCs from polyhydramnios samples (Figures 8E,G). Therefore, at this stage, the exact role of c-MYC in hAFSCs obtained from normal and fetus-affected gestations remains unclear and further more thorough investigations are needed. However, the cross-examination, involving hAFSCs from healthy gestations obtained at 32 weeks, is not eligible or ethical. Consequently, it is impossible to decipher the precise role of gestational age in the metabolic characteristics of tested cells.

Regarding neurogenic differentiation induction in hAFSCs from healthy gestations, the most effective results were achieved when using the combination of 50 ng/ml BDNF + 100 ng/ml NGF + 2  $\mu$ M RA + 5 mM KCl (Protocol No. II; Figures 5A,B, 6B, 7B,C). For example, the highest expression of neural differentiation-associated genes NCAM2, NES, MAP2, VEGFA, BDNF, and NTF4 was registered upon neurogenic induction with the aforementioned chemical cocktail. However, the most characteristic neuro-like morphology was observed when this treatment was supplemented with 1 mM 8-Bromo-cAMP and 0.3 mM IBMX (Protocol No. III; Figure 3A). Our results coincide with Bonaventura et al. (2015) (Bonaventura et al., 2015), who demonstrated that a similar chemical cocktail (1 mM dbcAMP + 0.5 mM IBMX + 20 ng/ml EGF + 40 ng/ml

bFGF + 10 ng/ml NGF + 10 ng/ml BDNF) was potent in hAFSC neurogenic differentiation induction. However, the chemical combination consisting only of 1 mM 8-Bromo-cAMP, 0.3 mM IBMX, 2  $\mu$ M RA, and 5 mM KCl (protocol No. I) was the least efficient, while treatment with 50 ng/ml BDNF + 100 ng/ml NGF + 2  $\mu$ M RA + 5 mM KCl proved to be the most effective in neurotrophic factors' gene induction (Figures 7B,C). For this reason, we further tested the secretome of hAFSCs upon neural differentiation induction with this particular chemical combination. Recent studies by other authors (Kukumberg et al., 2021) showed that hAFSCs under hypoxic conditions, in comparison to normoxic state, secrete larger quantities of growth factors such as BDNF and VEGF. Results of our ELISA analysis revealed that secretion of BDNF and VEGF proteins is also increased after the induction of neurogenic differentiation by a comparable degree in hAFSCs from both normal and pathological pregnancies (Figures 8C,D). In addition, upon neurogenic differentiation induction in hAFSCs, the intracellular levels of neuronal differentiation-associated proteins Nestin and LIN28A were upregulated more strongly in cells from polyhydramnios samples in comparison to cells obtained from healthy gestations. These observations may suggest that hAFSCs obtained from polyhydramnios should also be tested further for their neurotrophic potential and possible clinical applicability.

Surprisingly, in hAFSCs from polyhydramnios samples, secretion of pro-inflammatory cytokine TNF $\alpha$  was also detected (Figure 8F). However, upon neurogenic differentiation, it was significantly reduced. We wondered if secretion of TNF $\alpha$  by hAFSCs obtained from polyhydramnios samples may be associated with the intensity of ROS generation within these cells. Results of cellular ROS analysis revealed that hAFSCs from polyhydramnios samples indeed produce higher quantities of intrinsic ROS (Figures 2D–F). In addition, TNEA gene expression was also significantly higher in hAFSCs from pathological gestations (Figure 8F). Previous research by other authors (Kim et al., 2012) demonstrated that increased CD13 (aminopeptidase N) expression reduces ROS generation in cancer stem cells. In our study, such a negative correlation between the expression of CD13 (Figure 1C) and ROS production was also evident in hAFSCs. We believe that all these observations could possibly be explained by the inflammatory state of polyhydramnios itself, as treatment with the anti-inflammatory agents is suggested for the reduction of amniotic fluid volumes (Hamza et al., 2013). However, further research is needed in order to explain the role and molecular pathways of TNF $\alpha$  and ROS in the biology of hAFSCs obtained from polyhydramnios.

Nevertheless, subsequent analysis of inflammation-associated cytokines (IL-1 $\beta$ , IL-6, and IL-10) revealed that hAFSCs from polyhydramnios samples do not differ from healthy fetuses-derived hAFSCs in secretion of these cytokines, as no secretion of IL-1 $\beta$  and IL-10 was detected at all and levels of secreted IL-6 were comparable between tested groups (Figure 8E). Although IL-6 is generally regarded as a major inducer of immune and inflammatory cascades, accumulating data emphasize its role within the central nervous system as well, as IL-6 promotes differentiation of neural stem cells into glutamate-responsive neurons and several astroglia cell types (Islam et al., 2009).

In addition, IL-6 was also recently described to have an anti-inflammatory activity, as its effect depends on concentration and combination with other pro-inflammatory cytokines (Borsini et al., 2020). As it is evident from the results of our research, IL-6 secretion increases upon neural differentiation induction in hAFSCs from the Pathology group, whereas in hAFSCs from normal gestations, secretion of IL-6 slightly diminishes, although these differences are not statistically significant. Obviously, more comprehensive examination of hAFSC secretome would be necessary in order to refine the whole picture of paracrine activities of these cells. Recent research performed by Costa et al. (2021) showed that fetal hAFSCs (from the second trimester of gestations) and perinatal hAFSCs (obtained during scheduled C-sections) do differ in cytokine and chemokine profile. For example, several proteins, such as extracellular matrix metalloproteinase inducer (EMMPRIN) and interleukin 8 (IL-8), were found to be exclusively enriched in fetal but not in perinatal hAFSCs upon hypoxic preconditioning. In the aforementioned study, BDNF protein was enriched in all hypoxia-induced extracellular vesicles of hAFSCs regardless of gestational age, similarly to our study, where the level of BDNF secretion was comparable in both “Normal” and “Pathology” groups. Furthermore, recent research by Castelli et al. (2021) revealed that the secretome of hAFSCs was able to activate pro-survival and anti-apoptotic pathways and exhibited neuro-protective activity in an ischemia/reperfusion SH-SY5Y cell model, while activating intracellular BDNF signaling.

To sum up, results of our research expand the knowledge about the general characteristics and neurogenic potential of hAFSCs obtained from healthy and fetus-affected gestations. In this study, we demonstrated that hAFSCs from healthy gestations and gestations with fetus pathology concomitant with polyhydramnios do differ in their metabolic status, as hAFSCs from polyhydramnios samples rely on oxidative phosphorylation more heavily and are more energetic compared to hAFSCs from healthy fetuses. Although hAFSCs from normal gestations were shown to have stronger neurogenic potential, hAFSCs from these two different sources are comparable in neurotrophic factor secretion, in both control (untreated) and neuro-induced states. However, different patterns of pro-inflammatory cytokine TNF $\alpha$  secretion were characteristic for tested hAFSC groups, as hAFSCs from polyhydramnios samples were producing extracellular TNF $\alpha$ , whereas no secretion of TNF $\alpha$  was detected from hAFSCs, obtained from healthy gestations. Therefore, in future studies, *in vivo* potential as well as strategies that could improve the characteristics of hAFSCs derived from diseased fetuses should be investigated in order for those cells to be successfully applied for regenerative medicine purposes, particularly for infants, either in the prenatal or neonatal stage.

## LIMITATIONS OF THIS STUDY

It should be emphasized that sample groups in this study were quite small (three samples per group). Groups of studied hAFSCs were also different in gestational age (cells from healthy pregnancies were obtained at 16–17 weeks of gestation,

whereas cells from polyhydramnios were obtained at 32 weeks of gestation). As we have already stated, it is impossible to obtain hAFSCs from healthy pregnancies at 32 weeks of gestation in the clinical practice, as such interventions have no clinical utility and are not ethical. In addition, hAFSCs from gestations with polyhydramnios may also be obtained only when polyhydramnios condition occurs (in most cases, polyhydramnios develops late in the second or in the third trimester of pregnancy). Therefore, this particular shortcoming of our study is determined by the settings in the clinical practice and pathophysiology of polyhydramnios itself. The heterogeneity in diagnoses in the “Pathology” group samples is also a limitation of this study. However, this group was uniform for gestational age and concomitant polyhydramnios state.

## DATA AVAILABILITY STATEMENT

The raw data supporting the conclusions of this article will be made available by the authors, without undue reservation.

## ETHICS STATEMENT

The studies involving human participants were reviewed and approved by Vilnius Regional Biomedical Research Ethics Committee, No. 158200-18/7-1049-550, version No. 1. The patients/participants provided their written informed consent to participate in this study.

## AUTHOR CONTRIBUTIONS

GV conceived the idea and research questions, performed a formal analysis, investigation, and visualization, supervised the ongoing study, and prepared the first complete draft of the manuscript. AZ performed a formal analysis, investigation, and visualization, and aided in manuscript preparation and editing. EB performed investigation and formal analysis. RN reviewed and edited the manuscript. All authors approved the final manuscript.

## FUNDING

This work was supported by a Vilnius University Science promotion fund grant (MSF-LMT-3/2020).

## SUPPLEMENTARY MATERIAL

The Supplementary Material for this article can be found online at: <https://www.frontiersin.org/articles/10.3389/fcell.2021.700634/full#supplementary-material>

## REFERENCES

- Abe, Y., Ochiai, D., Masuda, H., Sato, Y., Otani, T., Fukutake, M., et al. (2019). In utero amniotic fluid stem cell therapy protects against myelomeningocele via spinal cord coverage and hepatocyte growth factor secretion. *Stem Cells Transl. Med.* 8, 1170–1179. doi: 10.1002/sctm.19-0002
- Abe, Y., Ochiai, D., Sato, Y., Otani, T., Fukutake, M., Ikenoue, S., et al. (2021). Amniotic fluid stem cells as a novel strategy for the treatment of fetal and neonatal neurological diseases. *Placenta* 104, 247–252. doi: 10.1016/j.placenta.2021.01.009
- Ahn, S. Y., Park, W. S., Sung, S. I., and Chang, Y. S. (2021). Mesenchymal stem cell therapy for intractable neonatal disorders. *Pediatr. Neonatol.* 62, S16–S21. doi: 10.1016/j.pedneo.2020.11.007
- Alessio, N., Pipino, C., Mandatori, D., Di Tomo, P., Ferone, A., Marchiso, M., et al. (2018). Mesenchymal stromal cells from amniotic fluid are less prone to senescence compared to those obtained from bone marrow: an in vitro study. *J. Cell. Physiol.* 233, 8996–9006. doi: 10.1002/jcp.26845
- Bonaventura, G., Chamayou, S., Liprino, A., Guglielmino, A., Fichera, M., Caruso, M., et al. (2015). Different tissue-derived stem cells: a comparison of neural differentiation capability. *PLoS One* 10:0140790. doi: 10.1371/journal.pone.0140790
- Borsini, A., Di Benedetto, M. G., Giacobbe, J., and Pariante, C. M. (2020). Pro- And anti-inflammatory properties of interleukin in vitro: relevance for major depression and human hippocampal neurogenesis. *Int. J. Neuropsychopharmacol.* 23, 738–750. doi: 10.1093/ijnp/pyaa055
- Cadrin, C., and Golbus, M. S. (1993). Fetal tissue sampling - Indications, techniques, complications, and experience with sampling of fetal skin, liver, and muscle. *West. J. Med.* 159, 269–272.
- Cao, Y., Guo, W., Tian, S., He, X., Wang, X., Liu, X., et al. (2015). miR-290/371-Mbd2-Myc circuit regulates glycolytic metabolism to promote pluripotency. *EMBO J.* 34, 609–623. doi: 10.15252/embj.201490441
- Castelli, V., Antonucci, I., d'Angelo, M., Tessitore, A., Zelli, V., Benedetti, E., et al. (2021). Neuroprotective effects of human amniotic fluid stem cells-derived secretome in an ischemia/reperfusion model. *Stem Cells Transl. Med.* 10, 251–266. doi: 10.1002/sctm.20-0268
- Cheng, E. Y. (2018). "Prenatal Diagnosis," in *Avery's Diseases of the Newborn*, 10th Edn, eds C. A. Gleason and S. E. Juul (Philadelphia, PA: Elsevier Inc.), 190–200.e1.
- Costa, A., Ceresa, D., De Palma, A., Rossi, R., Turturo, S., Santamaria, S., et al. (2021). Comprehensive profiling of secretome formulations from fetal-and perinatal human amniotic fluid stem cells. *Int. J. Mol. Sci.* 22:3713. doi: 10.3390/ijms22073713
- Daum, H., Ben David, A., Nadjari, M., Zenvirt, S., Helman, S., Yanai, N., et al. (2019). Role of late amniocentesis in the era of modern genomic technologies. *Ultrasound Obstet. Gynecol.* 53, 676–685. doi: 10.1002/uog.20113
- Di Bernardo, J., Maiden, M. M., Hershenson, M. B., and Kunisaki, S. M. (2014). Amniotic fluid derived mesenchymal stromal cells augment fetal lung growth in a nitrofen explant model. *J. Pediatr. Surg.* 49, 859–865. doi: 10.1016/j.jpedsurg.2014.01.013
- Fang, Y. H., Wang, S. P. H., Chang, H. Y., Yang, P. J., Liu, P. Y., and Liu, Y. W. (2021). Progress and challenges of amniotic fluid derived stem cells in therapy of ischemic heart disease. *Int. J. Mol. Sci.* 22, 1–12. doi: 10.3390/ijms22010102
- Gasiūnienė, M., Petkus, G., Matuzevičius, D., Navakauskas, D., and Navakauskienė, R. (2019a). Angiotensin II and TGF-β1 induce alterations in human amniotic fluid-derived mesenchymal stem cells leading to cardiomyogenic differentiation initiation. *Int. J. Stem Cells* 12, 251–264. doi: 10.15283/ijsc.18126
- Gasiūnienė, M., Valatkaitė, E., and Navakauskienė, R. (2020). Long-term cultivation of human amniotic fluid stem cells: the impact on proliferative capacity and differentiation potential. *J. Cell. Biochem.* 121, 3491–3501. doi: 10.1002/jcb.29623
- Gasiūnienė, M., Zentelytė, A., Treigyte, G., Baronaitė, S., Savickienė, J., Utkus, A., et al. (2019b). Epigenetic alterations in amniotic fluid mesenchymal stem cells derived from normal and fetus-affected gestations: a focus on myogenic and neural differentiations. *Cell Biol. Int.* 43, 299–312. doi: 10.1002/cbin.11099
- Gatti, M., Zavatti, M., Beretti, F., Giuliani, D., Vandini, E., Ottani, A., et al. (2020). Oxidative stress in Alzheimer's disease: in vitro therapeutic effect of amniotic fluid stem cells extracellular vesicles. *Oxid. Med. Cell. Longev.* 2020:2785343. doi: 10.1155/2020/2785343
- Hamid, A. A., Joharry, M. K., Mun-Fun, H., Hamzah, S. N., Rejali, Z., Yazid, M. N., et al. (2017). Highly potent stem cells from full-term amniotic fluid: a realistic perspective. *Reprod. Biol.* 17, 9–18. doi: 10.1016/j.repbio.2017.02.001
- Hanza, A., Herr, D., Solomayer, E. F., and Meyberg-Solomayer, G. (2013). Polyhydramnios: causes, diagnosis and therapy. *Geburtshilfe Frauenheilk.* 73, 1241–1246.
- Huang, J., Ma, W., Wei, X., and Yuan, Z. (2020). Amniotic fluid mesenchymal stromal cells from early stages of embryonic development have higher self-renewal potential. *Vitro Cell. Dev. Biol. Anim.* 56, 701–714. doi: 10.1007/s11626-020-00511-z
- Islam, O., Gong, X., Rose-John, S., and Heese, K. (2009). Interleukin-6 and neural stem cells: more than gliogenesis. *Mol. Biol. Cell* 20, 188–199. doi: 10.1091/mbc.e08-05-0463
- Jafari, A., Rezaei-Tavirani, M., Farhadhosseiniabadi, B., Zali, H., and Niknejad, H. (2021). Human amniotic mesenchymal stem cells to promote/suppress cancer: two sides of the same coin. *Stem Cell Res. Ther.* 12:126. doi: 10.1186/s13287-021-02196-x
- Jain, M., Minocha, E., Tripathy, N. K., Singh, N., Chaturvedi, C., and Nityanand, S. (2019). Comparison of the cardiomyogenic potency of human amniotic fluid and bone marrow mesenchymal stem cells. *Int. J. Stem Cells* 12, 449–456. doi: 10.15283/IJSC18087
- Kim, H. M., Haraguchi, N., Ishii, H., Ohkuma, M., Okano, M., Mimori, K., et al. (2012). Increased CD13 expression reduces reactive oxygen species, promoting survival of liver cancer stem cells via an epithelial-mesenchymal transition-like phenomenon. *Ann. Surg. Oncol.* 19, 539–548. doi: 10.1245/s10434-011-2040-5
- Kim, H., Jang, H., Kim, T. W., Kang, B., Lee, S., Jeon, Y., et al. (2015). Core pluripotency factors directly regulate metabolism in embryonic stem cell to maintain pluripotency. *Stem Cells* 33, 2699–2711. doi: 10.1002/stem.2073
- Kleine, R. T., Bernardes, L. S., Carvalho, M. A., Carvalho, M. H., Krebs, V., and Francisco, R. (2016). Pregnancy outcomes in severe polyhydramnios: no increase in risk in patients needing amnioreduction for maternal pain or respiratory distress. *J. Matern. Fetal Neonatal Med.* 29, 4031–4034. doi: 10.3109/14767058.2016.1153060
- Kouamé, N., N'Goan-Domoua, A. M., Nikiéma, Z., Konona, A., N'guessanc, K. E., Sétchéoua, A., et al. (2013). Polyhydramnios: a warning sign in the prenatal ultrasound diagnosis of foetal malformation? *Diagn. Interv. Imaging* 94, 433–437. doi: 10.1016/j.diii.2013.01.002
- Kukumberg, M., Phermthai, T., Wichtwiengrat, S., Wang, X., Arjunan, S., Chong, S. Y., et al. (2021). Hypoxia-induced amniotic fluid stem cell secretome augments cardiomyocyte proliferation and enhances cardioprotective effects under hypoxic-ischemic conditions. *Sci. Rep.* 11:163. doi: 10.1038/s41598-020-80326-w
- Kunisaki, S. M. (2018). Amniotic fluid stem cells for the treatment of surgical disorders in the fetus and neonate. *Stem Cells Transl. Med.* 7, 767–773. doi: 10.1002/sctm.18-0018
- Kunisaki, S. M., Fuchs, J. R., Steigman, S. A., and Fauza, D. O. (2007). A comparative analysis of cartilage engineered from different perinatal mesenchymal progenitor cells. *Tissue Eng.* 13, 2633–2644. doi: 10.1089/ten.2006.0407
- Liu, T., Zhou, Y., Ko, K. S., and Yang, H. (2015). Interactions between myc and mediators of inflammation in chronic liver diseases. *Mediators Inflamm.* 2015:276850. doi: 10.1155/2015/276850
- Mobarak, H., Heidarpour, M., Rahbarghazi, R., Nouri, M., and Mahdipour, M. (2021). Amniotic fluid-derived exosomes improved spermatogenesis in a rat model of azoospermia. *Life Sci.* 274:119336. doi: 10.1016/j.lfs.2021.119336
- Nicholls, D. G. (2004). Mitochondrial membrane potential and aging. *Aging Cell* 3, 35–40. doi: 10.1111/j.1474-9728.2003.00079.x
- Nitkin, C. R., Rajasingh, J., Pisano, C., Besner, G., Thébaud, B., and Sampath, V. (2020). Stem cell therapy for preventing neonatal diseases in the 21st century: current understanding and challenges. *Pediatr. Res.* 87, 265–276. doi: 10.1038/s41390-019-0425-5
- Ramasamy, T. S., Velaithan, V., Yeow, Y., and Sarkar, F. H. (2018). Stem cells derived from amniotic fluid: a potential pluripotent-like cell source for cellular therapy? *Curr. Stem Cell Res. Ther.* 13, 252–264. doi: 10.2174/1574888x13666180115093800
- Schieke, S. M., Ma, M., Cao, L., McCoy, J. P., Liu, C., Hensel, N., et al. (2008). Mitochondrial metabolism modulates differentiation and teratoma formation

- capacity in mouse embryonic stem cells. *J. Biol. Chem.* 283, 28506–28512. doi: 10.1074/jbc.M802763200
- Shaw, S. W. S., Cheng, P. J., Chang, Y. L., Chao, A., Wang, T., Chang, S., et al. (2017). Human amniotic fluid stem cells have better potential in early second trimester of pregnancy and can be reprogramed to iPS. *Taiwan. J. Obstet. Gynecol.* 56, 770–774. doi: 10.1016/j.tjog.2017.10.012
- Shaw, S. W., Peng, S. Y., Liang, C. C., Lin, T., Cheng, P., Hsieh, T., et al. (2021). Prenatal transplantation of human amniotic fluid stem cell could improve clinical outcome of type III spinal muscular atrophy in mice. *Sci. Rep.* 11:9158. doi: 10.1038/s41598-021-88559-z
- Sisodiya, S., Thom, M., Strauss, K., Orlova, K. A., Tsai, V., Baybis, M., et al. (2012). Early progenitor cell marker expression distinguishes type II from Type I focal cortical dysplasias. *J. Neuropathol. Exp. Neurol.* 69, 850–863. doi: 10.1097/NEN.0b013e3181eac1f5.Early
- Tsogetbaatar, E., Landin, C., Minter-Dykhouse, K., and Folmes, C. D. L. (2020). Energy metabolism regulates stem cell pluripotency. *Front. Cell Dev. Biol.* 8:87. doi: 10.3389/fcell.2020.00087
- Ursachen, D. P., and Therapie, D. (2013). Polyhydramnios : causes, diagnosis and therapy. *Geburtshilfe Frauenheilkd* 73, 1241–1246.
- Yan, Z. J., Hu, Y. Q., Zhang, H. T., Zhang, P., Xiao, Z., Sun, X., et al. (2013). Comparison of the neural differentiation potential of human mesenchymal stem cells from amniotic fluid and adult bone marrow. *Cell. Mol. Neurobiol.* 33, 465–475. doi: 10.1007/s10571-013-9922-y
- Yang, C., Wu, M., You, M., Chen, Y., Luo, M., and Chen, Q. (2021). The therapeutic applications of mesenchymal stromal cells from human perinatal tissues in autoimmune diseases. *Stem Cell Res. Ther.* 12:103. doi: 10.1186/s13287-021-02158-3
- Yefet, E., and Daniel-Spiegel, E. (2016). Outcomes from polyhydramnios with normal ultrasound. *Pediatrics* 137:e20151948. doi: 10.1542/peds.2015-1948
- Yu, L., Ji, K. Y., Zhang, J., Xu, Y., Ying, Y., Mai, T., et al. (2019). Core pluripotency factors promote glycolysis of human embryonic stem cells by activating GLUT1 enhancer. *Protein Cell* 10, 668–680. doi: 10.1007/s13238-019-0637-9
- Yuan, J., Zhang, S., and Zhang, Y. (2018). Nrfl is paved as a new strategic avenue to prevent and treat cancer, neurodegenerative and other diseases. *Toxicol. Appl. Pharmacol.* 360, 273–283.
- Zentelytė, A., Gasiūnienė, M., Treigytyė, G., Baronaitė, S., Savickienė, J., Borutinskaitė, V., et al. (2020). Epigenetic regulation of amniotic fluid mesenchymal stem cell differentiation to the mesodermal lineages at normal and fetus-diseased gestation. *J. Cell. Biochem.* 121, 1811–1822. doi: 10.1002/jcb.29416

**Conflict of Interest:** The authors declare that the research was conducted in the absence of any commercial or financial relationships that could be construed as a potential conflict of interest.

Copyright © 2021 Vallulienė, Zentelytė, Beržanskytė and Navakauskienė. This is an open-access article distributed under the terms of the Creative Commons Attribution License (CC BY). The use, distribution or reproduction in other forums is permitted, provided the original author(s) and the copyright owner(s) are credited and that the original publication in this journal is cited, in accordance with accepted academic practice. No use, distribution or reproduction is permitted which does not comply with these terms.

## UŽRAŠAMS

# UŽRAŠAMS

Vilniaus universiteto leidykla  
Saulėtekio al. 9, III rūmai, LT-10222 Vilnius  
El. p. [info@leidykla.vu.lt](mailto:info@leidykla.vu.lt), [www.leidykla.vu.lt](http://www.leidykla.vu.lt)  
Tiražas 15 egz.